The role of Transforming Growth Factor beta in Mesothelioma collagen production and tumour growth

by

Michael Keith Wood
MB.BS (London), BSc (London), MRCP (UK)

A thesis submitted to the University of London for the degree of

Doctor of Philosophy

in the Department of Medicine

Centre for Respiratory Research
5 University Street
University College London
London WC1E 6JJ

ProQuest LLC
789 East Eisenhower Parkway
P.O. Box 1346
Ann Arbor, MI 48106-1346

Abstract

Malignant Mesothelioma (MM) is an aggressive, fibrotic tumour predominantly of pleural origin. It is poorly understood, insensitive to conventional therapy and its incidence is increasing with a peak predicted around 2020. Its fibrous nature is due to abundant extracellular matrix (ECM) deposition with collagen as its major component. ECM has essential roles in many cancers; as a scaffold for tumour growth and by interacting with tumour cells it is essential in tissue invasion, metastasis, angiogenesis and protection of tumours from chemotherapy. MMs produce growth factors, including TGFβ, which is pro-angiogenic, immunosuppressive, and a potent stimulator of collagen production. TGFβ signals predominantly through a unique signalling system - the Smad pathway. This involves Smad7, a negative feedback inhibitor of Smad signalling, which when over-expressed has been shown to inhibit TGFβ activity. This thesis examined the role of TGFβ and collagen in MM tumour growth, using 7 MM cell lines derived from 3 murine and 4 human tumours. *In vivo*, a murine model was used to assess tumour growth following subcutaneous inoculation with syngeneic MM cells. MM cell TGFβ production was assessed using a mink lung reporter assay, which confirmed high levels of TGFβ synthesis. High-pressure liquid chromatography (HPLC) was used to assess collagen production and MM cells found to synthesise large quantities of collagen, responding to TGFβ stimulation by increasing production. Furthermore, tumours contained abundant collagen, assessed histologically and using HPLC. Two approaches were used to inhibit TGFβ activity; TGFβ neutralising antibodies and transfection of Smad7. Assessment of collagen responses, at gene level (reporter assays) and protein level (HPLC), following inhibition of TGFβ found that TGFβ antibodies reduced the collagen response, but Smad7 transfection resulted in increased basal collagen production and no inhibition of TGFβ. Tumour growth and collagen production were reduced in mice systemically treated with TGFβ neutralising antibodies, but tumours derived from Smad7 transfected cells grew larger than controls. These paradoxical findings suggested the possibility of either alternative non-Smad signalling pathways or altered receptor expression. Smad and MAPK signalling were assessed using Western blotting and Smad found to be normally activated. MAPK signalling (ERK1/2 and p38 kinase)

was found to be directly activated by TGFβ, but inhibition using specific inhibitors found that these pathways may play a role in regulating basal collagen production but were not the signalling route for the TGFβ response. Finally, MM tumour expression of TGFβ type I receptors (TβRI) were examined and both the ALK1 and ALK5 isoforms found to be present. This novel finding of ALK1 was unexpected and its responses have previously been shown to oppose ALK5 effects. Conclusion: This work confirms the importance of TGFβ and collagen in MM with inhibition of TGFβ causing a reduction in tumour growth. Transfection of Smad7 resulted in paradoxical findings that might relate to changes in the expression of different isoforms of the TGFβ type I receptor in MM. These novel findings warrant further investigation that may lead to new therapeutic targets.

Dedication

"For Cynthia, Jakob, Rebekah and Isabella"

Acknowledgements

Thank you to all who helped me on the way. I am indebted in particular to my supervisors, Steve and Robin, to the boss, Geoff, and those whose experience I could always rely on for advice, Pat, Rachel, Mike, Geoff B, Steve B, and the Sarahs. Also thanks to Steve Spiro for setting me on the right path and introducing me to the lab.

To the students in the lab who kept me sane and amused, Keith, Rebecca, Nat, Adam, Dave, Danielle, Mark, Alex and Robin J.

Most of all I thank my long suffering family, especially Cynthia, without whose support this thesis would never have been written.

Contents

List of Tables

List of Figures

Abbreviations

ALK - activin receptor-like kinase

bFGF - basic-fibroblast growth factor

BMPs - bone morphogenic proteins

CBP - CREB-binding protein

CDKs - cyclin-dependent kinases

CREB - Ca^{2+} /cAMP response element-binding protein

DMEM - Dulbecco's Modified Eagle Medium

DMSO - dimethyl sulphoxide

ECM – extracellular matrix

EGF - epidermal growth factor

EGFR epidermal growth factor receptor

ERK1 - extracellular signal-related kinase 1

FCS - Foetal calf serum

GFP - green fluorescent protein

hCMV - human cytomegalovirus

HIV – human immunodeficiency virus

HPLC – high-pressure liquid chromatography

HRP – horse radish peroxidase

hyp – Hydroxyproline

IGF - insulin-like growth factor

IRES - Internal Ribosome Entry Site

JNK - Jun-NH2-terminal kinase

LAPs - latency associated proteins

LID – transfection vector comprising lipofectamine (L), an integrin binding peptide (I), and the plasmid of the selected cDNA (D)

LLC - large latent complex

LTBP - latent-TGFβ-binding protein

MAPK - mitogen activating protein kinase

MAPKK – MAPK kinase

MAPKKK - MAPK kinase kinase

MEKK1 - MAP or ERK kinase kinase

MH1 and **MH2** - Mad homology regions 1 and 2

MLEC - mink lung epithelial cell

MM – malignant mesothelioma

MMPs - matrix metalloproteinases

MSB – Martius Scarlet Blue staining for collagen analysis

PBS - phosphate buffered saline

PCR – polymerase chain reaction

PDGF - platelet derived growth factor

PGLIα - vector comprising the mouse promoter region of the COL1A1 gene for α_1 (I) procollagen upstream of the firefly luciferase gene

Rb - retinoblastoma susceptible gene

Smad – TGFβ signalling protein, name derived from the Drosophila signalling protein Mad (mothers against decapentaplegia) and the C.elegens signalling Sma proteins

STRAP - serine-threonine kinase receptor-associated protein E3 ubiquitin ligase,

Smurf1 - Smad ubiquination-related factor 1

SV40 - Simian virus 40

TβRI - TGFβ receptor type I

TβRII - TGFβ receptor type II

Tag - T antigen

TAK1 - TGFβ activated kinase 1

TGFβ – transforming growth factor beta

VEGF - vascular endothelial growth factor

Chapter 1. Introduction

1.1 Background

Malignant Mesothelioma (MM) is an aggressive tumour that arises predominantly from the pleura and is often associated with deposition of large amounts of collagen and other extracellular matrix (ECM) proteins. Its rising incidence as a cause of cancer mortality has lead to an urgent need for the development of new therapies, yet the tumour remains poorly understood and is almost completely insensitive to conventional forms of therapy. There is a considerable time lag of up to and beyond 40 years between exposure to asbestos fibres, the predominant cause of MM, and development of the tumour. However, following the onset of symptoms, there is a median survival time of only 10-14 months(Edwards *et al.* 2000;Peto *et al.* 1999;Treasure *et al.* 2004). The peak of MM cases in developed countries is predicted to occur between 2010 and 2020 with 2000 patients dying per year from MM in the UK and 100,000 patients dying in total across Western Europe (Peto *et al.* 1999;White 2003). Therefore, the need for a better understanding of MM tumour biology in order to develop new therapies cannot be overstated.

1.2 Asbestos and Malignant Mesothelioma

Mesothelioma cells are thought to be derived from mesothelial cells following their transformation by exposure to asbestos fibres. The normal mesothelium and its function is described in section 1.2.1 followed by a description of asbestos fibres and how they are thought to cause MM.

1.2.1 The normal mesothelium

The mesothelium is comprised of a single cell layer of mesodermal origin(Whitaker *et al.* 1982) that lines the pleural, pericardial and peritoneal cavities and the organs within those cavities. What appears to be a simple monolayer of mesothelial cells providing a frictionless surface for the organs in the body cavities has in fact a number of other dynamic functions. Its other primary function appears to be in response to injury, whether due to inflammation, infection, surgical or other insults, to maintain the integrity of the serosal space it lines(Antony 2003). Pleural

mesothelial cells are metabolically active and have cellular functions including the active transport of solutes, which can involve vesicular transport of protein(Zocchi 2002). In response to inflammatory stimuli, mesothelial cells release cytokines and growth factors, such as TGFβ, which aid in repair but these factors can also result in pleural fibrosis and the stimulation of pleural effusions(Lee and Lane 2001). TGFβ has been shown to stimulate pleural vascular endothelial growth factor (VEGF) during inflammatory pleural responses(Cheng *et al.* 2000), which appears to have a principle role in the formation of exudative pleural effusions and may also promote tumour growth(Grove and Lee 2002).

The healing properties of mesothelial surfaces are unique and distinguish it from other epithelial surfaces. Although the mechanisms of healing remain controversial, an injury to the mesothelial layer is repaired by diffuse healing across the injury rather than by healing from the edges inward as for other epithelial-like cell layers (Mutsaers 2002). Normal skin wounds epithelialize from the borders inwards and the size of the injury affects the healing time. In serosal trauma, an injury to the mesothelium results in the simultaneous mesothelialization of the entire surface irrespective of the size of the lesion(Mutsaers 2002). This mechanism of healing is thought to be involved in the formation of intraperitoneal adhesions, a dynamic process whereby surgically traumatized tissues in apposition bind through fibrin bridges.

1.2.2 Types of asbestos

Asbestos fibres are of two main sub-types – Serpentine and Amphibole. The division between the two types of asbestos is based upon the crystalline structure. Serpentines have a sheet or layered structure whereas amphiboles have a chain-like structure. Once mined, asbestos rock mineral is crushed and processed producing long fibres, which are strong, durable, and resistant to many chemicals, heat and fire, which are the properties, along with its high tensile strength, that made it so popular. There are three main types of asbestos that are mined commercially: the Serpentine asbestos - Chrysotile (white) is highly flexible and easily spun and woven into cloth as soft and as flexible as cotton, yet fireproof, the Amphiboles - Amosite (brown) and Crocidolite (blue), which are coarser and stronger than chrysotile, and have been used predominantly in lagging and construction. All three types are very adaptable and are

often mixed. These three types are highlighted in figure 1.1, which groups the different asbestos fibres.

After processing, Serpentine fibres are longer (1-20nm in length, but can be up to 100nm) and more curly than amphibole fibres, which contain shorter, rod-like fibres and it is these, especially crocidolite, that have the strongest causal link of all to MM.

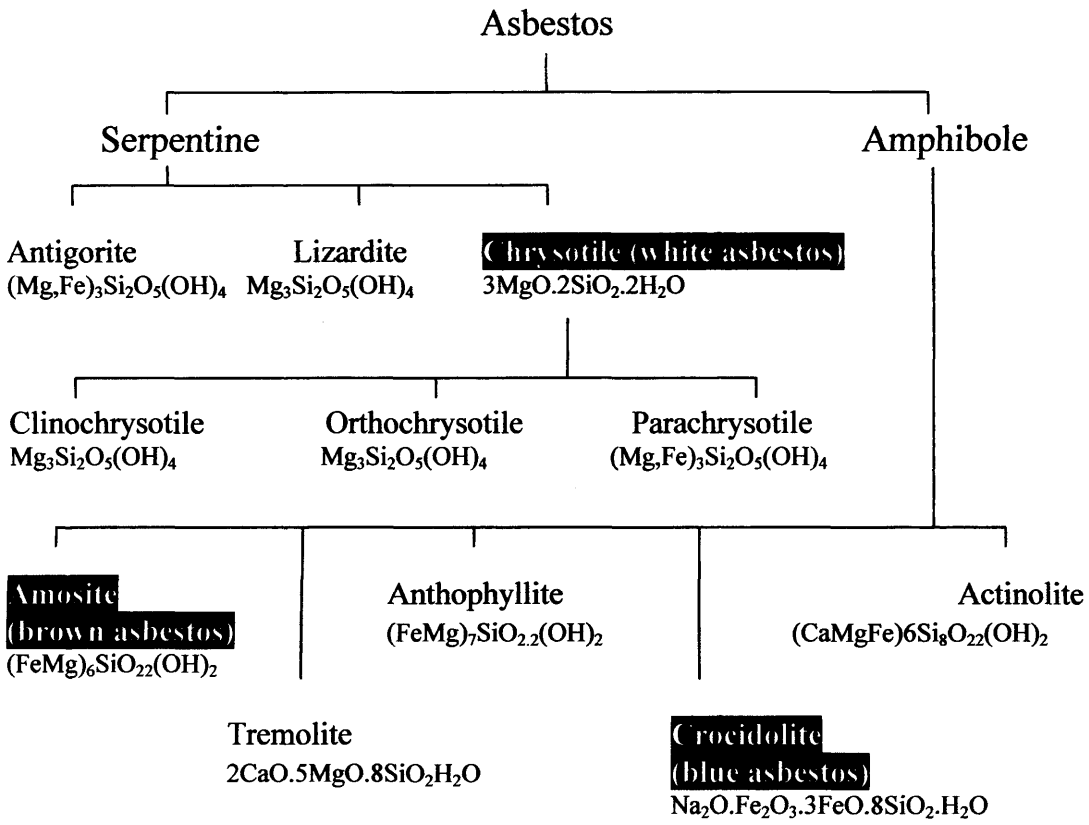

Figure 1.1 The different basic forms of asbestos fibre. Asbestos fibres are divided into Serpentine and Amphibole types depending upon their physical properties (see text). The three commercially mined types of asbestos (chrysotile, amosite and crocidolite) are highlighted. (Adapted from Encyclopaedia Britannica, www.concise.britannica.com.)

1.2.3 Producers and users of asbestos

In South Africa, asbestos has only recently been officially accepted as a dangerous substance, yet South Africa has been one of the world's major producers of amphibole fibre along with Australia (McCulloch 2003). Australia mined and

imported large amounts of amosite and crocidolite reaching a peak in 1958, later importing chrysotile up until the 1970s. Australia has the highest reported rate of MM anywhere in the world but has now banned the use of asbestos (Leigh and Driscoll 2003;Xu *et al.* 1985). China, Russia and Brazil are increasing their production with large local markets and Thailand, India, South Korea and Iran, who are major importers of asbestos(Joshi and Gupta 2004). Korea has been mining asbestos since the 1920s, but the first national asbestos related ill-health survey was only carried out in 1993. There are 100 asbestos factories in Korea and lung cancer is their fastest growing cancer (Paek 2003). These countries will inevitably have huge numbers of MM cases in the future.

Canada is the only developed country that still produces asbestos and is the world's second largest producer of chrysotile (18% of world's production) (Harris and Kahwa 2003). This is justified on the grounds of improved handling and greater purity of the fibres since people within the asbestos industry purport that MM following chrysotile exposure is due to amphibole contamination. Chrysotile fibres are thought to be 2-4 times less potent than amphibole fibres in causing MM but are equally as potent in causing lung cancer(Landrigan *et al.* 1999). Chrysotile fibres also cause asbestosis, an untreatable form of pulmonary fibrosis.

There are geographical areas that have high environmental levels of airborne fibres. In south central Turkey, erionite (an amphibole related fibre) is a naturally occurring air-borne fibre and in this region there is endemic MM and lung cancer (Baris *et al.* 1996). Erionite is a component of the stone used to build houses in this region and in the villages of Karain and Tuzkoy half the villagers are purported to die from mesothelioma (Emri *et al.* 2002). This has recently been linked to a genetic susceptibility within these communities(Carbone *et al.* 2002;Roushdy-Hammady *et al.* 2001).

1.2.4 The history of asbestos and Malignant Mesothelioma

Asbestos had been suspected of causing MM and lung cancer long before the epidemiological proof was established, yet unfortunately its use continued in large quantities in Western countries until only recently and its use in many developing countries is expanding – see section 1.2.3. The heat resistant property of asbestos was recognised in ancient times – everlasting lamp wicks used at the temples of the vestal

virgins were made from asbestos. Its dangers were also suspected, the 1st Century AD Roman historian, Pliney the Elder, advised his friends not to buy slaves from asbestos mines "because so many of them die young".

In the UK, in 1929, a Leeds Coroner called for a public enquiry following the death of an employee of Turner and Newell, which was the UK's biggest producer of asbestos. In 1930 Merewether and Price reported to Parliament concluding that the development of "asbestosis" was irrefutably linked to the prolonged inhalation of asbestos dust(Greenberg 1994). Following this, in 1931, regulations to limit the amount of dust exposure allowed were introduced. In 1955, Richard Doll published evidence that asbestos caused lung cancer(Doll 1955) and in 1960 Wagner *et al.*, produced evidence linking asbestos to the then rare tumour Mesothelioma(Wagner *et al.* 1960). In 1970 the 1969 Asbestos Regulations (replacing the 1931 regulations) were instituted. In 1985, The Asbestos Prohibition Regulations were introduced to prohibit the import, supply and use of many asbestos products and applications (allowing only some chrysotile products). By now epidemiological studies by Craighead and Mossman (Craighead and Mossman 1982) had demonstrated conclusively that asbestos caused the majority of MM cases by showing the direct relationship between exposure to fibres and tumour development. In 1988, The Control of Asbestos at work Regulations (1987) was introduced to further limit use of chrysotile asbestos. Regulations were further tightened and revised during the 1990s until a final total European Union ban was passed in 1999, and was implemented in the UK that year. The ban is to have pan-European effect from January 2005. In 1964, at the New York Academy of Sciences, much of the evidence showing the harmful effects of asbestos was gathered together, but a total ban on asbestos in America was not passed through Congress until 2003 (Greenberg 2003).

The "magical properties" of asbestos lead to its widespread use with large numbers of mainly men being exposed to inhalation of fibres. Not only people working in asbestos mines and those who worked at and/or lived near asbestos processing plants have been exposed but anyone working in the building trade up until the 1980s is likely to have been exposed to asbestos due to its almost universal use(Burdorf *et al.* 2003;Koskinen *et al.* 2002;Wang *et al.* 1999). Dockyard workers were at particularly high risk, mainly because of the use of amphibole asbestos for insulation in naval ships. The exposure was particularly high in laggers, boilermakers, painters, welders and burners, and shipwrights (Sheers and Coles 1980). In Australia,

Yeung et al., examined the distribution of MM in different occupational groups from 1979 – 1995. The building industry had the largest number of MM victims, followed by ship building and repair, asbestos cement production, crocidolite mining and milling, rail locomotive construction and repair, coal-fired power stations, and other engineering operations. Occupations with high rates were plumbers, carpenters, machinists and car mechanics(Yeung *et al.* 1999;Yeung and Rogers 2001). Electricians also had high exposure to asbestos, as it was used as lagging to insulate cables, leading to a high incidence of MM in this group(Robinson *et al.* 1999). Exposure by car mechanics to asbestos from asbestos lined brake cables has recently been questioned as a risk factor for MM and recent studies suggest that this is not a high risk factor(Goodman *et al.* 2004;Hessel *et al.* 2004;Laden *et al.* 2004).

A famous victim of Mesothelioma was the actor Steve McQueen, who died aged 50. His asbestos exposure was said to be due to him breathing through asbestos containing fire protective clothing worn as a racing driver, but he had had multiple exposures in the many jobs he'd undertaken before his acting success, including work on construction sites and in ships. When in the marines, while in the brig, he had had to clean an engine room, which involved cleaning pipes coated with asbestos that were ripped down producing a very dusty atmosphere (Penina Spiegel: McQueen The untold story of a bad boy in Hollywood).

1.2.5 The tumorigenesis of asbestos fibres

Amphibole fibres can remain unchanged for decades, whereas chrysotile fibres can undergo fragmentation by organic acids leading to progressive clearance (Churg and DePaoli 1988). This may partly explain why amphibole fibres have the highest mutagenic potential. Stanton *et al,* (Stanton *et al.* 1977), demonstrated that the risk of mesothelioma is related to the concentration of long amphibole fibres (>8μm) (Stanton *et al.* 1981). The tumorigenic potential of an asbestos fibre is partly dependent upon its physical properties, with longer, thicker fibres having a greater effect (Barrett *et al.* 1989;Lippmann 1988;Stanton *et al.* 1977;Stanton *et al.* 1981). There is a dose response with carcinogenesis directly related to the intensity of exposure, which is true of both serpentine and amphibole fibres(Davis *et al.* 1978;Iwatsubo *et al.* 1998;Prehn 1975;Suzuki and Kohyama 1984). Interestingly, fibres greater than 10μm in length and thicker than 0.15μm in diameter are more

closely associated with lung cancer (Barrett *et al.* 1989;Lippmann 1988). This may be partly due to where the fibres become lodged within the respiratory system, as these longer fibres may not be able to reach the pleura, although the route by which asbestos fibres reach the pleura is controversial - a direct path through the lung parenchyma or a circuitous route via the lymphatics?(Bignon *et al.* 1979;Boutin *et al.* 1996;Gibbs *et al.* 1991;Sebastien *et al.* 1980)

Mesothelial cells seem to be particularly susceptible to the mutating effect of the fibres. Boutin *et al.*, 1996 (Boutin *et al.* 1996) showed that following inhalation, asbestos fibres gather near the mesothelial cell layer in "black spots", seen at thoracoscopy and predominantly distributed in the lower costal and diaphragmatic zones. These appear to be the sites of particle collection on the mesothelial surface and are related to sites of lymphatic drainage from the mesothelium and blood vessels(Muller *et al.* 2002) (Mitchev *et al.* 2002). The exact mechanism of fibre tumorigenesis is unclear, but they are known to produce chronic inflammatory responses leading to the stimulation of oxidant pathways(Manning *et al.* 2002a). These produce oxygen and nitrogen species that lead to cell proliferation and apoptosis(Kinnula 1999) Oxidative stress and the free radicals produced are also associated with malignant transformation (Barrett 1994;Gulumian 1999). The ever present asbestos fibres initiate and perpetuate inflammatory cytokine release and proliferative responses that can activate signalling pathway proteins such as epidermal growth factor (EGF) and mesothelial cell EGF receptor expression(Pache *et al.* 1998). This results in the stimulation of the mitogen activating protein kinase (MAPK) cascade through extracellular signal-related kinase (ERK1) activity(Zanella *et al.* 1999), which can result in changing the expression of ECM components such as matrix metalloproteinases (MMPs)(Davidson *et al.* 2003;Tanimura *et al.* 2003).

A common feature of MM cells, presumably transformed from mesothelial cells, is the loss of the tumour suppressor gene $p16^{INK4a}$ (Cheng *et al.* 1994;Hirao *et al.* 2002;Kratzke *et al.* 1995;Lechner *et al.* 1997;Papp *et al.* 2001). $p16^{INK4a}$ is a member of a family of inhibitors specific for cyclin-dependent kinases (CDKs), which play essential roles in the cell cycle by mediating the phosphorylation of the retinoblastoma susceptible gene (Rb). Phosphorylation of Rb inactivates its growth-suppressive properties at the centre of the cell cycle, as shown schematically in figure 1.2. $p16^{INK4a}$ is also required for p53-independent G1 arrest in response to DNA-damaging agents(Shapiro *et al.* 2000).

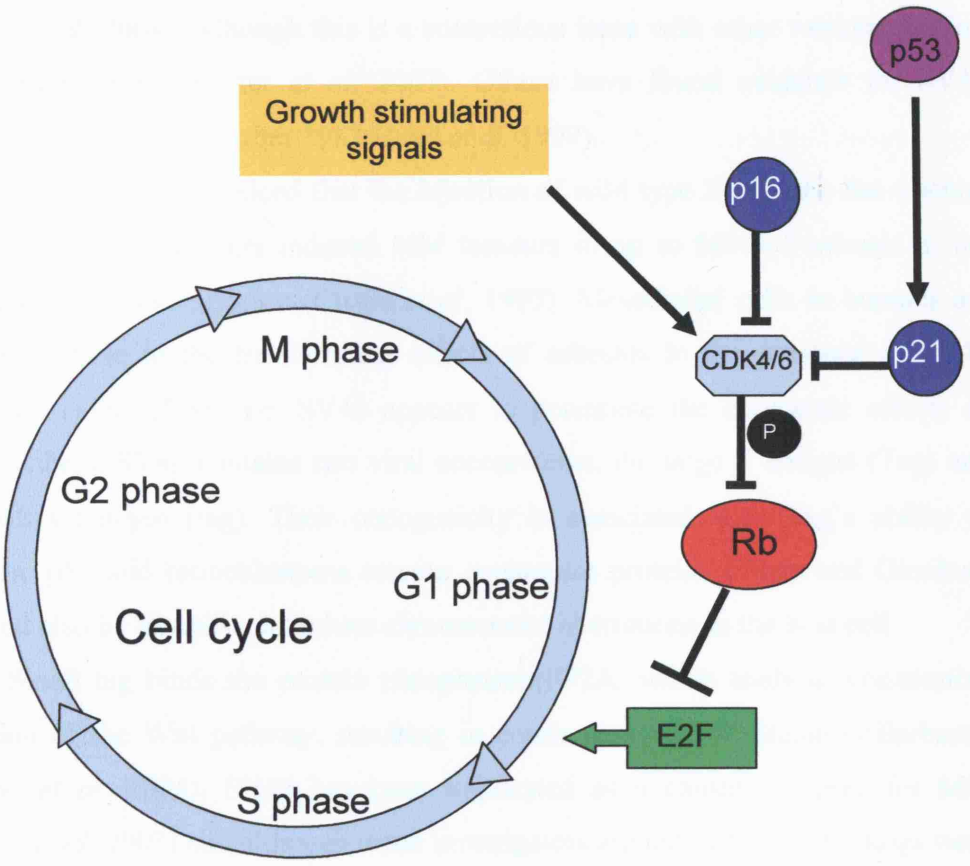

Figure 1.2 The cell cycle. Rb is phosphorylated by cyclin D dependent kinases (CDKs) resulting in its inactivation. This releases Rb-bound E2F, triggering the expression of key cell cycling enzymes including dihydrofolate reductase, thymidine kinase and thymidine synthetase. These allow the cell cycle to move from G1 (gap phase) into the S phase (DNA synthesis). The inhibitory activity of the cyclin dependent kinase inhibitor p16 and the action of p53 are shown. P53 activates p21, which inhibits CDK4 and CDK6, as does p16, hence preventing the phosphorylation of Rb and allowing it to bind E2F, rendering it inactive. Further cyclins and cyclin-dependent kinases act at different points around the cell cycle, but are not shown for simplicity.

1.2.6 A role for SV40 in malignant transformation of mesothelial cells

Oncogenes may also be important in the transformation of mesothelial cells and there has been great controversy over the role of Simian virus 40 (SV40) in the pathogenesis of MM. SV40 is a monkey virus that may have been introduced into the human population by contaminated poliovaccines, produced in SV40-infected monkey cells, between 1955 and 1963(Dang-Tan *et al.* 2004). More recent epidemiological evidence suggests that SV40 may be contagiously transmitted by

person to person regardless of previous SV40 contaminated vaccination (Barbanti-Brodano *et al.* 2004), although this is a contentious issue with other workers finding no evidence for this(Carter *et al.* 2003). Others have found evidence for SV40 infection in children born after 1982(Butel *et al.* 1999).

In 1993, it was noticed that the injection of wild type SV40 into the visceral cavities of Syrian hamsters induced MM tumours in up to 50% of animals in the absence of asbestos exposure (Cicala *et al.* 1993). Mesothelial cells in humans are more susceptible to the transforming effects of asbestos in the presence of SV40 (Bocchetta *et al.* 2000), i.e. SV40 appears to potentiate the oncogenic effects of asbestos fibres. SV40 contains two viral oncoproteins, the large T antigen (Tag) and the small t antigen (tag). Their oncogenicity is associated with Tag's ability to inactivate p53 and retinoblastoma tumour suppressor proteins (Testa and Giordano 2001)and also by its ability to induce chromosomal aberrations in the host cell.

Small tag binds the protein phosphatase PP2A, which leads to constitutive activation of the Wnt pathway, resulting in continuous cell proliferation(Barbanti-Brodano *et al.* 2004). SV40 has been implicated as a causative agent for MM (Cerrano *et al.* 2003) and although some investigators argued that these findings were due to laboratory contamination (PCR products) the most recent analyses show that SV40 is probably a co-mutagen with asbestos fibres in MM (Carbone *et al.* 2003). SV40 is not found in all tumour samples and there seems to be geographical variation, for instance, De Rienzo et al., found SV40 in 4 out of 11 MM samples from patients in the United States but none out of 9 Turkish samples(De Rienzo *et al.* 2002). A study of 17 MM tissue samples in the UK showed no evidence for the role of SV40 in the tumour aetiology(Mulatero *et al.* 1999).

1.3 Clinical features and natural history of Malignant Mesothelioma

1.3.1 Histopathology of MM

There are four main histological categories of MM: epithelial (~50% of cases), sarcomatous (~15%), biphasic or mixed (~25%) and poorly differentiated (~10%). The sub-type distribution is fairly consistent around the world. A study of 1,517 cases of MM in the New York area showed that epithelial cell type was predominant (61.1%), followed by biphasic (22.1%) and fibrosarcomatous (16.4%) (Suzuki 2001).

The histological diagnosis of MM is often difficult to reach and pathology panels are often necessary to reach a consensus – although even these only agree in up to 75% of cases(McCaughey *et al.* 1991). More recent investigations show that immunohistochemistry is helpful in distinguishing between MM and adenocarcinoma of the lung, for instance E-cadherin is much more common in adenocarcinoma than MM (Ordonez 2003). However, there is no histochemical technique available that gives 100% reliability in diagnosing MM.

1.3.2 Clinical presentation

Due to the aetiology and time-lag following exposure to asbestos and tumour development (30-40+ years), most cases present in late adulthood with men accounting for 70-80% of cases(Pelucchi *et al.* 2004). Presentation is usually with either chest pain or shortness of breath usually related to the formation of a pleural effusion, which is often the only clinical sign. Tumours appear to originate in the parietal pleura following the malignant transformation of mesothelial cells(Adams *et al.* 1986;Nishimura and Broaddus 1998). The tumour spreads around and encases the lung, invaginating along fissures as shown in the post mortem lung section in figure 1.3. It can spread directly into the chest wall and infiltrate the other structures of the thoracic cavity. It often tracks along planes of tissue and along biopsy tracts(Bydder *et al.* 2004)and at autopsy approximately one third of MMs have invaded the peritoneum(Suzuki 2001).

The disease is very rarely picked up early and it is unclear whether early diagnosis effects the long-term outcome. Screening radiologically for MM has not been useful but recent investigations of soluble mesothelin-related proteins measured in the serum has shown some promise for the detection of early MM(Robinson *et al.* 2003).

Figure 1.3. Section of lung from a victim of MM. The deposition of collagen results in gross thickening of the pleura with a large mass of collagen at the lung base in this example. The tumour can also be seen invaginating the oblique fissure between the upper and lower lobes.

1.3.3 Survival and treatment

The median survival time is from 10 – 14 months, with a 2 year survival of 20%(Edwards *et al.* 2000;Law *et al.* 1984;Ruffie *et al.* 1989). Those surviving for longer have certain good prognostic factors including epithelioid histology, good performance status, early disease stage, absence of pain at presentation and age less than 55(Baas 2003). As the disease progresses, dyspnoea, weight loss, anorexia and malaise become prominent features. Patients generally die from respiratory failure or pneumonia. Some deaths are due to pericardial or myocardial involvement or small bowel obstruction after intra-abdominal disease extension.

There has been no conclusive evidence that surgery is of any benefit for the treatment of MM, despite reports of good outcomes in highly selected patients with good prognostic features (Sugarbaker *et al.* 2004;Zellos and Sugarbaker 2002). These studies did not have a control arm and the natural history of patients in this better

prognostic group is not clear. A South African study comparing pleurectomy with extrapleural pneumonectomy showed that patients surviving the longest had early tumour stages, epithelial histology and absence of pain or weight loss pre-operatively. There was a trend toward improved survival in the extrapleural pneumonectomy treated group who also received adjuvant radiotherapy (de Vries and Long 2003). However, the published surgical studies are generally either retrospective or without control arms and so can only be interpreted cautiously.

Chemotherapy has marginal effects with the best results still only producing partial responses in ~20% of patients (Middleton *et al.* 1998;Steele *et al.* 2000). Recent studies with Pametrexed, a novel multitargeted antifolate that inhibits at least three enzymes in folate metabolism and purine and pyrimidine synthesis(Adjei 2003), have shown promise. In a phase III trial of 456 patients a response rate of 41% was achieved with pametrexed and cisplatin compared with 16.7% with cisplatin alone. This however, actually represents an improvement in median survival from 9.3 months in the cisplatin group to 12.1 months in the pametrexed and cisplatin combined group(Vogelzang *et al.* 2003). The BTS is currently running a multi-centre trial with three arms comparing active symptom control (ASC), MVP (mitomycin, vinblastine, cisplatin) and ASC, and vinorelbine and ASC. These chemotherapy regimens were selected as their effectiveness in terms of palliation have been fully reported previously and the study aims to examine effective palliation as well as any survival benefit(Muers *et al.* 2004;Vogelzang *et al.* 2003).

The role of radiotherapy appears to be limited to control of pain, particularly chest wall masses, and the prophylactic treatment of biopsy sites to prevent seeding of the tumour along needle or drain tracks (Senan 2003). The effects of local radiotherapy for pain control are often only relatively short-lived. The mainstay of treatment is the palliation of symptoms and even with this, pain control can be very difficult as the disease progresses.

1.3.4 Experimental treatment of Malignant Mesothelioma

There are a number of experimental approaches under investigation. Some use intrapleural techniques such as photodynamic light therapy, while others use knowledge gained from examining tumour biology to select potential therapeutic targets. Intrapleural induced hyperthermia using simple perfusing fluids or perfusions

of chemotherapeutic drugs, such as cisplatin and doxorubicin, at around 41°C have been used mainly in conjunction with cytoreductive surgery (Deraco *et al.* 2003;Monneuse *et al.* 2003;van Ruth *et al.* 2003). The theory being that this will have local cytotoxic effects to residual tumour cells without systemic side effects. The results have been mixed – some resulting in significant morbidity without much benefit, while others were better tolerated with good results in early stage disease, but again without controls the results can only be assessed cautiously. Other studies have used combinations of therapy such as debulking surgery followed by continuous hyperthermic peritoneal perfusion with cisplatin, and a single postoperative intraperitoneal treatment with fluorouracil and paclitaxel(Feldman *et al.* 2003). The results of this appeared good but depended upon good prognostic factors such as a lack of invasive growth and minimal residual tumour.

Another intrathoracic technique is photodynamic therapy. This involves the systemic administration of a photosensitising agent activated at a light wavelength specific to the absorption characteristics of the sensitizer in the presence of oxygen. Early stage III studies with first generation photosensitising agents showed that this technique could be employed in MM following cytoreductive surgery, but there was no prolongation of survival(Pass *et al.* 1997). More recent sensitising agents have shown more promise. In a porcine model of MM, xenografts were selectively destroyed without damaging thoracic organs(Krueger *et al.* 2003). It is hypothesised that there is differential uptake of the agent by tumour cells, but a recent study suggests that the effects are mediated by vascular damage in both normal and tumour tissue(Cramers *et al.* 2003). A more recent phase I trial of Foscan-mediated photodynamic therapy showed better toxicity profiles and appears to warrant a phase II trial(Friedberg *et al.* 2003).

Other approaches have attempted to stimulate immune responses to tumours. A multicentre stage II trial of immunotherapy by infusion of autologous activated macrophages and gamma-interferon showed good tolerance but no effect on tumour growth(Monnet *et al.* 2002). The immunomodulatory cytokine Interleukin-12 (IL-12) has shown high levels of anti-tumour effects when administered systemically to a murine model of MM, but the side effects are significant. MM cell gene transfection with IL-12 produced immunity against the tumour cells both locally and at a distant site in the murine model without side-effects(Caminschi *et al.* 1999).

Other work has targeted growth factors and signalling pathways. Many of these approaches work well in vitro, for instance the epidermal growth factor receptor inhibitor (EGFR) ZD1839 inhibited MM cell growth(Janne *et al.* 2002). This inhibitor was also shown to potentiate the radiation response of MM tumours in a murine model(She *et al.* 2003). Suramin, an inhibitor of extracellular growth factors also inhibited tumour growth in a mouse model of MM(Cook *et al.* 2003).

Other studies have attempted to address the apparent apoptotic resistance of MM cells. MM cells over-express the anti-apoptotic protein Bcl-xL. Treatment of human MM cell lines with antisense oligonucleotides to the gene, bcl-xl, resulted in greater apoptosis rates and this was more marked in combination with cisplatin treatment(Ozvaran *et al.* 2004). Inhibition of histone deacetylase using suberohydroxamic acid (SBHA) sensitised MM cells to TRAIL (TNF-related apoptosis-induced ligand) apoptosis and specific down-regulation of anti-apoptotic proteins, particularly Bcl-xL were demonstrated(Neuzil *et al.* 2004). These techniques have not yet progressed beyond the laboratory setting.

The final group of experimental approaches to MM has involved gene therapy. MM remains a good candidate tumour for gene therapy for a number of reasons. These include its localised nature, often in association with a pleural effusion, which allows easier local application of a vector. The pleural fluid in itself could be useful by acting as a reservoir for the gene therapy applied. These techniques have used suicide gene therapy, such as a stage I trial of adenoviral mediated intrapleural herpes simplex virus thymidine kinase/ganciclovir gene therapy(Sterman *et al.* 1998). This showed low toxicity and successful gene transfer, but as with most gene therapy techniques was limited by penetration of the gene therapy into the tumour. As with many of these approaches, gene therapy is most likely to work in combination with debulking surgery. In a murine model, combination gene therapy with interferon-β before surgical debulking improved tumour free long-term survival compared with surgery alone(Kruklitis *et al.* 2004). Other gene therapy approaches have used gene replacement therapy, replacing the deleted $p16^{INK4A}$ gene resulted in prolonged survival in nude mice with human xenograft MM tumours(Frizelle *et al.* 2000).

1.4 The extracellular matrix in cancer

A characteristic feature of MM is its highly fibrous nature with deposition of large quantities of ECM in and around the tumour. Collagen is the major structural protein component of the ECM and appears to be of great importance to MM pathogenesis. The ECM acts as a scaffold that the tumour cells can grow on and through but also has other functions in tumour progression described below.

1.4.1 The ECM in local tumour invasion and metastasis

ECM, predominantly composed of collagen, is deposited in and around MM tumours. The collagen is thought to be derived from both the surrounding stromal cells and from the MM cells themselves and is likely to have an important role in MM tumour growth. There is extensive literature demonstrating the importance of the ECM in the mechanisms that solid tumours use for growth, invasion of local structures and in metastasis.

The balance between tumour local invasion and metastasis appears to be related to its interaction with the surrounding ECM. At the primary tumour site, some malignancies such as melanoma, are surrounded by only minimal stroma (Varani 1987) and local invasion is limited. In others, for example squamous head and neck cancer, large quantities of ECM are produced by direct tumour synthesis and by stimulating ECM production from surrounding stromal cells(Hagedorn *et al.* 2001). These tumours are invasive locally but have much lower metastatic potential. This suggests that expression of collagen may be related to local invasion rather than metastasis, however the type of collagen and composition of the ECM is critical. Terranova et al., (Terranova *et al.* 1982), showed that laminin promotes the attachment of metastatic sarcoma cells to the basement membrane. The same group showed that in metastatic melanoma cells, removal of fibronectin or exposure to laminin lead to an increased tumour cell affinity for basement membrane collagen, resulting in greater cell invasion (Terranova *et al.* 1984). In MM, tumour cells have the ability to synthesise components of the basement membrane and enhanced attachment to ECM would be anticipated as laminin receptors are present in large numbers on the surface of MM cells(Kallianpur *et al.* 1990).

In laryngeal cancer, there is a lower incidence of neck metastases than in other cancers of the head and neck region. However, some show metastases at very early stages and these correlate with the expression of collagen IV. In these tumours, collagen IV in the stroma surrounding tumour cells is a bad prognostic factor (Krecicki *et al.* 2001). In human colorectal cancer, non-metastatic cancer cells induce mainly fibroblast proliferation, whereas metastatic cancer cells mainly induce fibroblast collagen synthesis, suggesting that the production of collagen is more important than fibroblast cell proliferation in the process of metastasis (Basso *et al.* 2001). In these two examples increased production of collagen is pro-metastatic.

Stromal changes at the invasion front include the appearance of myofibroblasts, cells that share characteristics with both fibroblasts and smooth muscle cells. Fibroblasts are the main precursors of myofibroblasts and the transdifferentiation is modulated by cancer cell-derived cytokines, such as TGFβ(Grotendorst *et al.* 2004). Myofibroblasts produce pro-invasive signals, such as N-Cadherin, that are implicated in positive invasion signalling pathways (De Wever and Mareel 2003). In human melanoma, secretion of $TGF\beta_1$ by tumour cells stimulates fibroblasts to deposit ECM within and around the tumour. The high expression of collagen and other matrix proteins correlates with the number and size of metastases (Berking *et al.* 2001). These studies suggest that TGFβ effects on the ECM are important in both local invasion and metastasis.

Loss of contact between cells and the ECM induces apoptosis in non-malignant cells such as fibroblasts. Loss of contact between tumour cells and the ECM does not necessarily result in cell death, as tumour cells upregulate anti-apoptotic proteins such as Bcl 2 and have reduced or absent p53 activity(Jin and Varner 2004;Meredith, Jr. *et al.* 1993).

1.4.2 Integrins and the ECM in malignancy

Interactions between cells and the ECM have been shown to influence gene expression by the cell and that the balance between proteases and their inhibitors greatly influence cell-matrix interactions (Stetler-Stevenson *et al.* 1993). Many of these interactions are now thought to occur via integrins. Integrins are adhesion receptors on the cell surface that interact with their immediate environment and

respond to changes in ECM by integrin-ligand interactions. This enables information to flow into and out of the cell (Newham and Humphries 1996). Integrins are composed of two subunits, α and β, and αβ combinations form to create their own binding and signalling properties(Giancotti and Ruoslahti 1999). Some integrins, such as α5β1 recognise predominantly a single ECM component, in this case fibronectin. Others recognise several ligands, such as αvβ3, which binds vitronectin, fibronectin, fibrinogen and denatured collagen. They differ from growth factor receptors in having no intrinsic enzymatic activity. They activate integrin-regulated signalling pathways by co-clustering with kinases in focal adhesion complexes(Jin and Varner 2004).

The ECM plays an essential role in coordinating the signalling processes involved in the growth, tissue invasion and metastasis of tumours and the effects of the ECM are primarily mediated by integrins(Jin and Varner 2004). Integrin signalling regulates the activity of cytoplasmic kinases and growth factor receptors and controls the intracellular actin cytoskeleton(Giancotti and Ruoslahti 1999). Integrin activation initiates cell signalling pathways such as the MAPK cascade leading to the activation of transcription factors that regulate the expression of genes critical for ECM degradation or cell migration, such as the matrix metalloproteinases (MMPs) (see section 1.4.4) (Crowe and Shuler 1999). Specific integrin expression enhances malignant progression in some cancers, such as colon carcinoma, where a higher expression of α5β1 is found in invasive cell lines compared with poorly invasive lines. The invasive cell lines demonstrate greater cell adhesion to the ECM protein fibronectin (Gong *et al.* 1997). Adherence of tumour cells to the ECM, degradation of matrix components by MMPs and movement of the cell bodies are all essential processes that require the tumour cells to interact with ECM via integrins.

1.4.3 Protection of tumour cells against chemotherapy by ECM

The formation of ECM and stroma around tumour cells may be a reason for the lack of response of some solid tumours to anticancer drugs. Sethi *et al.*(Sethi *et al.* 1999), demonstrated that in small cell lung cancer the presence of tumour cell interactions with the ECM, specifically through β1 integrins, made the cells resistant to chemotherapeutic agents. If this finding applies to other tumours then the resistance of highly fibrotic MM tumours to conventional therapy becomes more understandable. In other work, cells grown on collagen coated Teflon membranes had

slower penetration by anticancer drugs (cisplatin, etoposide, gemcitobine, paclitaxel, vinblastine) than cells grown on Teflon alone (Tannock *et al.* 2002). In human gastric cancer the amount of stromal collagen was found to be a significant predictor of disease relapse and this was associated with reduced CD8+ T-cell infiltration. This is because CD8 cells induce tumour cell apoptosis in gastric carcinoma patients (Ohno *et al.* 2002).

1.4.4 Matrix metalloproteinase (MMP) interactions with the ECM in tumour progression and metastasis

There are currently 23 MMP genes identified in humans and many are implicated in cancer (Itoh and Nagase 2002). They have essential functions in tumour cell migration and invasion through their effects on the ECM. Before tumour cells can invade local structures or metastasise to other organs they must locally degrade ECM components that would otherwise act as a physical barrier. To do this they have enhanced production of MMPs, with MMP2 and MMP9 (also known as gelatinases A and B) and collagenase-1 (MMP-1), which has its predominant effect on collagen, being the most common MMPs present in lung diseases(Atkinson and Senior 2003;Beeh *et al.* 2003;Cataldo *et al.* 2001;Ohbayashi 2002)including MM, which has increased expression of MMP2 and MMP9(Edwards *et al.* 2003;Giancotti and Ruoslahti 1999;Liu *et al.* 2001). MMPs degrade different ECM components including basement membrane collagen, interstitial collagen, and proteoglycans - active in normal tissue remodelling and repair. Their proteolytic activity is normally regulated by specific tissue inhibitors of MMP (TIMPs). Over-activity of MMPs without up-regulation of TIMP activity is a common feature of many tumours, although the interaction between MMPs and TIMPs is complex(Khasigov *et al.* 2003). The action of MMPs is essential to cancer cell migration, which occurs in two ways: single cell locomotion and cohort migration (cell movement en mass keeping cell-cell contact). MMPs are essential for this migration, through remodelling of the ECM, and are found localised at leading edges in both types of cell migration (Nabeshima *et al.* 2002;Ohbayashi 2002). MMPs have other important functions in the malignant process, such as the activation of TGFβ - see section 1.6.2.

1.4.5 Malignant Mesothelioma and the ECM

There has only been a limited amount of research into the relationship between MM and the ECM despite the high levels of ECM protein deposition around many of these tumours. MM cells have the ability to synthesise components of the ECM and have a high expression of laminin receptors that bind to the ECM(Kallianpur *et al.* 1990). If grown on collagen I *in vitro*, MM cells show increased cell separation and invasiveness compared with cells grown on an intact basement membrane, which appears to inhibit cell invasion(Ehlers *et al.* 2002). The three different histological types of MM described in section 1.3.1 all express ECM to varying degrees. Scarpa *et al.*, examined expression of 3 ECM components: laminin, fibronectin and collagen IV. Epithelial MM cells have the highest expression of laminin and collagen IV, biphasic MM cells express the highest level of fibronectin and fibroid (sarcomatous) MM cells weakly express fibronectin, laminin and collagen IV. The Biphasic cells have the highest chemotactic and haptotactic motility, but fibroid MM cells migrate towards the lowest concentration of laminin. Epithelioid MM cells have the lowest chemotactic and haptotactic motility for each of the ECM components (laminin, fibronectin and collagen IV)(Scarpa *et al.* 1999). There are high levels of the interstitial collagens I and III expressed in MM tumours, which also synthesise hyaluronan(Liu *et al.* 2004), a major constituent of the ECM. CD44 receptors, an adhesive protein receptor which binds hyaluronan, are also expressed by MM cells and those with the highest amount of CD44 receptor show an increase in proliferation and haptotactic migration, demonstrating that the interaction between an adhesive protein receptor and the ECM plays a role in local tumour extension(Nasreen *et al.* 2002). Another component of the ECM, the glycoprotein Tenascin-C, is found in all histological types of MM and appears to be associated with a worse prognosis. It has anti-adhesive properties and is particularly high in the fibrotic stroma of tumours and around the tumour border, but mRNA levels are not particularly high within MM tumour cells(Kaarteenaho-Wiik *et al.* 2003). Tenascin-C synthesis is stimulated by TGFβ, which is also produced by MM tumours, and may be stimulating Tenascin-C production from stromal tissue.

1.5 Growth factors in Malignant Mesothelioma

MM cells, like many cancer cells, produce a large number of growth factors. Those reported in the literature include transforming growth factor beta (TGFβ)(Garlepp and Leong 1995;Kuwahara *et al.* 2001;Maeda *et al.* 1994), platelet derived growth factor (PDGF)(Gerwin *et al.* 1987), insulin-like growth factor (IGF) I and II(Lee *et al.* 1993), vascular endothelial growth factor (VEGF)(Konig *et al.* 1999), basic-fibroblast growth factor (bFGF)(Strizzi *et al.* 2001b) and granulocyte-colony stimulating factor (GCSF)(Kasuga *et al.* 2001). Most of these are thought to have both paracrine and autocrine functions in regulating tumour growth.

1.5.1 TGFβ in MM

TGFβ is found at high levels in MM associated pleural effusions in man (Maeda *et al.* 1994), and *in vitro* MM cell lines have been shown to produce 30-70 times more TGFβ than non-malignant mesothelial cells (Kuwahara *et al.* 2001). Immunolocalisation of TGFβ in human MM tissue sections shows there are high levels of $TGF\beta_2$ expression in the tumour cells and of $TGF\beta_1$ in the surrounding stroma(Jagirdar *et al.* 1997). TGFβ inhibits the differentiation of naïve CD4+ T cells toward Th-1 phenotype following presentation of purified protein derivatives to MM cells i.e. inhibits the immune response(Valle *et al.* 2003). Finally, inhibition of $TGF\beta_2$ responses, using antisense oligonucleotides, in MM cells and in a murine model of MM resulted in decreased cell and tumour growth(Fitzpatrick *et al.* 1994;Marzo *et al.* 1997). TGFβ is discussed at length section 1.6.

1.5.2 Platelet derived growth factor in MM

PDGF is expressed at much higher levels by MM cells than mesothelial cells (Gerwin *et al.* 1987). It appears to be predominantly the PDGF BB isoform that is important in MM cells, which remains at very low levels in normal mesothelial cells. This is true for the expression of both the growth factor and its receptor. The PDGF AA isoform remains relatively high in normal mesothelial cells but low in malignant lines suggesting autocrine roles of one isoform in malignancy and the other in normal

cells (Versnel *et al.* 1991). The function of PDGF in MM is unclear but it has been shown to be mitogenic and a chemoattractant for MM cells. The motile response of the MM cells in response to PDGF is dependent upon α3β1 integrins and their interaction with the matrix proteins fibronectin, laminin, and collagen type IV as adhesive substrates along which the cells can move. On a non-matrix adhesive substrate, poly-L-lysine, there is no cell migration, again highlighting the importance of the ECM (Klominek *et al.* 1998).

1.5.3 Insulin-like growth factors in MM

IGF-I and II are polypeptides that have effects upon cellular proliferation and differentiation. IGF-I and its receptor are also present on both normal mesothelial cells and MM cells and these cells proliferate in response to exogenous IGF-I (Lee *et al.* 1993). In a hamster mesothelioma model (SV40-induced), cells were electroporated with an inducible expression vector containing antisense cDNA to a fragment of the IGF-I receptor. This had an inhibitory effect on growth and tumorigenicity of the MM cells and reduced proliferation *in vitro* (Pass *et al.* 1998).

1.5.4 Vascular endothelial growth factor in MM

VEGF has an important role in angiogenesis as a regulator of endothelial cell proliferation both in normal and malignant tissue growth processes. Analysis of human MM tissue by immunohistochemistry and *in situ* hybridisation demonstrated increased VEGF associated with increased microvessel density (i.e. angiogenesis) (Konig *et al.* 1999). VEGF may also act by stimulating tumour growth directly through a mechanism involving activation of tyrosine kinase receptors (Strizzi *et al.* 2001a). Targeting of VEGF and a closely related protein VEGF-C simultaneously using antisense oligonucleotide complementary to VEGF inhibited MM cell growth *in vitro.* This result was confirmed using antibodies to the VEGF receptor and the VEGF-C receptor and by using a diphtheria toxin-VEGF fusion protein, which is toxic to cells that express VEGF receptors (Masood *et al.* 2003).

1.5.5 Basic fibroblast growth factor in MM

Basic FGF (bFGF) is another potent angiogenic factor that promotes *in vitro* endothelial cell growth and *in vivo* vessel formation. High levels of b-FGF in MM correlate with poor patient survival, but the mechanism is unclear and does not appear to be related to its angiogenic effects (Strizzi *et al.* 2001b). The mechanism may be due to effects upon the ECM, as b-FGF produced by MM cells stimulates hyaluranon and proteoglycan synthesis from fibroblasts and normal mesothelial cells (Asplund *et al.* 1993).

1.5.6 Granulocyte colony stimulating factor in MM

G-CSF has also been shown to be produced by human MM cell lines, although its production by MM cells appears to be extremely rare *in vivo* with only three reported cases. When G-CSF is produced patients usually suffer haematological complications such as elevated neutrophil levels (Kasuga *et al.* 2001)or chronic myelogenous leukaemia (Masuda *et al.* 1995).

1.6 The role of transforming growth factor β (TGFβ) in malignancy

1.6.1 TGFβ function and signalling

TGFβ is a secreted cytokine that is a member of a large group of multifunctional proteins including TGFβs ($TGF\beta_1$, $TGF\beta_2$ and $TGF\beta_3$), bone morphogenic proteins (BMPs), activins and inhibins. These proteins have diverse roles in development and tissue homeostasis regulating growth, differentiation, migration, adhesion, apoptosis and morphogenesis. Most members of this cytokine family, including TGFβ, are disulfide-bonded dimeric molecules. They bind to two different types of membrane receptors, which form hetero-tetrameric complexes, to activate an intracellular signalling pathway involving Smad proteins (see section 1.6.5)(Kretzschmar *et al.* 1999;Moustakas *et al.* 2002;Roberts and Sporn 1993).

The TGFβ sub-family ($TGF\beta_1$, $TGF\beta_2$ and $TGF\beta_3$) has multiple functions in growth and development, inflammation and repair, host immunity and is a potent

stimulator for the production of collagen and other matrix components(Clark and Coker 1998). It is of particular interest in cancer as it appears to have a dual role - initially acting as a tumour suppressor (see section 1.6.8), but later as a tumour enhancer (see sections 1.6.9 – 1.6.11)(Derynck *et al.* 2001). Many tumours, including MM, appear to escape from the tumour suppressor effects of TGFβ, and furthermore, produce TGFβ in significant quantities(Kuwahara *et al.* 2001;Maeda *et al.* 1994).

The various roles of specific TGFβ isoforms are uncertain in malignancy but there is some evidence to suggest differing effects. In breast cancer, Tamoxifen therapy leads to an up-regulation of $TGF\beta_2$ but has no effect on $TGF\beta_1$, suggesting that in this cancer $TGF\beta_2$ is protective (Brandt *et al.* 2003). In ovarian cancer there is up-regulation of all three isoforms but their differing functions are unclear(Nilsson and Skinner 2002). Chondrosarcoma cells grown *in vitro*, show a two-fold increase in DNA synthesis in response to all three isoforms in serum-fed confluent cell conditions. In serum-free confluent conditions, only $TGF\beta_1$ stimulates proliferation, $TGF\beta_2$ has no effect and $TGF\beta_3$ is inhibitory(Boumediene *et al.* 2001). However, in Giant cell tumours of the bone there appears to be an absence of $TG\beta_1$ expression but an increase of $TGF\beta_3$, although its affects are unclear(Franchi *et al.* 2001). Conversely, in colon cancer, $TGF\beta_1$ and $TGF\beta_2$ are up-regulated to a much greater extent than $TGF\beta_3$(Bellone *et al.* 2001). In the progression of keratinocyte skin cancer HaCaT-ras clones of increasingly aggressive nature show that $TGF\beta_1$ appears to be associated with a more differentiated state, $TGF\beta_2$ with a highly malignant and invasive cells and $TGF\beta_3$ with tumour stroma formation and angiogenesis(Gold *et al.* 2000).

The role of the different TGFβ isoforms is far from clear and all appear to have the potential for pro-tumorigenic effects, although this varies with the type of cancer examined.

1.6.2 TGFβ synthesis and activation in MM

$TGF\beta_1$, $TGF\beta_2$ and $TGF\beta_3$ are synthesised as a homodimeric proprotein (proTGFβ), which has a mass of 75 kDa. Dimeric propeptides called latency associated proteins (LAPs) are the N-terminal sequence of proTGFβ and are cleaved

from the active TGFβ dimer in the trans Golgi. Hydrophobic interactions, further strengthened by an intersubunit disulfide bridge stabilises the active TGFβ dimer(Shi and Massague 2003). Disulfide links are formed between cysteine residues of LAP and cysteine residues in the latent-TGFβ-binding protein (LTBP). LTBP is a member of the LTBP/fibrillin protein family(Kanzaki *et al.* 1990;Ramirez and Pereira 1999), which contain multiple epidermal growth factor–like repeats and a unique domain containing cysteine residues(Kanzaki *et al.* 1990). In this large latent complex (LLC), comprising TGFβ, LAP and LTBP, TGFβ cannot bind to its receptors. This complex is shown in figure 1.4.

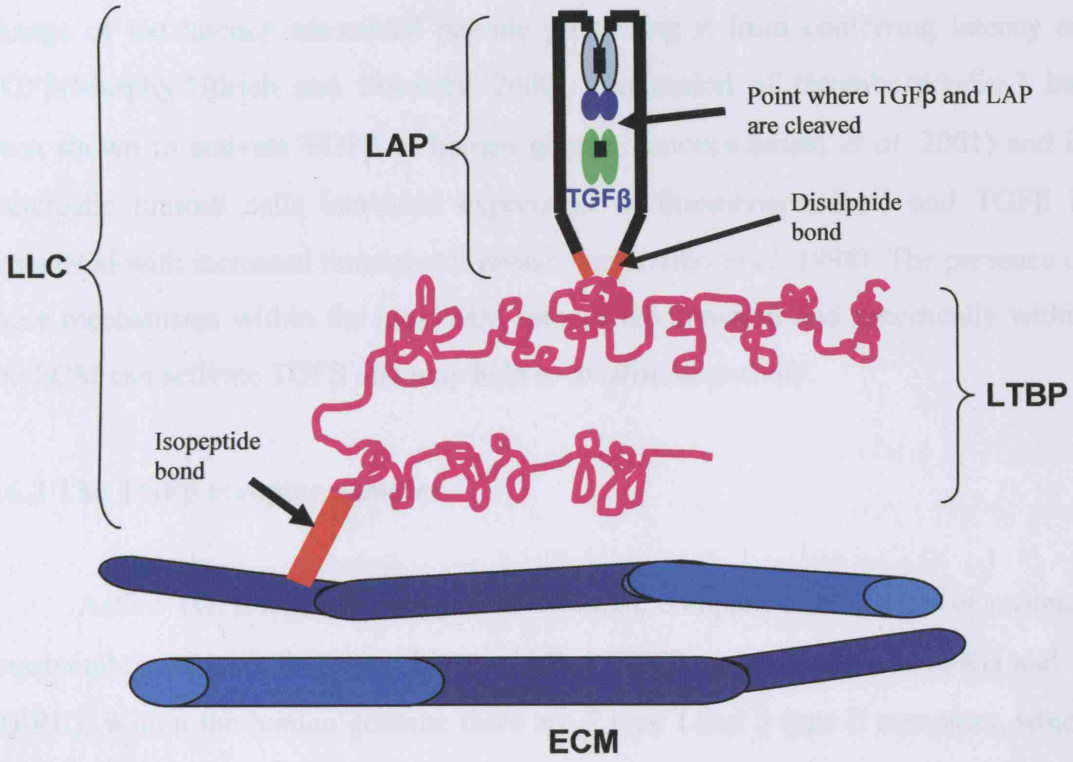

Figure 1.4 The TGFβ large latent complex (**LLC**) comprises the active TGFβ dimer, latency associated proteins (**LAP**), and latent TGFβ binding protein (**LTBP**). TGFβ and LAP are proteolytically cleaved as indicated. TGFβ remains noncovalently associated with LAP, which is bound to LTBP by disulfide bonds. The LLC is covalently linked to the ECM through an isopeptide bond at a region that is protease-sensitive to allow LLC to be released from the ECM. Adapted from Annes et al., 2003(Annes *et al.* 2003).

The LLC is covalently linked to the ECM where it is sequestered. The association with LAP keeps the TGFβ dimer inactive and TGFβ must be released from LAP before it can bind to its receptor. This can therefore provide a large reservoir of secreted TGFβ within the ECM. Activation is thought to be through

proteases that preferentially degrade the pro-segments of the TGFβ complex (LAP) releasing the active stable dimer(Annes *et al.* 2003).

There are a number of proteases associated with malignant cells that can activate TGFβ by degradation of LAP, including MMP-9 and MMP-2 (Yu and Stamenkovic 2000). In MM tumours, both MMP-9 and MMP-2 are produced by the tumour and are able to activate TGFβ. Similarly, plasmin converted from plasminogen at sites of tumour cell migration and invasion can also activate TGFβ (Andreasen *et al.* 1997). Finally, non-protease activating mechanisms such as thrombospondin-1, an ECM protein, may activate TGFβ by causing a conformational change of the latency associated peptide preventing it from conferring latency on TGFβ(Murphy-Ullrich and Poczatek 2000). Expression of thrombospondin-1 has been shown to activate TGFβ in human glioma tumours(Sasaki *et al.* 2001) and in pancreatic tumour cells increased expression of thrombospondin-1 and TGFβ is associated with increased tumour cell invasiveness(Albo *et al.* 1998). The presence of these mechanisms within the local MM tumour environment and specifically within the ECM can activate TGFβ and may help to localise its activity.

1.6.3 The TGFβ receptor complex

Active TGFβ signals through a heteromeric complex of two types of receptor transmembrane serine/threonine kinases called TGFβ receptor type I (TβRI) and II (TβRII). Within the human genome there are 7 type I and 5 type II receptors, which are used by different members of the large TGFβ family(Manning *et al.* 2002b). Type I and type II receptors contain approximately 500 amino acids, with an N-terminal extracellular ligand binding domain, a transmembrane region and an intracellular C-terminal serine/threonine kinase domain(Shi and Massague 2003). The TGFβ sub-family ($TGF\beta_1$, $TGF\beta_2$, $TGF\beta_3$) have only one type II receptor (TβRII), for which active TGFβ has a high affinity. TGFβ doesn't directly interact with the type I receptors (Massague 1998). The binding of the active TGFβ dimer to TβRII induces a conformational change, which exposes the binding epitope of the type I receptor(Hart *et al.* 2002) and since each receptor only binds to one monomer of the active TGFβ dimer, the activated receptor complex comprises four receptor molecules (two TβRII

and two TβRI)(Shi and Massague 2003). Within this complex TβRII kinase phosphorylates the Glycine-Serine (GS) sequence upstream from the TβRI kinase domain. This changes the GS region into a binding surface for receptor Smad proteins (described in section 1.6.4)(Huse *et al.* 2001) and activates the TβRI kinase, which phosphorylates the bound Smad receptor protein. Intracellular signalling then proceeds by activation of the Smad pathway (described in section 1.6.5).

There are a number of type I receptors called activin receptor-like kinase-1 (ALK1), ALK2, ALK3, ALK4, ALK5, ALK6, ALK7. ALK4, 5 and 7 are TGFβ activated type I receptors, ALK5 being the predominant signalling receptor for $TGF\beta_{1\text{-}3}$ activity(DaCosta *et al.* 2004), ALK1 is expressed specifically on endothelial cells and is essential for angiogenesis(Mo *et al.* 2002), but can also bind $TGF\beta_1$ and this appears to have counteracting effects to $TGF\beta_1$/ALK5 activation in endothelial cells during angiogenesis(Goumans *et al.* 2002). ALK2, 3 and 6 are activated by bone morphogenic proteins (see table 1.1 above).

1.6.4 Smad signalling proteins

Smads are a family of intracellular signalling proteins so called after the original Smad family members discovered as the Drosophila signalling protein Mad (mothers against decapentaplegia) and the C.elegens signalling proteins Sma2, 3 and 4 (Graff *et al.* 1996;Liu *et al.* 1996;Savage *et al.* 1996;Sekelsky *et al.* 1995). The Smads are divided into 3 classes dependent upon their function. Types and function of Smad proteins are described in table 1.1. Smad proteins contain 3 regions that are highly conserved between Smad types and between species. The structure of Smad proteins is described in figure 1.5.

Receptor Smads	Co-Smads	Antagonist (or inhibitory) Smads
Smad1, Smad5, Smad8 **Smad2, Smad3** Mad (Drosophila) Sma2, Sma3 (C. elegans)	**Smad4** Mcd (Drosophila) Sma4 (C.elegans)	Smad6, **Smad7** Dad (Drosophila)

Table 1.1 The Smad signalling proteins. The function of receptor Smads, co-Smads and inhibitory Smads are explained in the text. In TGFβ signalling, the receptor Smads are Smad2 and Smad3, the co-Smad is Smad4 (common to all Smad signalling pathways) and the inhibitory Smad is Smad7.

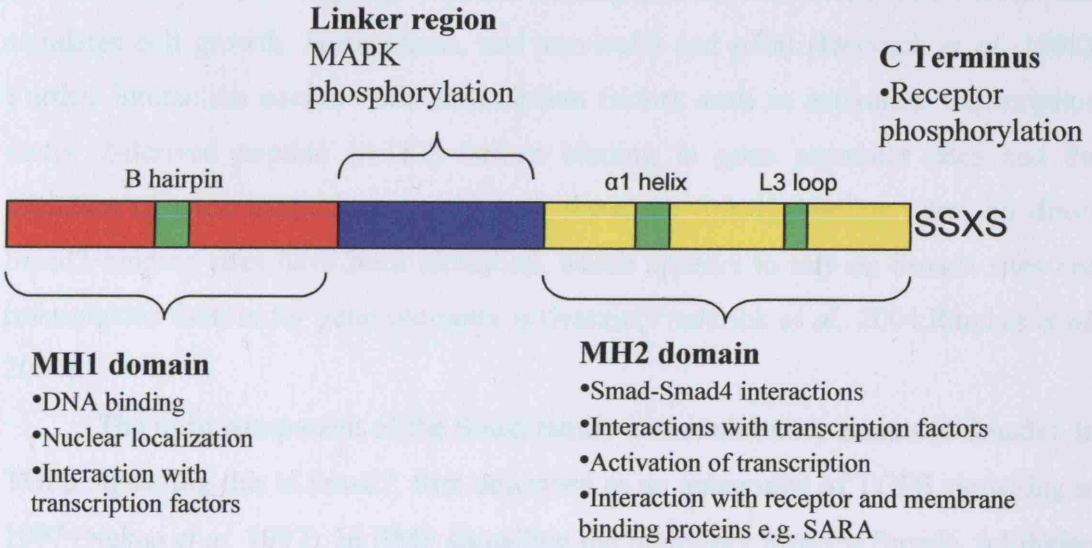

Figure 1.5 Smad proteins. Smad proteins are comprised of 3 regions. Mad homology regions 1 and 2 (MH1 and MH2) are highly conserved at the N and C termini of the protein. There is a non-conserved linker region. Phosphorylation in response to TGFβ occurs at 2 terminal serines in an SSXS motif at the C terminus (Abdollah *et al.* 1997). In the MH2 region the α1 helix and L3 loop determine the specificity of R-Smad-receptor interactions (Chen *et al.* 1998;Chen and Massague 1999).

1.6.5 Smad Signalling

In TGFβ (and activin) signalling there are receptor regulated Smads (R-Smads); Smad2 and Smad3, which are anchored to the cell membrane through membrane bound proteins such as the Smad-anchor for receptor activation (SARA; (Tsukazaki *et al.* 1998)). These R-Smads are activated following phosphorylation at the TβRI serine/threonine kinase site. The second class of Smad protein is the common mediator Smad or co-Smad, Smad4, which neither binds to the receptor site nor is phosphorylated by it, but forms a hetero-oligomeric complex with the activated phosphorylated R-Smads(Heldin *et al.* 1997). The formation of this complex is essential for the passage of the R-Smads across the nuclear membrane and in binding to gene targets. In the nucleus there is further interaction with co-repressors such as c-Ski (Akiyoshi *et al.* 1999) and SnoN oncoprotein (Sun *et al.* 1999) and with co-activators such as the major histone acetyltransferases CBP (CREB-binding protein (CREB; Ca^{2+} /cAMP response element-binding protein, is a transcription factor that regulates cell growth, homeostasis, and survival)) and p300 (Derynck *et al.* 1998). Further interaction occurs with transcription factors such as activating transcription factor 2-derived peptide (ATF2) before binding to gene promoter sites and the initiation of gene transcription. Although there are Smad3 binding sites, no direct Smad2 binding sites have been identified, which appears to rely on Smad4 sites and transcription factors for gene promoter activation(Frederick *et al.* 2004;Randall *et al.* 2004).

The third component of the Smad family is the inhibitory Smads (I-Smads). In TGFβ signalling this is Smad7, first described as an antagonist of TGFβ signalling in 1997 (Nakao *et al.* 1997). In BMP signalling the inhibitory Smad is Smad6, inhibiting the activation of Smad1 and Smad5. Smad7 is released from the nucleus and its transcription is initiated following TGFβ signalling, as the gene promoter site has a Smad3 and Smad4 binding site (von Gersdorff *et al.* 2000). Smad7 crosses the nuclear membrane and binds to TβRI in synergy with another protein, designated STRAP (serine-threonine kinase receptor-associated protein), blocking the phosphorylation site and preventing the activation of the R-Smads. An E3 ubiquitin ligase, Smad ubiquination-related factor 1 (Smurf1), interacts with Smad7 in the nucleus inducing ubiquitination and translocation into the cytoplasm (Ebisawa *et al.* 2001;Suzuki *et al.* 2002). It associates with the TβRI via Smad7 with subsequent enhancement of

turnover of both TβRI and Smad7 by initiating their ubiquination. The signalling sequence is illustrated schematically in figure 1.6.

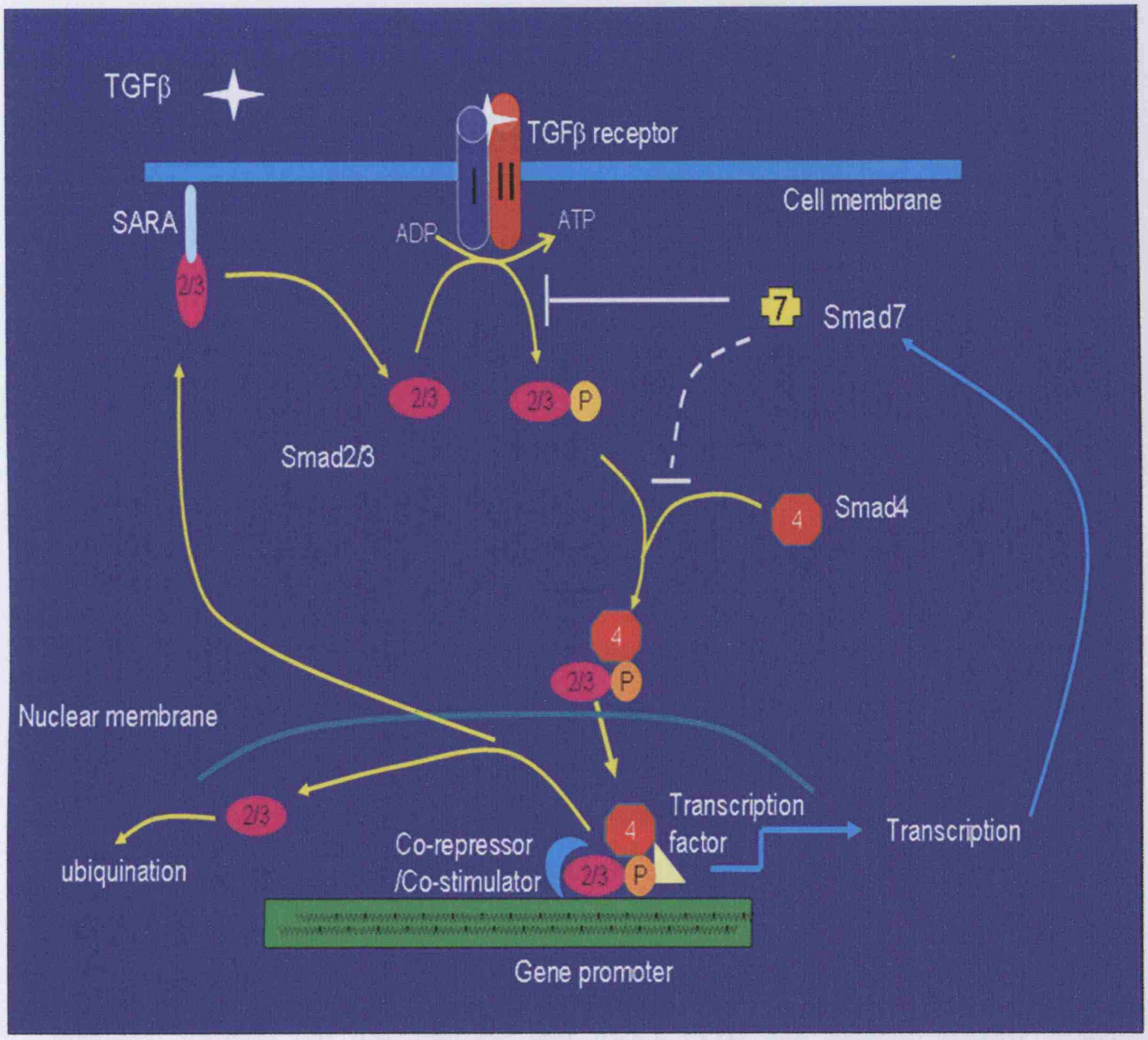

Figure 1.6. The Smad pathway. This is described in detail within the text. Briefly, activated TGFβ binds to the TGFβ receptor type II (TβR II), which then phosphorylates and activates the type I TGFβ receptor (TβR I). This exposes a serine/threonine phosphorylation site that phosphorylates and activates the receptor Smads 2 and/or 3, which are then able to form oligomeric complexes with Smad4, the co-Smad, which carries the signal to the nucleus. Within the nucleus this complex interacts with transcription factors, co-stimulators and/or co-repressors before binding to transcription sites within target gene promotor regions. Following this, breakdown of the complex occurs predominantly by ubiquination with some recycling of the R-smads. Transcription of Smad7, the inhibitory Smad, is stimulated by the transcriptional activity of the receptor Smads and is transported into the cytoplasm where it binds TβR I, blocking the active site and inhibiting further activity.

1.6.6 TGFβ cross-talk with other signalling pathways

Three major interactions with other pathways that affect the Smad pathway have been identified. The first is the regulation of R-Smads by the mitogen activated protein kinase (MAPK) signalling family; the second is the effect of co-factors, stimulated by other pathways, interacting with the Smad pathway at transcriptional sites, such as Ski(Akiyoshi *et al.* 1999); the third is the stimulation of I-Smads by other signalling proteins.

1.6.7 MAPK signalling and TGFβ

The MAPK signalling family has three major pathways comprising the extracellular signal-regulated kinase (ERK) 1/2, the stress-activated protein kinases c-Jun-NH2-terminal kinase (JNK) and p38 kinase. These are illustrated in figure 1.7.

Mutations in the MAPK pathways are common in human cancers and increased activity following upstream mutations are also relatively common. They can affect the Smad pathway in many ways that can either enhance or inhibit Smad effects. For instance, the activation of ERK1/2 by the frequently mutationally activated oncogene Ras inhibits the Smad pathway by phosphorylation of the linker region (see figure1.5) of Smad2 or Smad3 (Kretzschmar *et al.* 1999). Conversely, in untransformed lung and interstitial epithelial cells, $TGF\beta_3$ can induce $TGF\beta_1$ mRNA by induction of an AP-1 complex at the $TGF\beta_1$ gene promoter and the signal is mediated through the Ras cascade and ERKs (Yue and Mulder 2000b). Stable expression of dominant-negative Smad3 or Smad4 significantly inhibits the ability of $TGF\beta_3$ to stimulate the $TGF\beta_1$ promoter. MAPK can also enhance TGFβ mediated signalling via an ERK-dependent pathway in epithelial cells through a pathway that includes the activation of Smad2 by MEKK1 (MAP or ERK kinase kinase), an upstream activator of JNK (Brown *et al.* 1999). In rat chondrocytes, TGFβ has been shown to activate ERK1/2 but not p38 kinase or JNK (Yonekura *et al.* 1999).

Another MAPKKK (MAPK kinase kinase), TAK1 (TGFβ activated kinase 1), and its activator TAB1 (TAK1 binding protein) are activated by TGFβ leading to p38 kinase activity (Hanafusa *et al.* 1999) although the direct route of this activation is still unclear. In BMP2 signalling (another member of the TGFβ family), BMP2-

induced neurite outgrowth involves the activation of TAK1 and hence p38 kinase. Smad6 (the other I-Smad, important in BMP signalling) and Smad7 are up-regulated by BMP2 stimulation and have been found to interact physically with TAK1-binding protein, which is necessary for TAK1 activation (Yanagisawa *et al.* 2001).

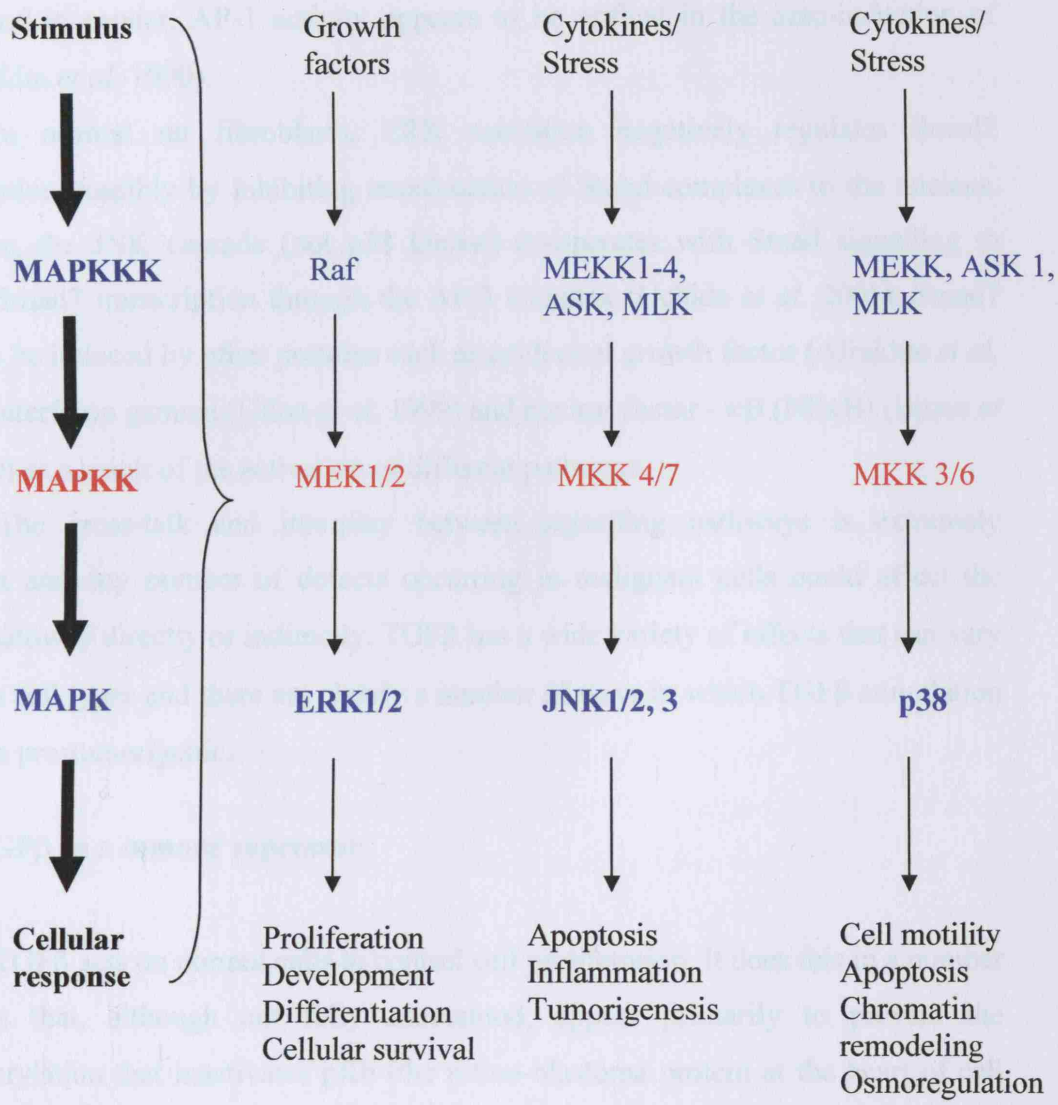

Figure 1.7 MAPK signalling. The three MAPK signalling pathways, ERK, JNK and p38 kinase, are each made up of a cascade of MAPK kinase kinase (MAPKKK), MAPK kinase (MAPKK) and the MAP kinase, illustrated in the flow chart above (Adapted from Cowan and Storey, 2003. J Exp Biol 206: 1107-1115).

One of the key transcription elements regulated by Smads is the activator-protein 1 transcription protein (AP-1) complex. This is also activated by activation transcription factor-2 (ATF-2), a constitutively expressed member of the c-Jun family

that is a downstream substrate of the JNK and p38 pathways. ATF-2 is transcriptionally activated as a result of an interaction of Smad3 and 4 (Sano *et al.* 1999) and is another example of this complex signalling interplay whereby AP-1 is activated by MAPK/Smad-interdependent amplification (de Caestecker *et al.* 2000). AP-1 activity is essential in the process of obtaining a metastatic phenotype (Denhardt 1996) and in cancer, AP-1 activity appears to be critical in the auto-induction of TGFβ (Kim *et al.* 1990).

In normal rat fibroblasts, ERK activation negatively regulates Smad7 transcription possibly by inhibiting translocation of Smad complexes to the nucleus. However, the JNK cascade (not p38 kinase) co-operates with Smad signalling to induce Smad7 transcription through the AP-1 complex (Uchida *et al.* 2001). Smad7 can also be induced by other proteins such as epidermal growth factor (Afrakhte *et al.* 1998), interferon gamma (Ulloa *et al.* 1999) and nuclear factor - κB (NFκB) (Bitzer *et al.* 2000) as a result of the activation of different pathways.

The cross-talk and interplay between signalling pathways is extremely complex and any number of defects occurring in malignant cells could affect the TGFβ pathway directly or indirectly. TGFβ has a wide variety of effects that can vary between cell types and there are clearly a number of ways in which TGFβ stimulation becomes pro-tumorigenic.

1.6.8 TGFβ as a tumour repressor

TGFβ acts on normal cells to control cell proliferation. It does this in a number of ways that, although not fully understood, appear primarily to prevent the phosphorylation that inactivates pRb (the retino-blastoma protein at the heart of cell cycle regulation), hence blocking the advance of the cell cycle through G1 (as illustrated in figure 1. 2).

This can occur by TGFβ suppression of the c-myc gene at a transcriptional level, which regulates the G1 cell cycle machinery (Moses *et al.* 1990). Different Smad transcription factor complexes can cause the synthesis of proteins p21 and $p15^{INK4B}$, which block the cyclin/CDK complexes responsible for pRb phosphorylation (Datto *et al.* 1997).

In epithelial cell renewal, TGFβ maintains the balance between cell number and cell loss by inhibiting cell proliferation and inducing apoptosis (Perlman *et al.* 2001). It has been recognised as a tumour suppresser and the loss of sensitivity to TGFβ is recognised as an important early feature of tumorigenesis. This loss of sensitivity may occur through a number of mechanisms; in hereditary non-polyposis colorectal cancer (a hereditary form of colon cancer) a somatic mutation of TGFBR2, the gene encoding TβRII, occurs leading to TGFβ insensitivity resulting in growth advantage and clonal expansion with progression to tumour(Togo *et al.* 1996). A number of human tumours show loss of heterozygosity at gene loci within different components of the TGFβ signalling pathway resulting in loss of tumour suppresser activity (see table 1.2). For example, Smad4 was first described as the tumour suppresser DPC4, common in pancreatic cancer (Hahn *et al.* 1996). The majority of these mutations are associated with microsatellite repeat sequences. These are mutations due to inactivation of the DNA mismatch repair system resulting in hypermutable states that make simple repetitive DNA sequences unstable during DNA replication. If this occurs in critical coding or regulatory regions of the gene, then a functional change may result.

TGFβ tumour suppressor effects may also be lost due to the mutation of other downstream targets such as the deletion of the locus encoding $p16^{INK4b}$ (Chin *et al.* 1998). As described above, this protein blocks cyclin/CDK complexes responsible for Rb phosphorylation. The loss of this function results in increased cell cycling and proliferation.

Gene	Protein	Tumour type Microsatellite instability = (+) No microsatellite instability = (-)	Frequency
TGFBR2	TβRII	Colon (+)	~ 30 %
		Colon (-)	~ 15 %
		Gastric (+)	30-80 %
		Gastric (-)	< 5 %
		Glioma (+)	~70 %
		Glioma (-)	< 5 %
		NSCLC (+)	~ 75 %
		NSCLC (-)	< 5 %
		Pancreas	< 5 %
TGFBRI	TβRI	Ovarian	< 5 %
		Metastatic breast	< 5 %
		T-cell lymphoma	< 5 %
MADH4 (DPC4)	Smad4	Pancreas	25-90 %
		Colon (+)	30 %
		Colon (-)	< 5 %
MADH2	Smad2	Colorectal	< 5 %
		Lung	< 5 %

Table 1.2 Mutations in Smad genes. All the genes in the table are tumour suppressors, mutated in human tumours, with subsequent loss of heterozygosity. NSCLC = Non-small cell lung cancer. (Adapted from Akhurst RJ and Derynck R 2001 (Akhurst and Derynck 2001)).

1.6.9 TGFβ and the tumour microenvironment – the pro-tumorigenic role

As described in section 1.4 there are a number of factors in the tumour microenvironment that can increase the levels of and activate TGFβ e.g. plasmin generation by tumour cells, increased protease expression such as MMP2 and MMP9, which activates TGFβ sequestered to the ECM, and increased expression of TGFβ by tumour cells. Many different tumours have been demonstrated to grow in association

with TGFβ production (Pasche 2001). The three key features of the pro-tumorigenic effects of TGFβ are angiogenesis (new vessel formation from pre-existing vessels), immune modulation and the stimulus of ECM production.

1.6.10 TGFβ and angiogenesis

Angiogenesis is a pre-requisite for solid tumour growth, invasion and metastasis. Blood is essential for the delivery of nutrients and oxygen to tumour cells and blood vessels act as portals for tumour cells to intravasate the vasculature leading to metastasis. TGFβ is a pro-angiogenic growth factor in both normal cells and in cancer and the ECM acts as scaffolding through which new vessels can form. In embryogenesis, TGFβ receptor type II deficiency results in defects of yolk sac vasculogenesis (de novo vessel formation) (Oshima *et al.* 1996) and in TGFβ type I receptor null mice there is abnormal angiogenesis (Larsson *et al.* 2001), both of which are embryonically lethal. In 3D matrigel cocultures, TGFβ is required for the induction of mesenchymal cells to smooth muscle cells as part of the formation of capillary-like structures (Darland and D'Amore 2001). In hereditary haemorrhagic telangiectasia, a hereditary condition of multisystemic angiodysplasia in man, the genetic defects are primarily within TGFβ signalling(Lux *et al.* 1999;McAllister *et al.* 1994).

In tumours, $TGF\beta_1$ activated at the tumour/stroma border induces VEGF expression at the tumour periphery (Breier *et al.* 2002). VEGF is a potent inducer of angiogenesis and can act as a survival factor for immature blood vessels (Benjamin *et al.* 1999). In prostate carcinoma cells transfected with $TGF\beta_1$, there is potent induction of angiogenesis, whereas TGFβ neutralising antibodies reduce tumour angiogenesis (Ueki *et al.* 1992). In breast cancer, high levels of $TGF\beta_1$ mRNA are associated with increased microvessel density and both TGFβ levels and microvessel density correlate with poor patient prognosis (de Jong *et al.* 1998). The ability of endothelial cells to migrate and invade in the process of angiogenesis is enhanced by the expression of MMP-2 and MMP-9 and down-regulation of TIMPs. This occurs in response to TGFβ in both tumour cells and endothelial cells (Madri *et al.* 1988;Yang and Moses 1990).

1.6.11 TGFβ and immunosuppression in relation to malignancy

The second component of the pro-tumorigenic effects of TGFβ is to allow the tumours to escape from immunosurveillance. TGFβ is able to suppress the immune system in a number of ways. It can inhibit T-cell proliferation, T-cell differentiation into cytotoxic T cells and helper T cells, and inhibit the T-cell stimulatory functions of antigen-presenting cells. It can also inhibit the activity of natural killer (NK) cells, neutrophils, macrophages and B cells (Letterio and Roberts 1998). T helper cells type I (Th1) and cytotoxic T cells play major roles in immune-mediated tumour cell killing. The suppression of these functions by TGFβ at the site of tumours may go some way to explaining how these tumour cells escape the immune response. In MM, TGFβ appears to drive the shift in the Th1/Th2 balance toward Th2 dominance via IL-10 and leads to inhibition of the Th-1 type responses directly in MM cells(Maeda and Shiraishi 1996).

1.6.12 TGFβ and tumour related ECM

The third pro-tumorigenic role of TGFβ is in the stimulation of ECM synthesis. In most solid tumours, stromal fibroblasts and/or myofibroblasts are considered to be the major cell types responsible for the increased production of ECM in response to growth factors such as TGFβ released by tumour cells (Bosman *et al.* 1993;Dahlman *et al.* 2000;Faouzi *et al.* 1999;Kauppila *et al.* 1998;Minamoto *et al.* 1988). There is also evidence of tumour cells themselves producing ECM proteins in response to autocrine tumour TGFβ production. For example, in breast cancer, $TGF\beta_1$ production can result in over-expression of tenascin-C by the tumour cells, which is associated with a migratory and invasive tumour cell type(Maschler *et al.* 2004). Tumour cell derived $TGF\beta_1$ has been shown to increase the deposition of fibronectin and tenascin-C by oral tumour cells(Dang *et al.* 2004). There can be marked ECM deposition in glioma, and $TGF\beta_1$ synthesised by tumour cells stimulates an autocrine production of collagen I by the glioma cells(Paulus *et al.* 1995). $TGF\beta_1$ produced by Moser colon cancer cells stimulates the production of fibronectin and laminin by the same tumour cells(Huang and Chakrabarty 1994). The ECM has a number of key roles necessary for tumour growth as discussed above (see section 1.4).

1.7 Experimental inhibition of TGFβ

Inhibition of TGFβ has been investigated in many fibrotic diseases and more recently, following the recognition of the pro-tumorigenic effects of TGFβ, those techniques and others have been used as tools or as possible therapies in cancer research. There are five broad methods for inhibiting TGFβ activity: 1) inhibition of TGFβ before it binds to its receptors by ECM constituents such as the proteoglycan decorin, 2) antibodies to neutralise TFGβ activity, 3) inhibition of receptor activation by the use of soluble TGFβ type II receptors, 4) Smad signalling blockade by numerous gene manipulation techniques including antisense to Smad2 and Smad3 and transfection of the inhibitory Smad7, and more recently, 5) the use of small molecular weight inhibitors to block TGFβ receptors. Each of these is discussed below.

1.7.1 Inhibition of TGFβ before receptor binding

Decorin is an endogenous proteoglycan that naturally inhibits TGFβ. In pulmonary fibrosis, TGFβ is a key mediator of collagen deposition and fibrosis. In a murine model of pulmonary fibrosis, transfection of decorin before bleomycin instillation resulted in a reduction of bleomycin-induced fibrosis(Kolb *et al.* 2001). In a rat glioma model, glioma cells transfected with decorin resulted in tumours that grew initially but then regressed compared with control transfected tumour cells, which all resulted in death(Stander *et al.* 1998). Decorin probably does not work by simply binding to and inactivating TGFβ since it has recently been shown to possibly function by interaction with Smad2 (Abdel-Wahab *et al.* 2002). Also, gene transfer of decorin inhibited colon and squamous cell cancer xenograft tumour growth via inactivation of the EGF receptor tyrosine kinase (Reed *et al.* 2002).

1.7.2 TGFβ neutralising antibodies

TGFβ neutralising antibodies have been used to block the activity of TGFβ in a number of experimental settings. In models of renal nephropathy, TGFβ antibodies have been used to inhibit the pro-fibrotic effects of TGFβ, which in a murine model

resulted in reduced deposition of collagen III (Ling *et al.* 2003). In a rat model of progressive nephritis, systemic TGFβ antibodies were shown to reduce TGFβ/Smad signalling responses with reduced renal scarring(Fukasawa *et al.* 2004). Interestingly, there seems to be a dose response to TGFβ antibodies, demonstrated in a rat model of nephropathy in which only lower doses of the antibody reduced sclerosis(Ma *et al.* 2004). Higher levels did not and this does produce some difficulties in finding the most effective antibody dose. In other systems, corneal fibrosis was reduced in a rabbit model with the demonstration of reduced collagen deposition (Jester *et al.* 1997). Following a successful preliminary trial (Siriwardena *et al.* 2002), a $TGF\beta_2$-specific antibody is under controlled clinical trials in humans to reduce collagen contraction and deposition in glaucoma filtration surgery. In the nervous system, pan-specific TGFβ antibodies have been used to reduce collagen deposition around a crushed sciatic nerve in a rat model of nerve injury(Nath *et al.* 1998).

In cancer, TGFβ reduces the immune response to tumour cells, as described in section 1.6.11. In a dendritic cell based tumour vaccine model, TGFβ antibodies enhanced the ability of dendritic cells to present antigen in mammary tumour bearing mice resulting in increased T cell stimulation and reduced tumour growth(Kobie *et al.* 2003). In a human xenograft model of prostate cancer, $TGF\beta_1$ neutralising antibodies reduced angiogenesis and tumour growth in mice(Tuxhorn *et al.* 2002). In another approach, TGFβ antibodies enhanced the effects of cisplatin treatment against human breast cancer tumour cells by reducing the induction of p21 cyclin dependent kinase (Cdk) inhibitor and enhancing the activity of Cdk 2. These resulted in facilitating the progression of S phase into G2M phase of the cell cycle with resultant increased DNA fragmentation, implying that $TGF\beta_1$ may protect the tumour cells from DNA damage(Ohmori *et al.* 1998).

1.7.3 Soluble receptor complexes to inhibit TGFβ

Soluble TGFβ type II receptors (TβRII) have been shown to inhibit TGFβ activity. Soluble TβRIIs transfected into hepatoma cells lead to a reduction in tumour growth when those cells are used to grow tumours in a rat model(Zhao *et al.* 2002b). Most work involving soluble TβRIIs and cancer have examined the effects on metastasis. Transfection into pancreatic ductal adenocarcinoma cells that were then

injected into athymic mice inhibited the metastatic potential(Rowland-Goldsmith *et al.* 2002). Systemic administration of soluble Fc:TGF-beta type II receptor fusion protein in murine transgenic and transplantable breast cancer models did not reduce the size of the primary tumour but did reduce tumour cell motility, intravasation, and formation of lung metastases(Muraoka *et al.* 2002).

1.7.4 Gene transfection techniques to inhibit TGFβ and Smad signalling

There are a number of ways to block TGFβ using gene transfection by targetting different parts of the TGFβ signalling pathway. As described above, TGFβ can be reduced by the over-expression of the proteoglycan decorin (a natural inhibitor of TGFβ) by gene transfer (Zhao *et al.* 1999). Antisense can be delivered to TGFβ specific isoforms as demonstrated by Fitzpatrick *et al.*, 1994(Fitzpatrick *et al.* 1994), and Marzo *et al.*, 1997(Marzo *et al.* 1997), who showed that in MM, antisense oligonucleotides to $TGF\beta_2$ reduced TGFβ production with the consequence of inhibited anchorage-independent growth, reduced tumorigenicity and delayed tumour growth *in vivo.*

The TGFβ receptor is another target for gene transfection. In a rat model of liver fibrosis, a vector expressing a dominant-negative TGFβ receptor was transfected into the liver. This resulted in inhibition of both TGFβ signalling and fibroblast activity leading to reduced collagen deposition i.e. reduced fibrosis (Ueno *et al.* 2001). Inhibition of TGFβ can also be achieved by blocking the Smad signalling cascade. This can be accomplished by transfection of the inhibitory Smad, Smad7, or by using antisense to the receptor Smads, Smad2 and 3 (Zhao *et al.* 1998), or to the co-Smad, Smad4 or by transfection of dominant negative constructs for Smad4 or the receptor Smads. In an animal model of lung fibrosis, transfection of lung cells with Smad7 inhibited TGFβ-induced lung fibrosis (ECM deposition, assessed by quantifying collagen deposition) in a bleomycin induced murine model of lung fibrosis (Nakao *et al.* 1999). In a rat kidney model of renal fibrogenesis, TGFβ-mediated collagen deposition has been blocked by the over-expression of Smad7 using a doxycycline inducible stable expression transfection system (Li *et al.* 2002).

1.7.5 Small molecular weight inhibitors of TGFβ

Finally, small molecular weight inhibitors of TGFβ receptor activation have recently been demonstrated to inhibit activity. SB431542 is a small molecular weight inhibitor of the $TGF\beta_1$ receptor. This has been shown to block phosphorylation and translocation of Smads (from the receptor to the nucleus), with resultant inhibition of VEGF production and inhibition of proliferation of glioma cells(Hjelmeland *et al.* 2004). Another small molecular weight inhibitor, halofuginone, used in a mouse model of squamous cell carcinoma, inhibits side effects of radiotherapy i.e. radiation-induced fibrosis. Halofuginone inhibits the effects of TGFβ by elevating the levels of Smad7, reducing the phosphorylation of Smad2 and Smad3 and reducing the expression of cytosolic and membrane TβRII, resulting in the amelioration of radiation-induced fibrosis(Xavier *et al.* 2004).

1.8 Summary

MM is increasing in incidence and will continue to do so for the next 10-20 years in Western countries and may increase for many years in developing countries that are still using large amounts of asbestos. It is an aggressive tumour that is unresponsive to conventional treatment with a median survival of 10-14 months. The primary cause is asbestos fibres, although co-factors such as SV40 may have synergistic effects. Following asbestos exposure, there is a time lag before presentation of MM of 30-40+ years. A key characteristic of this tumour is that it is extremely fibrous due to the excessive deposition of collagen within the ECM.

The ECM has been shown to have an essential role in the growth of many solid tumours, acting as a scaffold through which the tumour can grow, and by multiple interactions with tumour cells that are important for local tissue invasion, metastasis, angiogenesis and in protecting the tumour from chemotherapeutic agents.

Like many tumours, MM produce growth factors including TGFβ. TGFβ has three basic pro-tumorigenic effects: it is pro-angiogenic, immunosuppressive and stimulates production of ECM proteins. Inhibition of TGFβ in other cancers has shown great potential. The levels of TGFβ produced by MM tumours are reported as

high and are likely to be responsible for much of the fibrous tissue associated with MM through the stimulation of collagen synthesis.

What is not known is how essential TGFβ is for MM tumour growth and how important the role of collagen deposition is. If collagen is important, then the necessity off TGFβ stimulation for its production is also not known. Inhibition of TGFβ may result in blocking MM collagen production and limiting tumour growth by inhibiting an autocrine growth loop between collagen deposition and tumour growth. The importance of different TGFβ isoforms is uncertain in cancer as discussed in section 1.6.1. Specific TGFβ antibodies can be used to block the different TGFβ isoforms, whereas inhibition of the intracellular signalling pathway should block all isoforms.

TGFβ is thought to signal predominantly through the Smad pathway, which is unique to the TGFβ family (see table 1.1). Part of this signalling involves Smad7, a natural inhibitor of the Smad signal, which acts as negative feedback, and has been used in transfection experiments to inhibit TGFβ signalling. Smad7 is therefore a potentially useful tool with which to inhibit the signalling and hence the activity of TGFβ. The Smad pathway has been shown to interact with other pathways and in collagen regulation there appears to be a role for the MAPK signalling cascades. The importance of the MAPK signalling pathways is unclear in relation to TGFβ and collagen synthesis in MM cells, as these pathways have both inhibitory and stimulatory effects on TGFβ activity in other cell types (as discussed in section 1.6.7). Whether these signalling pathways are important or not for collagen production in MM is not known.

The cell biology of MM is not fully understood and since current therapies are inadequate, a better understanding of factors that enhance the growth of these tumours will potentially identify novel therapeutic targets.

1.9 Hypothesis

MM cell synthesis of TGFβ stimulates MM cell collagen production and promotes tumour growth. Strategies to inhibit TGFβ activity or signalling will inhibit MM collagen production and limit tumour growth.

1.10 Aims

Aim 1.

To assess the relationship between TGFβ and collagen production in MM cells by measuring collagen and TGFβ synthesis in 7 MM cell lines (3 murine, 4 human) and examine the effect of TGFβ stimulation on MM cell collagen production.

Collagen production: the amount of collagen produced basally and in response to TGFβ will be assessed *in vitro* by measuring hydroxyproline production using reverse-phase HPLC.

TGFβ production: the production of active TGFβ by MM cells will be demonstrated and quantified using a mink lung epithelial cell assay.

Smad signalling: an assessment of the Smad signalling pathway in MM cells will be made by measuring phosphorylated (activated) Smad2 levels at different time points following TGFβ stimulation using Western blotting.

Aim 2.

To assess the effects of inhibiting TGFβ on tumour growth using an established murine model of MM

Murine model of MM: An established murine model of MM using syngeneic cells will be used to assess the effects of inhibiting TGFβ on MM tumour growth *in vivo*.

TGFβ neutralising antibodies *in vivo*: Pan-specific, $TGF\beta_1$-specific and $TGF\beta_2$-specific neutralising antibodies and their controls will be administered systemically to mice and the effects on collagen production and tumour growth assessed by measuring tumour weight, tumour collagen content using reverse-phase HPLC and by histological examination of tumour sections

Aim 3.

To assess the effects of blocking the Smad signalling pathway by over-expression of Smad7, as an alternative means of inhibiting all three isoforms of TGFβ, on MM cell collagen response and tumour growth.

Transient transfection of Smad7 *in vitro* using the LID transfection system: this system will be optimised for the transfection of MM cells by transfection of green fluorescent protein (GFP) to assess transfection efficiency with different LID components. It will then be used in the assessment of MM cell collagen gene responses.

Gene response: this will be assessed by transiently transfecting an α_1(I) pro-collagen gene promoter luciferase reporter into MM cells with dual transfection of Smad7 or a control vector, using the LID system, and measuring basal and TGFβ stimulated reporter activity.

Retroviral transfection of Smad7 to create stable transfections of MM cells over-expressing Smad7: this system will be used to produce cell cultures in which all cells are over-expressing Smad7, which will be used to assess total collagen production and the effects of Smad7 on tumour growth.

Collagen production: using HPLC measurements of hydroxyproline synthesis to measure collagen production by Smad7 or control vector expressing MM cells.

Tumour growth: using the murine model to grow tumours from MM cells that have been stably transfected to over-express Smad7, or a control protein, the effects of

Smad7 on tumour growth will be assessed by measuring tumour weight and collagen content (using reverse-phase HPLC).

Aim 4.

To investigate the role of MAPK signalling in the collagen response of MM cells to TGFβ stimulation

MAPK activation by TGFβ: the activation of MAPK pathways (ERK, p38 kinase and JNK activation) will be measured by Western blotting of lysates from MM cells *in vitro* following their exposure to TGFβ, to examine for the activated MAPK proteins

Inhibition of MAPK signalling: the collagen response of MM cells to TGFβ at gene and protein levels while blocking ERK activity, p38 kinase activity and JNK activity, using specific inhibitors, will be assessed at gene and protein levels:

Gene response: by transfecting MM cells with the α_1(I) pro-collagen gene promoter luciferase reporter assay (as above), using the LID system, and treating the cells with the specific MAPK inhibitors before exposure to TGFβ.

Protein response: collagen production will be assessed by measuring total collagen production, using reverse-phase HPLC measurement of hydroxyproline, by MM cells treated with the specific inhibitors.

Aim 5.

To examine the TGFβ receptor for expression of different isoforms

An initial assessment for the presence of different subtypes of the type I receptor – ALK1 and ALK5 – and, since Smad7 stimulates down regulation of these receptors in other systems, the effects of Smad7 transfection on ALK1 and ALK5 expression by MM cells will be assessed using immunohistochemical and Western blotting techniques.

Chapter 2. Materials and Methods

2.1.1 Cell lines

Seven Malignant Mesothelioma (MM) cell lines were studied. Four cell lines were derived from human tumours and three from murine ascitic fluid. The human lines JU77, NO36, LO68 and ONE58, were established from MM cells isolated from pleural effusions as described previously (Manning *et al.* 1991). AB1 and AB22 (murine) MM cell lines were derived from tumours induced by inoculation of crocidolite asbestos into BALB/c mice and the AC29 cell line from crocidolite inoculated CBA mice as described previously (Davis *et al.* 1992). All seven cell lines were kindly donated by Professor Bruce Robinson, Department of Medicine, University of Western Australia.

2.1.2 Materials

Tissue culture plastic ware was purchased from TTP, Helena Biosciences, Sunderland, UK and Sarstedt Ltd, Leicester, UK. Culture medium, Dulbecco's Modified Eagle Medium (DMEM), Trypsin-EDTA, Penicillin/Streptomycin and L-Glutamine were purchased from GibcoBRL, UK. Foetal calf serum (FCS) was purchased from Autogen Bioclear, Wiltshire, UK.

2.1.3 Cell culture conditions

Cells were routinely grown in 75 cm^2 tissue culture flasks in DMEM containing 10% FCS (v:v), penicillin (100 U/ml) and streptomycin (100 μg/ml) and grown in a humidified atmosphere of 10% CO_2 at 37°C. Culture medium was changed every 3-4 days and cells passaged at visual confluence with a 1:5 to 1:10 split ratio. Routine tests for Mycoplasma were carried out at regular intervals using a commercial mycoplasma detection kit (Boehinger Mannheim).

2.1.4 Cell Passage

At visual confluence the culture medium was removed from the flask. The cell layer was washed twice with 5 ml of phosphate buffered saline (PBS, Oxoid Ltd, UK)

to remove remaining serum, which would deactivate trypsin. The PBS was removed and 1ml of trypsin/EDTA introduced into the flask. The flask was briefly rocked to spread the trypsin/EDTA evenly over the confluent cell monolayer and then placed in an incubator for 2 – 4 minutes at 37°C until the cell layer had visibly detached from the plastic. Detachment and rounding of the cells was confirmed using an inverted-phase contrast light microscope (Olympus CK2, Olympus Optical company Ltd, Japan). DMEM (4 ml) containing 10% FCS was then added to neutralize the trypsin/EDTA and the cells resuspended by passing them several times through a 10 ml pipette. Aliquots of either 1 ml (1:5 ratio) or 0.5 ml (1:10) of the cell suspension were then added to a fresh flask with 10 ml of culture medium.

2.1.5 Storage of cells under liquid Nitrogen

Cells were stored in a cell bank by freezing in dimethyl sulphoxide (DMSO) and submerging under liquid nitrogen. Briefly, cells were grown to confluence in 75 cm^2 flasks, washed with PBS and trypsinised as described in section 2.1.4. Following re-suspension in 5 ml media containing 10% FCS the cells were spun in 15 ml polypropylene tubes at 300g, 6 min, 4°C. The supernatant was discarded and the cells re-suspended in 1.5 ml of freezing solution (DMSO 10%, FCS 20%, DMEM, penicillin (100 U/ml) and streptomycin (100 µg/ml)), which was added slowly over 2 min to avoid a rapid change of the osmotic gradient across the cell membrane that would damage the cells. The cells were then placed into cryovials (2 ml volume), labelled and wrapped in tissue paper before being covered in a polystyrene case to slow down the freezing time. This was then placed in a -80°C freezer before being transferred to a liquid nitrogen cell bank the following day. Cells could be re-used at any time by thawing in a waterbath at 37°C for 2-3 min before adding to 10 ml 10% FCS in a 75 cm^2 tissue culture flask. The growth medium is replaced the following day.

2.1.6 Cell Counting

At visual confluence cells were trypsinized as described. The cells were resuspended in 5 ml of fresh media and 10 µl of this cell suspension was introduced into an Improved Neubauer Haemocytometer (BDH/Merck) and visualised under an

inverted phase-contrast light microscope. As the volume of one grid in the chamber is 10^{-4}ml the number of cells/ml was calculated by taking the average of the four grids on the chamber multiplied by 10^4. Cells were then seeded in tissue culture plates at the required concentration

2.2 Bioassay for TGFβ

A mink lung epithelial cell (MLEC) bioassay system was selected to measure levels of active TGFβ produced by MM cells. There are a number of assays available to measure TGFβ levels but this assay has been shown to be robust and both highly sensitive and specific(Abe *et al.* 1994). It is a quantitative bioassay that has a further advantage over other assays in that it doesn't involve radioactive elements. TGFβ is known to induce plasminogen activator inhibitor-1 (PAI-1) expression and this has been exploited to produce the bioassay. By creating MLECs that are stably transfected with an expression construct containing a truncated PAI-1 promoter fused to a firefly reporter gene, luciferase activity can be stimulated from the construct by exposure of the cell to TGFβ. The luciferase is measured, using a luminometer, from the MLEC lysates (since the luciferase remains intracellular) after 16 hours of exposure to either TGFβ or conditioned media thought to contain TGFβ, and the level of luciferase activity is dose-dependent for TGFβ concentrations. Each time the bioassay is used a number of set concentrations of TGFβ are also measured to produce a standard curve for each experiment, since luciferase activity will vary due to other variables including the number of passages performed on the MLEC cells, the cell number and the time taken for incubation. This means that although luciferase activity varies between experiments the level of TGFβ quantified, by correction to the TGFβ standard curve, remain consistent. The bioassay is described in more detail below.

2.2.1 Mink Lung Epithelial Cell line

The assay uses mink lung epithelial cells (MLEC), kindly supplied by DB Rifkin (Department of Cell Biology, New York University Medical Centre, New York), that have been stably transfected with an 800 bp fragment of the 5' end of human plasminogen activator inhibitor-1 (PAI-1) gene promoter (Mimuro *et al.* 1989)

upstream of the firefly luciferase gene in a p19LUC-based vector(Abe *et al.* 1994). The cells were maintained in DMEM supplemented with 10% FCS, penicillin (100 U/ml), streptomycin (100 μg/ml) and Geneticin (200 μg/ml) and grown at 37°C in 10% CO_2. Geneticin resistance is produced by the transfected construct and so incubation in the presence of this antibiotic allows only the transfected MLEC cells to grow. The cell line was maintained by passage and splitting of cells in a 1:10 ratio. The cells were used to assay test samples for active TGFβ.

2.2.2 Assaying of active TGFβ

Confluent or subconfluent MLEC were trypsinised gently and resuspended in growth media at 1.6 x 10^5cells/ml and plated at 100 μl/well in 96 well tissue culture plates. Cells were incubated at 37°C in 10% CO_2 for three hours to allow cell attachment. The medium was then aspirated and 100 μl of the test sample (conditioned media – see section 2.2.3) added directly to the attached cells with triplicate repeats. Dilutions of $TGF\beta_1$ (0.01–1.2 ng/ml) were made in media similar to the test media and added to attached MLEC cells in triplicate repeats to create a standard curve. The samples and standard $TGF\beta_1$ dilutions were incubated for 16 hours overnight at 37°C in 10% CO_2. The culture media was gently aspirated from the cells and the cells gently washed with 50 μl of PBS. The cells were then lysed with 100 μl of lysis buffer (Boehinger Mannheim) and incubated at room temperature for 20 min, to allow for complete cell lysis. The lysates (45 μl sample repeated in triplicate) were centrifuged at 300g for 2 min to remove cell debris and transferred to an opaque 96 well plate. 100 μl of luciferase substrate buffer was added to each sample and the luciferase activity from each measured in a microplate luminometer (Tropix 717, PE Applied Biosystems). Samples of the lysates (45 μl) obtained from the cells exposed to standard $TGF\beta_1$ dilutions (in triplicates) were also transferred to the 96 well plate. The mean value of luciferase activity for each triplicate repeat was calculated and recorded and the concentration of TGFβ in the sample calculated by comparison with the luciferase activity measured from the standard $TGF\beta_1$ dilutions.

2.2.3 Conditioned medium

Seven different MM cells (4 human, 3 murine) were grown in 75 cm^2 flasks at 37°C in 10% CO_2 containing 10% FCS. At confluence, the medium was removed and washed with PBS. 5 mls of serum-free medium was then placed on the cells and left for 24hr. The medium was then removed for subsequent use in the MLEC assay to assess for active TGFβ concentrations. The number of cells in each flask was recorded, as described in section 2.1.7, so that values of TGFβ concentrations could be corrected for cell number.

2.2.4. Effects of TGFβ neutralising antibodies on MLEC luciferase activity

To confirm that the luciferase activity produced following exposure of the cells to TGFβ or conditioned media was due to TGFβ and not other factors present in the serum, luciferase activity was measured following the pre-treatment of the TGFβ standards with pan-specific TGFβ neutralising antibody (Cambridge Antibody Technologies (CAT), Cambridge, UK) at 50 μg/ml and 100 μg/ml (antibody concentrations recommended by CAT). Following this, pan-specific TGFβ antibody, at 100μg/ml, was added to the conditioned media samples from AB22 and AC29 cells before application to the MLEC cells to confirm that luciferase activity was due to TGFβ. AB22 and AC29 cells were assessed as these were the predominant cell lines used throughout the study.

2.2.5 Effects of different TGFβ isoform specific neutralising antibodies on $TGF\beta_1$ stimulated MLEC luciferase activity

Since a $TGF\beta_1$-specific (CAT) and a $TGF\beta_2$-specific antibody (CAT) were to be used in the murine model of MM (see section 2.7) these antibodies were also used to pre-treat $TGF\beta_1$ standards before application to the MLEC cells and activity compared with results obtained from pan-specific TGFβ antibody treatment. This was to assess the specificity of the antibodies and to compare the effectiveness of $TGF\beta_1$-specific antibody with the pan-specific antibody when used at the same concentration (100μ/ml), which should inhibit the activity of the chosen dose of $TGF\beta_1$ (0.3 ng/ml –

selected as the mid-point of the $TGF\beta_1$ standard curve concentrations). $TGF\beta_2$-specific antibody should not inhibit the activity of $TGF\beta_1$ induced luciferase.

2.3 Vector preparation for use in transfection experiments

Two Smad7 vectors were prepared for use in transfection experiments. The first was a Smad7 cDNA plasmid in an expression vector for use in a transient transfection system. The second vector was more complex for use in a lentiviral transfection system. The preparations of these two vectors are described below, followed by a description of how they were used in transfections. The reason for using two separate transfection systems is explained in section 2.4.

2.3.1 Smad7 vector

A Smad7-Flag construct containing Smad7 cDNA and a small peptide "tag", coding for Flag, as an amino terminal addition that has been cloned into a specific restriction site of the 5.4 kb expression vector pcDNA3 (Nakao *et al.* 1997), was kindly provided by CH Heldin (Ludwig Institute for Cancer Research, Upsala, Sweden). The Flag tag can be identified easily using anti-Flag antibody. The Smad7 insert is 1.3kb in length cloned into the pcDNA3 vector (see figure 2.1) at restriction sites using cloning enzymes BamH I and Xho I at the 5' and 3' ends respectively.

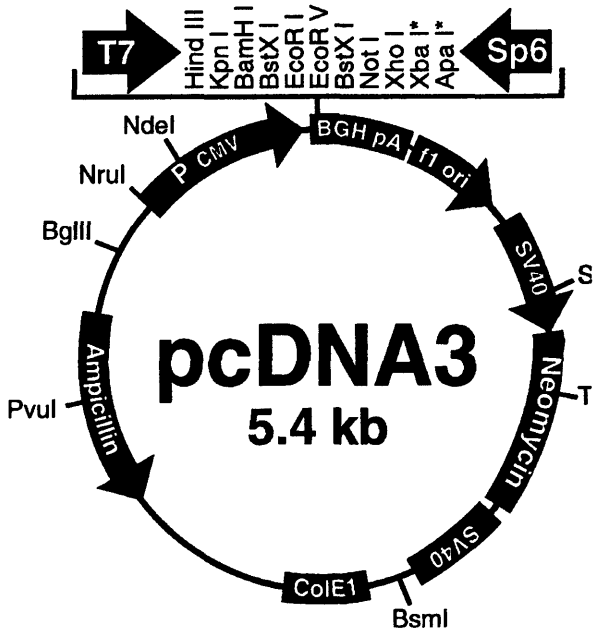

Restriction enzyme site between T7 CMV promoter and Sp6 promoter with restriction enzymes active at this site listed. This is the point at which 1.3 kb Smad7-Flag is inserted using restriction enzymes BamH I and Xho I.

Figure 2.1 Schematic of the pcDNA3 vector used in these experiments as published by Invitrogen. Flag/Smad7 cDNA was inserted into this vector between restriction sites BamHI and XhoI at the restriction site indicated, as described in the text. This vector was also used, as shown above, as a control vector.

2.3.2 Confirmation of plasmid insert size

To confirm that the insert was 1.3kb in size, consistent with being Smad7, a double digest was performed to cut the insert out of the construct and the products of the digest reaction separated in a 1% agarose gel. Briefly, approximately 15 μg Smad7-pcDNA3 plasmid DNA (as supplied) was dissolved in 50 μl TE buffer and 2 μl of this was added to an eppendorf (repeated in quadruplicate). To each sample the following were added: 1 μl of restriction endonuclease BamHI, 0.5 μl of restriction endonuclease XhoI, 2 μl of reaction buffer D (Promega, Tris-HCl 6mM, $MgCl_2$ 6mM, NaCl 150 mM, DTT 1mM, pH 7.9) and 15 μl ddH_2O. This mixture was then incubated for 1 hour at 37^0C. The digested sample was then run at 50mV in a 1% agarose gel (1g agarose added to 100 ml TBE buffer and melted in a microwave oven followed by the addition of 5 μl ethidium bromide (10 mg/ml stock)) with the uncut sample (i.e. original undigested plasmid) as a control and a 1kb DNA ladder. The

DNA bands were visualised under UV light and compared with the DNA size ladder as shown in figure 2.2, confirming that the insert size was 1.3kb.

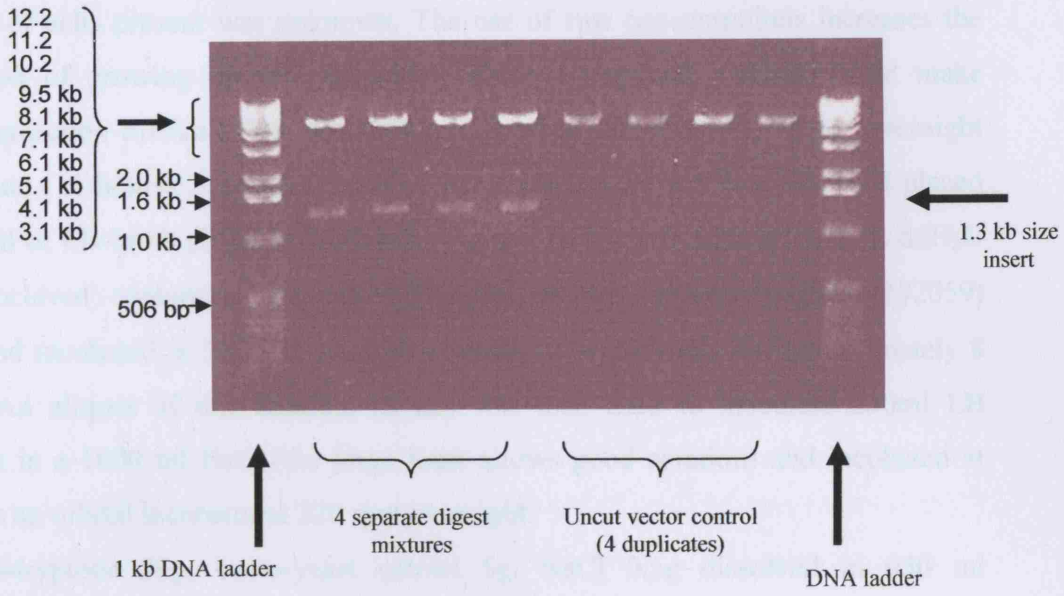

Figure 2.2. Gel showing DNA bands following double digest of pcDNA3/Smad7 cDNA to confirm that the insert size is ~1.3kb, which is consistent with it being Smad7. Four repeat digests were run and all confirmed that the insert size was ~1.3kb.

Following confirmation of correct insert size the quantity of plasmid was increased by transformation, purification and amplification as described in sections 2.3.3 and 2.3.4.

2.3.3 Transformation and Amplification Procedure for plasmid DNA

A 2 µl aliquot of Smad7 plasmid DNA diluted in TE buffer to 1ng/µl (determined using a spectrophotometer, 1 OD_{260}=50µg/ml) was added to 50 µl of DH5α *E. coli* competent cells and incubated for 30 min on ice in a pre-chilled falcon tube. The cells were then heat-shocked for 45 seconds at 42°C in a water bath, allowing plasmid to cross through the cell membrane, and immediately placed back on ice for 2 minutes, preventing further movement of plasmid across the membrane. The cells were suspended in 450 µl of SOC buffer (20mM glucose added to SOB medium*) and shaken at 220rpm, 37°C for 1 hour. Agar plates containing ampicillin

(50 μg/ml) were pre-heated at 37°C and 10 and 100 μl of the cells in the SOC medium were plated separately and allowed to dry before being inverted and incubated over night at 37°C. The two quantities of 10 and 100 μl of medium were used as the number of cells present was unknown. The use of two concentrations increases the likelihood of growing discrete colonies without overgrowth, which would make colony selection difficult. The remaining cells were stored at 4°C. After overnight incubation (16 hours) 2 discrete colonies were selected from either plate and placed into 2 ml of LB-broth (25g LB broth mix, Sigma Chemical Company, and 1L ddH_2O and autoclaved) containing ampicillin (50 μg/ml) in 14 ml Falcon "snapcap" (#2059) tubes and incubated at 37°C, in an orbital incubator at 220 rpm for approximately 8 hours. An aliquot of this medium (2 ml) was then used to inoculate 250ml LB medium in a 1000 ml flask (the large flask allows good aeration) and incubated at 37°C, in an orbital incubator at 220 rpm overnight.

(*bacto-tryptone 20g, bacto-yeast extract 5g, NaCl 0.5g dissolved in 950 ml deionized water. 10 ml of 250mM KCl solution added and pH adjusted to 7.0 with 5N NaOH. The volume was adjusted to 1 litre with water and the medium sterilised by autoclaving. Just before use, 5 ml of a sterile solution of 2M $MgCl_2$ was added)

2.3.4 Purification of plasmid DNA

Purification of plasmid DNA was performed using a Qiagen EndoFree Plasmid Maxi kit (Qiagen Ltd, West Sussex, UK). Briefly, bacterial cells were grown as described in section 2.3.3 and harvested by centrifugation at 6000 x g for 15 minutes at 4°C. The supernatant was aspirated and the bacterial pellet resuspended in 10 ml of resuspension Buffer P1 (50mM Tris-Cl, pH 8.0, 10mM EDTA, 100μg/ml Rnase A, Qiagen EndoFree Plasmid Maxi kit), which contains RNase, ensuring that no cell clumps remained. 10 ml of lysis Buffer P2 (200 mM NaOH, 1% SDS (w/v), Qiagen) was added and mixed gently by inverting 4-6 times, followed by incubation at room temperature for 5 min (vortexing is avoided as this would shear the genomic DNA). 10 ml of chilled neutralization Buffer P3 (3.0 M potassium acetate, pH 5.5, Qiagen) was added to the lysate to enhance precipitation and mixed immediately by inverting 4-6 times. The mixture was poured into the barrel of the QIAfilter cartridge and incubated at room temperature for 10 minutes (this allows a precipitate of

proteins, genomic DNA and detergent to float to the top and form a layer allowing easier filtration without clogging). The outlet nozzle cap was removed and the lysate filtered into a 50 ml tube. 2.5 ml of buffer ER (Qiagen Proprietary formulation) was added to the filtrate and mixed by inverting the tube 10 times followed by 30 min incubation on ice. During this time a QIAGEN-tip 500 was equilibrated by applying 10 ml of equilibration Buffer QBT (750 mM NaCl, 50mM MOPS, pH 7.0, 15% isopropanol (v/v), 0.15% Triton® X-100 (v/v), Qiagen) and the column allowed to empty by gravity flow. The filtered lysate was applied to the QIAGEN-tip and allowed to enter the resin by gravity flow. The tip was then washed through with 2 x 30 ml of wash Buffer QC (1.0 M NaCl, 50 mM MOPS, pH 7.0, 15% isopropanol (v/v), Qiagen) to remove contaminants (such as traces of RNA and protein) from the plasmid preparation and also to disrupt non-specific interactions, and remove any nucleic acid binding proteins without the use of phenol. The DNA was eluted with 15 ml of elution Buffer QN (1.6 M NaCl, 50 mM MOPS, pH 7.0, 15% isopropanol (v/v), Qiagen) and collected in a 30 ml endotoxin-free tube. The DNA was precipitated by adding 10.5 ml of isopropanol at room temperature, which was mixed and centrifuged immediately at 15,000 x g for 30 minutes at 4°C. The supernatant was removed and the pellet washed with 5 ml endotoxin-free 70% ethanol (to remove precipitated salt) at room temperature and centrifuged at 15,000 x g for 10 minutes. The DNA pellet was then air-dried for 5 minutes and re-dissolved in 75 µl of endotoxin-free TE (10 mM Tris-Cl, pH 8.0, 1mM EDTA) buffer.

The final DNA concentration was calculated by diluting 2 µl of the solution in 500 µl on ddH_2O and reading the OD_{260} and OD_{280} on a spectrophotometer. The ratio of OD_{260} to OD_{280} gives an estimate of the purity of the DNA (a value of 1.8 equates with a pure DNA sample) and using the OD_{260} value the concentration of the sample was calculated (1 OD_{260}=50 µg/ml). The DNA was stored in ampoules at -20°C.

2.3.5 Creation of a Smad7 vector for use in retroviral transfection.

The expression vector "pHR-CMV-EGFP" was supplied by Dr Walter Low in collaboration with Professor Mary Collins (Institute of Immunology and Molecular Pathology, University College London) and was used for retroviral transfection. This vector contains a 700 bp region encoding LacZ, between the restriction sites XhoI and

BamHI. These two restriction sites are also at the 5' and 3' end of the Smad7-Flag region of the Smad7-pcDNA3 construct described in section 2.3.1. This allows the Smad7-Flag to be inserted into the pHR vector in the correct orientation, after excision of the 700 bp LacZ region, using the same restriction enzyme sites.

The 700 bp LacZ region was first cut from the pHR vector to leave a linear cDNA strand of the remaining expression vector. A test cut was first performed using 0.5 ml of pHR-CMV-EGFP vector (at 1 μg/ml by diluting the DNA in TE buffer following calculation of the DNA concentration using spectrophotometry as described in section 2.3.4) added to 2 μl of reaction buffer B (Promega), 1 μl of restriction enzyme XhoI, 1 μl of restriction enzyme BamHI and made up to 20 μl with 15.5 μl of ddH_2O in ependorfs and incubated at 37°C for 1 hour. Three other reaction mixtures were made using DNA and reaction buffer in the same amounts in the presence or absence of restriction enzymes. Each mixture was corrected to 20 μl with ddH_2O. A 5 μl sample of each reaction mixture was mixed with 1 μl of 5 x loading buffer and run in parallel at 80 mV in a 1% agarose gel (see section 2.3.2) to confirm that appropriate sized pieces of DNA resulted from the reaction. The results are shown in figure 2.3

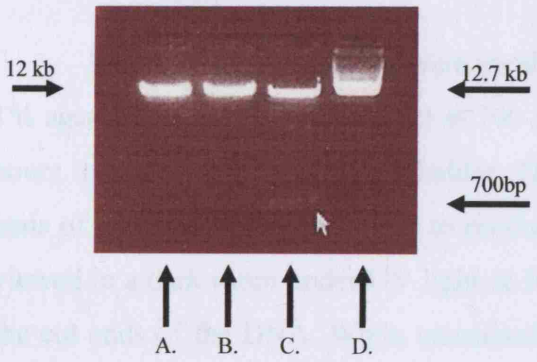

Figure 2.3 Gel showing restriction enzyme cutting of the pHR-CMV-EGFP vector using a double digest with XhoI and BamHI. Single digests using either XhoI or BamH1, shown in lanes A & B, result in linearisation of the vector, shown uncut in lane D. A double digest using both restriction enzymes results in two bands (the smaller 700bp band is just visible) in lane C. The small 700 bp section is the LacZ region, which is being removed from the vector at the point where Smad7 is to be inserted.

2.3.6 Gel extraction of DNA from plasmid constructs

The optimal molar ratio for ligation of DNA insertions to vector constructs is insert: vector, 3:1. Given that i) the Smad7 insert is 1.3 kb in length, ii) the Smad7-pcDNA3 vector is 5.2 kb uncut, and iii) the retro-viral vector insert pHR is 9 kb in length, quantities of each construct were calculated so that a ratio of cut vector (pHR) to Smad7-Flag insert of 1:3. This was obtained following two double digest reactions of the retroviral vector and the Smad7 vector. The following reaction mixtures were prepared:

	Retroviral vector	**Smad7 vector**
	25 µl DNA (=20µg)	60 µl DNA (=100µg)
	12 µl Buffer B (10x) (Promega)	12 µl Buffer B
	5 µl XhoI (restriction endonuclease)	20 µl XhoI
	5 µl BamHI (restriction endonuclease)	20 µl BamHI
	73 µl ddH_2O	8 µl ddH_2O
Totals	120 µl	120 µl

The reactions mixtures were incubated at 37°C for 2 hours and then run on a 1% agarose gel (see section 2.3.2) at 100 mV for 15 min followed by 20 mV for 16 hours together with a DNA size ladder. These reactions result in the cutting of both ends of the insert from the vector to produce two pieces of linear DNA. The gel was viewed in a dark room under UV light at 365 mHz. This wavelength will not damage the cut ends of the DNA. While visualised under UV light the Smad7 insert and the retroviral vector were identified by size and cut from the gel using a scalpel and placed into separate ependorfs. This is shown in figure 2.4.

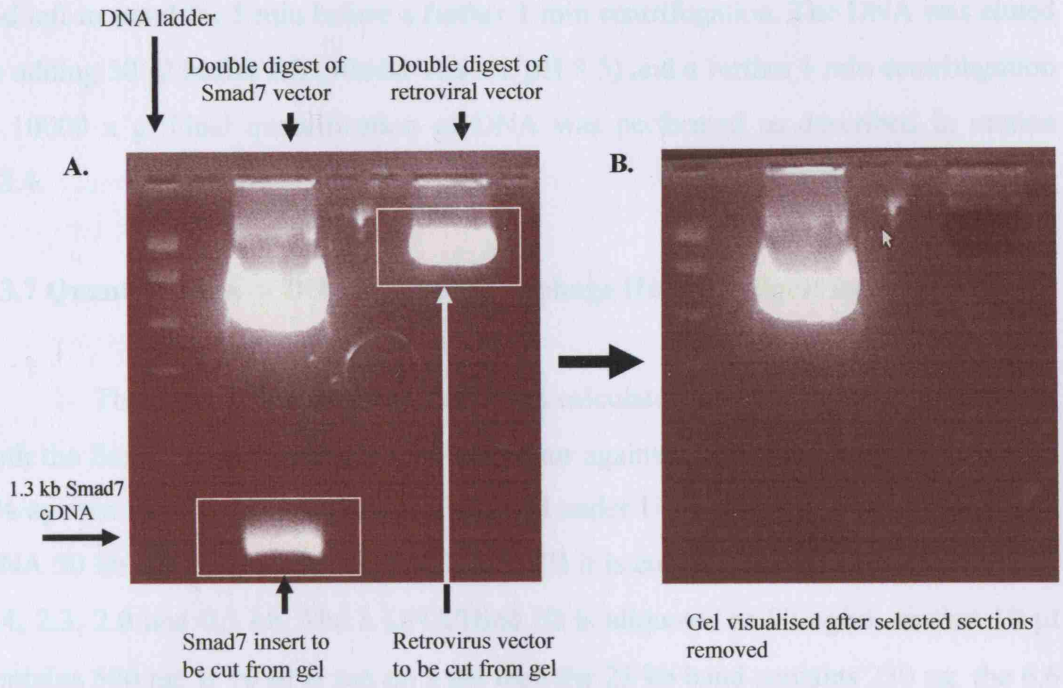

Figure 2.4. A. Double digests of the pcDNA3/Smad7 vector and the retroviral pHR vector containing LacZ were performed as described in the text. The 700bp cDNA of LacZ is not seen as it has run off beyond the end of the gel. The cDNA of interest were identified (boxed on gel image) and cut out from the gel using a scalpel, leaving the remaining vector components (**B**) to be discarded.

The size of each gel piece was kept to a minimum by removing extra agarose. The gels were weighed and the DNA extracted from the gel using a QIAquick Gel Extraction Kit (Qiagen Ltd). Briefly, to solubize the gel, 3 volumes of buffer QG (proprietary solubilisation and binding buffer, Qiagen Ltd) were added to 1 volume of gel (100 μg ~ 100 μl) for both the insert and the vector. Each was incubated at 50°C for 10 min (or until the gel had dissolved). Buffer QG contains a pH indicator, which is yellow at pH≤ 7.5. Following this, 1 gel volume of isopropanol (i.e. volume of isopropanol equals weight of gel) is added to the mixture of the retroviral vector gel as this increases the yield of DNA fragments <500bp and > 4kb. Each sample was applied to a column that binds DNA and spun for 1 minute at 10000 x g in a table top microcentrifuge (Beckman GS-15R Centrifuge, Beckman Ltd, UK). The column was then washed with buffer QG and centrifuged for 1 min at 10000 x g, which removes all trace of agarose. The column was washed with buffer PE (Qiagen)

and left to stand for 5 min before a further 1 min centrifugation. The DNA was eluted by adding 50 µl buffer EB (10mM Tris-Cl, pH 8.5) and a further 1 min centrifugation at 10000 x g. Final quantification of DNA was performed as described in section 2.3.4.

2.3.7 Quantification of DNA using λ DNA phage Hind III digest ladder

The quantity of DNA produced was calculated by running 5 µl and 10 µl of both the Smad7 insert and the retroviral vector against a λ DNA/Hind III ladder in a 1% agarose gel (section 2.3.2) and visualised under UV light. The λ DNA is a phage DNA 50 kb long. When digested with Hind III it is cut into fragments of 23, 9.3, 6.6, 4.4, 2.3, 2.0 and 0.5 kb. The λ DNA/Hind III is aliquoted at 50 ng/µl, so that 10 µl contains 500 ng. If 10 µl is run on a gel then the 23 kb band contains 230 ng, the 6.6 kb band 66 ng etc. By comparing the intensity of the plasmid bands in the gel with the λ/Hind III marker the amount of DNA in the band is estimated and the concentration calculated. See figure 2.5 for DNA quantification using Hind III ladder.

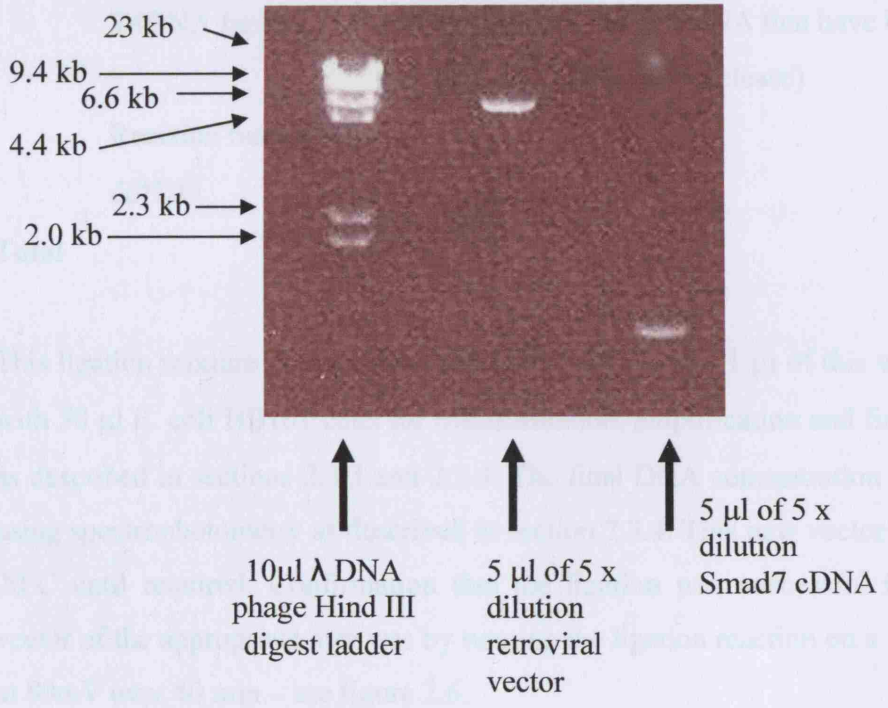

Figure 2.5. Quantification of DNA concentrations by comparison of band densities from 5µl of both the retroviral vector and the Smad7 cDNA run in conjunction with a λ Hind III phage on a 1% agarose gel.

Using this data, the amounts of both the vector and insert are calculated for a ligation reaction, such that the vector : insert molar ratio is 1 : 3 as described in section 2.3.8.

2.3.8 Ligation of vector and insert to form new construct pHR-CMV-Smad7-Flag-EGFP

Following quantification of the DNA concentration described in section 2.3.7 the final concentration of the retroviral vector was calculated as 94 μg/ml and the Smad7 insert was 50 ng/ml. Given that a molar ratio of the vector : insert of 1 :3 is required and the size of the vectors are 9 kb for the vector and 1.3 kb for the insert, then for 100 ng of vector 43.33 ng of insert is optimal. This was approximately equivalent to 1 μl vector (at 94 μg/ml) to 1 μl (50 ng/ml) insert. Therefore for ligation of these two pieces of DNA the following ligation reaction was mixed:

Vector	1 μl
Smad7 insert	1 μl
T4DNA ligase	1 μl (which binds the ends of DNA that have been cut by the same restriction endonuclease)
Reaction buffer	4 μl
ddH2O	13 μl
Total	**20 μl**

This ligation mixture was incubated at 14°C for 16 hours. 1 μl of this was then grown with 50 μl E. coli HB101 cells for transformation, amplification and final purification as described in sections 2.3.3 and 2.3.4. The final DNA concentration was calculated using spectrophotometry as described in section 2.3.4. This new vector was stored at -20°C until required. Confirmation that the ligation was successful in producing a vector of the appropriate size was by running the ligation reaction on a 1% agarose gel at 80mV over 40 min – see figure 2.6.

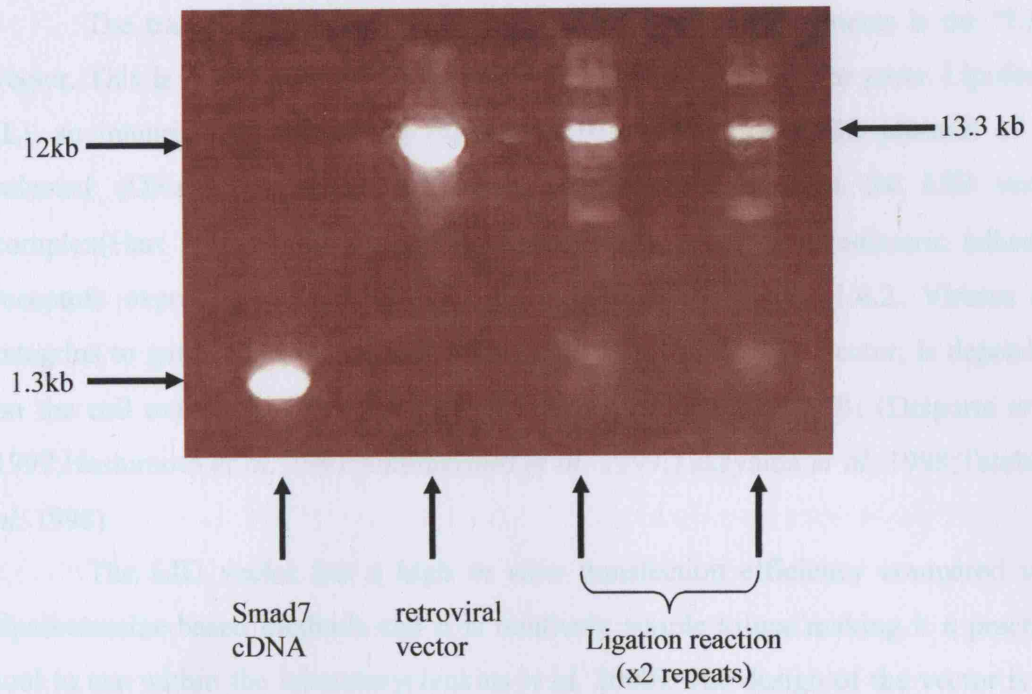

Figure 2.6 Ligation reaction. 1% agarose gel showing bands from samples from the ligation reactions run in conjunction with the non-ligated components. This confirmed that ligation had occurred to create the new vector pHR-CMV-Smad7-Flag-EGFP. Small amounts of non-ligated DNA at the Smad7 size can be seen, but the bulk of the reaction mixture is at the correct size confirming successful ligation.

2.4 Gene Transfection Techniques

Gene transfection is a useful way of introducing genes into a cell in order to modify cell behaviour. This technique is used in a number of experiments described in this thesis. Transfection can be either transient or stable i.e. a relatively short-lived expression of the gene by the transfected cell or continuous expression of the gene, which is also passed on to daughter cells. Both of these techniques are used in these investigations. Transient transfection is particularly useful for studies of reporter gene assays, as only the activity of transfected cells is measured and so very high levels of transfection are not required to obtain meaningful results. This technique is also useful in permitting dual transfections of two vectors simultaneously, as will be described in section 2.5.4, to assess the effects of Smad7 transfection on the response of a procollagen promoter gene reporter.

The transient transfection technique used in these experiments is the "LID" vector. This is a novel integrin targeting vector that comprises three parts: Lipofectin (L), an integrin binding peptide (I) with a 16-lysine tail, and the plasmid of the selected cDNA (D), which combine electrostatically to form the LID vector complex(Hart *et al.* 1998). Integrins are a family of αβ heterodimeric adhesion receptors expressed on almost all cells, described in section 1.4.2. Viruses use integrins to gain entry to cells and adenovirus, as a transfection vector, is dependent on the cell expression of integrin $\alpha_v\beta_5$ and to a lesser extent $\alpha_v\beta_3$ (Delporte *et al.* 1997;Hashimoto *et al.* 1997;Summerford *et al.* 1999;Takayama *et al.* 1998;Tatebe *et al.* 1998).

The LID vector has a high *in vitro* transfection efficiency compared with lipofectamine-based methods and it is relatively simple to use making it a practical tool to use within the laboratory(Jenkins *et al.* 2000). The design of the vector is for the integrin targeting element, a small peptide, to bind the vector to the target cell and enhance gene transfection. The effectiveness of LID transfection integrin is thought to depend upon the integrin profile of the target cell and also the cationic properties of the peptide (Hart *et al.* 1998). In principle, modifications in the peptide should allow different integrins to be targeted. The technique is established in this laboratory for transient transfections. The protocol is described in detail below, section 2.4.1 – 2.4.6. MM cells have not been transfected with this system previously and so initial experiments were to establish optimal transfection conditions.

Stable transfection produces cell lines in which all cells contain the transfected gene and this is passed onto daughter cells with cell expansion and passage. This is useful for measuring changes in total cell collagen production following transfection of a vector producing an intracellular protein such as Smad7, since transient transfection will transfect perhaps 20% of cells, but a 20 % change in collagen production in a cell culture may not yield significant changes. By using stable transfection to produce cell lines in which all cells are transfected, any change in collagen production is more likely to be measurable. In the *in vivo* model of MM, described in section 2.7, tumours are induced from cells grown in culture and so stably transfected cells can also be used to grow tumours and assess the effect of Smad7 over-expression on tumour growth.

A retroviral technique was used in collaboration with Dr Walter Low and Professor Mary Collins (Institute of Immunology and Molecular Pathology, University College London) to create stable transfectants. The technique is well established in Professor Collins laboratory, with Dr Walter Low providing expertise in the transfection process. The system uses HIV derived replication-defective retroviral particles generated by transient co-transfection of human kidney cells with a three plasmid combination required for packaging, reverse transcription and integration(Naldini *et al.* 1996). The packaging plasmid construct contains the human cytomegalovirus (hCMV) immediate early promoter, which drives the expression of all viral proteins required in transfection. The second plasmid encodes a heterologous envelope protein with high stability, which allows for viral vector concentration by ultra-centrifugation. The third plasmid is the transducing vector, containing the cis-acting sequences of HIV required for packaging, reverse transcription and integration as well as unique restriction sites in to which the cDNA of the chosen gene for transfection can be cloned.

Once the vector has been created, it is applied to the target cells and results in the stable transfection of the chosen gene. These cells will continue to express the chosen gene and can be used both *in vitro* and *in vivo* to examine the effects of the resulting gene over-expression.

2.4.1 Transient transfection using the lipofectin-integrin-DNA (LID) system

This is a liposome based method of transfection that targets integrins to increase transfection efficiency, using a lipofectin-integrin-DNA (LID) vector (Hart *et al.* 1998).

2.4.2 Transfection mixture

The transfection mixture is composed of three elements: Lipofectin (L; a cationic liposome preparation), an integrin-targeting peptide (I; that has a sixteen-lysine tail which allows it to bind DNA), and cDNA (D; the plasmid for transfection) – see section 1.8.1. These elements are combined in a specific optimised weight ratio of Lipofectin : integrin-targeting peptide : DNA of 0.75: 4: 1 respectively (Hart *et al.* 1998), where upon they combine electrostatically to form the LID complex. The

transfection mixture was made by diluting the stock components in OptiMEM (Gibco-BRL) freshly on the day of transfection. The integrin targeting peptide, "Peptide 6" (produced by Zinsser Analytic, Maidenhead, UK), which is designed to bind specifically to the integrin α5β1 (sequence - $[K]_{16}$GACRRETAWACG), was dissolved in OptiMEM at a concentration of 0.1 mg/ml. Plasmid DNA was dissolved in OptiMEM at 1 μg/100 μl and lipofectin dissolved in OptiMEM at a concentration of 0.75 μg/100 μl (Lipofectin is supplied at 1 mg/ml (Gene Medicine, Texas, USA)). Lipofectin was mixed with the peptide before adding the plasmid. The complexes were then allowed to form for 30-60 min before further dilution with Optimem to the required concentration of DNA. Two other peptides were also used, peptide 8 (sequence – $[K]_{16}$GACDCRGDCFCA), which targets integrin α4β1 and peptide 1 (sequence - $[K]_{16}$GACRGDMFGCA), which targets the RGD component of integrins non-specifically. These peptides were used in the LID complex to assess its transfection efficiency of targeting different integrins in MM cells.

2.4.3 Assessment of transfection efficiency in MM cells

The LID vector has not previously been used to transfect MM cells and so the initial experiments were to determine the optimal transfection conditions for MM cell transfection using this system. This involved finding the most efficient peptide of those available, comparing different DNA concentrations and assessing the level of maintained protein expression over time following transfection, to see if levels remained constant for the duration of experiments using transfected cells.

2.4.4 Comparison of peptides used in LID complex

Vector induced expression of green fluorescent protein (GFP) was used to assess cell transfection rates *in vitro.* The GFP plasmid is a 4.7kb expression vector (pEGFP-N3 see figure 2.7) that encodes a red-shifted variant of wild-type GFP, which has been optimised for brighter fluorescence and higher expression in mammalian cells(Chalfie *et al.* 1994). It is available commercially and can be amplified (see section 2.3.3) to maintain stocks. This plasmid was used in the LID complex at 1μg/ml final concentration as described in section 2.4.1 and three separate transfection mixtures made using peptides 1, 6 and 8 (see section 2.4.1).

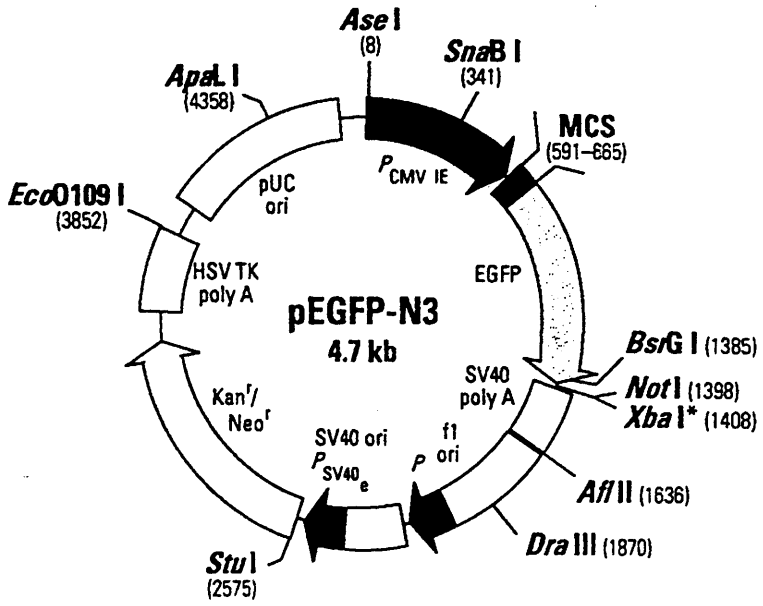

Figure 2.7 pEGFP-N3 vector. Restriction sites are shown. As published by Clontech Laboratories Inc.

MM cells were seeded into 24 well plates and grown until visual confluence in culture medium (normal cells transfect more efficiently when sub-confluent, however the MM cells appeared to transfect as efficiently or more efficiently when the cultures are dense). The media was then removed from the cells and the cells washed with PBS. 0.25 ml of the LID transfection medium was applied to each well at room temperature. Four wells were treated with each of the three transfection mediums. Cells were incubated with the transfection medium for 5-6 hours at 37°C in 10% CO_2. The transfection medium was then removed and replaced with culture medium containing 1% FCS to allow recovery following transfection (10% FCS is sometimes used for cell recovery following transfection, but for the MM cells using the LID vector, 1% FCS was adequate). Transfected cells are identified by expression of GFP, visualised under an inverted fluorescent microscope. To calculate the transfection rate, the cells were trypsinised at 24 hr post transfection (allowing enough time for GFP synthesis) and counted as described in section 2.1.7 under normal light conditions and then under fluorescent light for visualizing transfected cells. The percentage of cells expressing GFP is then calculated for each of the three groups. This was repeated twice in the murine cell lines, AB22 and AC29.

2.4.5 Comparison of DNA concentration used in the LID complex

To compare the effect of using different DNA concentrations in the transfection medium, three separate LID complexes composed of peptide 6 were prepared with GFP plasmid at a final DNA concentration of 1, 2 and 5 μg/ml. Transfection efficiency was calculated as described in section 2.4.3.

2.4.6 Assessment of transfection over time

AB22 cells were transfected as described in section 2.4.4 with a LID complex containing peptide 6 and GFP at a final concentration of 1μg/ml. Total and fluorescing cells were counted at 24 and 56 hours to assess GFP expression over time.

2.4.7 Retroviral Stable Transfection

A retroviral system based on the human immunodeficiency virus (HIV) was used for stable gene transfer into MM cells creating lines over-expressing either Smad7 or a control vector. The technique, described by Naldini *et al.*, 1996(Naldini *et al.* 1996), uses HIV derived replication-defective retroviral particles generated by transient co-transfection of 293T human kidney cells with a three plasmid combination required for packaging, reverse transcription and integration. The three-plasmid expression system was obtained from and used in collaboration with Professor Mary Collins and Dr Walter Low at the Institute of Immunology and Molecular Pathology, University College London. Essentially, it contains the packaging plasmid construct, containing the human cytomegalovirus (hCMV) immediate early promoter, which drives the expression of all viral proteins required in transfection. This plasmid is defective for the production of the viral envelope and the accessory protein Vpu. Cis-acting sequences crucial for packaging, reverse transcription and integration of transcripts derived from the packaging plasmid have been eliminated. The second plasmid encodes a heterologous envelope protein – the vesicular stomatitis virus glycoprotein (VSV-G) with high stability, which allows for particle concentration by ultra-centrifugation. The third plasmid is the transducing vector (pHR), containing the cis-acting sequences of HIV required for packaging, reverse transcription and integration as well as unique restriction sites in to which the

Smad7-Flag cDNA (cut from the pcDNA3 vector described in section 2.3.1) was cloned to create the vector pHR'CMV-Flag-SMAD7-IRES-EGFP (see section 2.3.5).

293T human kidney cells, which are highly transfectable, were grown in 6 well plates using DMEM containing 10% FCS and penicillin/streptomicin (100U/ml). At sub-confluence (~70%) they were transfected in OptiMEM (Invitrogen) with plasmid at a mass ratio of 3:3:1 of packaging:transfer:envelope (to a total of 30μg DNA) using Lipofectamine (Invitrogen), which contains a liposome suspension, according to the manufacturer's instructions. Lipofectamine transfection produces near 100% transfection rates in human 293T cells. The transfection medium was left on the cells for 16 hours and the transfection medium then exchanged for 10% FCS in DMEM. The cells were left in DMEM containing 10% FCS for 2 days and the virus particles generated by the 293T cells harvested by filtration of the cell medium through a 450nm filter (Sartorius) followed by ultra-centrifugation. The medium was spun at 50,000g for 2 hr at room temperature using a AH629 rotor in a Beckman refrigerated centrifuge (Beckman instruments, Palo, CA). The pellet was resuspended in 1ml DMEM containing 10% FCS, which could be stored at -80°C. A second harvest was taken 2-3 days later.

To titrate the viral stocks, cultured 293T cells were seeded at $5x10^5$ cells on a 24 well plate and grown until 70% confluence. They were then transduced with serially diluted, concentrated viral vector stocks. GFP-positive fluorescent cells were counted using con-focal microscopy and excitation-emission at 470 nm measured. Viral vector titre was determined as the average number of GFP-positive cells per 20 1-mm^2 fields multiplied by a factor to account for plate size, and dilution of the viral stock. The viral titre was calculated at 5×10^6 per ml. MM cells were transfected by application of 2×10^6 viral particles in 0.25 ml of DMEM to sub-confluent MM cells (70-80%) in six well tissue culture plates. Four human MM cell lines were transfected: JU77, LO68, ONE58, and NO36 and three murine MM cell lines: AB1, AB22, and AC29. Each cell line was transfected with the Smad7 expressing construct pHR'CMV-FLAG-SMAD7-IRES-EGFP (that also expresses GFP) and a parallel group transfected with its control pHR'CMV-IRES-EGFP, which expresses GFP alone. Cells that had been transfected express GFP as well as Smad7 and this can be visualised by fluorescence microscopy. This confirmed that all cells seen were expressing GFP i.e. all cells had been transfected and no further cell selection was

performed – see results section 3.2.5. Following transfection, the cells were grown to confluence, passaged and grown in 75 cm^2 flasks to confluence before being frozen down and placed in the cell bank (see section 2.1.5) until required.

2.5 Assessment of collagen expression by MM cells

The production of collagen by MM cells and their response to stimulus or specific inhibitors was measured in two ways. The first measured the response at gene level by assessing the activity of a pro-collagen gene promoter reporter vector transfected into MM cells. This method allows rapid measurements of gene activity from a reporter vector transfected into the target cells by measuring luciferase activity, as the truncated promoter region of procollagen is linked to a firefly luciferase gene. When the promoter region is stimulated the construct produces luciferase that can then be measured as described in section 2.2.2. The level of activity of the reporter was measured under a number of conditions described, including transfection with Smad7 i.e. a dual transfection of the gene reporter vector and Smad7.

2.5.1 Procollagen gene promoter activity in MM cells following transfection of a procollagen gene promoter luciferase reporter

To assess the collagen gene response of MM cells to TGFβ, a procollagen gene promoter reporter system was used. An expression vector containing a 2.3kb fragment (sequences between –2310 to +115) of the mouse promoter region of the COL1A1 gene for α_1 (I) procollagen (PGLIα), upstream of the firefly luciferase gene was kindly provided by Dr Jill Norman, Department of Medicine, UCL, London(Norman *et al.* 2001). This construct was used in a LID complex using a DNA concentration of 1μg/ml as described in section 2.4.1 to transfect murine AC29 cells. A similar expression vector containing a 3.5kb fragment of the human α_2 (I) procollagen promoter gene (based on the vector described by Boast *et al.* (Boast *et al.* 1990), with luciferase cDNA cloned into the vector in place of CAT) kindly supplied by Francesco Ramirez, Brookdale Centre for Molecular Biology, Mount Sinai School of Medicine, New York, was used to transfect human derived Ju77 cells. 0.25 ml of the LID transfection media was added to each well in 24 well plates with four repeats per group. After 6 hours the transfection media was removed and replaced by 1% FCS

supplemented culture medium for 16hr. The medium was replaced with serum-free media for 6 hours, then treated with 1 ng/ml $TGF\beta_1$ in serum-free medium. Luciferase activity was measured between 15 and 24 hours in four repeats as described in section 2.2.2. From this an optimal time-point was selected for the assay with these cells.

2.5.1.1 Assessment of procollagen gene promoter reporter luciferase activity

Following incubation with $TGF\beta_1$, cells grown under the conditions described in section 2.5.1 were harvested for luciferase activity. Briefly, the media was removed and the cells washed with cold PBS (chilled to 4°C). Cell lysis buffer (100 µl, Promega, Southampton, UK) was added to each well for 20 – 30 min at room temperature. Remaining cells were disrupted with a cell scraper if still attached to the plate. The lysate was centrifuged at 300g at 4°C for 5 min and 10 µl of the supernatant added to 100 µl of luciferase assay substrate (Promega). Luminescence was measured in a single channel luminometer (TD-20/20, Steptech Instruments, Stevenage, UK) for 15 seconds following a 3 second delay. All measurements were repeated in groups of four and the mean calculated and expressed as relative light units (RLU). The total protein concentration was measured for each lysate using a protein assay kit (BCA, Pierce, Rockford, USA) with bovine serum albumin used as a standard control (described in section 2.6.6). Each individual luciferase reading was corrected for protein concentration to give a final reading of luciferase activity expressed as RLU per mg of protein.

2.5.1.2 Dual transfection of MM cells with a procollagen gene promoter luciferase reporter and Smad7

A LID transfection medium was made using the PGL1α procollagen promoter luciferase reporter plasmid and Smad7-Flag plasmid as a dual transfection complex. Essentially, the transfection process is the same as that described in section 2.4.4, but using two separate DNA plasmids instead of one. The DNA plasmid concentrations are each halved so that the final DNA concentration remains constant. A control dual transfection medium was made using the reporter plasmid and the empty vector pcDNA3 as a control for the Smad7. AC29 MM cells were grown in 24 well tissue culture plates and at confluence LID transfection medium added to the cells (at DNA

concentration of 1μg/ml using 0.25ml per well), repeated in quadruplicate. Following transfection, overnight serum rescue and 6 hours pre-incubation, as described in section 2.3.1, the cells were treated with 1ng/ml $TGF\beta_1$ in fresh serum-free medium. The experiment was stopped after 24 hours and luciferase activity measured as described in section 2.5.2. 10 μl of each lysate was used to measure the protein concentration as described in section 2.6.6.

2.5.2 Assessment of Collagen Production by MM cells

The second method of assessing collagen expression is to measure the total production of collagen by cells by measuring Hydroxyproline (hyp) levels using reverse-phase HPLC(Campa *et al.* 1990). Hyp is an essential component of collagen that makes up 12.2% of the total collagen protein (w:w). The method, developed by this laboratory produces extremely accurate measurements of pico-molar amounts of hyp and can be used to measure *in vitro* collagen production and the collagen content of tissue samples, such as MM tumours.

2.5.2.1 Measurement of Hydroxyproline

The effect of 0 – 10 ng/ml $TGF\beta_1$ on collagen production in MM cells was determined. Furthermore, collagen production was assessed following inhibition of the Smad pathway by Smad7 transfection (see section 2.4.7 on the creation of stably expressing Smad7 MM cell lines), inhibition of ERK1/2 activity using the specific MEK1 inhibitors UO126 and PD98059, and inhibition of p38 kinase using SB203580.

2.5.2.2 Cell culture conditions

Cells were grown to visual confluence, trypsinised as described in section 2.1.4, and re-suspended in DMEM containing 10% FCS before being seeded at a density of 2.5 x 10^4 cells/well in 24-well plates. Once confluent, the media was removed and replaced with 0.5 ml of pre-incubation medium containing 4 mM glutamine, 50 μg/ml ascorbic acid, 0.2mM proline and 1% FCS or serum-free medium and incubated for 24h. The medium was replaced with 0.5 ml fresh pre-incubation medium alone or 0.5ml pre-incubation medium containing 10 μM UO126,

50 μM PD98059 or 1.5, 10 or 15 μM SB203580 and incubated for 15 minutes (this allowed the cells a brief exposure to treatments before $TGF\beta_1$ was added) at 37°C. The medium was removed and replaced with 0.5 ml of fresh media containing either $TGF\beta_1$ (1ng/ml) alone or $TGF\beta_1$ with 10 μM UO126, 50 μM PD98059 or 1.5, 10 or 15 μM SB203580, or the inhibitors alone. Control groups consisted of MM cells exposed to fresh pre-incubation media alone for the 24h incubation period. As the UO126, PD98059 and SB203580 compounds are diluted in DMSO, the same amount of DMSO was added to other groups in experiments involving these compounds (i.e. 50μl for PD98059 experiment, 10μl for UO126, 1.5, 10 or 15 μl for SB203580, all in 0.5 ml medium). A plate containing cells exposed to fresh pre-incubation medium was stored at –40°C without further incubation to determine the background level (t_0) of hydroxyproline present in the culture medium and cell layer at the start of the incubation period and cell counts performed on an identical plate. The remaining plates were then incubated for a further 24h with parallel sets of plates treated in the same way to determine cell number. At the end of the incubation period, cell counts were performed on these plates (see 2.5.8) whilst plates set up for hydroxyproline measurements were frozen at –40°C, prior to analysis.

2.5.2.3 Parallel tissue culture plates for cell counts

Cell counts were performed on 24 well plates treated in parallel to those for measuring hydroxyproline with four repeat wells per group. At the end of the incubation period, culture media was removed and the cell layer washed with 1 ml PBS to remove any remaining serum. 250 μl of trypsin/EDTA was added and the cells incubated for approximately 2 minutes. Rounding and detachment of the cells was observed using an inverted phase-contrast light microscope. To re-suspend the cells and protect them from prolonged exposure to active trypsin, 750 μl of DMEM containing 10% FCS was added to the cell suspension. An aliquot from each well was removed and counted as described in section 2.1.7.

2.5.2.4 Cell harvesting and recovery of ethanol-insoluble fraction

Frozen plates described in section 2.5.4 were left to thaw at RT and then the cell layer scraped into the medium (total volume 0.5 ml) and aspirated. Each well was washed with 0.5ml PBS and the washings combined with the initial aspirate. 2 ml of absolute alcohol was added to give a final concentration of 67% (v/v) ethanol and proteins were precipitated in this solution at 4^0C overnight. Free amino acids and small peptides remain in the ethanol soluble fraction, which was separated from the ethanol insoluble fraction by passing the samples through 0.45 μm Durapore® membrane filters (Millipore). The protein pellet was washed by passing with a further 2ml of 67% (v/v) ethanol through the filter.

2.5.2.5 Acid Hydrolysis

Each 0.45 μm filter was placed in a Pyrex heat/acid resistant tube using forceps and 3ml of 6M HCl added. Each tube was capped and hydrolysed at 110°C for 16 hours. After cooling a small aliquot of charcoal was added to each tube and vortexed to de-colorize the sample. The solution was then filtered through a 0.65 μm membrane filter (Millipore) to leave a colourless solution. 150 μl of this sample was then transferred to an ependorf tube with a perforated cap and evaporated to dryness under vacuum using a centrifugal sample concentrator (Savant SpeedVac Plus SC110, Life Science International).

2.5.2.6 Amino acid derivatisation

The dried samples were dissolved in 100 μl of water and buffered with 100μl of potassium tetraborate (0.4 M, pH 9.5). A 100 μl aliquot of 36 mM 7-Chloro-4-nitrobezo-2-oxa-1, 3-diazole (NBD-Cl) in methanol (144 mg NBD-Cl in 20 ml methanol) was added and the solution derivatised for 20 min at 37°C protected from light. The reaction was stopped by reducing the pH with addition of 50 μl of 1.5M HCl and 150 μl of concentrated Buffer A (167 mM sodium acetate, pH 6.4, in 26% acetonitrile (v/v)). Samples were then filtered through a Durapore® (Millipore) 0.2

μm pore size filter before loading on to the High-Pressure Liquid Chromatography (HPLC) auto-sampler.

2.5.2.7 Chromatographic conditions

The auto-sampler injects 100 μl of derivatized sample onto the HPLC column. Samples were separated on a Beckman System Gold HPLC apparatus (Beckman Ltd, High Wycombe, UK), with a reverse-phase cartridge column (LiChroCART LiChrospere, 250 mm x 4 mm diameter, 5 μm particle size, 100RP-18) protected by a directly coupled precolumn (LiChrosorb, 4 x 4mm diameter, 5 μm particle size, 100RP-18). NBD derivatives were eluted with an acetonitrile gradient, generated by changing the relative proportions of buffers A and B over time (see table 2.1). Buffer A (8% (v/v) acetonitrile and 50mM sodium acetate, pH 6.4) was freshly prepared and run through the column for 40 minutes before the first sample in order to equilibrate the column. Solutions of hydroxyproline (hyp) were prepared and used as standards (50pmol hyp). These were run as the first three and last three samples in each HPLC run. Absorbance was monitored at 495nm and processed on a chromatography computing integrator for quantitative analysis.

2.5.2.8 Quantification of hydroxyproline

A peak corresponding to hyp eluted after 5-6 min and the hyp content was determined by comparing the peak area of samples generated on the chromatogram to that generated from the average of the standard solutions. To correct for the amount of hyp present in the cell layer and the medium at the start of the incubation, the quantity of hyp present in the samples derived from the t_0 plate (see section 2.5.8) was measured and this subtracted from values of subsequent samples. All values were then corrected for cell number and expressed as nmol of hyp/10^6 cells/24hours. Hyp is quantified using the following calculation:

$$\text{Nmol hyp} = \frac{\text{acid hydrolysis volume (3000µl)}}{\text{Volume aliquot dried (150 µl)}} \times \frac{\text{500µl reaction mix}}{\text{100 µl loaded on column}} \times \frac{\text{HPLC value}}{1000}$$

$$\text{To correct for cell number :} \quad \frac{\text{nmol hyp}}{\text{cell number}} \times 10^6 = \text{nmol} / 10^6 \text{ cells} / 24 \text{ hr}$$

Collagen is calculated assuming a hydroxyproline content of 12.2% (w/w).

Mobile phase	A – 8% Acetonitrile (v/v), 50mM sodium acetate, pH 6.4 B – 75% Acetonitrile (v/v), 25% water	
Flow rate	1.00ml/min	
Temperature	40°C	
Detection	495 nm	
Gradient	Time (min)	% B
	0	0
	5	5
	6	80
	12	80
	12.5	0
	25	0

Table 2.1 Chromatographic conditions for Hydroxyproline analysis by Reverse-Phase Liquid Chromatograpy (modified from Campa *et al.*,(Campa *et al.* 1990))

2.6 Protein analysis - Western Blotting and Protein Assay

Western blotting was used to examine cells for the expression of specific proteins. To confirm that the stable transfection of MM cells using the retroviral vector had been successful, Western blotting was performed to look for the Flag peptide, which is expressed when Smad7 is expressed as a result of transfection. This differentiates it from endogenously expressed Smad7.

To assess cell signalling activity, measurement of phosphorylated signalling proteins was performed using Western blotting. Smad signalling occurs following the phosphorylation of receptor Smads, such as Smad2. Similarly the phosphorylation of MAPK signalling proteins: ERK1/2, p38 kinase and JNK, are markers of their

activation. Measurement of the phosphorylated form of these proteins using specific antibodies therefore demonstrates signalling activity. Western blotting is also useful to assess the expression of particular proteins by cells. In these experiments the expression of the TGFβ type I receptors ALK1 and ALK5 are measured to assess whether there is differential expression of these receptors on MM cells. In the tumour model, differential expression of these receptors following the transfection of Smad7 is also measured since Smad7 should cause down-regulation of the receptor.

Protein quantification was also performed using a commercial protein assay (Pierce BCA Protein Assay), described in section 2.6.6, and used for the quantification of protein concentration for the luciferase assays described in 2.5.1.

2.6.1 Cell culture conditions and sample processing for Western blotting

MM cells were grown as a monolayer in six well plates with 10 % FCS supplemented DMEM. At confluence, cells were pre-incubated in serum-free media for 24 hours. Cells were then incubated with fresh media containing $TGF\beta_1$ (1 ng/ml) for between 1 min and 4 hours. The media was removed and the cell layer rinsed with PBS at 4°C. For examination of phosphorylated signalling protein; phospho-Smad2, phospho-ERK and phospho-p38 kinase, the cell layer was rinsed with a chilled (4°C) mixture of sodium vanodate 50 mM and sodium fluorate 1 mM in PBS to inhibit dephosphorylation. This step was not required for examining non-phosphorylated proteins; β-actin, activin receptor-like kinases 1 and 5 (ALK1, ALK5) and the labelling peptide Flag, targeted to confirm Smad7 expression. 200 µl of Tris Glycine SDS lysis buffer (Invitrogen) was added to each well and the plates frozen at –40°C. The samples were later thawed and the cell layer scraped into the buffer. The sample was transferred to an ependorf tube and urea added to a final concentration of 2M and mercaptoethanol at final concentration of 4% (v:v) added to each sample. The caps of the ependorfs were pierced and the samples incubated at 95^0C for 5 minutes. This process denatures and breaks down sulphide bonds between proteins.

2.6.2 Protein gel electrophoresis

After cooling to room temperature, 10-30 µl samples of cell preparations described in section 2.6.1 were loaded onto a 10% polyacrylamide gel (20.25 ml

ddH_2O, 12.5 ml 1.5 M Tris-HCl (ph 8.8), 0.5 ml 10 % (v:v) SDS stock, 16.5 ml Acrylamide/Bis (30% stock), 250 µl 10% ammonium persulphate, 25µL TEMED (N,N,N',N'tetramethylethylenediamine)) using a Hamilton syringe. 10 µl of protein ladder (SeeBlue, Invitrogen) was also loaded and gels run at 120-130 V for 2-3 hours.

2.6.3 Protein transfer

The gel was laid on a nitro-cellulose membrane (Hybond ECL, Amersham Pharmacia Biotech, UK) between two sets of four pieces of blotting paper and two pairs of sponges to compress the gel/membrane interface within the transfer block. Electrophoretic transfer onto the nitrocellulose membrane was carried out across a gradient of 200 mA for 1-2 hours. Confirmation of protein transfer was made by covering the membrane in Ponceau S solution (0.1% Ponceau (w/v) in 5%acetic acid (v/v), Sigma-Aldrich Ltd) for 2-3 min and rinsing under dH_2O. Protein bands appeared red. The band density directly correlated with protein concentration giving an indication of protein loading and any variation between lanes.

2.6.4 Antibody labelling

The membrane described in section 2.6.3 was washed in TBS (50 mM Tris-HCl (pH 7.4), 150 mM NaCl) and incubated on a shaker for 2 hours at room temperature in a blocking solution (skimmed milk powder in TBS at 5% concentration (w/v)) to block non-specific antibody binding sites. The membrane was transferred to a 50 ml polypropylene tube and incubated with agitation overnight at 4^0C or between 30 and 60 minutes at room temperature (see table 2.2) with the primary antibody diluted in blocking solution. The membrane was then washed briefly in TBST (TBS and 0.05% Tween®) or ddH2O and incubated on a shaker at room temperature for 1 hour with horse radish peroxide (HRP) conjugated secondary antibody (see table 2.2). Finally it was washed in TBST for 30 minutes with at least three wash changes.

2.6.5 Antibody binding visualisation

Binding was visualised by adding 2 ml of luminol reagents (1:40 solution A:B, ECLplus Western blotting reagents, Amersham International, UK) to the membrane and incubating at room temperature for 5 min. The excess reagent was then allowed to run off the membrane, which was then wrapped in Saran film and exposed to ECL photo film (Kodak, Amersham Pharmacia Biotech, UK) in the dark. The reagent becomes fluorescent following activation by the horseradish peroxidase conjugated to the secondary antibody. This fluorescence is detected on the ECL film at sites of antibody binding. The time of film exposure was varied following an initial 30 second exposure, which gave an indication of band luminescence (seen after development in a film processor (Fuji X-ray film processor, Fuji Photo Film Comp. Ltd, Japan)) and ranged between 10 seconds and 10 minutes. The antibody labelled protein bands appear as dark linear bands on a transparent background.

Target protein	Primary Antibody	Secondary Antibody
FLAG	5μg/ml Anti-FLAG® M2 monoclonal antibody isolated from a murine cell culture that binds to FLAG fusion proteins (Sigma). 30 minutes at room temperature	1:2000 Anti-mouse HRP conjugated IgG. 30 minutes at room temperature (Sigma)
Phosphorylated Smad2	0.5 – 2 μg/ml rabbit immunoaffinity purified IgG to phospho-Smad2 (Ser465/467) (Upstate cell signalling solutions, NY 12946). 4°C overnight	1:2000 Anti-rabbit HRP conjugated IgG. 1 hour at room temperature (Santa Cruz Biotechnology Inc)
ALK1	2.5 – 5 μg/ml polyclonal antibody against carboxy terminus of ALK1 (Santa Cruz Biotechnology Inc). Overnight at 4°C.	1:2000 Anti-rabbit HRP conjugated IgG. 1 hour at room temperature (Santa Cruz Biotechnology Inc)
ALK5	5 – 10 μg/ml rabbit polyclonal antibody against a peptide mapping within an internal domain of TGFβ RI (ALK5) (Santa Cruz Biotechnology Inc) Overnight at 4°C.	1:2000 Anti-rabbit HRP conjugated IgG. 1 hour at room temperature (Santa Cruz Biotechnology Inc)
β-Actin	1:1000 polyclonal rabbit antibody. 4°C overnight. (Sigma)	1:2000 Anti-rabbit HRP conjugated IgG. 1 hour at room temperature (Santa Cruz Biotechnology Inc)
Phosphorylated ERK	1:1000–1:2000 rabbit polyclonal antibodies to phospho-Thr202/Tyr204 peptide of human p44 MAP kinase (supplied in 200μl solution, antibody concentration not specified, Cell signalling Technology, Inc). 4 hours at 4°C	1:2000 Anti-rabbit HRP conjugated IgG. 1hour at room temperature (Santa Cruz Biotechnology Inc)
Phosphorylated p38 kinase	1:1000 rabbit polyclonal to Thr180/Tyr182 peptide of phospho-peptide of p38 kinase (supplied in 200μl solution, antibody concentration not specified, Cell signalling Technology, Inc), 4 hours at 4°C	1:2000 Anti-rabbit HRP conjugated IgG. 1hour at room temperature (Santa Cruz Biotechnology Inc)

Table 2.2 Antibodies used in Western blotting showing the concentrations of antibody used and incubation conditions.

2.6.6 Protein Assay

The assay (Pierce BCA Protein Assay) reagent assesses the reduction of Cu^{2+} to Cu^{1+} by protein in an alkaline medium by sensitive and selective colorimetric detection of the cuprous cation (Cu^{1+}). A purple coloured reaction is produced by the chelation of two molecules of the reagent that contains bicinchoninic acid (BCA) with one cuprous ion. This complex is water-soluble and exhibits a strong absorbance at 562 nm that is linear with increasing protein concentrations over a working range of 20 to 2000 μg/ml. 10 μl of supernatant from each cell lysate was transferred into a well on a 96 well plate. 10 μl of each standard (bovine serum albumin was diluted from 2mg/ml stock solution using the same diluent as the cell samples (i.e. cell lysis buffer) to concentrations of 25μg/ml up to 2000μg/ml to produce standard protein concentrations) and 10 μl of diluent were each transferred into blank wells and this was repeated in quadruplicate. 200 μl of "working reagent" (50 : 1 parts A : B) was added to each well and the plate briefly mixed on a shaker for 30 seconds before being covered and incubated for 30 min at 37°C. After incubation, the plate was allowed to cool to room temperature before the absorbance was read at 562 nm on a plate reader (Titertek Multiscan MCC/340). Using the standard protein measurements a standard curve was constructed and the linear portion used to calculate the protein concentration of the lysate samples.

2.7 *In vivo* Animal Model of Malignant Mesothelioma

2.7.1 Animals and cell lines

Tumours were derived from the three murine MM cell lines AB1, AB22 and AC29 following transplantation into mice. Cells stably expressing Smad7 or control vector were created as described in section 2.4.7 such that for each of the three murine lines (i.e. non-transfected controls) there was a Smad7 expressing and a control vector expressing equivalent cell line. All AB1 and AB22 cell line derived tumours were grown following transplantation into BALB/c mice and all AC29 cell line derived tumours in CBA mice (syngeneic matches). Cells were counted and diluted in DMEM to a concentration of 1 x 10^7 cells per ml. BALB/c and CBA mice were obtained from

Harlan, UK (SPF, female, 6 to 8 weeks old) and maintained under standard conditions in the animal facility at University College London.

2.7.2 Establishing flank tumours

MM tumours were grown subcutaneously on the hind flanks of mice. The positioning of the tumour on the flank is useful as i) it allows easy access for MM cell inoculation, ii) the tumours are clearly visible allowing easy monitoring of size, and iii) the tumours appear to cause little or no distress to the animal. The mice were anaesthetized by inhalation of a combination of Halothane at 2 – 4 L/min and Oxygen (4 L/min) in an induction chamber and maintained on this combination of gases for the duration of the procedure. The hind flank of each mouse was shaved and 100 μl of the suspended cells at 1 x 10^7 cells per ml (i.e. 1 x 10^6 cells) injected subcutaneously into each flank (figure 2.8). The mice were recovered in a dry heated cage before being returned to their cage. In each experiment groups of 10 mice (one tumour on either flank) were used for each treatment regimen. 5 mice were sacrificed at 10 days post MM cell inoculation and 5 mice at day 15.

Figure 2.8. Murine model of MM. 1 x 10^6 MM cells injected sub-cutaneously into each shaven flank of syngeneic mice

In experiments examining the effect of over-expressing Smad7 in cell lines, 3 animal groups were established: i) non-transfected MM cells ii) control transfected MM cells and iii) Smad7 transfected cells. When tumours reached 1cm in largest diameter measured externally using callipers or at 28 days had passed then the experiment was ended and all animals culled by cervical dislocation. The tumours were removed and half placed in 4% paraformaldehyde for histological and immunohistological analysis and half placed directly in liquid Nitrogen to be used for

collagen analysis. The tumours were then weighed before further processing of the paraformaldehyde samples and storage of the frozen samples at –80°C.

2.7.3 Treatment of mice using systemic TGFβ neutralising antibodies

Using AC29 cells, the protocol described in section 2.7.2 was used to establish tumours in syngeneic BALB/c mice. Mice were pre-treated on the day prior to AC29 MM cells inoculation with TGFβ antibodies ($TGF\beta_1$-specific, $TGF\beta_2$-specific or pan-specific TGFβ, supplied in collaboration with Cambridge Antibody Technologies (CAT), Cambridge, UK), or matched IgG control antibodies (CAT supplied) or PBS. These were administered by intra-peritoneal injection to achieve systemic absorption. The dose of antibody was 5mg/kg diluted in 50μl of PBS for both the neutralising TGFβ antibodies and their controls, or 50μl of PBS alone. This treatment was repeated 3 times per week, following the initial dose on the day before MM cell inoculation, until the end of the experiment i.e. when tumours in any group had reached the maximum size permitted or at specific time points. In each treatment group there were either 5 or 10 mice allowing for either one or two timepoints depending on the experiment design.

2.7.4 Histological processing of tumour samples

Half of the tumours harvested were fixed overnight at 4°C in 4% paraformaldehyde as described in section 2.7.2. They were then washed in two changes of PBS for 30 min each and then placed in a solution of PBS and 15% sucrose overnight and washed for a further 30 min in PBS. The tumours were placed in 50% ethanol for 30 min and then stored in 70% ethanol. Tumours were then processed and embedded in paraffin in an automated tissue processor (LeicaTP 1050). Each tumour was orientated and formed into wax blocks before being placed on ice and 4 – 5 μm sections cut on a retraction microtome (Shandon, UK). Sections were collected on poly-L-lysine coated glass slides (4 μm) for immunohistochemical analysis or on glass slides (5 μm) for histological staining. After placement on the slides the sections were blotted once between damp blotting paper and left to dry at room temperature overnight before use the following day.

2.7.5 Processing of tumour samples for HPLC analysis of collagen content

Half the tumours harvested were snap-frozen in liquid nitrogen. Tumour samples were then crushed under liquid nitrogen and stored at –80°C. An aliquot of approximately 10mg was weighed and added to 2ml 6M HCl in a Pyrex tube. Each tube was capped and hydrolysed at 110°C for 16 hours. After cooling a small aliquot of charcoal was added to each tube and vortexed to de-colorize the sample. The solution was then filtered through a 0.65 μm membrane filter (Millipore) to leave a colourless solution. The solution was then diluted 1 in 200 using 6M HCl and 100 μl of this sample then transferred to an ependorf tube with a perforated cap and evaporated to dryness under vacuum using a centrifugal sample concentrator (Savant SpeedVac Plus SC110, Life Science International). Calculation of hydroxyproline content was then performed as described previously in section 2.5.6. with adjustments for the dilutions described above.

2.8 Histological and immunohistochemical staining Techniques

2.8.1 Martius Scarlet Blue (MSB) staining for collagen analysis

An assessment of tumour collagen deposition was made by histological examination of tumour sections following staining using MSB. This technique results in collagen being stained blue, which is then easily identifiable. The collagen content of the tumours was visually assessed following MSB staining of tissue sections. Briefly, sections were de-waxed and rehydrated through xylene and ethanol before being stained in an automated system (Sakura Diversified Stainer, Bayer Diagnostics, UK) capable of staining up to 60 slides simultaneously. Table 2.3 lists the steps involved in this staining procedure.

The sections were then cover-slipped in an automated cover-slip machine (Sakura Coveraid, Bayer Diagnostics, Hants, UK) and examined using an Olympus BX40 light microscope.

Step	Solution	Time (min)
1	Xylene	3
2	Xylene	3
3	100% ethanol	2
4	90% ethanol	2
5	70% ethanol	2
6	Lugol's Iodine	5
7	Thiosulphate (3%)	3
8	Wash	1
9	Celestine Blue	10
10	Wash	1
11	dH_2O	30 sec
12	Haematoxylin	5
13	Wash	30 sec
14	Acid alcohol	20 sec
15	Wash	30 sec
16	Wash	2
17	90% ethanol	30 sec
18	Orange G (0.2% in Picric alcohol)	8
19	dH_2O	5 sec
20	Red Mix (Ponceau de Xylidine 0.5% and Fuchsin 0.5% in 1% Glacial acetic acid)	7
21	dH_2O	20 sec
22	Phototungstic acid (1%)	30 sec
23	dH_2O	20 sec
24	Pontamine sky blue (1% in Glacial acetic acid)	5
25	1% Acetic acid	20 sec
26	70% ethanol	20 sec
27	90% ethanol	20 sec
28	100% ethanol	1
29	Xylene	1
30	Xylene	1
31	Xylene	2

Table 2.3 Modified MSB staining protocol showing the stages involved in the procedure and the time at each station.

2.8.2 Immunohistochemical staining of tumour sections

Tissue sections of tumours 4 μm thick (as described in section 2.7.4) were dewaxed and rehydrated by washing in a sequence of xylene x 2, 100% ethanol x 2, 90% ethanol, 70% ethanol, 50% ethanol, water and finally PBS. The slides were dried around the section without touching the section itself and the section marked and encircled using a wax pen. The slides were then treated with 3% hygrogen peroxide for 10 min in a humidified chamber by dripping the solution onto the horizontal slide – the wax pen mark keeping the solution within the marked area, followed by three washes with PBS for 5 min each wash. The slide was shaken of free liquid and treated with serum, at 1.5% dilution in PBS, for 20 min, in a humidified chamber, using the serum in which the secondary antibody was hosted. This acts as a non-specific tissue blocker. The serum was drained off, without washing, and the primary (i.e. target) antibody added at variable dilutions depending upon previous experience with the antibody. If a new antibody was being used then it was first titrated by running the experiment with a range of antibody dilutions of 0.5 to 20 μg/ml. The experiment was later repeated using the most appropriate antibody dilution. The sections were exposed to the primary antibody overnight in a humidified chamber at 4°C and then washed in PBS for 5 min 3 times. The peroxidase conjugated secondary antibody was then added and left for a further 1 hour at room temperature, in a humidified chamber. Different dilutions of secondary antibody were assessed to find the most effective concentration. At this point, mouse serum could be added for more non-specific blocking if previous results had shown a lot of background staining. The slide was then washed in PBS for 5 min x 3 and staining visualised by exposure to a solution of 600μg /ml 3,3'-diaminobenzidine (DAB; Sigma) and 0.03% H_2O_2. This was prepared using a DAB substrate mixed with 30% H_2O_2 (working solution – 6mg DAB, 10μl 30% H_2O_2 solution in 10ml PBS). The slide was exposed to DAB in a specified DAB chamber in a fume cupboard for 3 - 10 min before being rinsed with ddH_2O. The slide was then counter stained with haematoxylin in an automated staining machine (see section 2.12) and mounted using an automated cover-slip machine (Sakura Coveraid, Bayer Diagnostics, Hants, UK). Finally it was examined using an Olympus BX40 light microscope. In each experiment negative controls were also run. These were a matched IgG primary antibody or no primary antibody or no secondary antibody. The

maximum number of sections to be examined during one experiment was between 15 and 20. Antibodies used were ALK1 and ALK5 as shown in table 2.4, which also shows secondary antibodies used.

Target protein	Primary Antibody	Secondary Antibody
ALK1	2.5 – 5 μg/ml polyclonal antibody against carboxy terminus of ALK1 (Santa Cruz Biotechnology Inc). Overnight at 4°C.	10 μg/ml Anti-rabbit HRP conjugated IgG. 1 hour at room temperature (Santa Cruz Biotechnology Inc)
ALK5	5 – 10 μg/ml rabbit polyclonal antibody against a peptide mapping within an internal domain of TGFβ RI (ALK5) (Santa Cruz Biotechnology Inc) Overnight at 4°C.	10 μg/ml Anti-rabbit HRP conjugated IgG. 1 hour at room temperature (Santa Cruz Biotechnology Inc)

Table 2.4 Antibodies and dilutions used in immunoperoxidase staining of tumour tissue sections.

Chapter 3. Results and Discussion

3.1 The effect of TGFβ blocking antibodies on Malignant Mesothelioma collagen production and tumour growth

This chapter examines collagen production and TGFβ synthesis by Malignant Mesothelioma cells. The hypothesis that TGFβ stimulates collagen production, which enhances tumour growth, is tested by using neutralising TGFβ antibodies to block this proposed autocrine loop.

3.1.1 TGFβ stimulates MM cell collagen production

A fundamental principle of this study is that there is an autocrine growth loop involving TGFβ and collagen synthesis in MM cells, which in turn regulates tumour growth. For this to occur, MM cells have to produce both TGFβ and collagen and furthermore up-regulate collagen synthesis in response to TGFβ. To confirm this, human and murine MM cell lines described in section 2.1.1, were assessed for basal and $TGF\beta_1$ induced hydroxyproline (hyp) production by HPLC (nmol hyp/10^6cells/24hr), as a measurement of collagen synthesis (as described in section 2.5.2). Table 3.1.1 shows collagen production measured basally and following stimulation with 0.1, 1, and 10 ng/ml $TGF\beta_1$ in 4 human and 3 murine MM cell lines. Six of the MM cell lines significantly increased collagen production in response to $TGF\beta_1$ in a dose dependent manner. One human cell line, LO68, demonstrated a maximal response at 0.1 ng/ml $TGF\beta_1$ (basal collagen production of 0.84 ± 0.09 (mean ± SEM) increasing to 1.01 ± 0.12 nmol hyp/10^6cells/ 24hr, $p < 0.05$) with no further increase in collagen production with increasing doses of $TGF\beta_1$. With the exception of LO68 the combined average fold increase in collagen production by these MM cell lines in response to 0.1, 1 and 10 ng/ml $TGF\beta_1$ was 1.6 ± 0.2, 2.9 ± 0.3, and 4.4 ± 0.8. The dose response of two murine MM cell lines, AB22 and AC29, used extensively throughout the study, are also shown graphically in figure 3.1.1.

There are three histological types of MM: sarcomatous, epithelioid and mixed-type. AC29 cells have a sarcomatous morphology whereas AB22 cells are epithelial-like. However, both demonstrate production of high levels of collagen, which increases in response to exogenous $TGF\beta_1$. In humans, both epithelial and

sarcomatous MM are associated with large amounts of collagen deposition, although sarcomatous are the most fibrotic. The basal level of collagen synthesis in AC29 cells was 0.72 ± 0.09 nmol hyp/10^6cells/24hr with fold increases above basal levels of 1.4, 3.3 and 5.3 after 0.1, 1, and 10 ng/ml of TGFβ_1 respectively ($p<0.01$). In AB22 cells basal collagen production of 0.66 ± 0.01 nmol hyp/10^6cells/ 24hr increased by 1.3, 1.8 and 3 fold ($p<0.01$ compared with basal levels for each increase) with 0.1, 1, and 10 ng/ml TGFβ_1 respectively.

Cell line	Hydroxyproline (nmol / 10^6 cells / 24 hours) following TGFβ_1 (ng/ml)				
	0	0.1	1	10	
AB22	0.66 ± 0.01	0.88 ± 0.12**	1.21 ± 0.04**	1.98 ± 0.14**	Murine
AC29	0.72 ± 0.09	1.01 ± 0.10**	2.37 ± 0.22**	3.81 ± 0.31**	
AB1	0.51 ± 0.21	0.72 ± 0.08**	1.31 ± 0.07**	1.53 ± 0.04**	
JU77	0.46 ± 0.16	0.82 ± 0.21**	1.37 ± 0.31**	3.22 ± 0.45**	Human
ONE58	0.27 ± 0.12	0.56 ± 0.10**	0.98 ± 0.17**	1.01 ± 0.27**	
LO68	0.84 ± 0.09	1.01 ± 0.12*	0.93 ± 0.05	0.81 ± 0.11	
NO36	0.62 ± 0.17	0.93 ± 0.09	1.46 ± 0.28	3.27 ± 0.51	

Table 3.1.1 Procollagen production in mesothelioma cell lines following TGFβ_1 stimulation. HPLC was used to measure hyp in confluent MM cells (grown in 0.4 % FCS) 24 hours after treatment with TGFβ_1 (0.1, 1, 10 ng/ml). Hyp levels (nmol / 10^6 cells / 24 hours ± SEM) were corrected for cell number and a students t test performed to assess significant changes between basal and TGFβ_1 –induced procollagen production. * = $p < 0.05$, ** = $p < 0.01$.

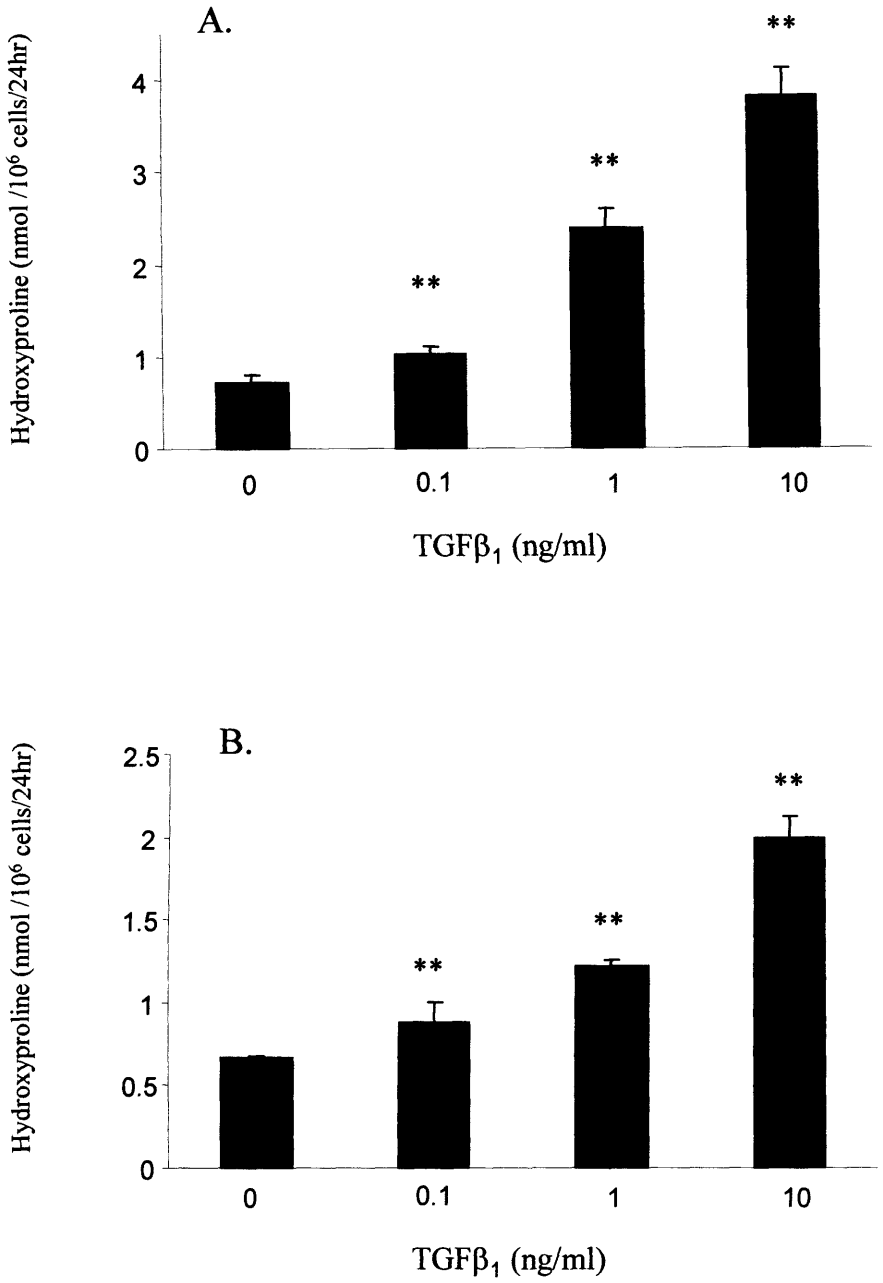

Figure 3.1.1 Collagen production in murine MM cells in response to TGFβ. **A** and **B** show the production of hydroxyproline (nmol/10^6cells/24hr) in response to increasing doses of $TGF\beta_1$ (ng/ml) in AC29 and AB22 MM cells respectively. Each represents the mean of 6 replicates ± SEM. ** = $p < 0.01$ compared with basal non-$TGF\beta_1$ treated levels. The graphs demonstrate a dose dependent increase in collagen production following stimulation by $TGF\beta_1$.

3.1.2 TGFβ synthesis by MM cells

Secreted active TGFβ levels were measured from the seven MM cell lines using the mink lung epithelial cell (MLEC) bioassay, a PAI-1 luciferase assay described in section 2.2. Conditioned medium was generated from each cell line and total cell number recorded. For each experiment a standard curve is generated using known concentrations of TGFβ. A standard curve is shown in figure 3.1.2A demonstrating increased luciferase activity in response to increasing doses of $TGF\beta_1$. The linear portion of the standard curve lies in a range between 0.05 and 0.5 ng/ml. Figure 3.1.2B shows the luciferase activity recorded following MLEC exposure to conditioned medium. The levels of active TGFβ production, corrected for cell number (ng/ 10^6 cells/ 24hours), are shown in figure 3.1.2C and are representative of three repeat experiments. All MM cell lines tested produced significant levels of active TGFβ. Of the murine cell lines, AC29 cells produced the most TGFβ (0.58-0.82 ng/ 10^6 cells/ 24hours) and of the four human lines, NO36 was the most consistent producer of active TGFβ, producing 0.35-0.8 ng/ 10^6cells/ 24 hours. The results of the two repeat experiments are shown in the table 3.1.2 below.

Cell line	Active TGFβ production (ng / 10^6 cells / 24 hr) ± SEM	
	Repeat experiment 1.	Repeat experiment 2.
AC29	0.62 ± 0.010	0.51 ± 0.103
AB22	0.42 ± 0.021	0.32 ± 0.021
AB1	0.55 ± 0.008	0.56 ± 0.009
JU77	0.12 ± 0.011	0.11 ± 0.023
Lo68	0.18 ± 0.019	0.19 ± 0.017
No36	0.58 ± 0.029	0.75 ± 0.031
ONE58	0.86 ± 0.028	0.67 ± 0.048

Table 3.1.2 MM cell active TGFβ production measured using the MLEC bioassay in two repeat experiments.

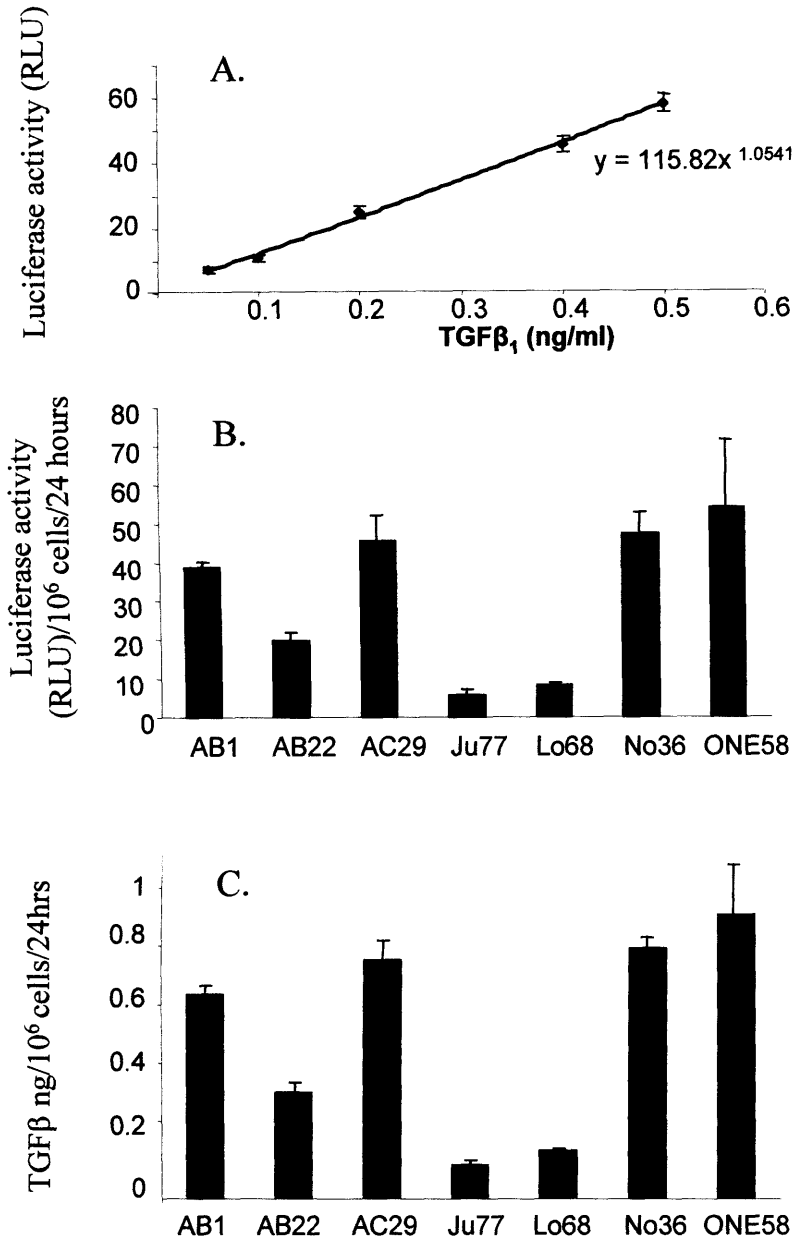

Figure 3.1.2 TGFβ production by MM cells assessed using the MLEC bioassay. **A.** A standard curve for $TGF\beta_1$ stimulated activity was created by assessing luciferase activity (relative light intensity, RLU) over 15 seconds from MLEC cell lysates following incubation with $TGF\beta_1$. Each point represents the mean of 3 replicates ± SEM. The graph equation is shown. **B.** MLEC luciferase activity was then assessed following exposure to the conditioned media samples from 3 murine MM cell lines (AB1, AB22, AC29) and 4 human MM lines (Ju77, Lo68, No36, ONE58) and corrected for cell number. The standard curve (**A**) is then used to calculate active TGFβ production/million cells/24hr, as shown in **C** (each represents the mean of 3 replicates ± SEM).

3.1.2.1 Inhibition of MLEC responses to TGFβ using TGFβ antibodies

To confirm that the luciferase activity measured in the MLEC bioassay was TGFβ induced, activity was measured following exposure of MLEC cells to $TGF\beta_1$ in the presence of a TGFβ pan-specific blocking antibody. Figure 3.1.3 shows that the pan-specific TGFβ antibody suppressed luciferase activity by approximately 90% confirming a TGFβ specific luciferase response. Control murine IgG antibody did not reduce TGFβ-induced luciferase activity.

3.1.2.2 Confirmation of MM cell conditioned medium TGFβ activity in the MLEC bioassay by inhibition with TGFβ antibodies

Experiment 3.1.2.1 was repeated using conditioned medium from MM cells (AB22 and AC29 cells were selected as these were the cell lines used for most experiments) in the presence of neutralising TGFβ antibody and inhibition of luciferase activity was again demonstrated (figure 3.1.4). This showed that TGFβ antibodies inhibited the activity of the luciferase reporter in the presence of MM cell conditioned media, confirming that the activity was specifically due to MM cell produced TGFβ.

3.1.3 Effects of neutralising antibodies on collagen production by MM cells

Pan-specific, $TGF\beta_1$-, and $TGF\beta_2$-specific antibodies were used, along with their matched IgG controls (as supplied by Cambridge Antibody Technologies (CAT) and described in section 2.7.3), to assess the effects of blocking TGFβ on MM cell collagen production. AC29 cells were grown in culture and treated with $TGF\beta_1$ (1ng/ml) pre-exposed to the neutralising or control antibodies, and hyp levels measured after 24 hours incubation (as described in section 2.11). AC29 cells were chosen for these experiments as this cell line was selected for the *in vivo* experiments (reasons outlined in section 3.1.6). Figure 3.1.5A shows the increase in collagen production, expressed as a percentage above basal values. It demonstrates that the $TGF\beta_1$-specific, $TGF\beta_2$-specific and pan-specific TGFβ neutralising antibodies all reduced the collagen response of MM cells to exogenous $TGF\beta_1$, whereas cells

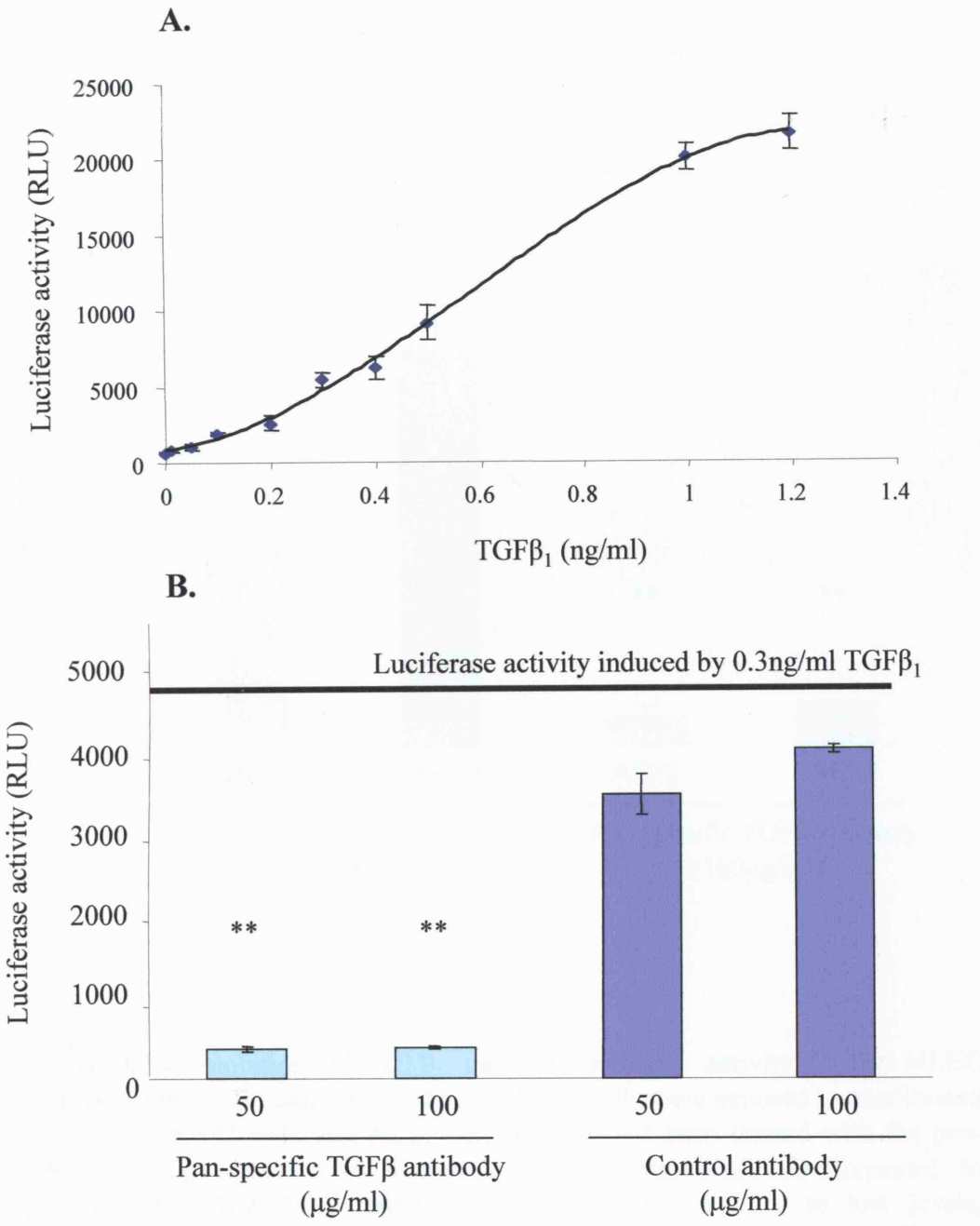

Figure 3.1.3 Inhibition of TGFβ $_1$ induced luciferase activity in the MLEC bioassay using TGFβ blocking antibody. In **A** the standard curve shows the MLEC luciferase activity in response to $TGF\beta_1$ in a 0-1.2 ng/ml dose range. The linear portion of the curve lies in a range between 0.05 and 0.6 ng/ml $TGF\beta_1$ and the dose in the mid-range of this, 0.3 ng/ml, was chosen to test the inhibiting activity of a pan-specific antibody shown in **B**. MLEC cells were exposed to 0.3 ng/ml of $TGF\beta_1$ having first been treated with the pan-specific TGFβ antibody or a matched IgG control antibody (repeated in quadruplicate). The TGFβ antibody reduced activity to very low levels, whereas the control antibody had no significant effect confirming that the activity was due to TGFβ. ** $p < 0.01$

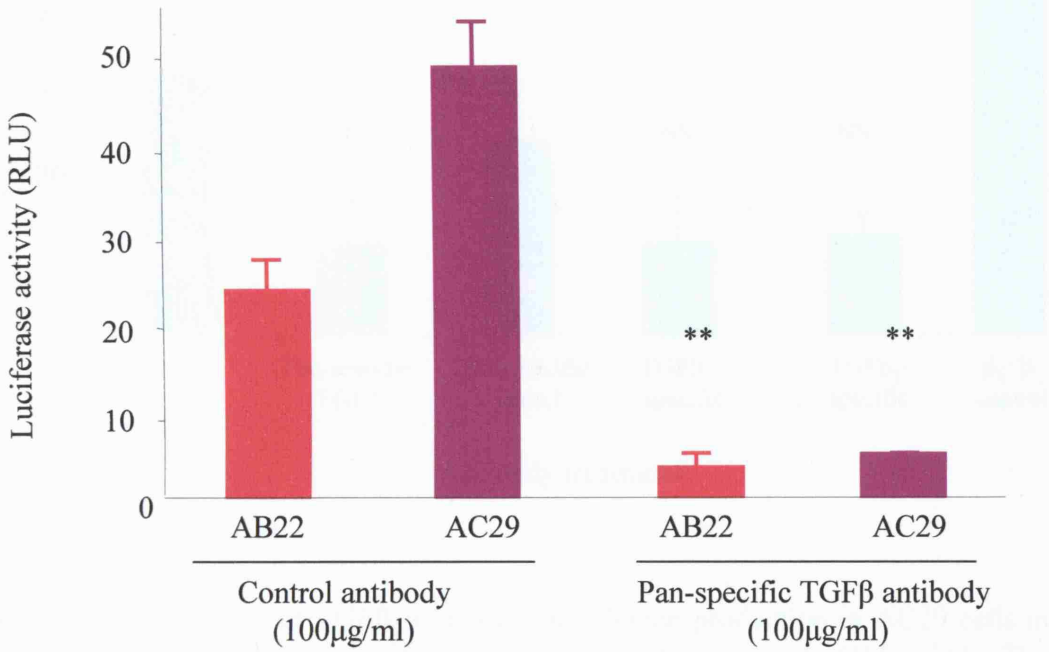

Figure 3.1.4 Inhibition of $TGF\beta_1$ induced luciferase activity in the MLEC bioassay using TGFβ blocking antibody. MLEC cells were exposed to conditioned media from AB22 cells and AC29 cells having first been treated with the pan-specific TGFβ antibody or a matched IgG control antibody (repeated in quadruplicate). The TGFβ antibody reduced MLEC activity to low levels, confirming that the effects on the MLEC cells from MM conditioned media was due to TGFβ. ** $p < 0.01$

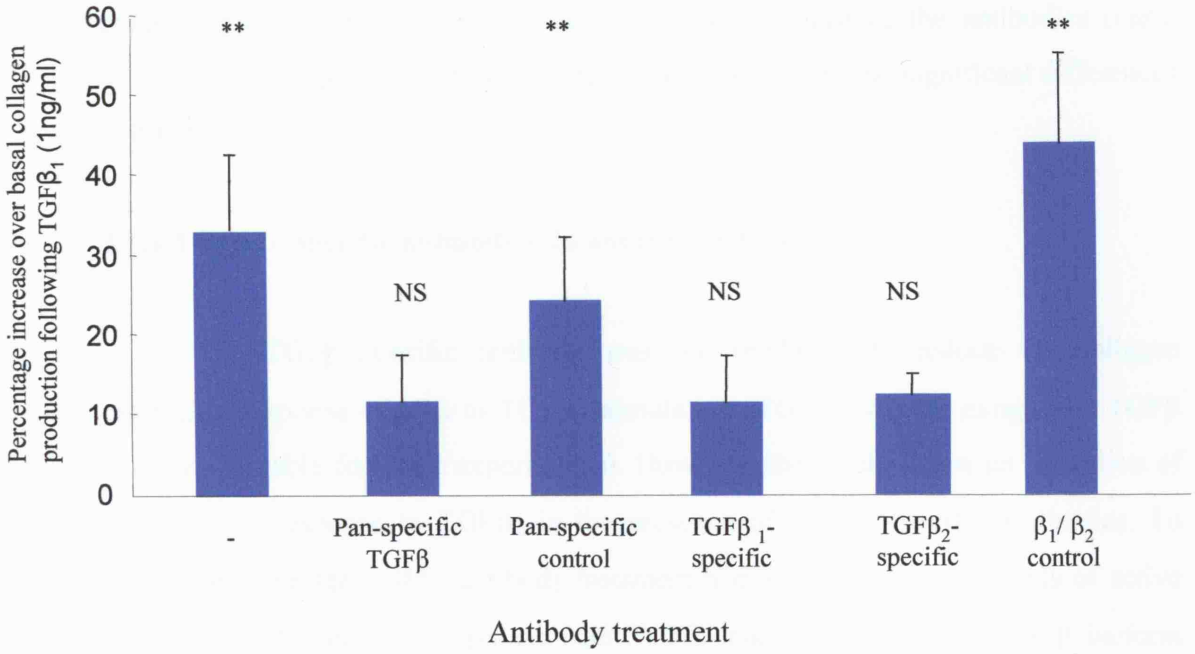

Figure 3.1.5A Effect of $TGF\beta_1$ (1ng/ml) on collagen production in AC29 cells in the presence of TGFβ neutralising antibodies or their controls (100μg/ml). The results are expressed as percentage increases of hydroxyproline production above basal levels at 24 hrs (the mean basal level of hydroxyproline production was 1.01 nmol/10^6 cells). The $TGF\beta_1$-specific, $TGF\beta_2$-specific and pan-specific TGFβ antibodies reduced the collagen response to exogenous $TGF\beta_1$. The basal level of collagen production was not inhibited by either TGFβ neutralising or control antibodies (data not shown). ** = significant increase above basal levels. NS = non-significant increase above basal production.

exposed to the control antibodies still significantly increased collagen production. This was unexpected as TGFβ$_2$-specific antibodies should not have reduced the response to TGFβ$_1$. This is investigated further in section 3.1.4. The basal levels of collagen production remained unchanged in the presence of the antibodies (basal collagen production is not shown on the graph as there were no significant differences between groups).

3.1.4 TGFβ$_2$ – specific antibodies do not inhibit TGFβ$_1$

The TGFβ$_2$-specific antibody was not predicted to reduce the collagen producing response of MM to TGFβ$_1$ stimulation (TGFβ$_1$ was the exogenous TGFβ isoform available for these experiments). However, the results show an inhibition of the collagen response to TGFβ$_1$ in the presence of TGFβ$_2$-specific antibodies. To investigate whether TGFβ$_2$ antibody treatment had any effect on the levels of active TGFβ$_1$, MLEC cells were treated with TGFβ$_1$ and exposed to the TGFβ isoform specific antibodies. A treatment dose of TGFβ to be neutralised was selected by generating a standard curve for TGFβ (figure 3.1.5.B1) and using the linear portion of this curve (figure 3.1.5.B2), a dose of 0.3 ng /ml TGFβ$_1$ was shown to produce luciferase activity at the mid-point of the dose response. Therefore, this dose (0.3 ng /ml TGFβ$_1$) was used to test the effectiveness of the antibodies in inhibiting stimulation of the MLEC bioassay. Figure 3.1.5.B confirms that TGFβ$_2$-specific antibodies have no effect on the response of MLEC to TGFβ$_1$. Therefore, the reason for the inhibition of TGFβ$_1$ induced collagen by TGFβ$_2$-specific antibodies remains unclear, but it is not due to cross-reactivity between the TGFβ$_2$-specific antibody and TGFβ$_1$. Interestingly, TGFβ$_1$-specific antibodies reduced the response to TGFβ$_1$ by 60%, whereas pan-specific TGFβ antibodies reduced activity by more than 90% - see discussion section 3.1.14.

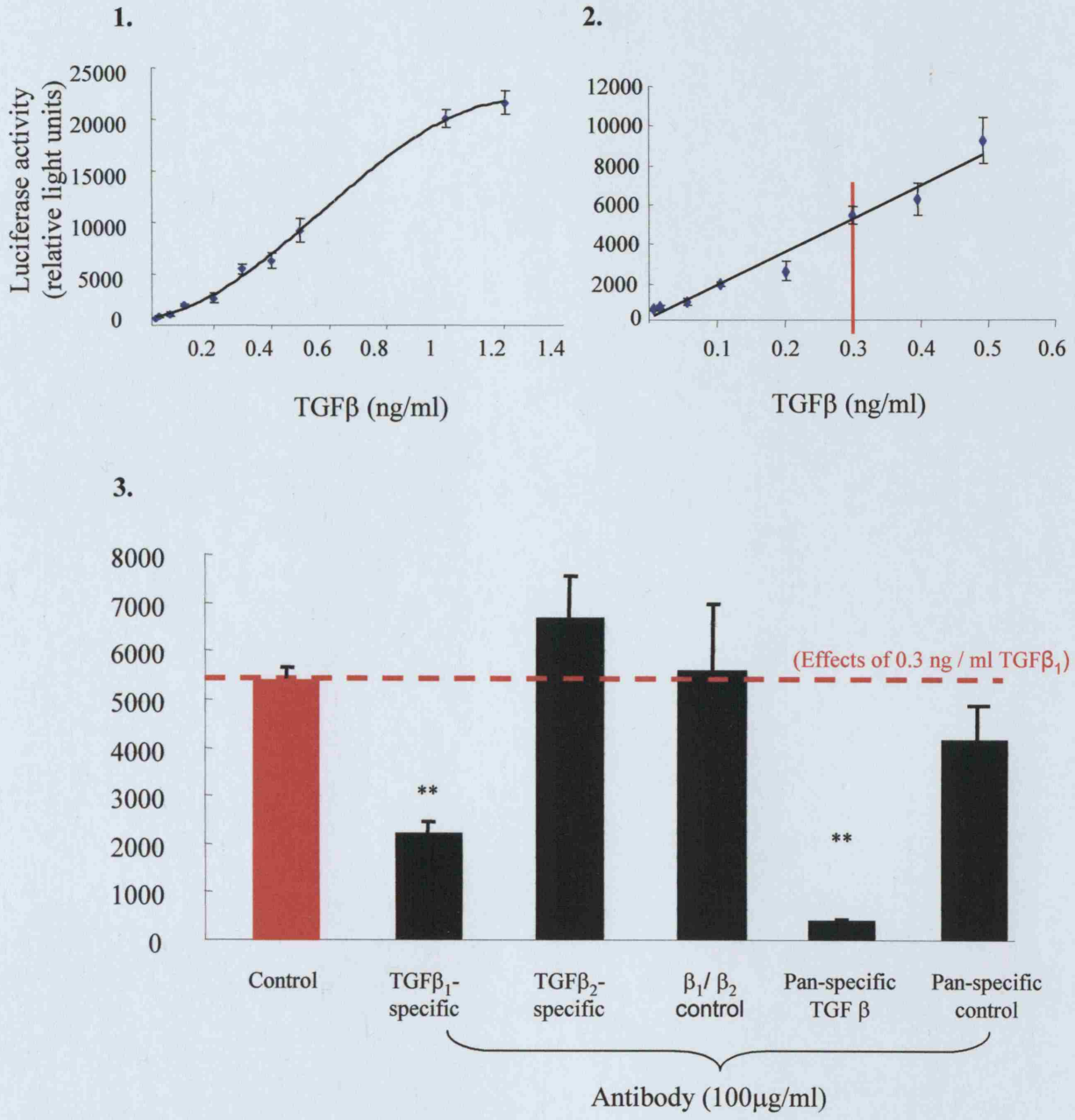

Figure 3.1.5B The effects of TGFβ neutralizing antibodies on the activity of the MLEC bioassay. **1**. Standard curve achieved following increasing doses of $TGF\beta_1$. **2.** shows the linear portion of this curve and the level of activity at the midway point (0.3 ng/ml $TGF\beta_1$) is marked. MLECs were then exposed to $TGF\beta_1$ at the selected dose (0.3 ng/ml) along with the neutralising antibodies at 100 μg/ml (**3**.) Pan-specific TGFβ antibodies almost completely block the effect of $TGF\beta_1$. $TGF\beta_1$-specific antibodies reduce the activity by 60% and the $TGF\beta_2$-specific antibodies have no significant effect. There are no significant effects with the control antibodies. ** = $p < 0.01$ compared with control

3.1.5 Murine model of MM to assess the effect of TGFβ neutralising antibodies on tumour growth

To assess the effects of TGFβ antibodies on the growth of tumours *in vivo*, a murine model of MM tumour growth, described in section 2.7.2, was used. Mesothelioma tumours were grown on the flanks of syngeneic mice using AB1, AB22 and AC29 cells. Tumours tended to grow as discrete nodules on the flanks of the animals following sub-cutaneous injection of MM cells. Figure 3.1.6 shows tumours in vivo. These were relatively easy to remove from the surrounding tissue, unless inoculation had occurred at a deeper level i.e. into the muscle layer rather than the sub-cutaneous space – see below. New vessel formation was seen supplying the tumour from adjacent stromal tissue, indicated in the figure. All three tumour lines grew tumours, but AC29 cell tumours grew faster than the other two cell lines. Histologically, all three tumour lines contained high quantities of ECM, indicated by blue stained collagen on Martius Scarlett Blue (see 2.8.1) stained tissue sections cut from paraffin wax embedded tumours, shown in figure 3.1.7. The AC29 derived tumours histologically appeared to be the most abundant in collagen deposition. Figure 3.1.8 shows an example of a tumour section indicating some of the basic tumour structures. Tumours were highly cellular with marked deposition of ECM. New blood vessels are seen carrying red blood cells. Although mitotic cells are seen throughout the tumour section, they are predominantly found in the outer regions and tissue margins. This reflects the high cell turnover and rapid growth of these tumours with the most active areas occurring at the tumour borders. This is the area where tumour cell turnover, interaction with the surrounding normal tissues, and angiogenesis is thought to occur, allowing tumour growth and local tissue invasion.

If MM cells were inoculated into the deeper muscle layer of the flank they behaved more invasively and less predictably. Figure 3.1.9 shows that there is a greater deposition of collagen and increased invasion by MM cells along tissue planes at these deeper inoculation sites. These tumours required greater dissection to separate them from the surrounding normal tissue and clear tumour borders could not always be delineated. These were interesting findings as they suggest different tumour cell behaviour dependent upon surrounded normal cell types and could warrant further investigation. For the purposes of these experiments it was considered best to inoculate cells sub-cutaneously only, as this site produced tumours that were more

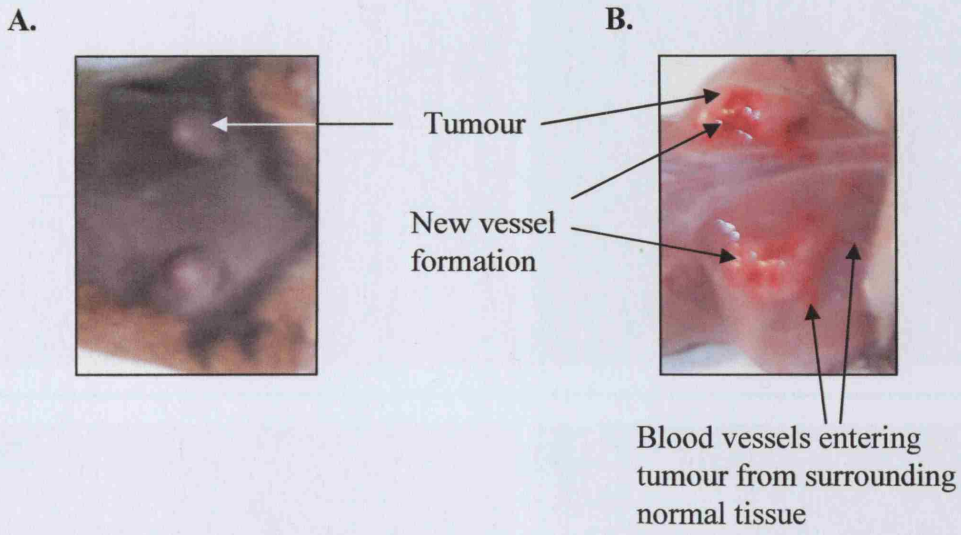

Figure 3.1.6 Murine model of MM. Tumours grown on the flanks of syngeneic mice are clearly visible subcutaneously (A) allowing for estimation of size (a maximum of 1cm external diameter is permitted). At dissection the tumours are situated on the flanks on top of the connective tissue layer above the muscle layer (B). The tumours were well vascularised with blood vessels noted to be growing in to the tumour from surrounding normal structures.

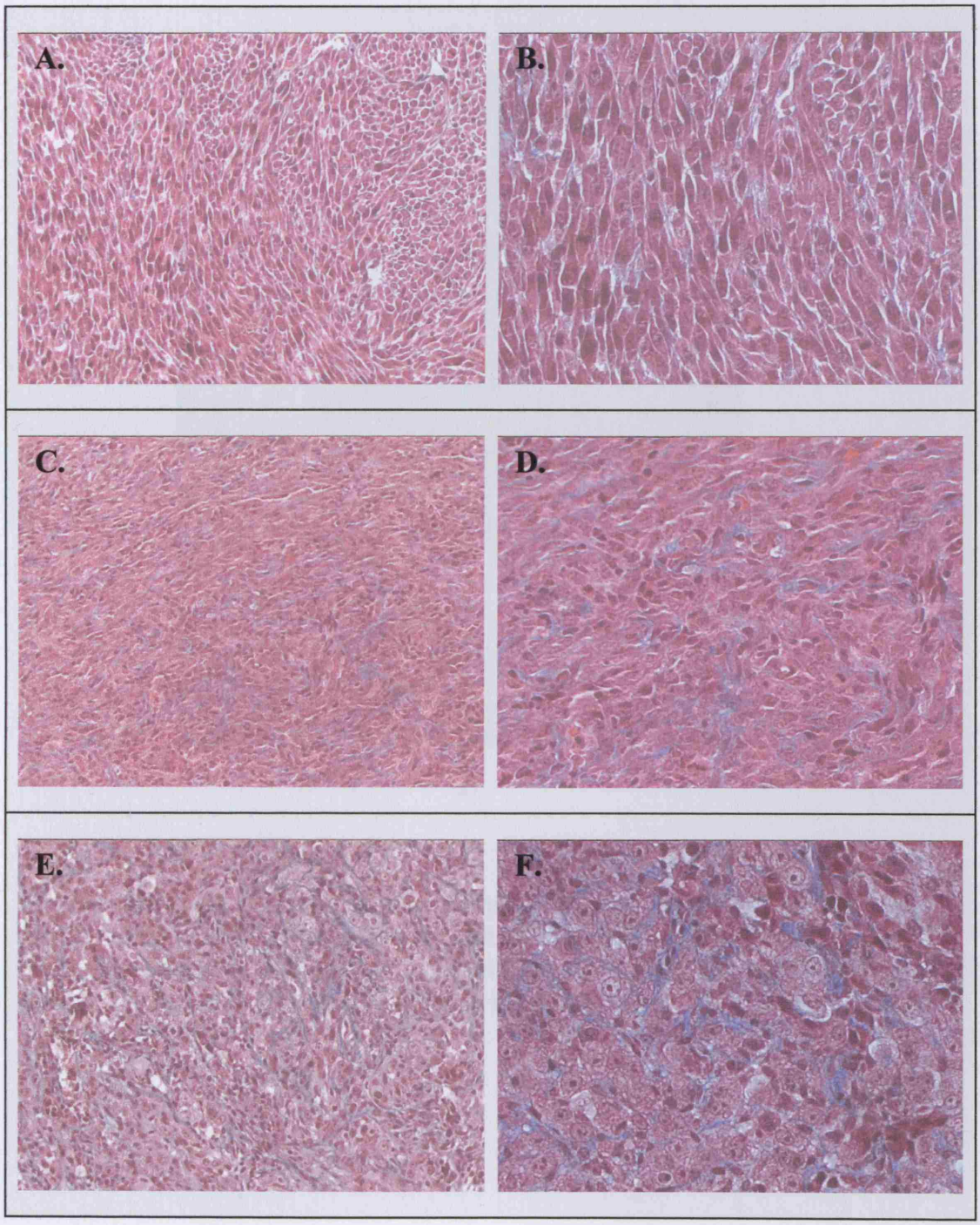

Figure 3.1.7 Martius Scarlet Blue (MSB) staining of murine mesothelioma tumour sections highlighting collagen content. **A** AB1 derived tumour section at 20x normal magnification and **B** at 40x. **C** AB22 derived tumour section at 20x and at 40x magnification in **D**. **E** shows AC29 cells at 20x and **F** at 40x. Collagen is stained blue and varies in its intensity and deposition between tumours derived from different cell lines. AC29 derived tumour appear to contain the most collagen. These figures are representative of sections from each of the three cell lines.

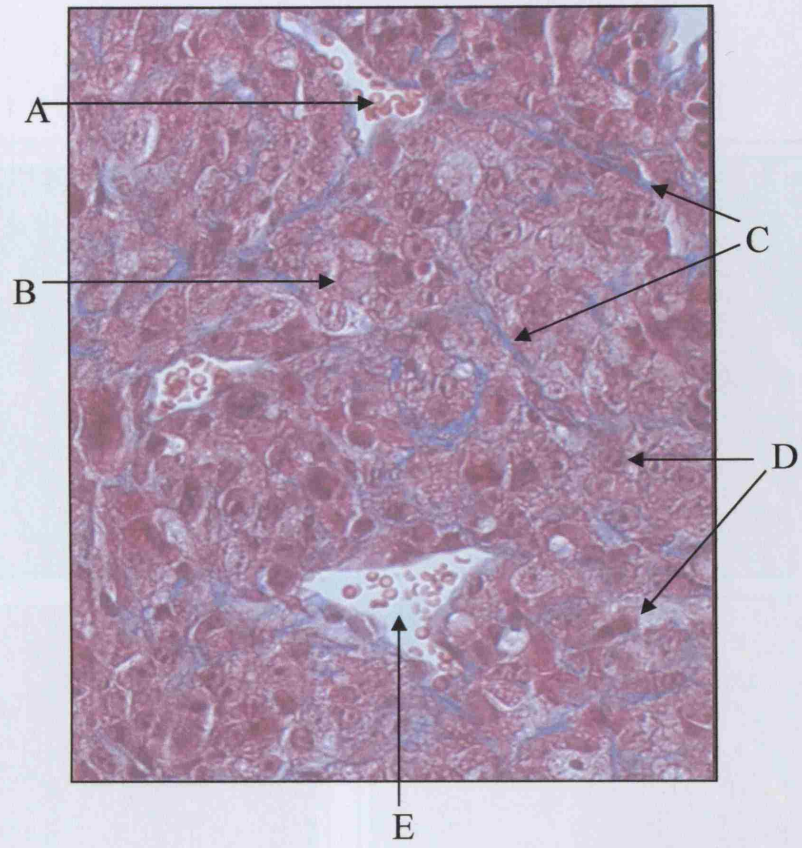

Figure 3.1.8 MM tumour structures**.** Section through an AC29 cell derived murine mesothelioma tumour stained with MSB highlighting typical structures (x40 magnification). **A** Red blood cells within a newly formed blood vessel. **B** typical tumour cells. **C** strands of blue stained collagen. **D** Mitotic tumour cells. **E** blood vessel

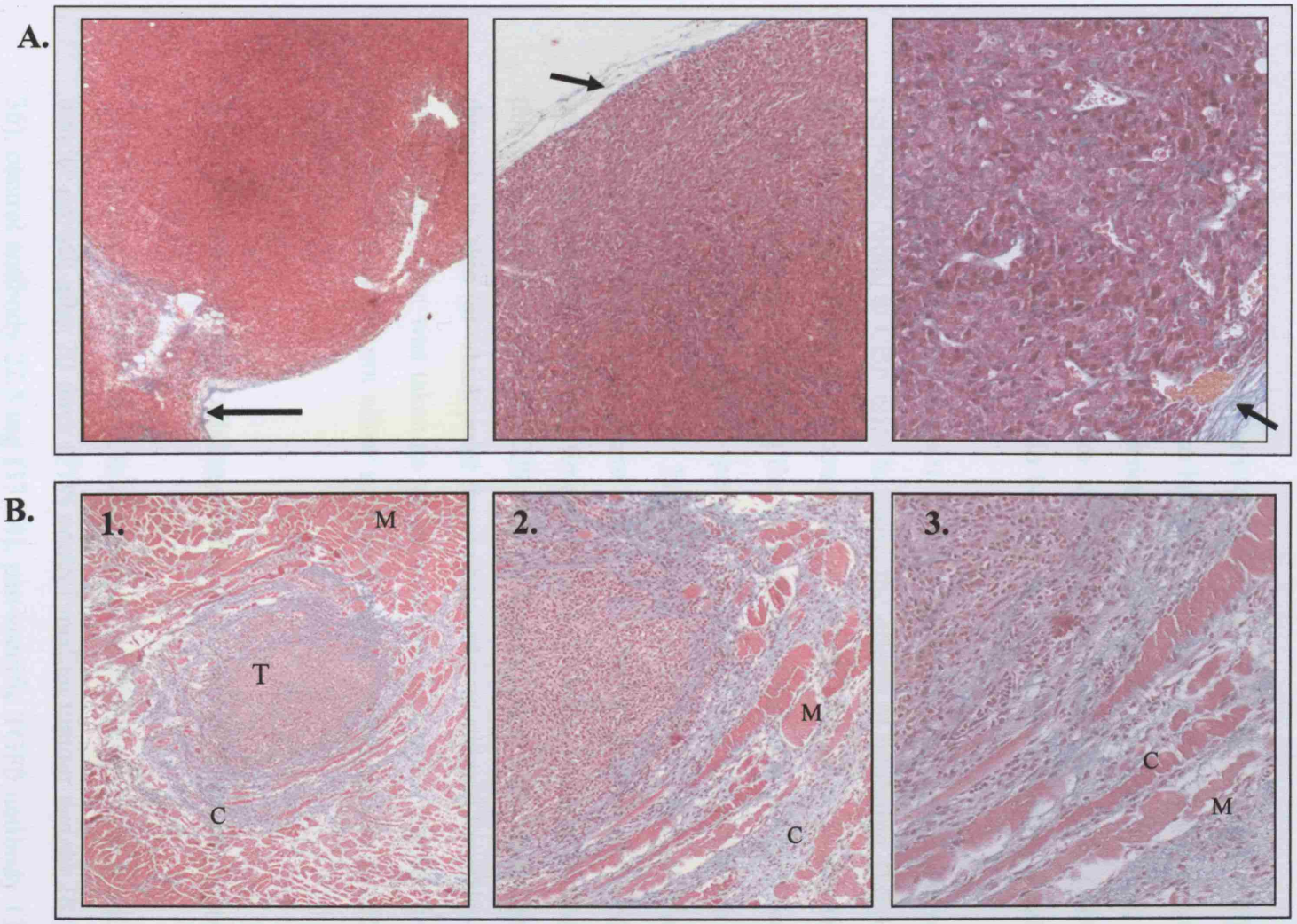

Figure 3.1.9 Tumour interaction with normal tissue. Panel **A** shows examples of tissue capsule formation (arrowed), which is blue stained with MSB demonstrating its high collagen content, at 10x (1), 20x (2), and 40x (3) normal magnification (taken from different sections). Panel **B** shows tumour situated in muscle fibres at 10x, 20x and 40x magnification (1.,2., and 3. respectively). The tumour T, is surrounded by large depositions of collagen C. Tumour cells are infiltrating the surrounding area and muscle fibres (M) with a predilection to invade through the matrix between muscle fibres.

discrete and were consistent in morphology between experiments. These tumours could be more accurately removed with clear separation from normal tissue - an important prerequisite in comparing tumour weights.

3.1.6 TGFβ neutralising antibodies inhibit *in vivo* MM tumour growth

AC29 cells were chosen for the *in vivo* experiments using TGFβ antibodies as this cell line had been shown to be the greatest producer of both collagen and TGFβ *in vitro*, and were the most consistently tumorigenic cell line *in vivo*, producing the fastest growing tumours from the murine cell lines available (AB1, AB22, and AC29). These findings were in keeping with previously published data of these cell lines (Davis *et al.* 1992).

Neutralising antibodies to TGFβ were systemically administered, via an intra-peritoneal route, to CBA mice to assess the effects of inhibiting TGFβ on the growth of tumours following the inoculation of AC29 MM cells (as described in section 2.7.3). The effects of blocking the three different isoforms of TGFβ were assessed by using $TGF\beta_1$-specific, $TGF\beta_2$-specific, pan-specific and a combination of $TGF\beta_1$- and β_2- specific antibodies (no $TGF\beta_3$-specific antibody was available). In each experiment a 10 day time-point and a 15 day time-point were used to assess the growth of tumours. The latter time-point was chosen as initial experiments had shown this to be a time at which AC29 derived tumours began to show signs of ulceration through the skin (at which point the experiment was stopped for ethical reasons). The 10 day time-point was taken as an intermediate time-point. Earlier time-points were not used as they did not allow sufficient growth of tumours to detect differences in size.

3.1.6a Pan-specific neutralising antibodies reduce MM tumour growth

Figure 3.1.10A shows that pan-specific TGFβ neutralising antibodies reduce tumour growth after 10 days (PBS control median tumour weight 18.0 mg (range 6-36), control antibody 22.5 mg (13-94), pan-specific TGFβ antibody 13.0 mg (4-27)). Using a Mann Whitney U test (since results were non-parametric) there was a significant difference between the pan-specific TGFβ antibody and its control

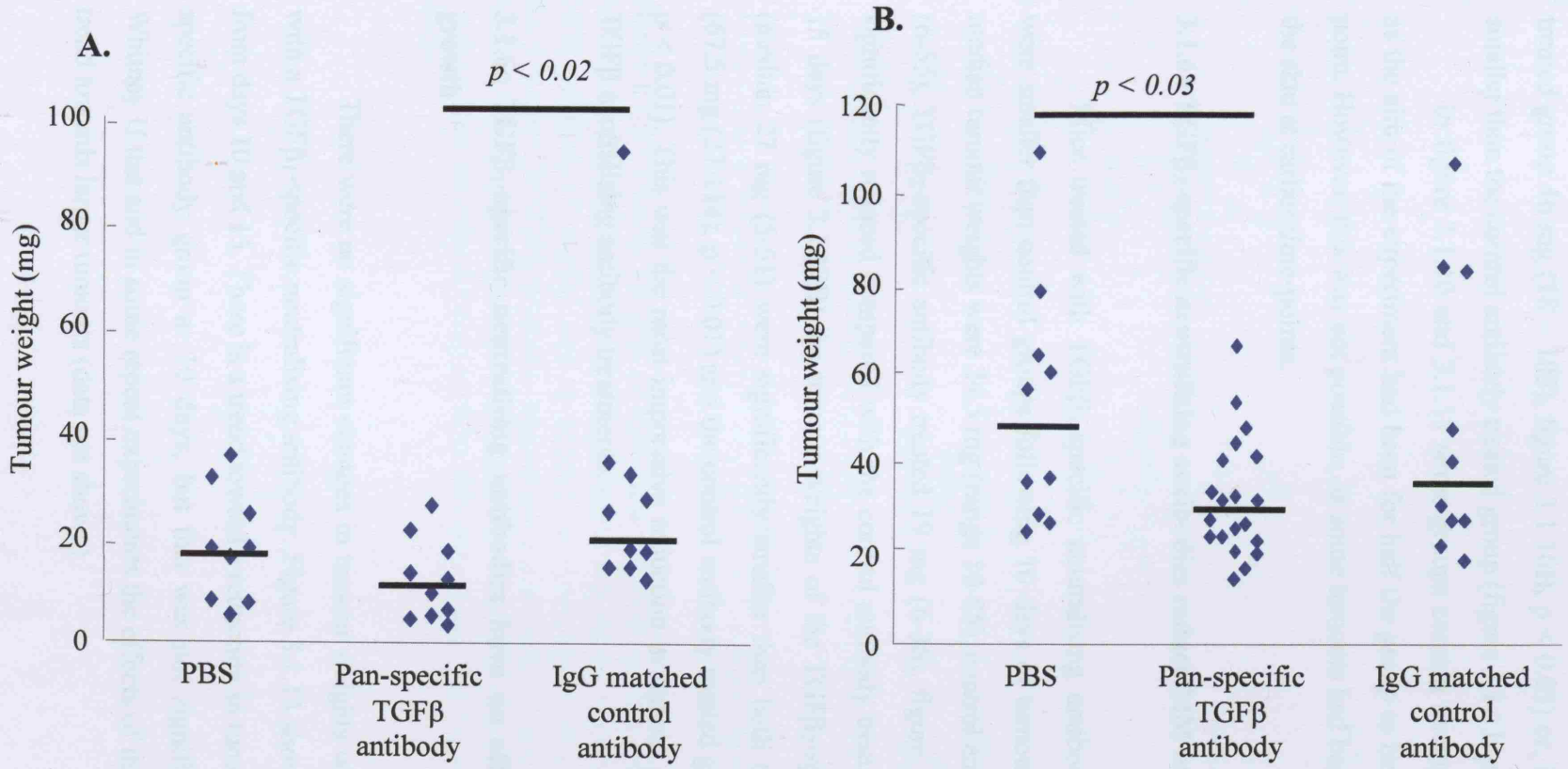

Figure 3.1.10 MM tumour weights 10 days (A) and 15 days (B) after inoculation with AC29 cells in mice treated with intraperitoneal injections of PBS, Pan-specific TGFβ antibody (5 mg/kg), or its IgG matched control (5 mg/kg). The pan-specific TGFβ antibody treated mice had tumours that were significantly smaller than their control antibody treated group at 10 days and smaller than the PBS controls at 14 days. Mann Whitney U test was used to test significance.

antibody ($p = 0.02$). At 15 days the mice treated with the neutralising antibody had tumours smaller than the PBS treated control group (antibody treated median tumour weight 30 mg (range 16 – 65), PBS treated group 46 mg (22 – 109), control antibody treated group 46 mg (18 – 105), figure 3.1.10B, $p < 0.03$) or, in a repeat experiment, smaller than the control antibody treated group (figure 3.1.11, $p = 0.05$).

In figure 3.1.10 and 3.1.11 some groups contain twenty tumours (=10 mice), as the aim of the experiment had been for half the group to be left for a longer time-point. However, this was not possible, as some tumours had began to ulcerate through the skin at earlier time-points.

3.1.6b TGFβ_2-specific neutralising antibodies reduce MM tumour growth

Mice treated with TGFβ_2-specific neutralising antibodies had tumours that were smaller than control groups following 10 days of tumour growth (PBS treated median tumour weights were 24.5 mg (range 10-85), control antibody treated 34.5 mg (6-55), TGFβ_2-specific antibody treated 19 mg (6-36), figure 3.1.12A). Growth was significantly reduced compared with the control antibody treated group, $p < 0.05$. At 15 days (figure 3.1.12B) the tumour weights of the TGFβ_2-specific antibody group (median 27 mg (5-51) were significantly smaller than both the PBS treated group (67.5 mg (27-114), $p < 0.01$) and the control antibody treated group (57 mg (35-193), $p < 0.01$). This was the most impressive reduction in tumour growth seen of all the TGFβ neutralising antibody treatments.

3.1.6c TGFβ_1-specific neutralising antibodies have no effect on MM tumour growth

There were no significant changes in tumour weights when mice were treated with a TGFβ_1-specific neutralising antibody. Figure 3.1.13 shows tumour weight data from days 10 and 15. There is a trend toward a reduction in tumour size in the TGFβ_1-specific antibody group at 10 days, but this was not significant using the Mann Whitney U test and in some repeat experiments the effects of the antibody produced a trend towards larger tumours (data not shown).

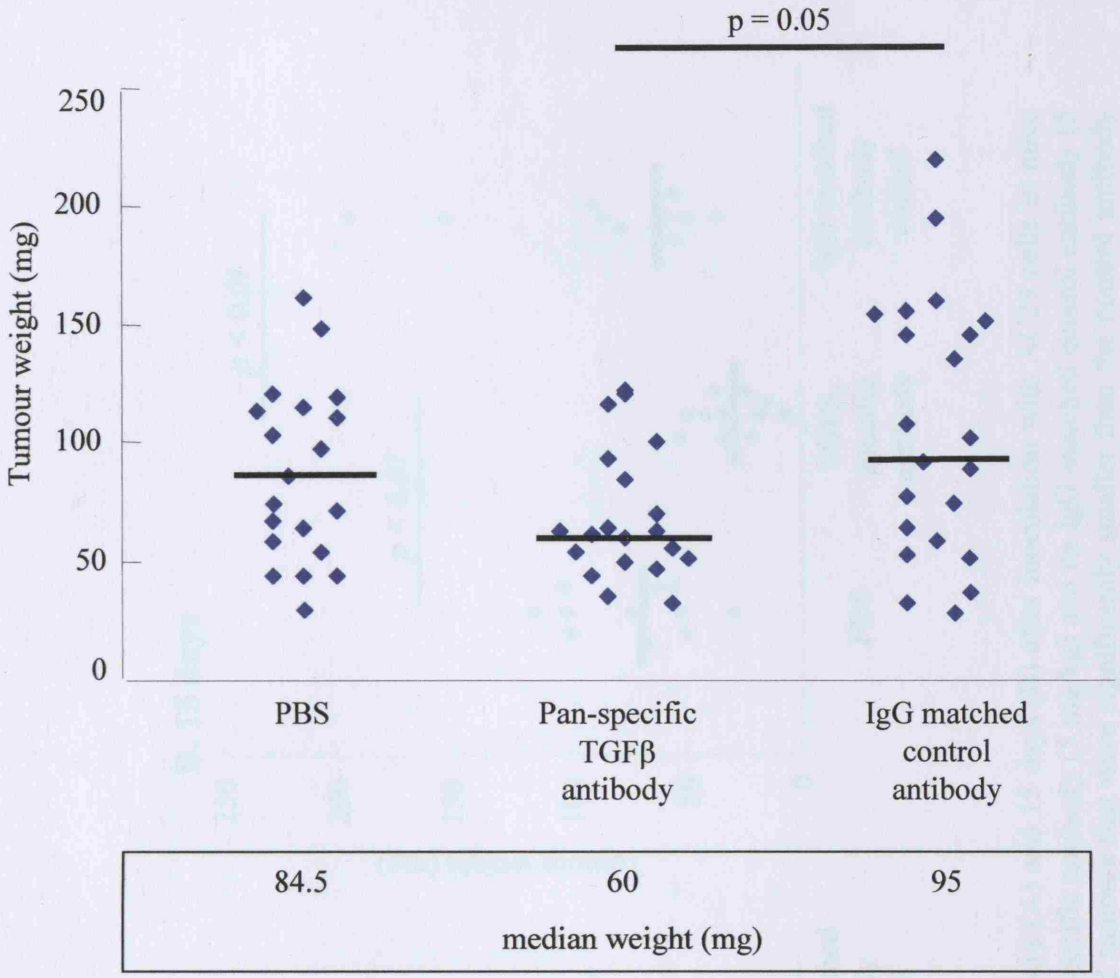

Figure 3.1.11 Tumour weights of MM tumours 15 days after inoculation with AC29 cells in mice treated with intraperitoneal injections of PBS, pan-specific TGFβ antibody (5 mg/kg) and its control IgG matched antibody (5 mg/kg). The pan-specific TGFβ antibody treated mice had tumours that were smaller than the control antibody treated mice. Median values are expressed in the box. P values were calculated using a Mann Whitney U test. Bars represent median values.

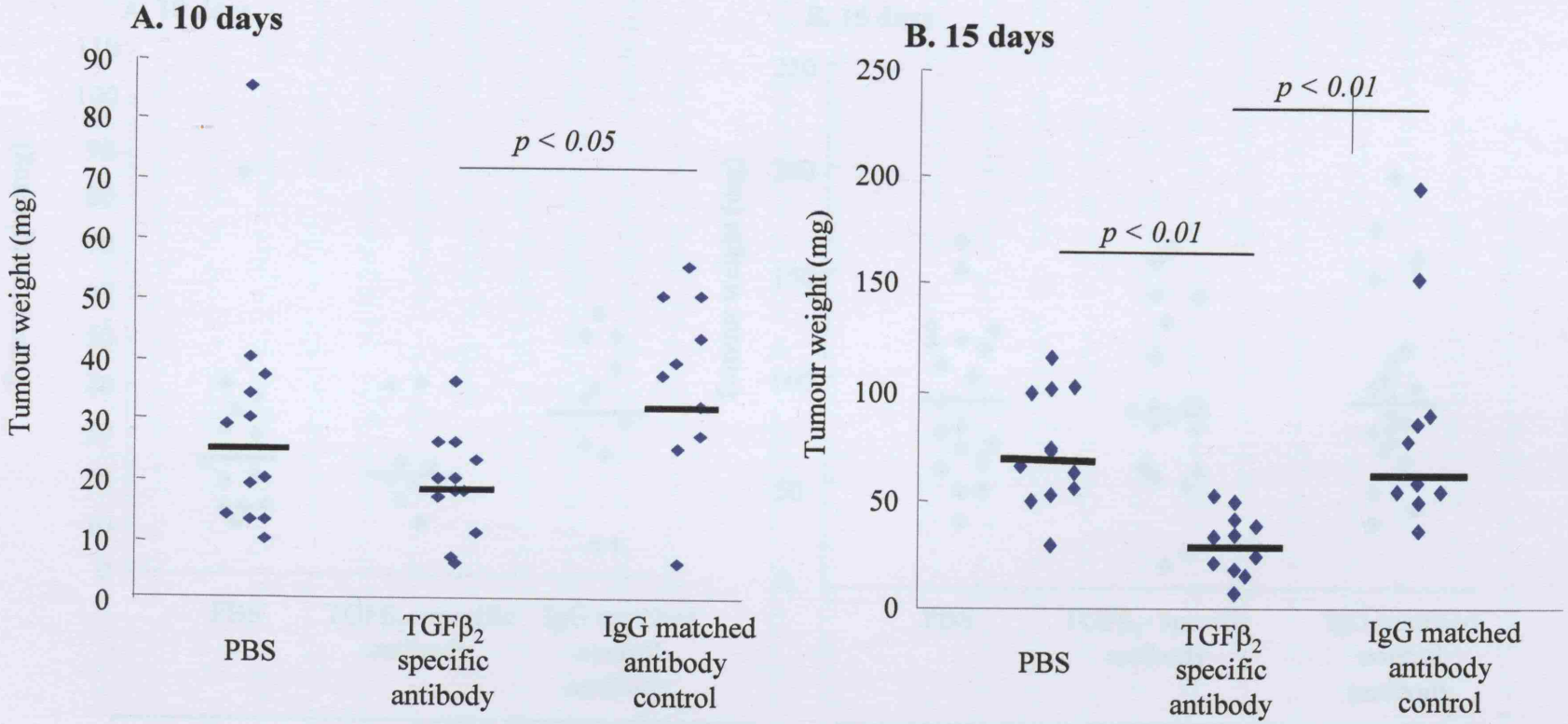

Figure 3.1.12. Tumour weights of MM tumours 10 days (A) and 15 days (B) after inoculation with AC29 cells in mice treated with intraperitoneal injections of PBS, $TGF\beta_2$-specific antibody (5 mg/kg) and its IgG matched control antibody (5 mg/kg). The $TGF\beta_2$-specific antibody treated mice had tumours that were significantly smaller than the control antibody treated group at 10 days. At 15 days, TGFβ2-specific antibody treated mice had tumours that were smaller than both control groups. Bars represent median values. Mann Whitney U test was used to test significance.

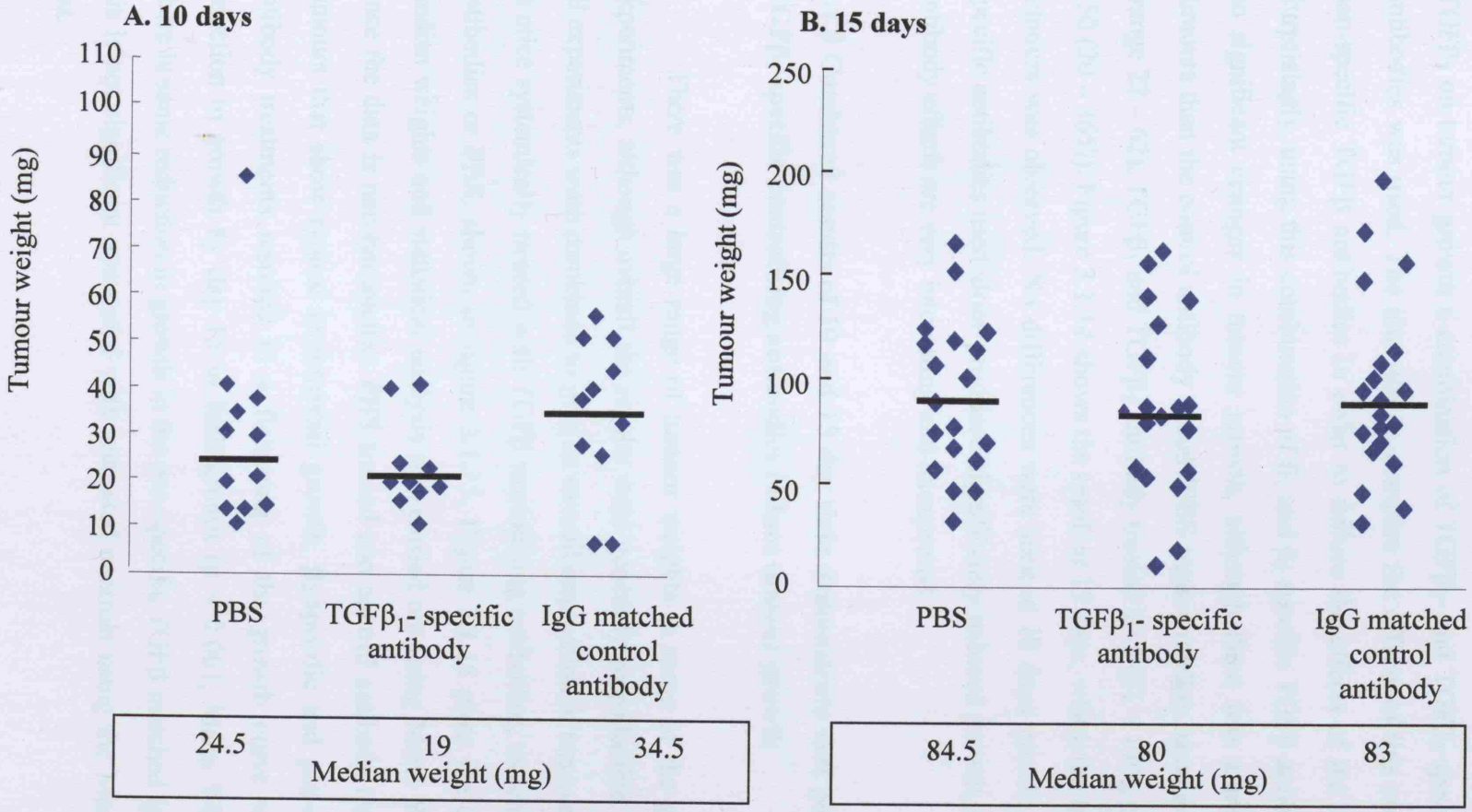

Figure 3.1.13. Tumour weights of MM tumours 10 (A) and 15 (B) days after inoculation with AC29 cells of mice treated with intraperitoneal injections of PBS, $TGF\beta_1$-specific antibody (5 mg/kg) or its IgG matched control antibody (5 mg/kg). There were no significant differences between the groups. Bars represent median values, also expressed in boxes. There is a trend for a smaller tumour size at 10 days but at 15 days this trend has vanished.

3.1.7 Combined TGFβ$_1$- and TGFβ$_2$-specific neutralising antibodies have little effect on tumour growth

Since no TGFβ$_3$-specific antibody was available, to assess possible effects of TGFβ$_3$ on tumour growth a combination of TGFβ$_1$- and TGFβ$_2$-specific neutralising antibodies was used. The aim was to compare the effects of this combination with pan-specific TGFβ antibodies in order to deduce the effects of the TGFβ$_3$ isoform. Surprisingly, using this combination of β$_1$ and β$_2$ specific TGFβ antibodies produced no significant changes in tumour growth, although there was a trend for smaller tumours than the control antibody group (PBS treated median tumour weight 84.5mg (range 22 – 62), TGFβ$_1$ and TGFβ$_2$ antibody treated 80.5 (21 – 170), control antibody 150 (20 – 365)). Figure 3.1.14 shows the result at 15 days, where the trend for smaller tumours was observed. No differences were seen at 10 days growth. Since TGFβ$_2$-specific antibodies used alone produced significantly reduced growth, these combined antibody effects are very interesting and unexpected.

3.1.8 Combined results of 10 and 15 day data demonstrate that pan-specific and TGFβ$_2$-specific neutralising antibodies reduce tumour growth

There was a large range of tumour weights in some of the groups between experiments, although overall the results were generally reproducible. The data from all experiments were combined to give an overall impression of tumour growth curves in mice systemically treated with TGFβ neutralising antibodies, matched IgG control antibodies or PBS, shown in figure 3.1.15. Figure 3.1.15 plots the data as tumour median weights and statistical analysis was carried out using Mann Whitney U test, since the data is non-parametric. PBS treated and control antibody treated mice had tumours that show typical exponential growth. β$_2$-specific and pan-specific TGFβ antibody treatments resulted in a flattening of the growth curve with a marked reduction in growth by day 15 in both groups ($p < 0.001$, Mann Whitney U test). There is some reduction in growth in the pan-specific TGFβ matched IgG control, but this is not significant compared with untreated controls using the Mann Whitney U test.

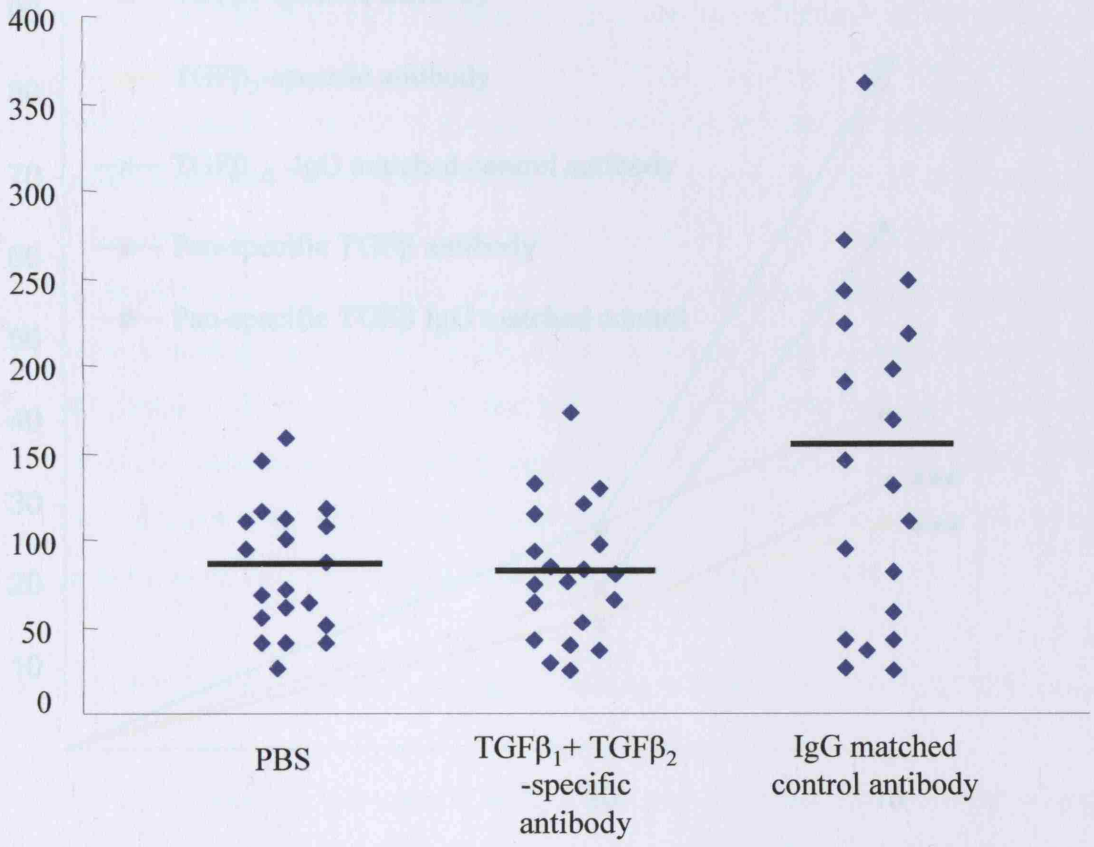

Figure 3.1.14. Tumour weights of MM tumours 15 days after inoculation with AC29 cells of mice treated with intraperitoneal injections of PBS, $TGF\beta_1$+ $TGF\beta_2$ -specific antibody mixture (both at (5 mg/kg) or an IgG matched control antibody (given at a dose of 2 x 5 mg/kg to match the dose of the combined TGFβ antibodies). There was a trend for the $TGF\beta_1$+ $TGF\beta_2$ -specific antibody mixture treated group to have smaller tumours than the control antibody treated group. Bars represent median values.

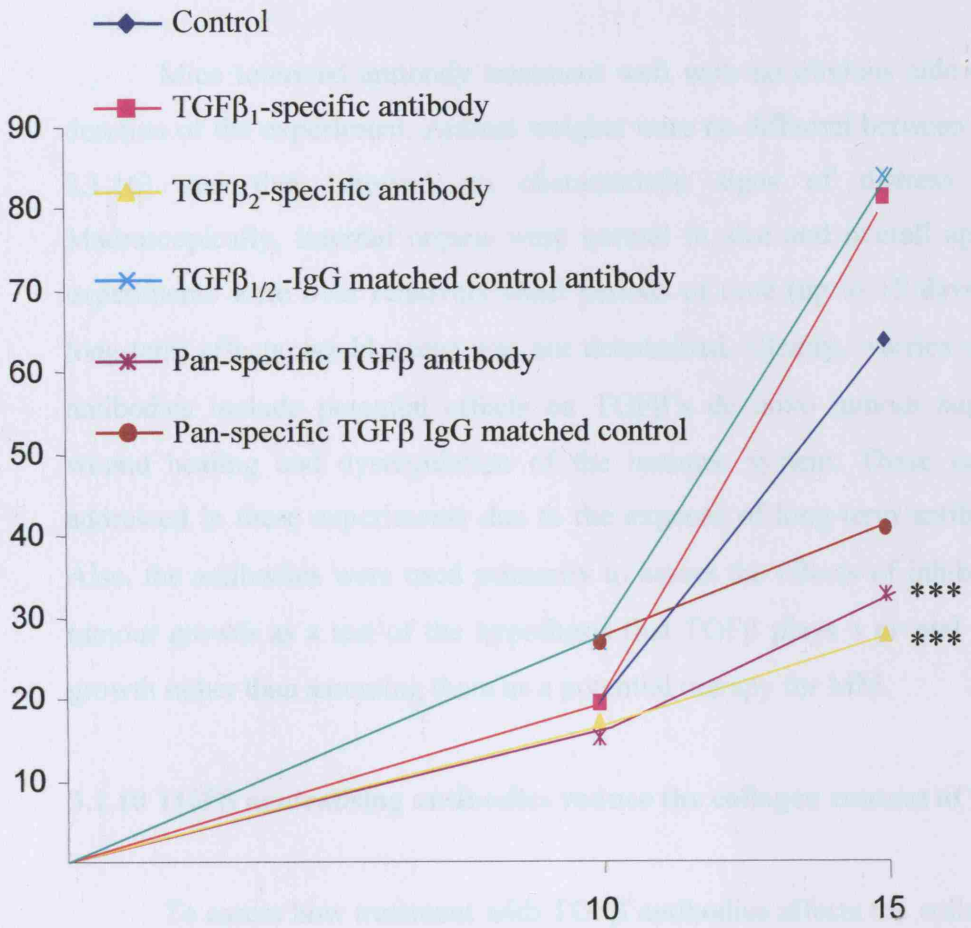

Figure 3.1.15 Combined data of all murine MM tumours grown using AC29 cells and treated with TGFβ neutralizing antibodies (5mg/kg). Tumour weights measured at 10 and 15 days are shown and expressed as median weight. The tumour size at day zero is taken as zero, representing 10^6 cells in suspension with no tumour structure. The reduction in tumour size at 15 days is highly significant in both the pan-specific TGFβ and the $TGF\beta_2$-specific antibody treated groups analyzed using Mann Whitney U test (using median values and assuming the results are non-parametric) and compared with either the PBS treated control group or the matched antibody treated control groups. *** = $p < 0.001$

3.1.9 TGFβ antibodies have no systemic short-term side-effects

Mice tolerated antibody treatment well with no obvious side effects for the duration of the experiment. Animal weights were no different between groups (figure 3.1.16) and they showed no characteristic signs of distress or ill-health. Macroscopically, internal organs were normal in size and overall appearance. The experiments were over relatively short periods of time (up to 15 days) and whether long-term effects would occur was not determined. Clearly, worries of using TGFβ antibodies include potential effects on TGFβ's de novo tumour suppressing role, wound healing and dysregulation of the immune system. These issues were not addressed in these experiments due to the expense of long-term antibody treatment. Also, the antibodies were used primarily to assess the effects of inhibiting TGFβ on tumour growth as a test of the hypothesis that TGFβ plays a pivotal role in tumour growth rather than assessing them as a potential therapy for MM.

3.1.10 TGFβ neutralising antibodies reduce the collagen content of MM tumours

To assess how treatment with TGFβ antibodies affects the collagen content of MM tumours, the level of hyp in tumours was measured using HPLC. Tumours from mice treated with pan-specific TGFβ, $TGF\beta_2$-specific and $TGF\beta_1$-specific antibodies and their controls that had been snap frozen and stored at –80°C were analysed as described in section 2.7.5. The collagen content of tumours (expressed as hyp /mg tumour) from mice treated with $TGF\beta_1$-specific, $TGF\beta_2$-specific neutralising antibodies or their controls is shown in figure 3.1.17. This shows that $TGF\beta_1$-specific antibodies had no effect on the collagen content of the tumour, whereas $TGF\beta_2$-specific antibodies produced a trend for smaller tumours compared with the control antibody treated tumours, but no significant difference compared with PBS treated mice. The amount of collagen in the pan-specific treated experiment is shown in figure 3.1.18. This shows that pan-specific TGFβ antibody treated tumours had significantly less collagen per mg tumour i.e. a reduction in collagen concentration, not just a reduced total collagen due to reduced tumour size (PBS control tumour collagen content 9.12 ± 0.76 (mmol hyp / mg tumour ± SEM), control antibody treated 6.67 ± 0.97, pan-specific antibody treated 4.50 ± 0.47, $p < 0.01$). To confirm

that the differences are not simply due to tumour size, a correlation curve plotting individual tumour weight against its collagen concentration was plotted and shown in figure 3.1.19. There is no direct correlation between tumour size and collagen concentration per se i.e. bigger tumours do not necessarily have increased collagen concentrations. This is because the control groups have more variable collagen content and tumour size. So the difference in collagen concentrations and tumour size between groups is likely to result directly from the effects of TGFβ antibodies. This reduced tumour collagen content is associated with a reduction in tumour size.

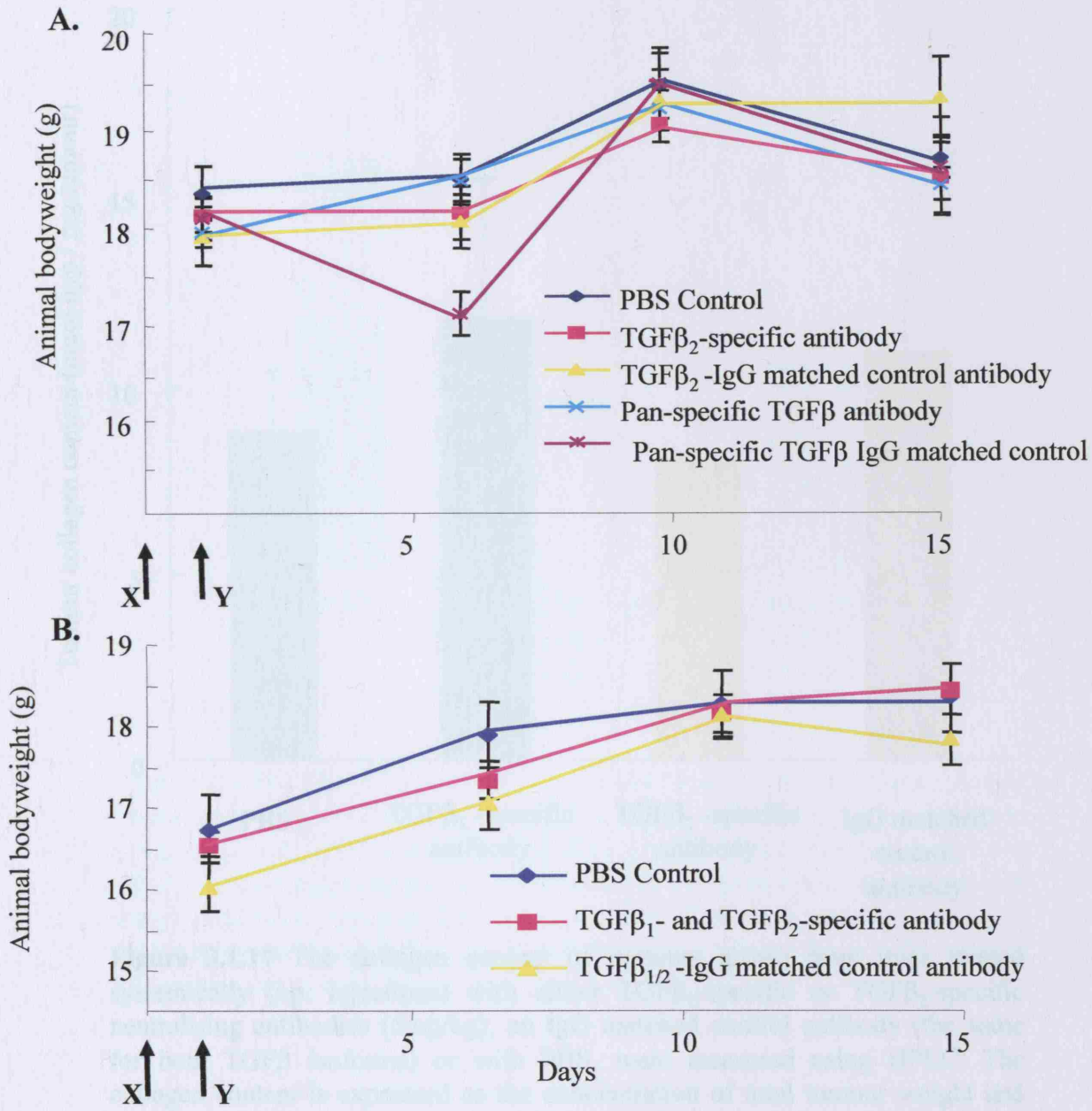

Figure 3.1.16 A. Bodyweights of animals following treatment with TGFβ antibodies and matched controls shows little change for the duration of the experiment. The results represent the mean of 10 animals per group at 1, 6 and 10 day timepoints and of 5 animals per group at the 15 day timepoint ± SEM. The only significant change was the decrease in weight of the pan-specific TGFβ IgG matched control antibody treated mice at day 6. **B**. Bodyweights of mice treated with a combination of $TGF\beta_1$ and TGF β_2-specific antibodies (both at 5mg/kg) and an equal dose of the matched control antibody. There were no significant variations in animal weights at 1, 6, 11 and 15 days. **X** = Start of antibody treatment, **Y** = inoculation of AC29 MM cells

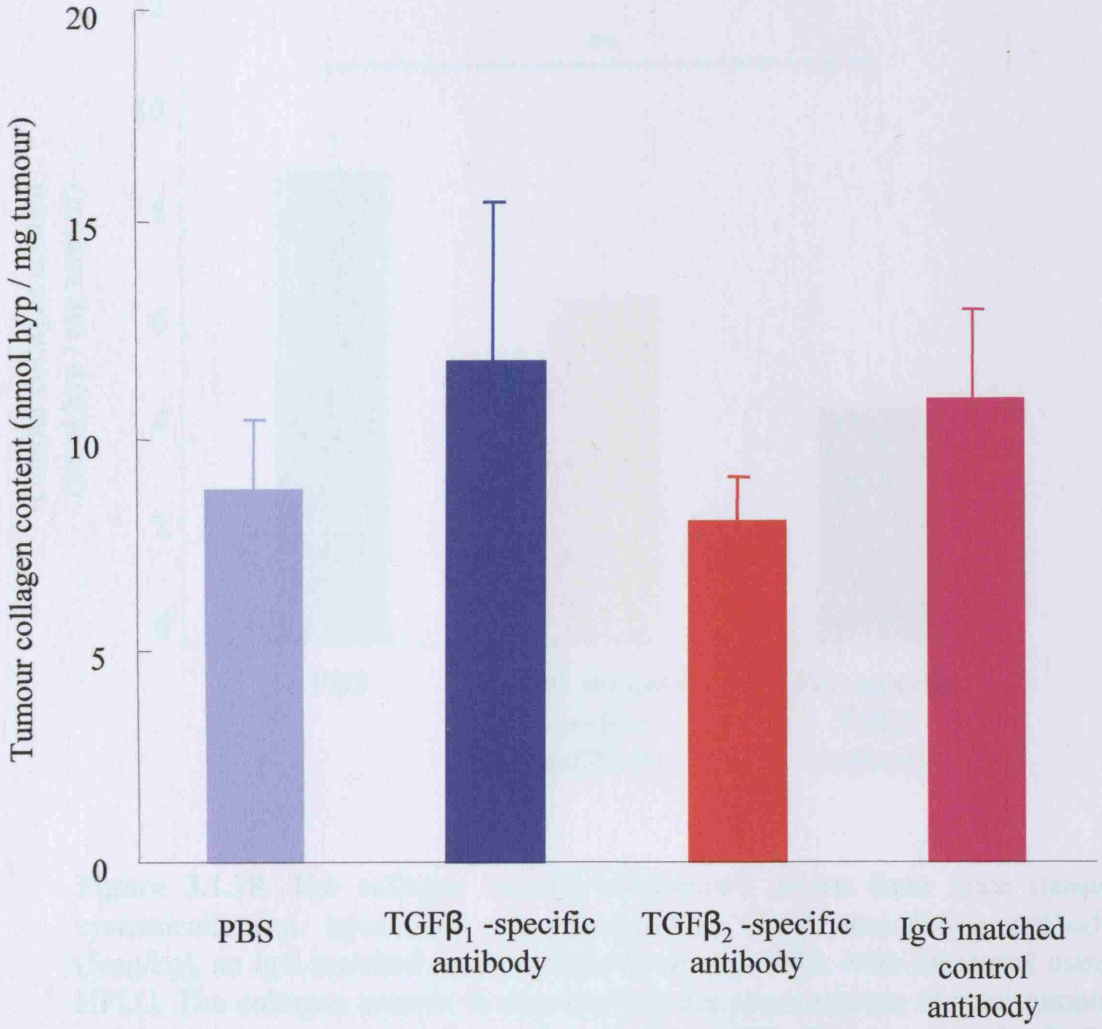

Figure 3.1.17 The collagen content of tumours grown from mice treated systemically (i.p. injections) with either $TGF\beta_1$-specific or $TGF\beta_2$-specific neutralising antibodies (5mg/kg), an IgG matched control antibody (the same for both TGFβ isoforms) or with PBS, were measured using HPLC. The collagen content is expressed as the concentration of total tumour weight and bars represent the mean values ± SEM. The $TGF\beta_2$-specific antibody treated tumours showed a trend for a reduction in collagen concentration compared with its IgG matched control antibody. $TGF\beta_1$-specific antibodies showed no change in collagen concentration. n = 10 tumours (10 animals) per group.

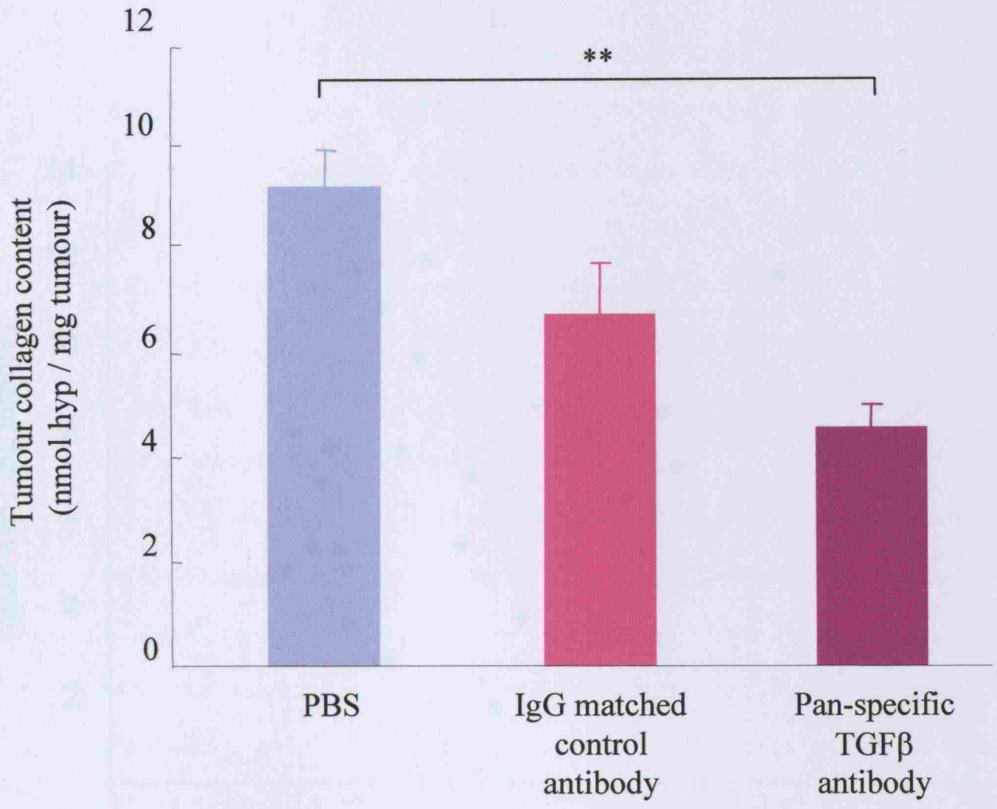

Figure 3.1.18. The collagen content of tumours grown from mice treated systemically (i.p. injections) with pan-specific TGFβ neutralising antibody (5mg/kg), an IgG matched control antibody or with PBS, were measured using HPLC. The collagen content is expressed as the concentration of total tumour weight and bars represent the mean values ± SEM. The pan-specific TGFβ antibody treated tumours had reduced collagen concentrations. n = 10 tumours (10 animals) per group. ** = $p < 0.01$ Student's paired t test

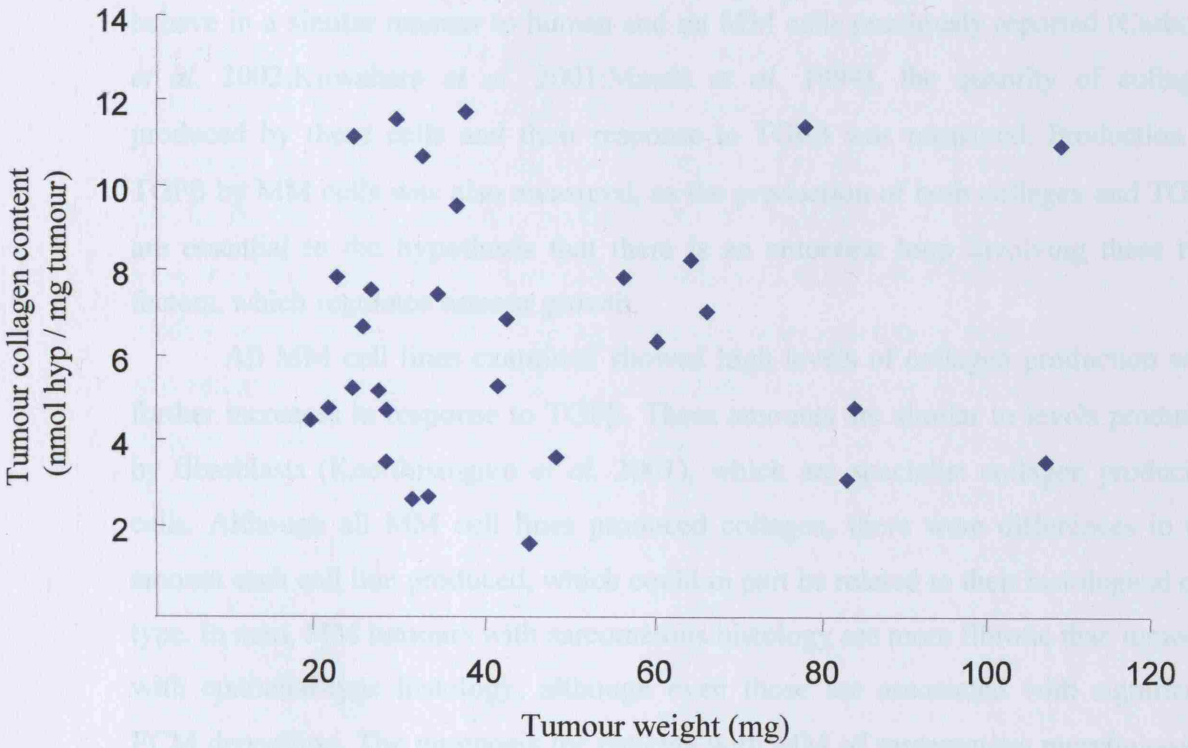

Figure 3.1.19. Tumour weight – collagen correlation curve. Each tumour from the experiment shown in figure 3.2.4A has been plotted as a weight against its collagen concentration. All tumours from the three groups have been plotted; PBS treated, control antibody treated and pan-specific TGFβ antibody treated. There is no direct correlation between total tumour weight and collagen concentration.

3.1.11 Discussion

Seven different MM cell lines have been used in this study. To assess the relationship between TGFβ and collagen production and to confirm that these cells behave in a similar manner to human and rat MM cells previously reported (Carbone *et al.* 2002;Kuwahara *et al.* 2001;Maeda *et al.* 1994), the quantity of collagen produced by these cells and their response to TGFβ was measured. Production of TGFβ by MM cells was also measured, as the production of both collagen and TGFβ are essential to the hypothesis that there is an autocrine loop involving these two factors, which regulates tumour growth.

All MM cell lines examined showed high levels of collagen production with further increases in response to TGFβ. These amounts are similar to levels produced by fibroblasts (Keerthisingam *et al.* 2001), which are specialist collagen producing cells. Although all MM cell lines produced collagen, there were differences in the amount each cell line produced, which could in part be related to their histological cell type. In man, MM tumours with sarcomatous histology are more fibrotic than tumours with epithelial-type histology, although even those are associated with significant ECM deposition. The prognosis for patients with MM of sarcomatous morphology is worse than for those with epithelioid morphology, in part due to lack of any response to treatment by sarcomatoid mesotheliomas, whereas epithelioid tumours may have partial responses (Ceresoli *et al.* 2001). However, whatever the cell type, the overall median prognosis is still only 10 - 14 months. This is consistent with the hypothesis that collagen deposition limits the effectiveness of tumour therapy.

In section 3.1.2, each cell line was shown to produce significant levels of active TGFβ. Although there is variation between cell lines that can not easily be associated with cell type, of the three murine cell lines assessed the biggest producer of TGFβ, AC29, also produced the most collagen, as described in section 3.1.1. However, the pattern is not consistent enough from these studies to conclude that the MM cells producing the most TGFβ are those that synthesise the most collagen.

These initial investigations confirm the two prerequisites necessary for the hypothesis that TGFβ and collagen production are involved in an autocrine loop that is important to mesothelioma tumour growth i.e. these cells produce both collagen and TGFβ and respond to the latter by increasing their collagen synthesis. These findings

are essential for the further studies attempting to interrupt this loop with the aim of inhibiting or partially limiting tumour growth.

In vitro studies demonstrated that the pan-specific TGFβ antibody completely inhibited exogenous $TGF\beta_1$, whereas the $TGF\beta_1$-specific antibody reduced the TGFβ response by only 60%. The suppliers (CAT antibodies) state that the $TGF\beta_1$-specific antibody works more effectively *in vivo* (personal communication), although the reason has not been determined, and for these studies this was assumed to be true. As predicted, the $TGF\beta_2$-specific antibody did not inhibit the response of the MLEC bioassay following $TGF\beta_1$ stimulation. Dose and treatment schedules used in these studies were recommended following extensive pharmacokinetic studies by CAT. The pan-specific antibody used, 1D11, has already been shown to reduce fibrosis in a number of earlier studies not related to this work. In a murine model of nephropathy induced by cyclosporin-A, the antibody prevented the development of nephropathy, reducing deposition of collagen III (Ling *et al.* 2003). In combination with an ACE inhibitor ID11 prevented proteinuria and overt renal nephropathy in a streptozotocin induced diabetic rat model, again by attenuating the deposition of collagen III (Benigni *et al.* 2003). Furthermore, in a rabbit model of corneal fibrosis the antibody reduced collagen deposition (Jester *et al.* 1997). The $TGF\beta_2$-specific antibody, CAT-152, has also been successfully used in a rat model of diabetic nephropathy in which there was a reduced rate of pathological fibrosis in antibody treated animals (Hill *et al.* 2001). Following a successful preliminary trial (Siriwardena *et al.* 2002), CAT-152 is under controlled clinical trials in humans to reduce collagen contraction and deposition in glaucoma filtration surgery. Interestingly, the $TGF\beta_1$-specific antibody has not been extensively used and this may reflect its lower activity or unexpected responses, consistent with the findings reported here. Other work in our laboratory showed that CAT-192 reduced airway remodelling by ~ 65% in a murine model of asthma (Rheinhardt *et al.*, abstract publication, ATS 2004).

The *in vitro* collagen response to exogenous TGFβ was reduced with $TGF\beta_1$-, $TGF\beta_2$- and pan-specific antibodies, although why the $TGF\beta_2$-specific antibody had an effect was unclear since the MLEC studies had shown it to have no $TGF\beta_1$-specific neutralising effects. However, none of the antibodies had any effect on the basal levels of collagen production despite the hypothesis that the cells respond to paracrine TGFβ synthesised and released by their neighbouring cells along with autocrine

TGFβ. The regulation of basal collagen production may be independent of TGFβ or it may be that the effects of the endogenous TGFβ are predominantly autocrine. It has been postulated that the autocrine responses to TGFβ occur within caveolae (pockets or crypts), at the cell surface, where there might not be exposure to the exogenous antibody before a response is elicited. Alternatively, the autocrine effects may occur by internal activation with no release of TGFβ into the surrounding milieu. Either of these scenarios would explain why basal levels of collagen production were unaffected by the antibodies. This could potentially be investigated further using immunogold-histochemistry and electron microscopy to label binding sites and TGFβ.

In vivo, to reduce animal wastage and expense, all experiments were performed using a single murine cell line, AC29, in CBA mice - the syngeneic strain from which these cells were derived. This cell line was selected as previous *in vivo* data has shown this cell line to be more tumorigenic than the other murine cell lines available, AB1 and AB22, despite all three cell lines having similar doubling times of between 27 to 30 hours(Davis *et al.* 1992). Preliminary *in vivo* data from this study confirmed that the AC29 cell line was the most tumorigenic, with tumours that grew faster and more consistently than any of the other murine MM cell lines.

Growth of these tumours was reduced using β_2- and pan-specific TGFβ antibodies. This confirmed the theory that TGFβ is pro-tumorigenic for these tumours and is consistent with the hypothesis that TGFβ may be involved in a growth loop involving TGFβ and collagen. The limited data available on tumour collagen content shows that tumours treated with pan-specific antibodies had a reduced concentration of collagen. This was not simply a reflection of overall size as the graphs in figure 3.1.19 show no direct correlation between tumour size and collagen content when all groups are combined. Tumours had a reduced mean level of collagen and a reduced size when treated with the antibody. Although these results do not prove that reduced collagen production resulted in reduced tumour growth, the findings are consistent with that hypothesis.

The $TGF\beta_1$-specific antibody did not reduce tumour growth. This may have been because the antibody was not effective in blocking TGFβ, as suggested by the *in vitro* studies. Alternatively, this isoform of TGFβ may not play an independent pro-tumorigenic role. Indeed, some of the experiments showed that $TGF\beta_1$-specific antibody treated mice grew tumours that were larger than controls, which might

suggest that if it plays any role in tumour growth, the TGFβ$_1$ isoform may be tumour restrictive. This may be a result of TGFβ anti-proliferative effects, which occur in normal cells, still functioning in MM cells *in vivo*. The anti-proliferative effects of TGFβ$_1$ may be more potent than its pro-tumorigenic actions, such as collagen stimulation or angiogenesis promotion in these cells. This was also suggested by the effects of combining β$_1$- and β$_2$-specific antibodies when the inhibition of tumour growth by blocking TGFβ$_2$ alone was lost (section 3.1.10).

The role of TGFβ$_3$ was not determined by these experiments. It was hoped that by comparing the results using the pan-specific with the results obtained using a combination of the β$_1$ and β$_2$-specific TGFβ antibodies, the effects of blocking TGFβ$_3$ could be deduced. As TGFβ$_2$-specific antibodies had reduced tumour growth, it was expected that at least a similar reduction would be observed when used in combination with the TGFβ$_1$-specific antibody. The finding that there was no significant change supports the idea that TGFβ$_1$ and TGFβ$_2$ may have opposing effects and would suggest that TGFβ$_1$ antibodies have enough tumour promoting activity *in vivo* to inhibit the effects of tumour inhibiting TGFβ$_2$-specific antibodies. The result also suggests that the TGFβ$_2$ isoform is specifically pro-tumorigenic, with the specific roles of TGFβ$_1$ and β$_3$ not determined.

These results suggest that different TGFβ isoforms may have different roles in MM. This difference between TGFβ isoforms is not surprising, as although the different isoforms each share approximately 70 % identical amino acid residues, they are all produced by separate genes. Other workers have shown differences in the actions of the different isoforms and this seems to be dependent on a number of factors including the cell type. In an experimental model of autoimmune encephalitis TGFβ$_3$ showed anti-proliferative properties towards encephalitigenic cells, whereas TGFβ$_1$ appeared to have an opposing role and was up-regulated (Matejuk *et al.* 2004). Other workers found that after spinal cord injury, TGFβ$_1$ was increased over the acute inflammatory phase modulating inflammation and neuronal processes and TGFβ$_3$ increased over the sub-acute period of scarring where it regulated glial cell collagen deposition (Lagord *et al.* 2002). In breast cancer, Tamoxifen therapy leads to an up-regulation of TGFβ$_2$ but has no effect on TGFβ$_1$, suggesting that in this cancer TGFβ$_2$ is protective (Brandt *et al.* 2003). Low concentrations of TGFβ$_1$, TGFβ$_2$ and TGFβ$_3$

stimulate colony-stimulating factor induced granulocyte-macrophage colony-forming units, but with high concentrations TGFβ$_2$ stimulates growth whilst the other two isoforms inhibit growth (Salzman *et al.* 2002). These are just some of the examples of different and sometimes opposing roles of the TGFβ isoforms. Clearly the inter-relationships are very complex and vary with cell type, concentration and cell function.

As a possible therapeutic option in man there are a number of potential problems in using TGFβ antibodies. The long-term side-effects are not known. Despite evidence from this study that there are no short-term side-effects of this form of therapy, over a longer period there are theoretically significant effects on the immune system and wound healing, as well as tumour suppressor effects, although in mice it has been demonstrated that long-term treatment with monoclonal TGFβ antibodies has no effect on immune function (Ruzek *et al.* 2003). TGFβ has a regulatory role in controlling T-cell function by suppression of the T-cell response (Gorelik and Flavell 2002). With long term antibody neutralisation of TGFβ there may be uncontrolled autoimmune consequences. Finally there is the bimodal role of TGFβ in cancer. In the late stages of cancer, as in the case of malignant mesothelioma, TGFβ is pro-tumorigenic. However, in the early stages of cell transformation and malignant cell growth TGFβ is a known tumour suppresser (as described in section 1.7), leading to fears that treatment may result in new tumour formation at other sites. There is an added problem in that host antibodies are likely to form against the TGFβ antibodies after approximately 10 days, which could render the neutralising antibodies ineffective over a longer exposure period.

TGFβ is clearly a good target in MM as a reduction in tumour growth has been demonstrated following the systemic administration of neutralising antibodies. Other ways of inhibiting TGFβ by targeting specific cells or acting only in a localised body region may offer a better therapeutic option. Similarly, by targeting specific pathways that respond to TGFβ within targeted cells using gene therapy would avoid deleterious effects of a global inhibition of TGFβ. One such method is to inhibit the Smad signalling pathway that is unique to TGFβ. The other advantage of blocking the cellular signalling in response to TGFβ is that it also specifically targets the autocrine effects that antibodies may not block. For instance, the basal levels of collagen

production were high, but were not affected by TGFβ neutralising antibodies *in vitro* and this may have been due to autocrine effects not inhibited by antibody treatment. If basal collagen production could be reduced then a much greater inhibition in tumour growth may be observed. This approach is examined in the following chapter.

3.2 Transient transfection of MM cells with Smad7 using the LID vector and stable transfection using a lentiviral vector - effects of Smad7 over-expression on collagen production and tumour growth.

Smad7 is the naturally occurring inhibitory protein within the TGFβ-Smad pathway, which is normally stimulated by activation of the Smad pathway in response to TGFβ. To inhibit Smad signalling in response to TGFβ, Smad7 was transfected into MM cells. This approach was aimed at inhibiting both autocrine and paracrine effects of TGFβ on MM cell collagen production and tumour growth. As TGFβ antibodies had demonstrated inhibition of tumour growth *in vivo* (chapter 3.1), the effects of transfecting cells with Smad7, the inhibitory component of the Smad pathway (described in chapter 1.5), were expected to be similar. As TGFβ antibodies had no effect on the *in vitro* basal collagen production by MM cells, possibly because there was no blockade of internal TGFβ autocrine effects, it was thought that by blocking the Smad pathway, basal collagen production would also be inhibited.

To assess the effects of Smad7 transfection on collagen production and tumour growth a method of transfecting Smad7 was first established. This chapter describes the results of transfecting MM cells with Smad7 using two methods; the LID vector for transient transfection and a retroviral method to create stable transfectants. It then describes the results of Smad7 transfection on MM cell collagen responses and tumour growth.

3.2.1 Transient transfection of MM cells using the LID vector

The LID vector transfection system (described in section 2.4.1) was optimised in this study to maximise the number of MM cells transfected. Peptide 6, as described in section 2.4.2, is designed to target α5β1 integrins and has been established as the most effective peptide used in this vector to transfect human cells. However, murine MM cells have an integrin profile that remains largely unexamined and therefore the most efficient integrin targeting peptide was not known. Similarly, MM cells may have different profiles of integrin expression to normal mesothelial cells.

3.2.1.1 Comparison of transfection efficiency using different peptides in the LID complex

To compare the transfection efficiency of different peptides, a green fluorescent protein (GFP) expressing vector was used in the LID complex with the three different peptides available (peptides 1, 6 and 8), and the number of transfected MM cells assessed, as described in section 2.4.4. The efficiency of peptide 6 was compared with peptide 8, which targets $\alpha 4\beta 1$ and peptide 1, which targets the RGD component, common to most integrins. Figure 3.2.1A shows that in AB22 cells, using 2 μg/ml of DNA, all peptides produced significantly greater transfection rates than having no peptide in the LID complex ($p < 0.01$ for peptides 1 and 6, $p < 0.05$ for peptide 8). Between peptides, peptide 6 was shown to produce greater transfection rates, for the same cDNA concentration in the LID mixture, transfecting more cells ($20 \pm 2.3\%$) than either peptide 1 ($11 \pm 1.9\%$, $p < 0.05$) or peptide 8 ($7 \pm 2.7\%$, $p < 0.01$). A similar result was found in AC29 cells, although a proportionally lower number of cells were transfected in each group ($14 \pm 3.1\%$, $7 \pm 2.5\%$ and $5 \pm 1.3\%$ with peptides 6, 1, and 8 respectively, fig 3.2.1B), again showing greater transfection with peptide 6 than with peptide 1, $p < 0.05$, or peptide 8, $p < 0.01$. These results show that the use of any of the peptides increases the transfection efficiency of the system, but peptide 6 was most effective for transfecting MM cells. Therefore, this peptide was selected for all further transfection studies using the LID complex.

3.2.1.2 The effect of LID vector cDNA concentration on transfection efficiency

To assess the effects of different concentrations of cDNA in the LID complex on cell transfection rates, increasing concentrations of GFP cDNA were used, as described in section 2.4.5. AB22 cells were used in these experiments, as these were the most readily transfected murine MM cells. Figure 3.2.2A shows increased transfection efficiency with increasing concentrations of DNA within the LID complex. At 5 μg/ml DNA over 30% of cells were transfected, which was reduced to 18.5% with 2 μg/ml (this is consistent with the data in figure 3.2.1, in which 2 μg/ml was used for transfection, demonstrating the reproducibility of transfection efficiency of this technique) and 14% with 1 μg/ml. This higher level of transfection using DNA

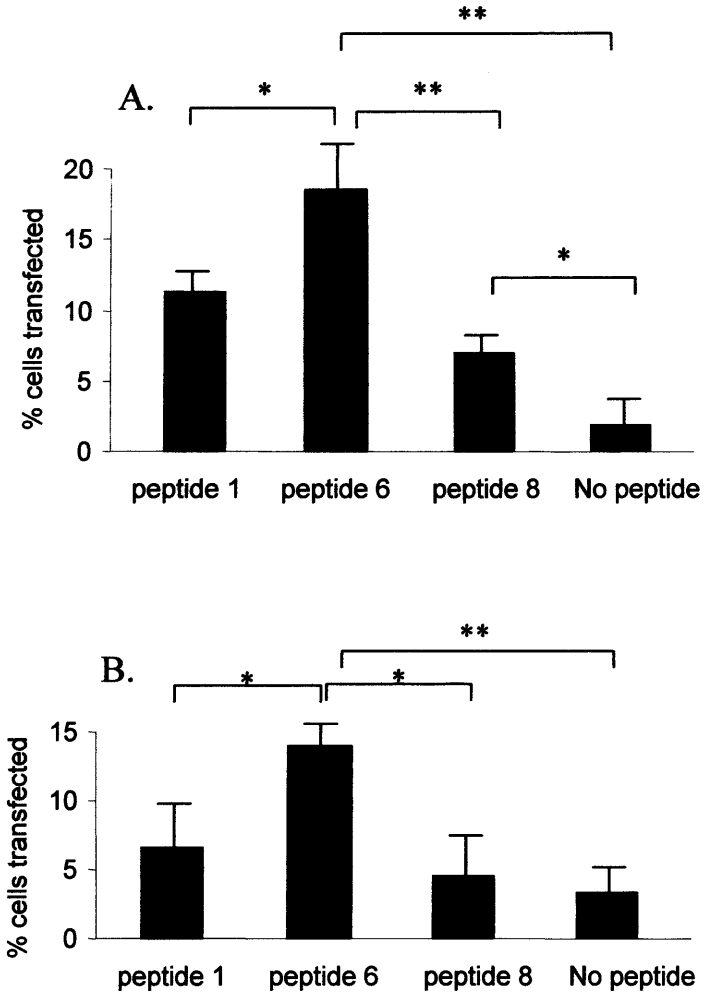

Figure 3.2.1 Transfection efficiency of different peptides in the LID complex in murine MM cells transfected with EGFP. **A** Confluent AB22 cells were transfected with EGFP (2 μg/ml) using a LID vector in 24 well flasks and incubated for a further 24 hours following transfection, then trypsinised and counted. The percentage of cells transfected was calculated by counting the number of fluorescent cells under fluorescent light and dividing by the total number of cells counted by light microscopy. Peptide 6 was the most effective peptide resulting in the highest transfection rate, transfecting more cells (20 ± 2.3%) than peptide 1 (11 ± 1.9%, $p < 0.05$) or peptide 8 (7 ± 2.7%, $p < 0.01$). All peptides were significantly more efficient than no peptide. Each represents the mean of 4 wells ± SEM. **B.** AC29 cells were also assessed and peptide 6 was again the most effective peptide within the LID complex. * $p < 0.05$

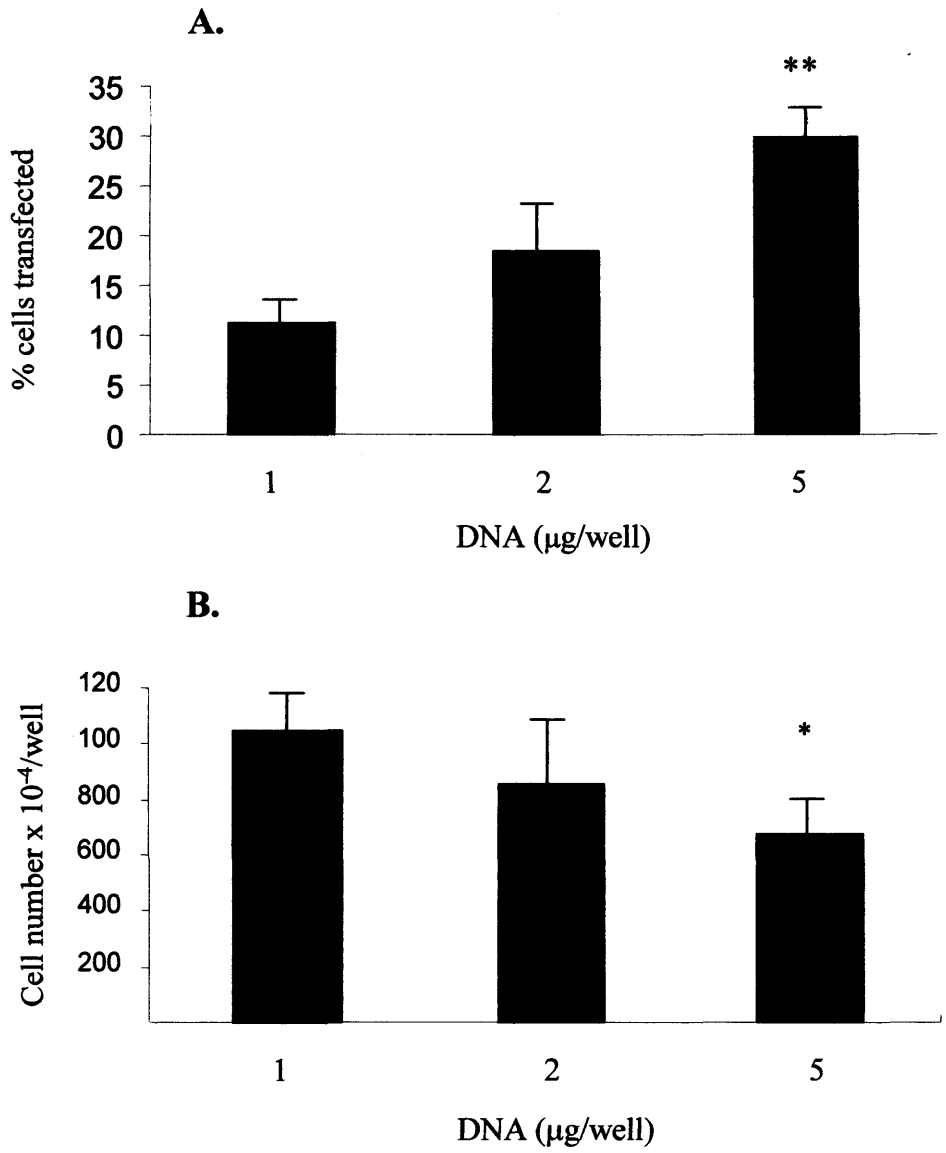

Figure 3.2.2 The effect upon transfection rates in AB22 cells of different concentrations of DNA used in the LID vector. **A.** The percentage of fluorescent AB22 cells after transfection with increasing concentrations of EGFP DNA in the LID complex, demonstrating an increase in transfection rate with increasing DNA concentration within the LID complex (** = $p < 0.01$, $n = 4$). **B.** The total number of cells following transfection with EGFP using the LID vector showing that increasing concentrations of DNA/well results in a significant fall in total cell numbers at 5μg/ml DNA.(* = $p < 0.05$, $n = 4$).

levels of 5μg/ml, was associated with a reduction in cell number per well by 36% compared with cells transfected with DNA at 1μg/ml, as shown in figure 3.3.2B. This suggests that cell death or inhibition of proliferation occurred at this concentration of GFP plasmid DNA. Cell death was not apparent morphologically when the cells were viewed by inverted light microscopy, but was predicted based on previous reported experience with other cell lines.

As a result of these preliminary experiments (section 3.3.1) peptide 6 and cDNA at a concentration between 1-2 μg/ml were selected as optimal conditions for all subsequent studies using the LID complex. This dose of DNA was chosen to limit potential cytotoxic effects of DNA on cells suggested by the data from figure 3.2.2.

3.2.1.3 Green fluorescent protein (GFP) expression over time following LID transfection

The duration required for transient gene transfection in the course of these studies was a maximum of 48 hours following transfection. To assess the effect of time following transfection on the number of cells expressing GFP, the presence of GFP in cells was assessed at 24 hours and 56 hours after the removal of the transfection medium. The results demonstrate that the number of cells expressing GFP remained high for this period of time. GFP cDNA was transfected at DNA concentrations of 1 and 5 μg/ml and the level of expression measured at the two time points (24 and 56 hours). Both the total cell number and the fluorescent cell number increased over the two time points as shown in figure 3.2.3. The number of fluorescing cells as a percentage of the total remained constant at 13%. As the copy number for transfection was not calculated, the reason for the sustained expression of GFP in the increasing cell population could be due to either plasmid or GFP protein being shared between daughter cells. However, these results do show that the number of cells expressing the protein appeared to remain constant for the time courses used in further experiments, where the maximum incubation following transfection was 48 hours.

In figure 3.2.3B the total cell number was reduced at 24 hours following transfection with higher DNA levels (5 μg/ml), which is consistent with the previous

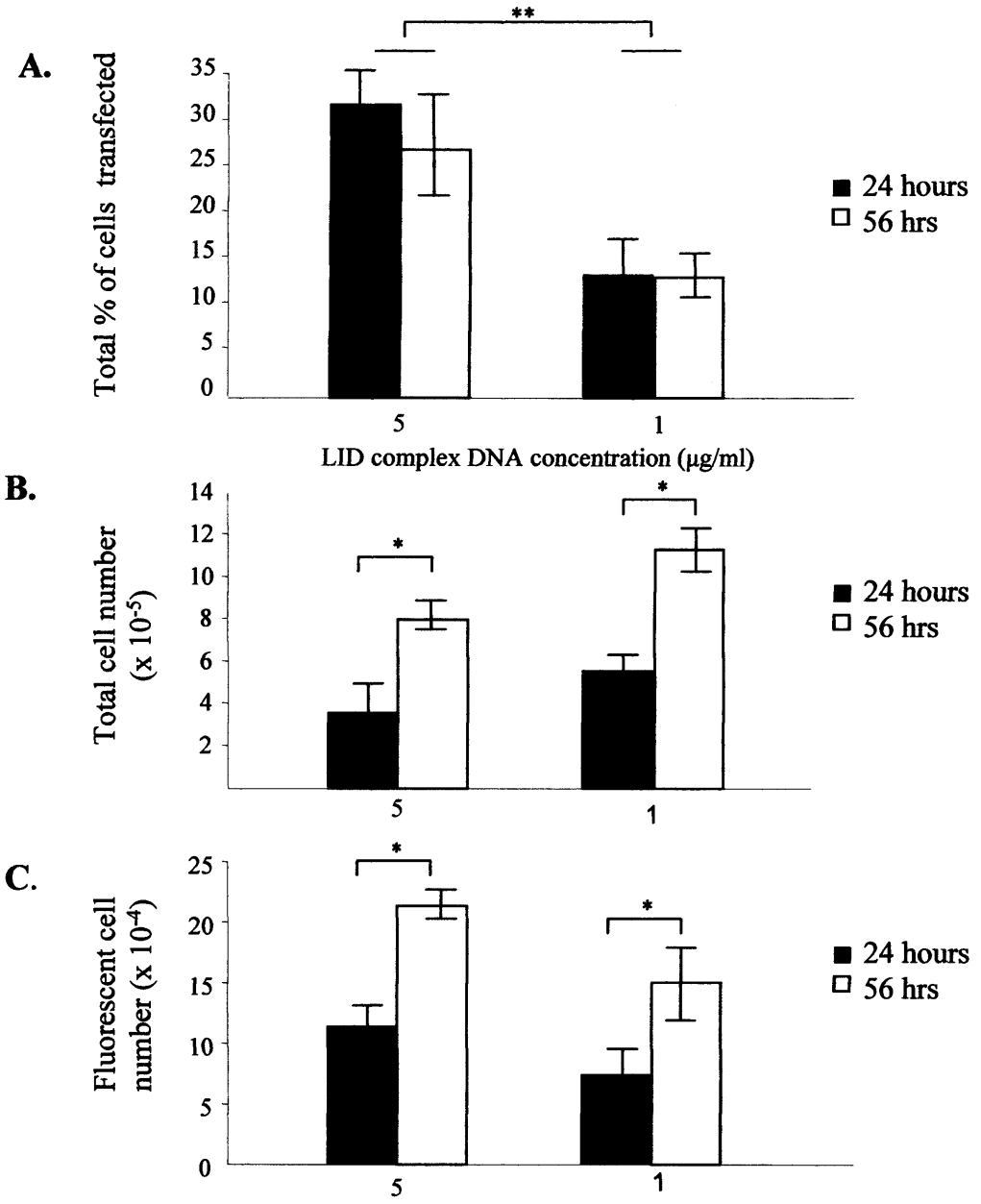

Figure 3.2.3 AB22 cell expression of transfected GFP over time and at different concentrations of DNA used in the LID complex. **A.** shows the percentage of cells expressing GFP (i.e. transfected cells) at 24 and 56 hours following transfection and also shows the difference in transfection rates when higher concentrations of DNA were used in the LID complex (x axis). There is no difference in the percentage of transfected cells between 24 and 56 hours and again the greater transfection efficiency of the higher concentration of DNA in the LID complex is demonstrated (32% with 5µg/ml DNA, 14% with 1 µg/ml). **B.** shows the total number of cells at the two time points demonstrating the reduced cell number when the cells have been exposed to higher concentrations of DNA in the LID complex. **C** shows that there is also a doubling in the total number of fluorescent cells. * = $p < 0.05$, ** = $p < 0.01$

experiment specifically examining the effects of DNA doses on transfection, shown in figure 3.2.2B. However, despite this apparent early loss of cells following transfection (using 5 μg/ml) the cells recover, since the total cell number does continue to increase at 56 hours and the percentage of transfected cells remains high. Lower doses of DNA were used in subsequent experiments since the incubation period of later experiments rarely exceeded 24 hours and this does not allow for the recovery of cells following the use of higher DNA concentrations in the LID system.

3.2.2 Stable transfection of MM cells with a Smad7 vector using a lentiviral technique

To assess the effect of Smad7 expression on total collagen production it was important that most or all of the cells over-expressed Smad7. This was because no bystander effects were predicted for Smad7 i.e. the effects of Smad7 transfection would be only on the transfected cell itself and not neighbouring cells. As such, transfection of approximately 15% of cells using the LID technique did not produce significant changes in collagen production (data not shown). Therefore, MM cell lines stably expressing Smad7 were created by transfecting cells using a retroviral technique, which incorporates the construct randomly into the MM cell genome (see section 2.4.7). The Smad7 vector (pHR'CMV-FLAG-SMAD7-IRES-EGFP) expresses GFP every time that Smad7 is expressed. This is because the two cDNA sequences of Smad7 and GFP are linked by a region that can mediate cap independent translation. This Internal Ribosome Entry Site (IRES) sequence follows directly after the Smad7 sequence and allows transcription of the GFP cDNA to start from within the ribosome rather than at the normal ribosomal initiation site. This allows simultaneous translation of two proteins from one single RNA transcript (cap-SMAD7-IRES-EGFP). GFP can only be transcribed if Smad7 has already been transcribed as the Smad7 sequence comes first. It is possible for Smad7 to be transcribed without GFP transcription as the IRES component is not 100% efficient.

Con-focal microscopy (Figure 3.2.4), confirmed that every MM cell expressed GFP following transfection indicating that they were also expressing Smad7. Figure 3.2.4 is of the JU77 cell line, as this gave the brightest GFP expression and best illustrates the successful transfection of all cells. All MM lines were

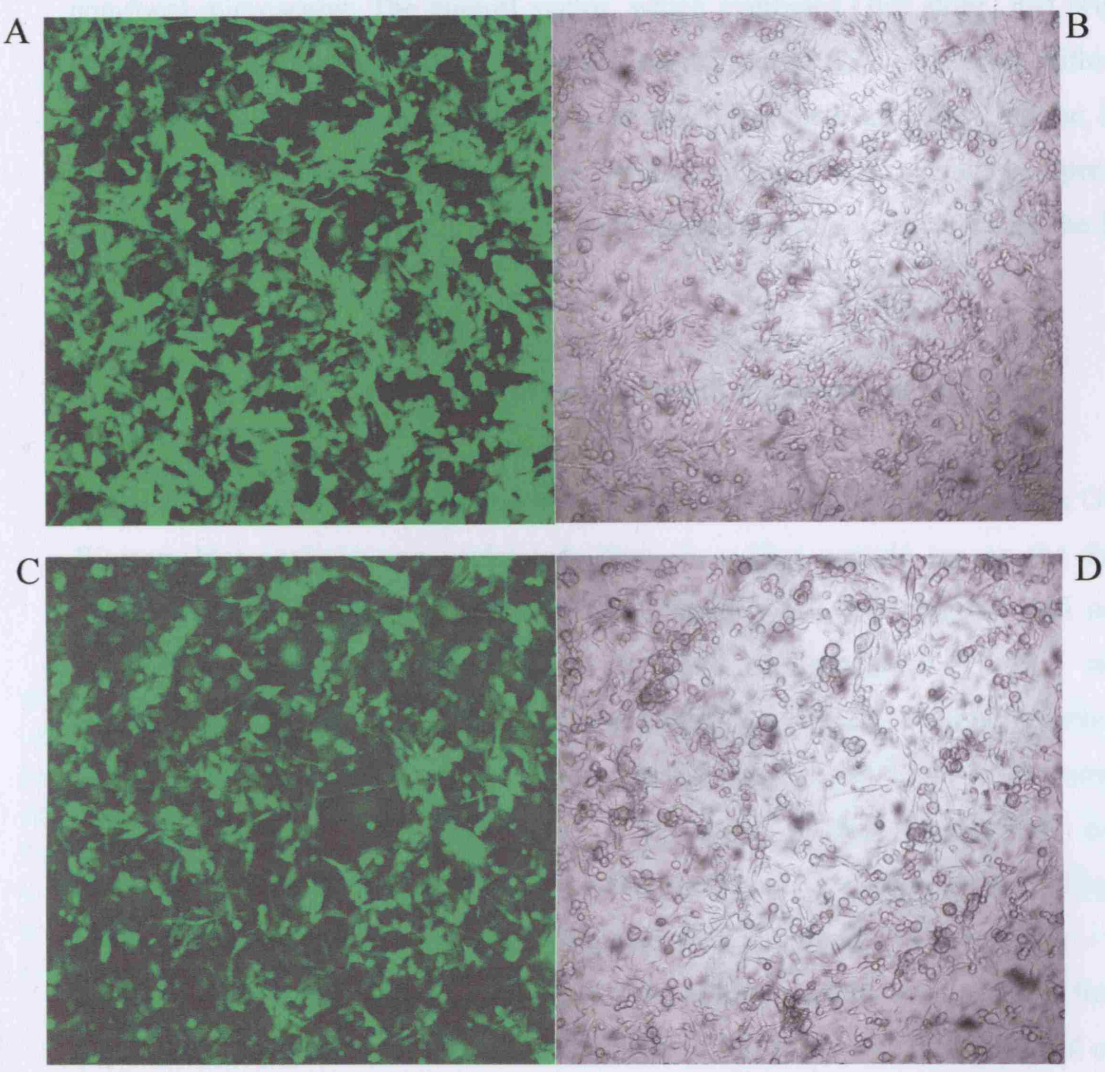

Figure 3.2.4 Con-focal images of Ju77 cells following stable transfection with Smad7-IRES-EGFP vector and its EGFP control. **A** EGFP transfected Ju77 cells viewed with confocal fluorescent microscopy showing all cells expressing GFP compared with the same cells viewed under normal light **B**, demonstrating successful transfection in all cells. **C** GFP expression associated with IRES linked Smad7 expression viewed under fluorescent conditions demonstrating high transfection rates compared with the same cells viewed by normal light microscopy **D**.

transfected using this technique with the same vector construct and all demonstrated expression of GFP (of varying intensity) in all cells, which could be visualised by con-focal microscopy. The control vector, which expresses GFP alone, had brighter expression of GFP. This may be because there is reduced GFP expression within the Smad7-IRES-GFP transfected cells due to the incomplete efficiency of the IRES sequence. This is a common observation using this technique (personal communication – Dr Walter Low) and may represent some inefficiency of the IRES component.

3.2.3 Western blot confirmation of stable Smad7 expression in MM cells

To confirm that transfected MM cells were making Smad7 as well as GFP, a Western blot analysis was performed. There is a Flag peptide tag on the Smad7 enabling easier detection of vector-induced Smad7 since this Flag tag will not be present on endogenous Smad7 (as described in section 2.6). This allows differentiation of transfected Smad7 from endogenous Smad7. In addition, the Flag antibody is much more sensitive and specific than Smad7 antibodies currently available. Western blot analysis (fig. 3.2.5) shows a clear band at the correct molecular weight for Smad7-Flag (48 kDa) confirming the expression of Flag and hence Smad7 in JU77 cells stably transfected with Smad7. Control cells - non-transfected and cells stably transfected with the control vector - were negative for Flag expression. The positive control is at 49.3 kDa as this is the size of the control carrier protein (BAP).

3.2.4 Smad activation in MM and HFLI cells

The use of Smad7 over-expression to block the effects of TGFβ relies on these cells having normal Smad activation. To confirm normal Smad signalling in the MM cell lines used in this study the phosphorylation of Smad2 (a receptor Smad – see section 1.6.4) was assessed in response to TGFβ. This is an accepted way of assessing Smad activation (Nakao et al, 1997. EMBO J. 16, 5353-5362). HFLI cells were also assessed as a comparison of normal cells known to signal through Smad following TGFβ. As described in 1.6.3 and 1.6.5, activation of the TGFβ receptor results in phosphorylation of Smad2/3 (the receptor Smads), which then interacts with Smad4 to

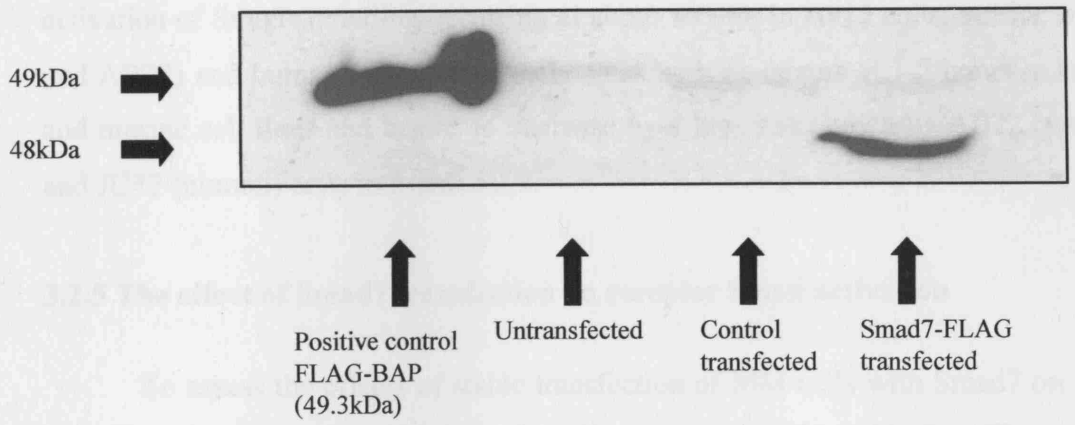

Figure 3.2.5 Flag expression by retroviral transfected MM cells. Western blot obtained from Ju77 cells stably transfected with Smad7-Flag-IRES-EGFP using a Flag antibody to detect Smad7 expression. The Flag tag peptide on the Smad7 was detected using Flag antibody (5µg/ml, Sigma) and visualized with a secondary horseradish peroxide labelled antibody. A positive control Flag is attached to a carrier protein (BAP), which is 49.3kDa in size. The Smad7-Flag protein is 48kDa in size. The untransfected Ju77 and the control transfected Ju77 line both remain negative.

transmit the signal to the nucleus. MM cells grown to confluence in 6 well plates were quiesced for 24 hours in serum-free medium and then treated with TGFβ_1 (1ng/ml) as described in section 2.6.1. Activation of Smad2 was then assessed by Western blot analysis of cell lysates, using an antibody specific to the phosphorylated form of Smad2, at time points from 5 min to 4 hours after TGFβ exposure. Figure 3.2.6 shows activation of Smad signalling occurring at about 15 min in HFLI cells, murine (AC29 and AB22) and human (JU77) MM cells. Peak activity occurs at 1-2 hours in human and murine cell lines and begins to decrease by 4 hours as shown by AB22 (murine) and JU77 (human) cells in figure 3.2.7.

3.2.5 The effect of Smad7 transfection on receptor Smad activation

To assess the effects of stable transfection of MM cells with Smad7 on Smad signalling, levels of phosphorylated Smad2 were assessed in stable Smad7 or control vector transfectants (created using the retroviral transfection system) and compared with non-transfected cells using Western blot analysis. NO36 MM cells were used as these were still expressing GFP visible by fluorescent microscopy. Other cell lines had much reduced expression at this time following multiple passage and the best GFP expressing cells, JU77 cells, had unfortunately been lost to infection. Ideally, these experiments would have been repeated in all cell lines used. Figure 3.2.8 shows that there is some activation of the Smad pathway in the Smad7 transfected cells, but the level of activity is markedly reduced (following correction against β-actin levels) compared with controls. To demonstrate that there is still some Smad activation in the Smad7 transfected cells a greater protein load was necessary, as shown by the levels of β-actin on the Western blot (figure 3.2.8). These results indicate a reduction in the activity of the Smad pathway compared with non-transfected and control transfected cells, but not total inhibition as a result of this method of transfection with Smad7 in these cell lines.

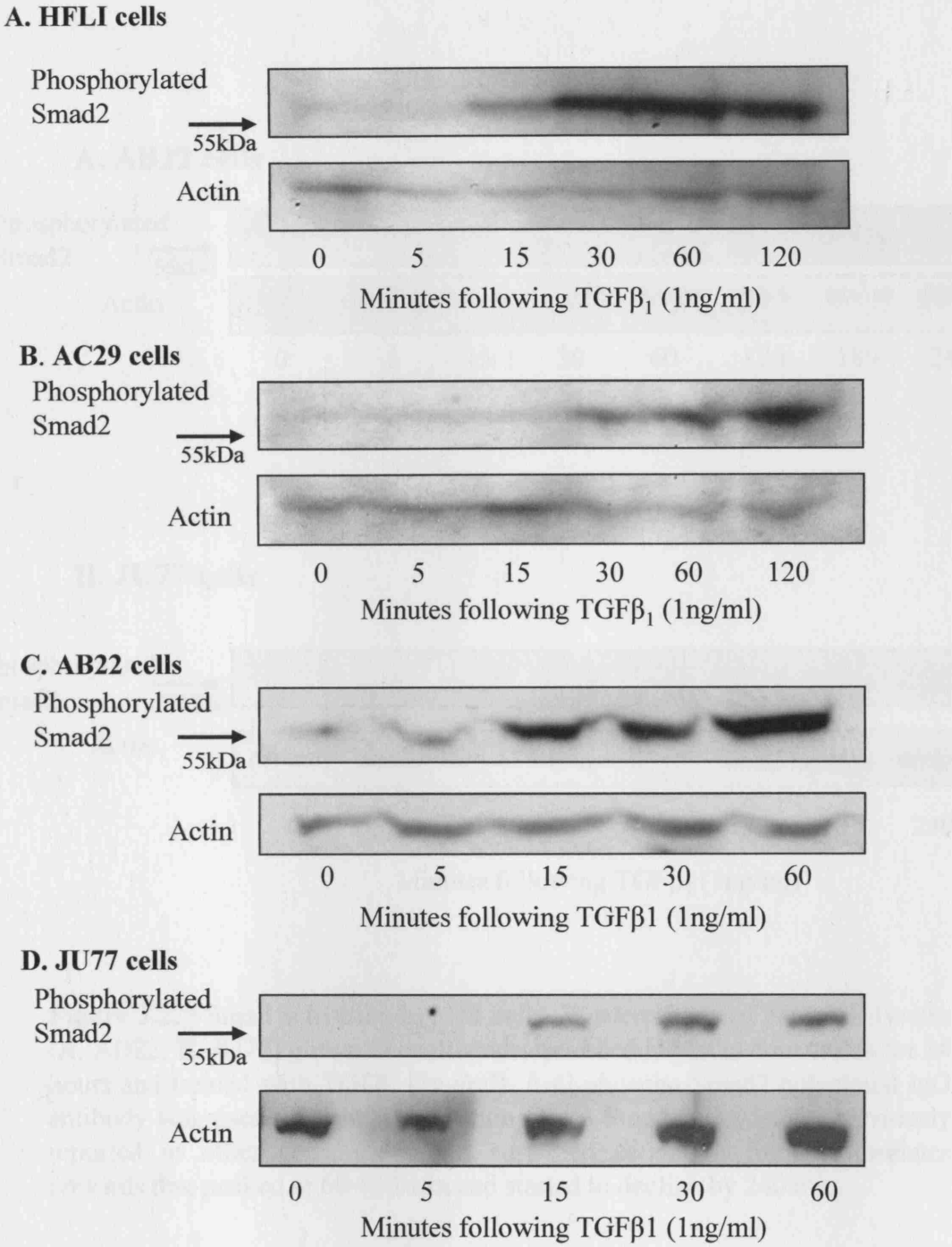

Figure 3.2.6 Western blot demonstrating phosphorylation of Smad2 (55-60 kDa) from 0 to 120 min following $TGF\beta_1$ exposure (1ng/ml) in HFLI cells (**A**) and AC29 cells (**B**). Each show phosphorylation of Smad2 occurring between 15 and 30 min after stimulation. Phosphorylation of Smad2 up to 60 min following $TGF\beta_1$ exposure (1ng/ml) is shown in AB22 (**C**) and JU77 (**D**) cell lysates. Actin labelled bands are shown to demonstrate protein loading of each lane.

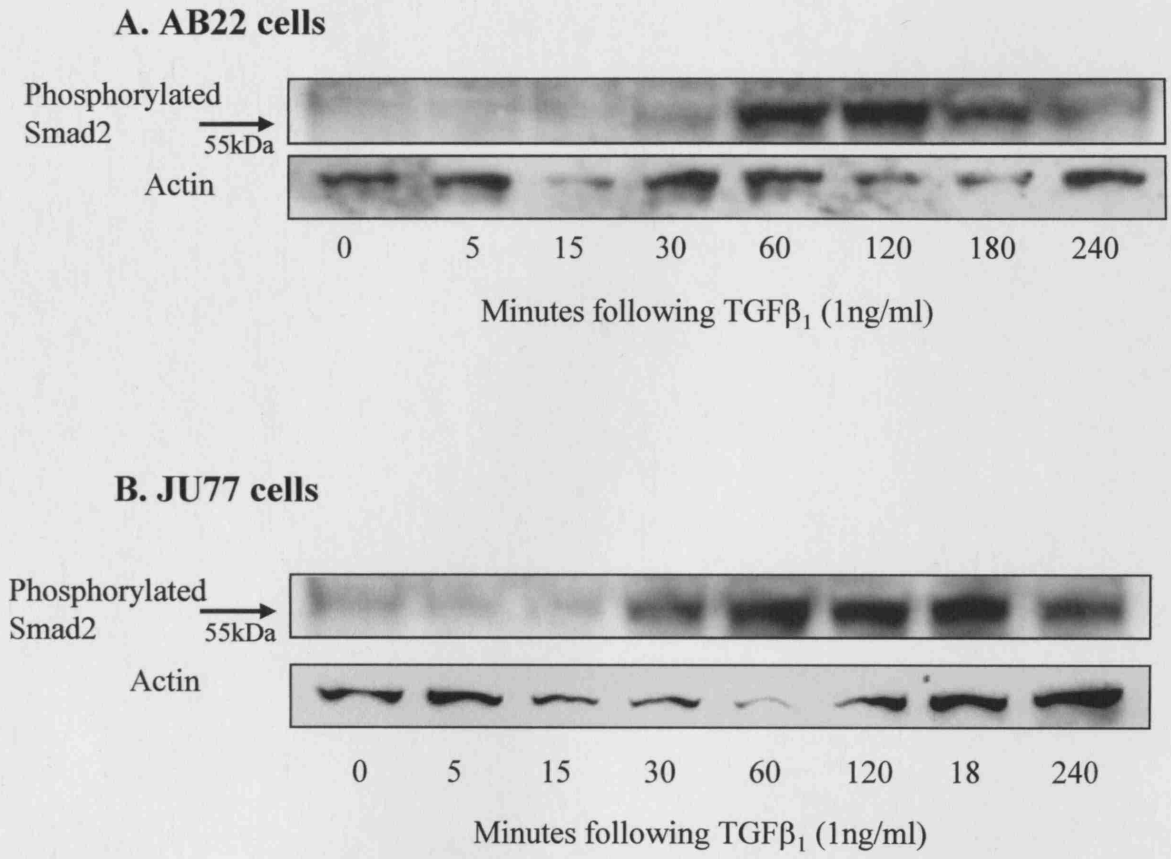

Figure 3.2.7 Smad activation in MM cells. Western blots of MM cell lysates (**A**. AB22, **B**. JU77) grown to confluence, quiesced in serum-free media for 24 hours and treated with $TGF\beta_1$ (1ng/ml). Anti-phospho-Smad2 polyclonal IgG antibody was used to identify activation of the Smad pathway. As previously reported in other cells, there was sustained activation from 15 minutes onwards that peaked at 60-120 min and started to decline by 240 min.

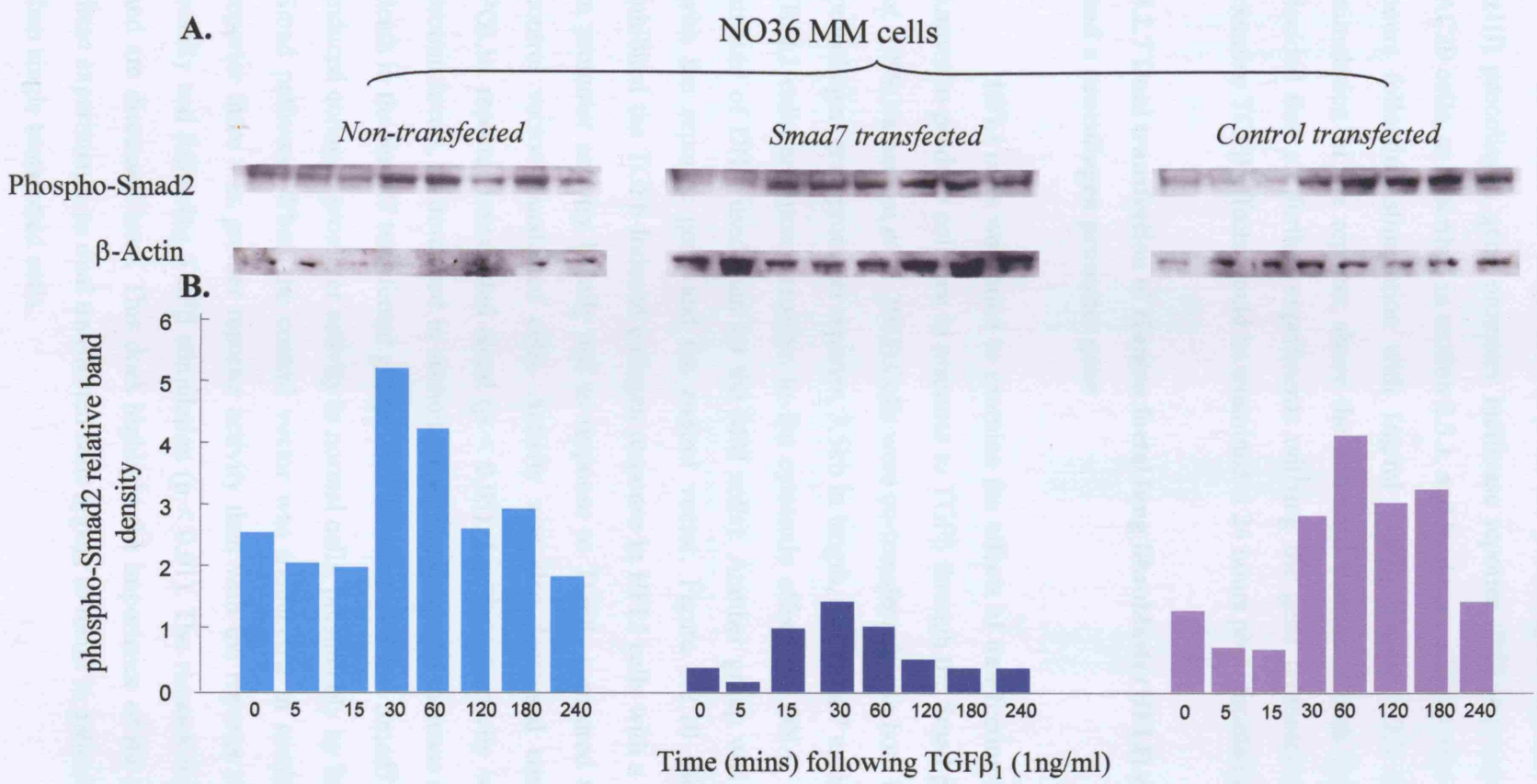

Figure 3.2.8 A. Effects of Smad7 transfection on Smad activation in MM cells. Western blots of NO36 cells that have been transfected to stably express Smad7 demonstrating reduced Smad activity. The Smad7 transfected cells needed much greater protein loading, shown by the much higher β-actin levels, which were used to correct the levels by comparisons of band densities shown in **B**. This shows the reduced signal in the Smad7 transfected NO36 cells compared with non-transfected and control transfected cells.

3.2.6 The effect of TGFβ on procollagen gene promoter activity in MM cells

To assess the effect of TGFβ on the procollagen response in MM cells an α1(I) procollagen gene promoter luciferase reporter (PGL1α) was transfected into AC29 cells, as described in section 2.5.1, and luciferase activity assessed at 16 and 24 hours following stimulation with 1ng/ml $TGF\beta_1$. Figure 3.2.9 shows significant stimulation of the reporter above the untreated control at both time-points. It was decided that all further experiments utilizing the gene promoter reporter assay to examine TGFβ effects would be examined at 24 hours post stimulation.

3.2.7 Dual transfection of Human foetal lung fibroblasts (HFLI) cells with Smad7 and a procollagen promoter gene

HFLI cells were used to examine the effects of transfecting Smad7 into cells known to produce collagen in response to TGFβ through the Smad pathway (Chen *et al.* 1999;Yamanaka *et al.* 2003).Cells were co-transfected with both the human α1 (I) procollagen gene promoter reporter, 3.5kb in length, and Smad7 using 0.2μg/ml DNA (HFLI cells are more sensitive to the cytotoxic effects of DNA, hence the lower amount of DNA used than for the MM cells). Another group was dual transfected with the reporter gene and the control vector. Figure 3.2.10 shows that Smad7 inhibited the TGFβ-induced collagen response in HFLI cells with a 10 fold decrease in promoter activity basally and in response to $TGF\beta_1$ compared with PGL1α and control vector transfected cells. Activity was also decreased compared with the PGL1α reporter transfected alone ($p < 0.05$). Luciferase activity was corrected for protein levels, as described in section 2.6.6. There was no increase in visualised cell death in the Smad7 transfected group. This demonstrated that Smad7 inhibited TGFβ-induced collagen promoter activity in normal cells, presumably by its blockade of the Smad pathway. When the control vector was transfected in combination with the reporter there was greater reporter activity than with the reporter transfected alone, basally and following TGFβ stimulation ($p < 0.01$). The reasons for this are unclear and are discussed later. This does highlight the importance of the control vector in these experiments, as dual transfected cells appear to result in greater reporter activity than single transfected cells.

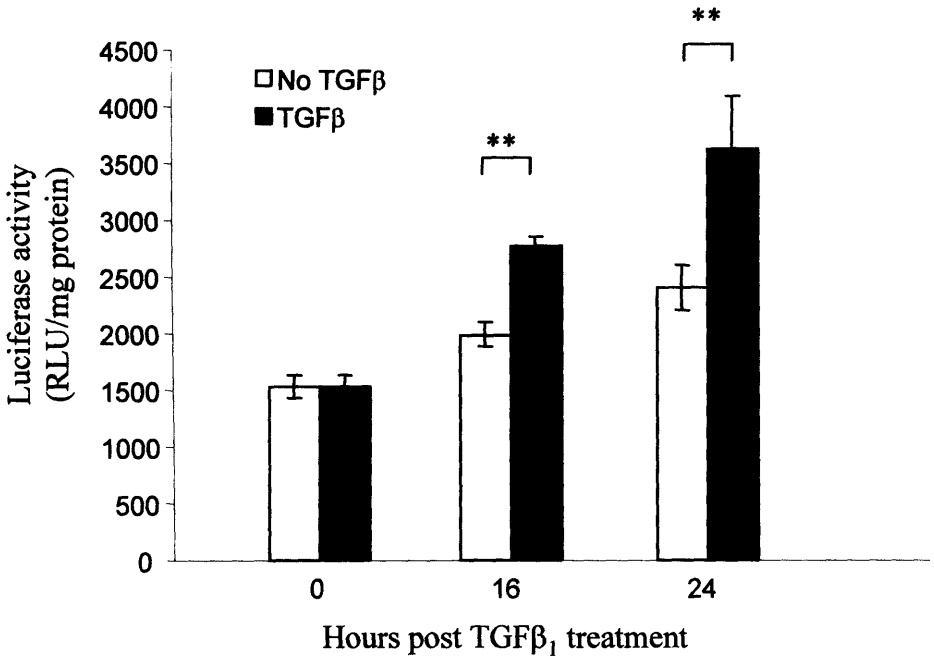

Figure 3.2.9 Procollagen α_1(I) gene promoter luciferase reporter activity in AC29 cells following stimulation with TGFβ. The activity of the PGL1α reporter was assessed over 24 hours following stimulation with $TGF\beta_1$ (1ng/ml). Four replicates were used per group and the bars represent the luciferase activity expressed as the mean RLU ± SEM. Empty bars represent non-$TGF\beta_1$ treated controls and black bars represent $TGF\beta_1$ treated cells, with time points shown on the x axis. Significant changes between controls and $TGF\beta_1$ treated controls are shown, ** = $p < 0.01$.

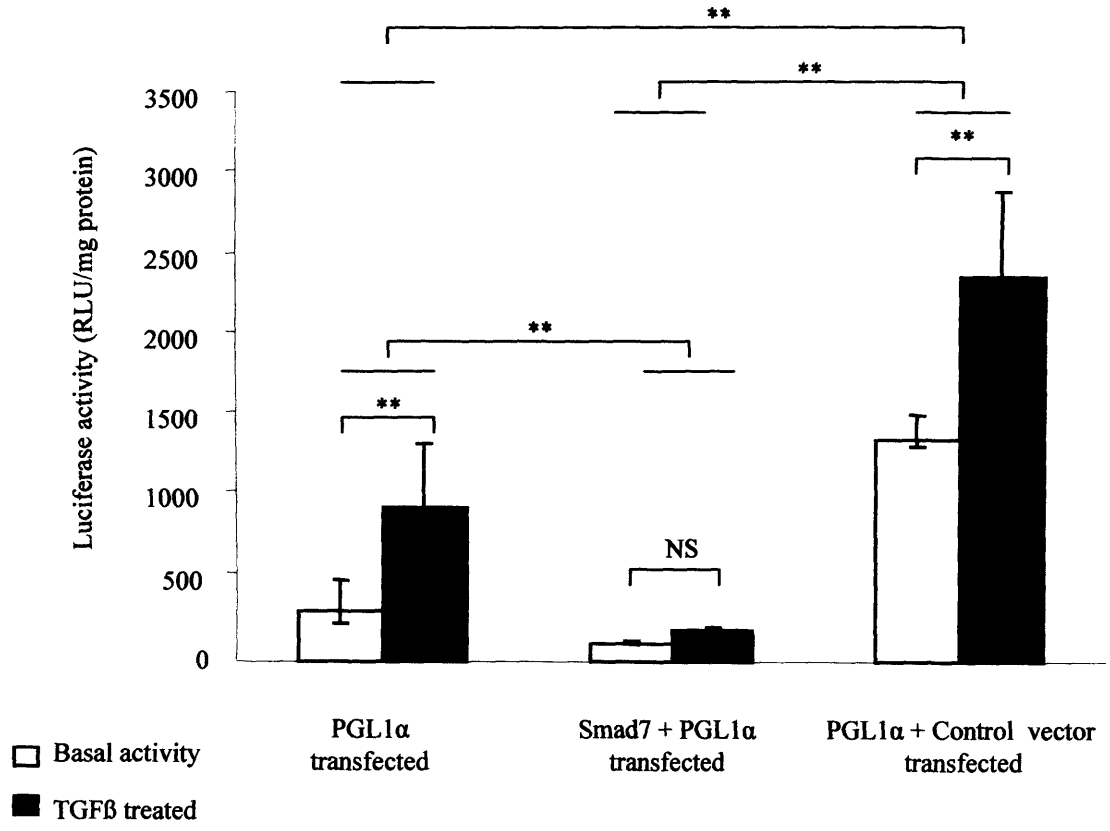

Figure 3.2.10 Dual transfection of Smad7 and a pro-collagen α1 (I) gene promoter in HFLI cells. HFLI cells were dual transfected with Smad7 and an α1 (I) pro-collagen gene promoter luciferase reporter. In these cells, expression of Smad7 resulted in significant inhibition of the basal reporter activity and loss of the response to $TGF\beta_1$. Interestingly, dual transfections with the control vector increases the basal activity of the reporter. There were normal responses to $TGF\beta_1$ with the control transfected cells. ** = $p < 0.01$, NS = not significant.

3.2.8 Dual transfection MM cells with a procollagen reporter and Smad7 vector

The effect of transfecting MM cells with Smad7 on TGFβ-induced procollagen synthesis was assessed by dual transfection with the α1 (I) pro-collagen gene promoter luciferase reporter (PGL1α) as described in section 2.5.1. In murine AC29 transfected cells (figure 3.2.11), TGFβ induced a 1.8 fold increase in luciferase activity in cells transfected with Smad7 ($p < 0.01$) compared with a 1.6 fold increase in cells transfected with control vector ($p < 0.01$). The dual Smad7 transfected cells had a 36% increased basal luciferase activity compared with the single reporter transfected control despite having been transfected using less reporter DNA in the LID complex (figure 3.2.11A). This result was a consistent finding in at least 4 repeat experiments, (the results of which were not amalgamated since each experiment had different baseline luciferase activity) shown in table 3.2.1. The experiment was repeated in JU77, a human MM cell line using a 3.5kb human reporter. Figure 3.2.11B shows that, as shown in the AC29 cells, dual transfection with Smad7 significantly increased the activity of the reporter basally (6 fold compared with dual control transfected cells), although there were no TGFβ responses in either the control cells or the Smad7 transfected cells.

JU77 cells did not have a significant response to $TGF\beta_1$ at this time-point (24 hrs) despite increased doses of $TGF\beta_1$ (data not shown). Smad7 expression was expected to reduce the response of the reporter to $TGF\beta_1$ but the activity of the reporter, basally and in response to $TGF\beta_1$, was surprisingly increased after dual transfection with Smad7 compared with controls. This is the opposite of the response seen in HFLI cells, where the predicted inhibition of the response is seen.

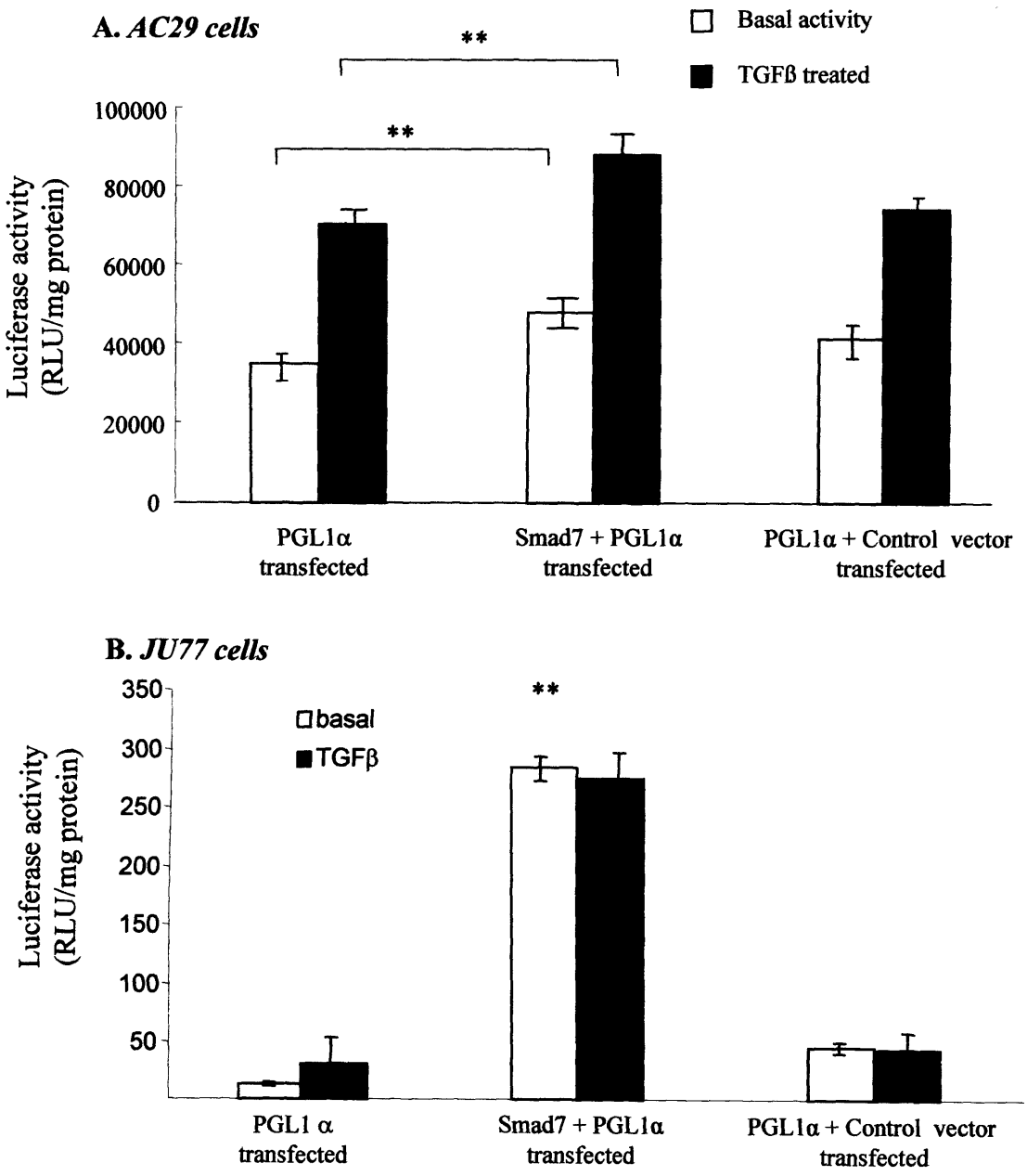

Figure 3.2.11 Dual transfection of Smad7 and PGL1α luciferase reporter in MM cells. **A** In AC29 cells the activity of the reporter is not inhibited by Smad7 expression but is significantly enhanced basally (empty bar) and at 24 hours following 1ng/ml $TGF\beta_1$ stimulation (filled bar) compared with cells transfected with the reporter alone (** $p < 0.01$). However, the increase is not significant when compared with the control dual transfected cells (representative of 6 repeat experiments). In **B** Ju77 cells transfected with the dual Smad7/procollagen gene promoter reporter showed an increase in the basal activity compared with either the single reporter transfected or control vector dual transfected cells (** $p < 0.01$). No TGFβ stimulated response is seen in any of the groups in this cell line at this time point (24 hours).

	Experiment 1		Experiment 2		Experiment 3		Experiment 4	
Transfection	**Basal**	**TGFβ treated**	**Basal**	**TGFβ treated**	**Basal**	**TGFβ treated**	**Basal**	**TGFβ treated**
PGL1α	3922 ± 115	6751 ± 547	74.71 ± 7.84	110 ± 6.67	767 ± 76	1127 ± 212	2219 ± 176	3689 ± 311
PGL1α + Smad7	4884 ± 32	8108 ± 715	424 ± 27.16	545 ± 51.35	1354 ± 109	2267 ± 221	4443 ± 432	7690 ± 288
PGL1α + PcDNA3	4411 ± 141	7702 ± 195	202 ± 24.25	206 ± 16.5	898 ± 98	1322 ± 142	3221 ± 357	4932 ± 552

Table 3.2.1 Results of repeat experiments assessing the effects of dual transfection of AC29 cells with PGL1α procollagen gene promoter reporter with either Smad7 or PcDNA3 control vector. Results are expressed as relative light units of luciferase activity ± SEM. The results show the repeated pattern of increased activity following Smad7 transfection. The basal luciferase activity varies considerably between experiments.

3.2.9 Collagen synthesis by MM cells expressing Smad7

The effects of Smad7 over-expression on collagen synthesis by MM cells was assessed by measuring hyp production (by HPLC) in MM cells stably transfected with Smad7. The human MM cell line, JU77 and the murine cell line, AB22, stably transfected with either Smad7 or control vectors, were selected for analysis as these two cell lines expressed more GFP than the other human and murine transfected lines respectively. This higher level of GFP expression indicated greater Smad7 production following transfection compared with the other MM cell lines. Cells were grown to confluence in 24 well tissue culture plates to assess collagen production basally and in response to $TGF\beta_1$ as described in section 2.5.5.

The results were analysed in three ways: 1) measurement of basal collagen production; 2) measurement of the response to TGFβ by each group; 3) by calculating the fold increase in production of collagen in response to TGFβ over basal levels. This last analysis was performed as each group had different basal levels of collagen

production and was therefore necessary in order to assess the stimulatory activity of TGFβ.

1) Cells transfected with Smad7 showed a 5.7 fold increase in basal collagen production compared with transfected controls and 2 fold increase over non-transfected controls (control transfected cells 0.11 ± 0.04, non-transfected controls 0.32 ± 0.06, and Smad7 transfected cells 0.65 ± 0.12 nmol hyp / 10^6cells / 24hr, $p < 0.01$), as shown in figure 3.2.12A.

2) In response to $TGF\beta_1$ stimulation collagen production increased in controls and Smad7-transfected cells (control 1.14 ± 0.04, control transfected 0.42 ± 0.18, Smad7 transfected 1.66 ± 0.06).

3) The fold increases over basal levels of collagen production show that Smad7-transfected cells have a smaller response to $TGF\beta_1$ than the control cells, as table 3.2.2 illustrates. This shows that the fold increase in collagen production following TGFβ in the control cells was 3.7-3.8, whereas the increase in the Smad7 transfected cells was 2.6 fold above basal levels.

The experiment was repeated in the murine AB22 MM cell line. Again there was increased basal collagen production in the Smad7 transfected cells ($p < 0.01$) with further increases following TGFβ stimulation (see figure 3.2.12B). Table 3.2.3 shows the levels of collagen measured and also the fold increases in each group following $TGF\beta_1$. As with the JU77 cells, the fold increase in the Smad7-transfected cells following TGFβ was less than the controls (although total collagen production was again higher).

These results concur with the procollagen reporter gene findings that suggest over-expression of Smad7 results in increased basal collagen production but with some reduction in the response to exogenous TGFβ.

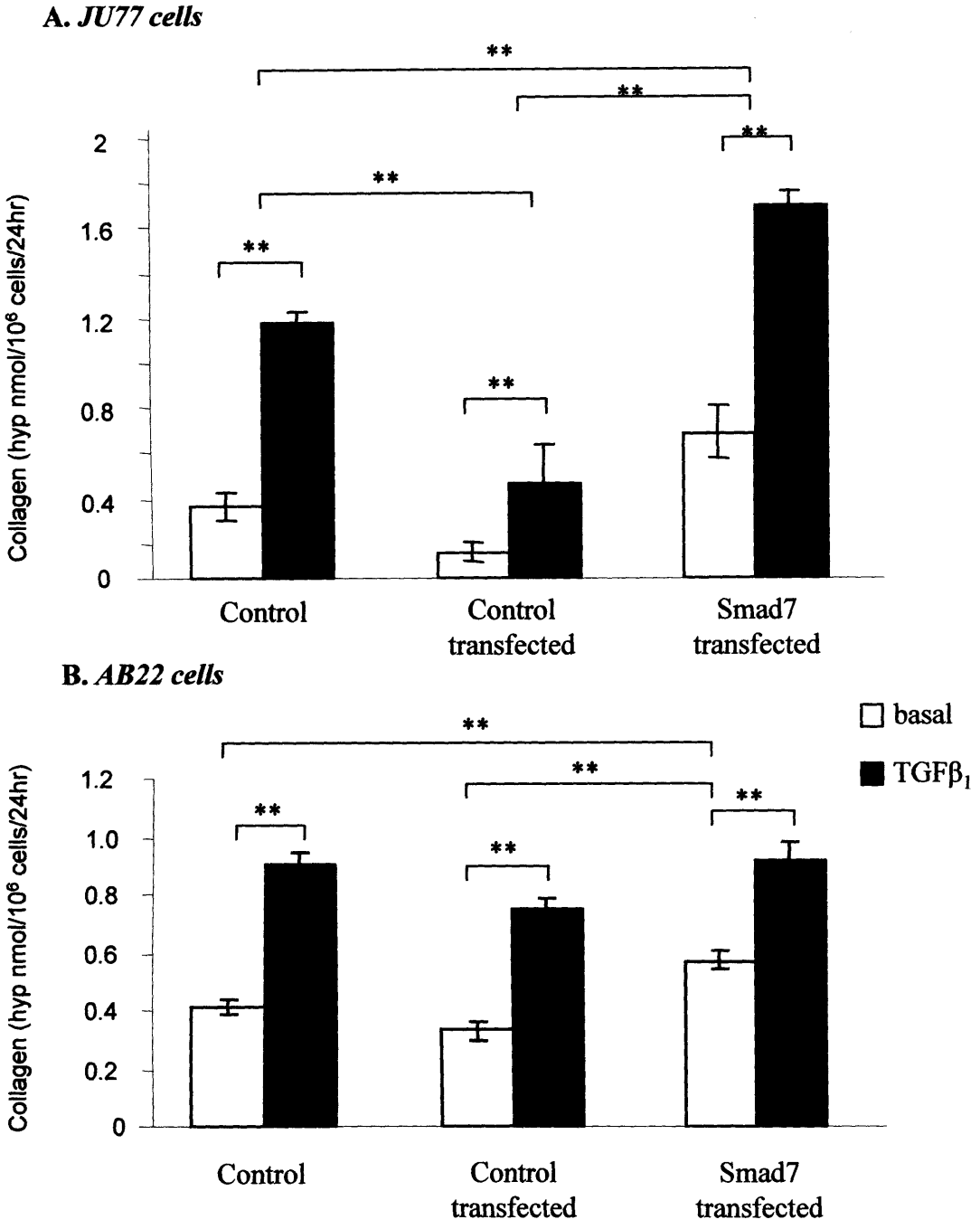

Figure 3.2.12 Increased collagen production in MM cells stably over-expressing Smad7 **A.** Hyp levels increase basally (empty bars) and 24hr after stimulation with 1ng/ml $TGF\beta_1$ (filled bars) in Ju77 MM cells stably over-expressing Smad7, ** $p < 0.01$ compared with non-transfected and transfected control. Each group is the mean of 6 replicates ± SEM. This graph is representative of three repeat experiments. **B.** A repeat experiment using murine AB22 cells stably expressing Smad7, also shows an increase in basal collagen production.

	JU77 non-transfected	JU77-HR	JU77-Smad7
Basal collagen ± SEM (nmol hyp / 10^6cells / 24hr)	0.31 ± 0.06	0.11 ± 0.04	0.65 ± 0.12
TGFβ_1 stimulated	1.14 ± 0.05	0.42 ± 0.18	1.66 ± 0.06
Fold increase	3.7	3.8	2.55

Table 3.2.2 Basal and TGFβ_1 (1ng/ml) stimulated collagen production in JU77 cells. JU77-HR = control vector transfected JU77 cells. JU77-Smad7 = Smad7 transfected JU77 cells. The TGFβ_1 stimulated fold increase in collagen above basal levels is shown in the bottom row of the table and shows the decreased response in Smad7 transfected cells.

	AB22 non-transfected	AB22-HR	AB22-Smad7
Basal collagen ± SEM (nmol hyp / 10^6cells / 24hr)	0.41 ± 0.03	0.33 ± 0.03	0.57 ± 0.03
TGFβ_1 stimulated	0.91 ± 0.04	0.75 ± 0.07	0.91 ± 0.03
Fold increase	2.2	2.2	1.6

Table 3.2.3 Basal and TGFβ_1 (1ng/ml) stimulated collagen production in AB22 cells. AB22-HR = control vector transfected AB22 cells. AB22-Smad7 = Smad7 transfected AB22 cells. The fold increase of basal collagen production following TGFβ_1 stimulation is shown in the bottom row of the table and shows the decreased response in the Smad7 transfected lines.

3.2.10 Tumour growth of MM cells expressing Smad7

Following the unexpected finding that MM cells stably transfected with Smad7 produced more collagen than control transfected and non-transfected MM cells, the effects of Smad7 transfection on tumour growth *in vivo* were analysed in a mouse model of MM, described in section 2.7. AC29, AB22 and AB1 cells and their stable Smad7 and control vector expressing equivalents were used to inoculate and grow tumours on the hind flanks of mice. In the AB22 and AB1 groups, the tumours were allowed to continue growing for 28 days at which point the experiment was stopped. In the AB22-Smad7 group (figure 3.2.13) the Smad7 tumours (median weight 313 mg, range 159-484) were significantly larger than the untransfected tumour group (median weight 186 mg, range 108-324, $p<0.01$) and were larger than the control transfected (median weight 32 mg, range 15-47, although the low number of tumours recovered from control transfected MM cell tumours made statistical analysis impossible). The AB1-Smad7 (figure 3.2.14) tumours (median weight 170 mg (69-301)) again showed a trend to be larger than the untransfected (median weight 148 mg (34-269)) and were larger than the control transfected tumours (median weight 27 (8-80), $p<0.01$). In the AC29 group, the experiment was stopped early (at 14 days) as some of the tumours reached the 1 cm maximum external diameter permitted by the Ethics Committee. Figure 3.2.15 shows that the Smad7 expressing cells induced growth of tumours that were larger than the untransfected AC29 induced tumours (median Smad7-transfected tumour weight 60 mg (15-359), control median tumour weight 22 (7-100), $p < 0.05$). There was a trend for the Smad7 transfected AC29 derived tumours to be larger than the control transfected AC29 derived tumours. As with the measurement of collagen production, tumour growth was the opposite of both the original prediction and the results using the TGFβ neutralising antibodies.

3.2.11 Collagen content of MM tumours grown from cells expressing Smad7

In vitro transfection of Smad7 resulted in increased activity of the procollagen gene promoter reporter and increased collagen production as described in sections 3.2.8 and 3.2.9. To assess the effects of Smad7 expression on the collagen content of tumours grown *in vivo*, tumours derived from the experiment described in section

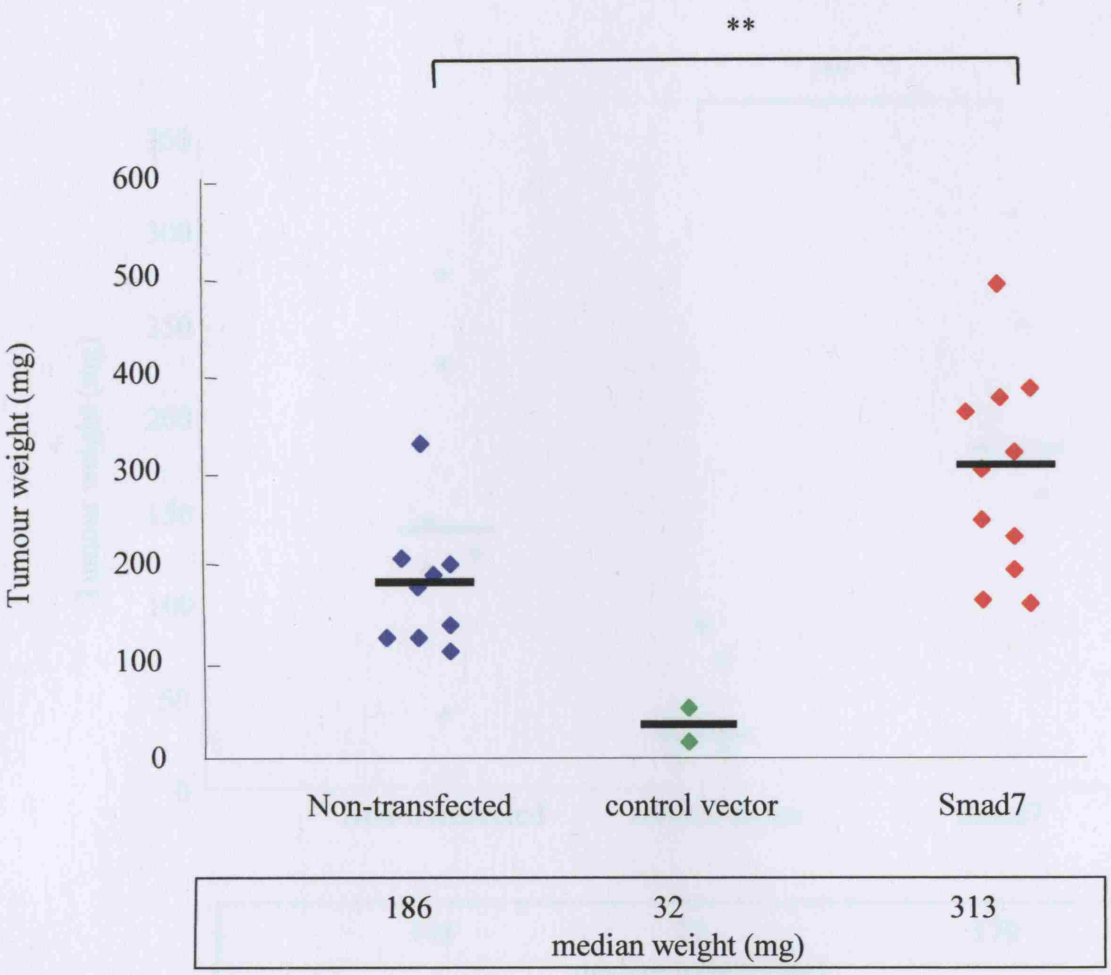

Figure 3.2.13 Weights of tumours grown from Smad7 expressing AB22 cells. Tumour weights of MM tumours grown in AB22 cells (non-transfected, control transfected, Smad7-transfected) at 28 days. Each point represents an individual tumour. The bar represents the median tumour weight in each group, which is also shown in the box below the graph. There is a significant increase in weight of tumours derived from Smad7 expressing cells. ** $p < 0.01$ Mann Whitney U test

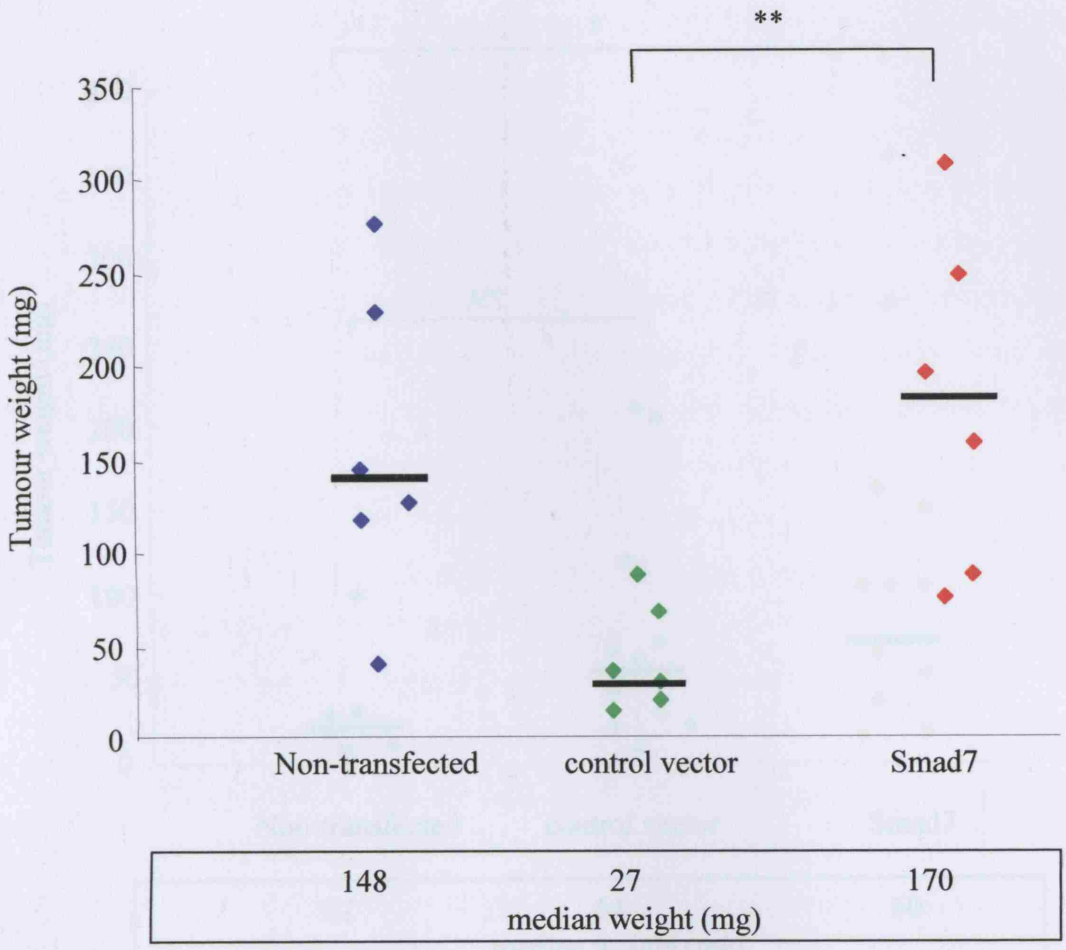

Figure 3.2.14 Weights of tumours grown from Smad7 expressing AB1 cells. Tumour weights of MM tumours grown in AB1 cells at 28 days. Each point represents an individual tumour. The bar represents the median tumour weight in each group, also shown in the box below the graph. Smad7 expressing cells were significantly larger than control transfected tumours with a trend for increased size compared with the non-transfected controls. ** $p < 0.01$ Mann Whitney U test

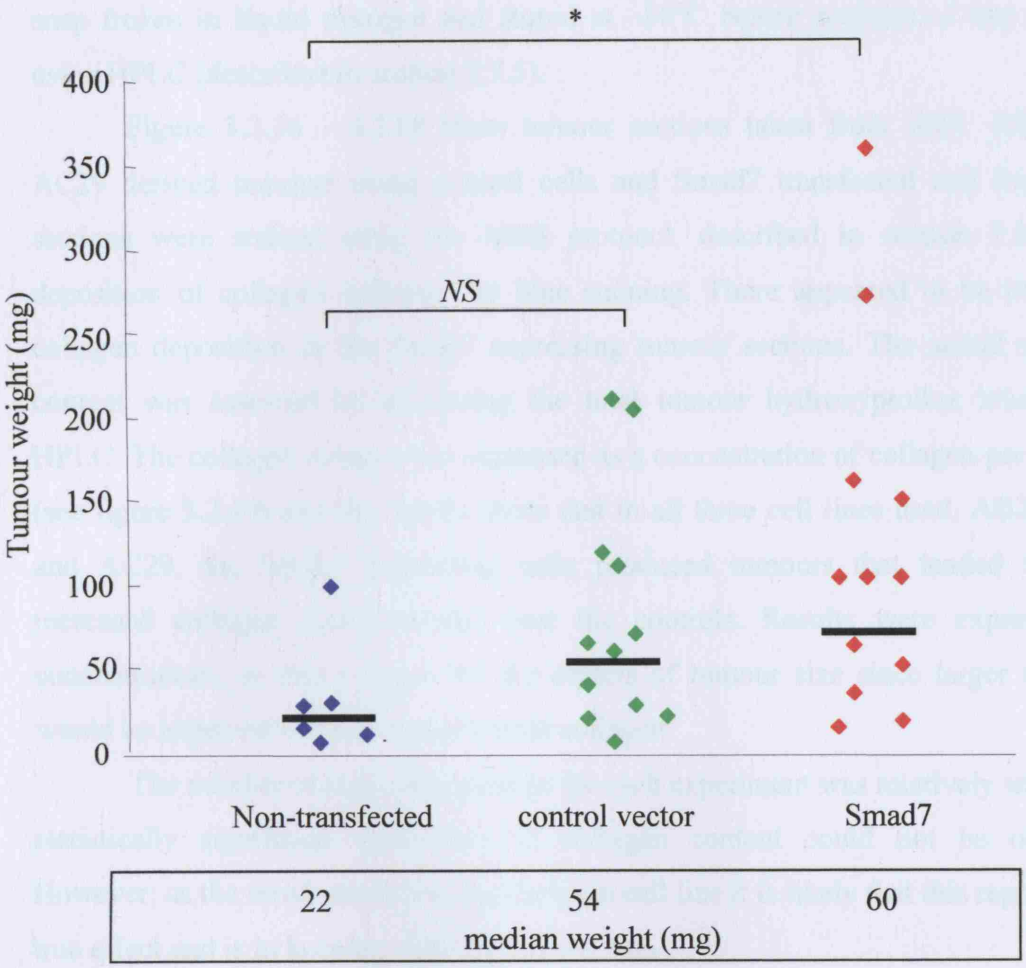

Figure 3.2.15 Weights of tumours grown from Smad7 expressing AC29 cells at 14 days. This experiment was ended early as some of the tumours had reached the maximum permitted size. Each point represents an individual tumour. The bar represents the median tumour weight in each group, also shown in the box. Tumours derived from Smad7 expressing cells were significantly larger than non-transfected control tumours with a trend for increased size compared with the transfected controls. ** $p < 0.05$ Mann Whitney U test. *NS* = non-significant

3.2.10 were either placed in paraformaldehyde before processing to be placed in paraffin blocks (as described in 2.7.4) and sectioned for histochemical staining or snap frozen in liquid nitrogen and stored at –80°C before analysis of hyp content using HPLC (described in section 2.7.5).

Figure 3.2.16 – 3.2.18 show tumour sections taken from AB1, AB22 and AC29 derived tumours using control cells and Smad7 transfected cell lines. The sections were stained using the MSB protocol, described in section 2.8.1, and deposition of collagen indicated by blue staining. There appeared to be increased collagen deposition in the Smad7 expressing tumour sections. The actual collagen content was assessed by measuring the total tumour hydroxyproline level using HPLC. The collagen content was expressed as a concentration of collagen per tumour (see figure 3.2.19) and the results show that in all three cell lines used, AB22, AB1 and AC29, the Smad7 expressing cells produced tumours that tended to have increased collagen concentrations over the controls. Results were expressed as concentrations, as this corrects for the effects of tumour size since larger tumours would be expected to have a greater total collagen.

The number of tumours available for each experiment was relatively small and statistically significant differences in collagen content could not be obtained. However, as the trend was consistent for each cell line it is likely that this represents a true effect and is in keeping with the *in vitro* data.

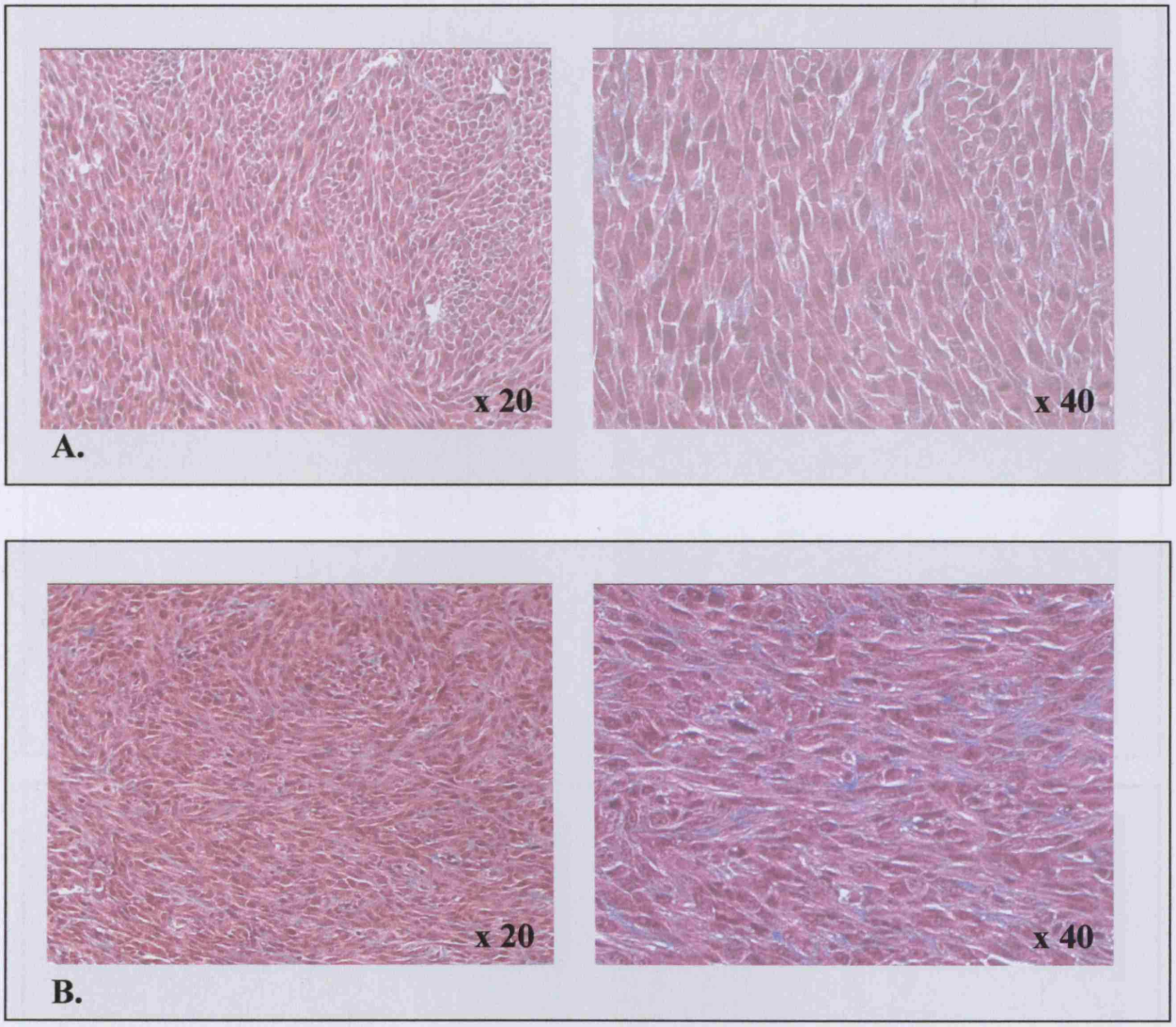

Figure 3.2.16 AB1 Smad7-transfected cell derived tumour section stained with MSB. Panel **A** shows non-transfected AB1 tumour sections at 20 and 40 x normal magnification as indicated. Panel **B** shows a section from a tumour derived from AB1 cells transfected with Smad7. These are representative samples of tumour sections showing relatively heterogeneic levels of collagen content. These sections suggest a possible increase in collagen in the Smad7 sections in panel **B** compared with panel **A**. However, they only represent a small area of one section of one tumour.

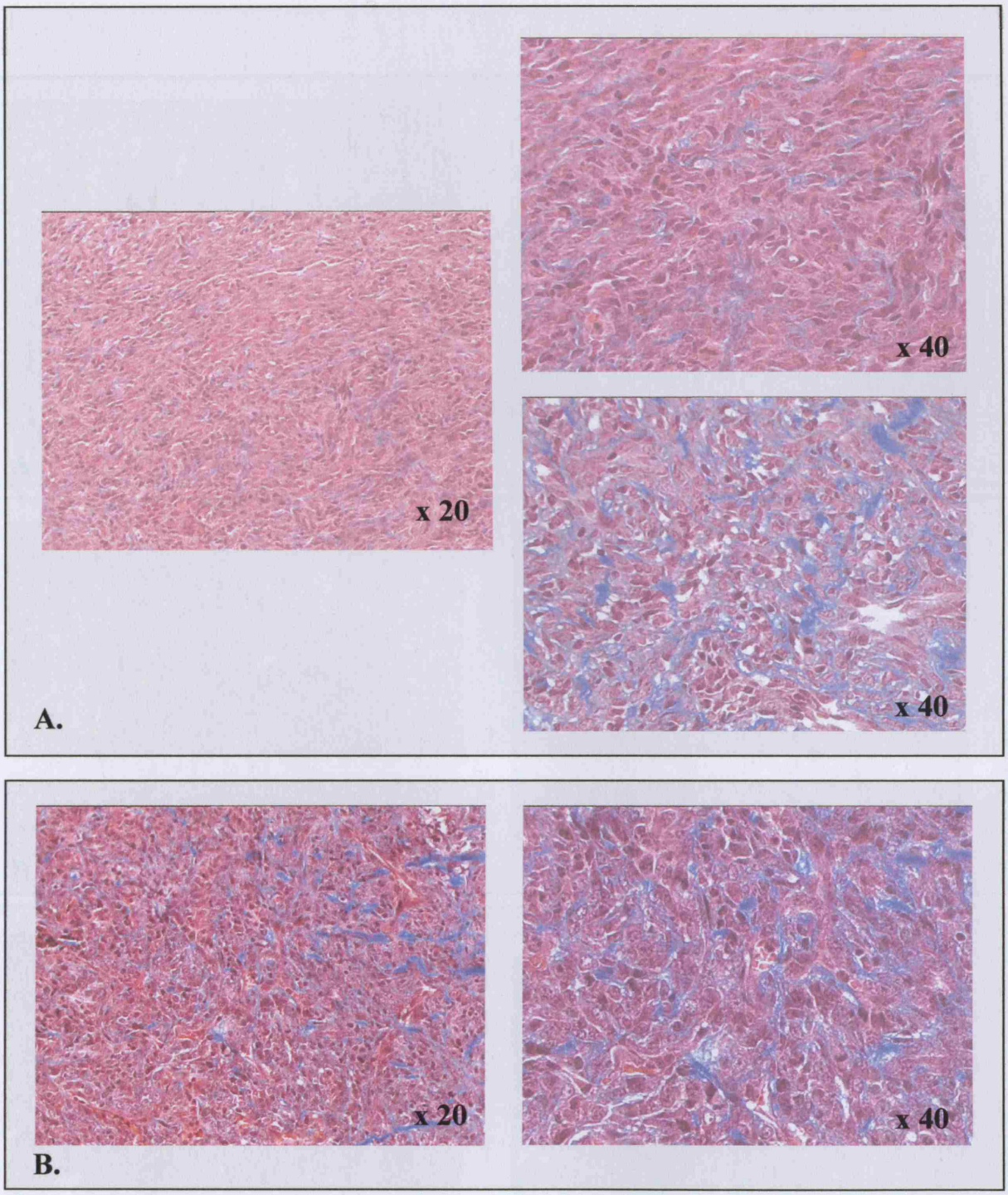

Figure 3.2.17 AB22 Smad7-transfected cell derived tumour sections stained with MSB. Panel **A** shows non-transfected AB22 derived tumour at x 20 and x 40. Two sections taken from the same tumour shown at x 40 show the heterogeneity of collagen deposition within a tumour section. Panel **B** shows sections through Smad7 transfected AB22 derived tumours. There is an appearance of greater collagen content within the Smad7 derived tumour sections.

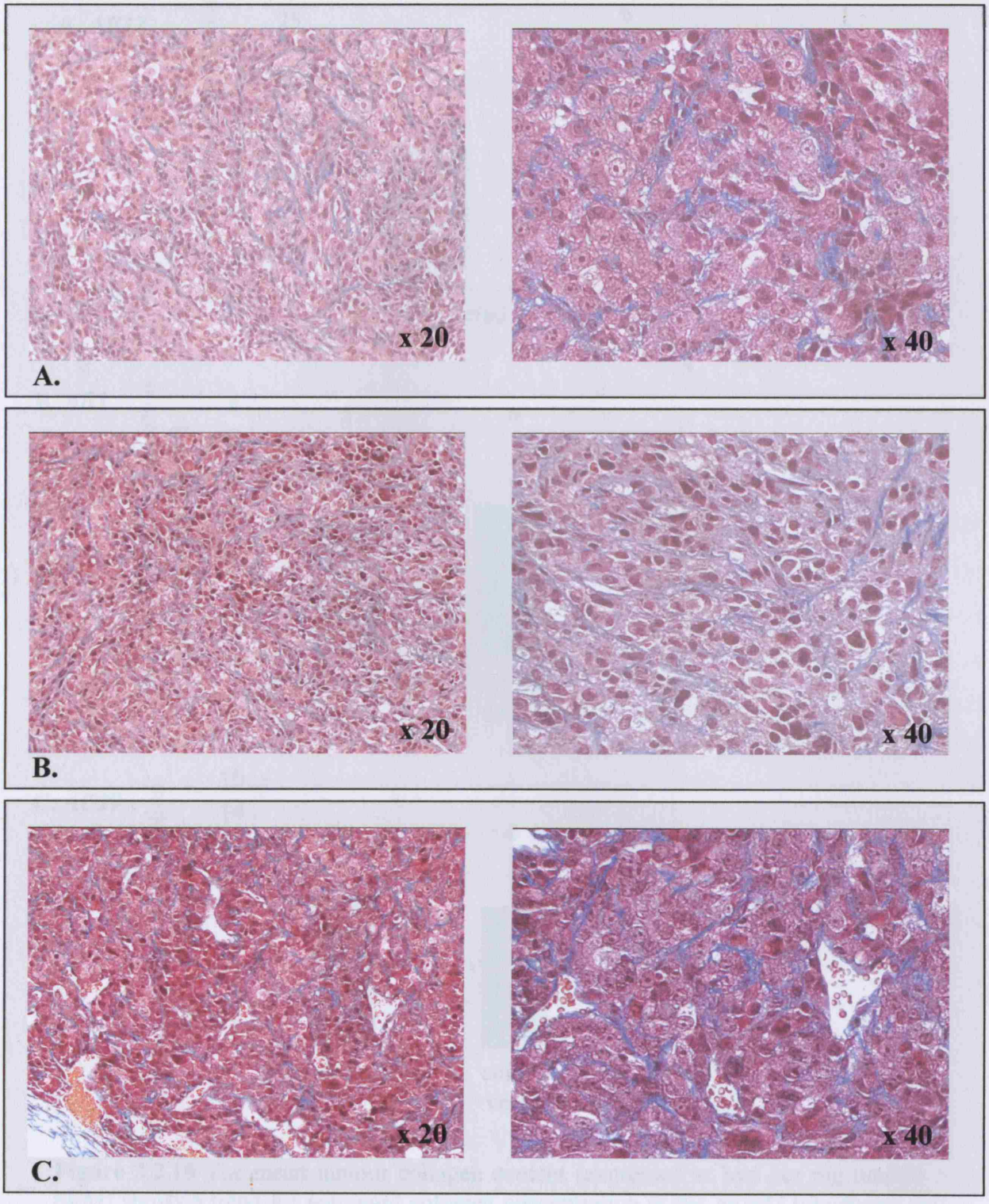

Figure 3.2.18 AC29 Smad7-transfected cell derived tumours stained with MSB. Panel **A** shows non-transfected AC29 cell derived tumour sections at 20x and 40x normal magnification. Panel **B** shows control vector derived AC29 cell tumours and panel **C** shows sections from tumours derived from Smad7 transfected AC29 cells. There appears to be more collagen staining (blue) in the sections seen in panel **C** i.e. tumour sections from Smad7 transfected cells.

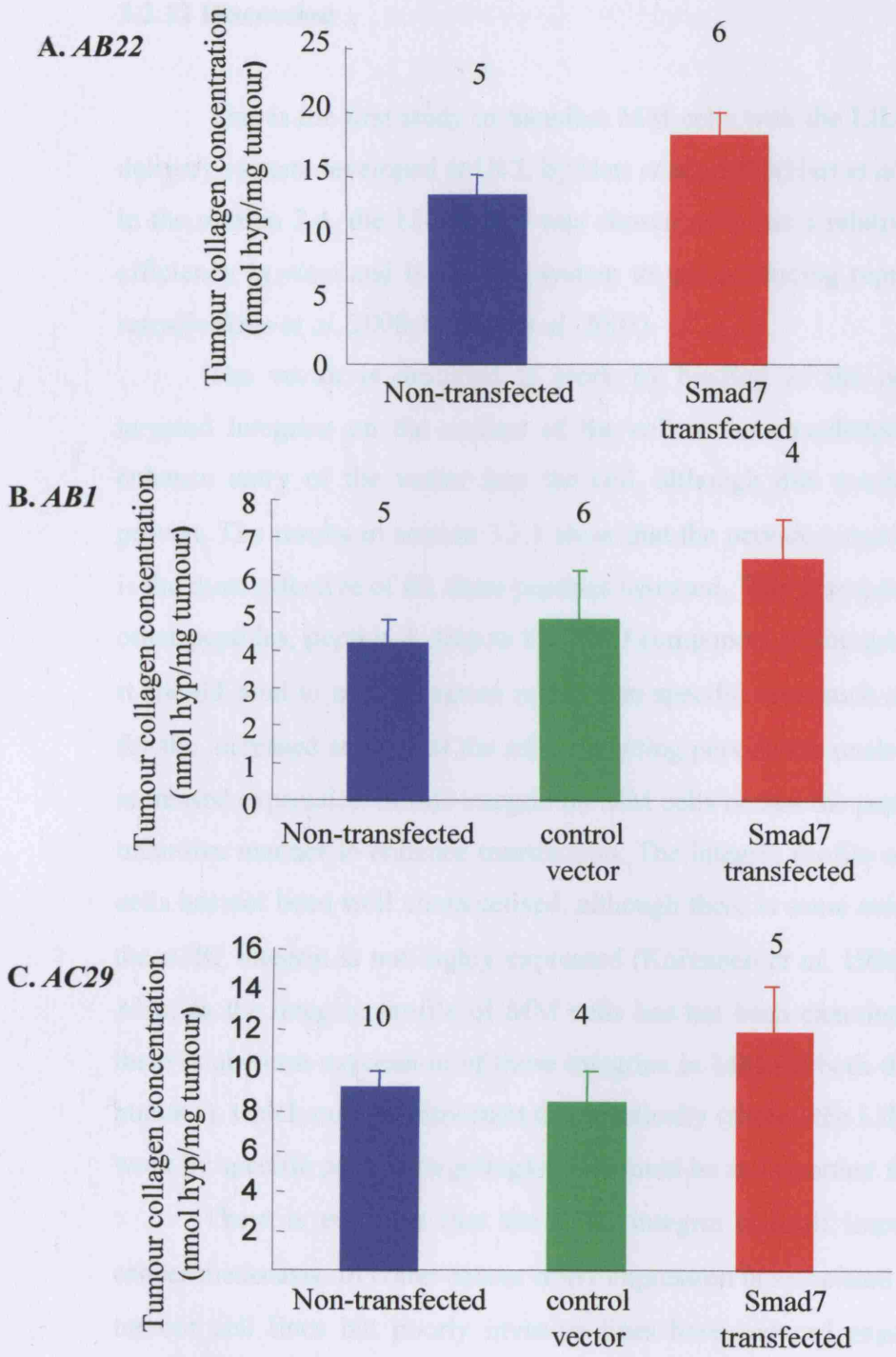

Figure 3.2.19 The mean tumour collagen content (expressed as hyp per mg tumour ± SEM) shows a trend for increased collagen concentration in the Smad7 transfected cell tumours in all three experiments, using three different cell lines, (**A**. AB22 **B**. AB1 **C**. AC29). Numbers above columns represents the number of tumours analysed. This was limited by recovery of tumour and the loss of some samples in the processing for analysis by HPLC. The number of AC29 non-transfected controls were bolstered from another experiment (TGFβ antibody expts).

3.2.12 Discussion

This is the first study to transfect MM cells with the LID vector, a novel gene delivery system developed at UCL by Hart *et al.*, 1998(Hart *et al.* 1998). As discussed in the section 2.4, the LID vector was chosen as it has a relatively high transfection efficiency *in vitro* and is an easy system to use producing reproducible transfection rates(Jenkins *et al.* 2000;Jenkins *et al.* 2003).

The vector is designed to work by binding of the peptide component to targeted integrins on the surface of the cell to be transfected. This is thought to enhance entry of the vector into the cell, although this mechanism has yet to be proven. The results in section 3.2.1 show that the peptide targeting the α5β1 integrin is the most effective of the three peptides assessed. This is surprising, since one of the other peptides, peptide 1, targets the RGD component of integrins, which means that it should bind to most integrins rather than specific ones such as α5β1. The reasons for the increased activity of the α5β1 targeting peptide are unclear but may be due to increased expression of this integrin on MM cells or that the peptide is working in an unknown manner to enhance transfection. The integrin profile of murine mesothelial cells has not been well characterised, although there is some evidence to suggest that the α5β1 integrin is not highly expressed (Koivunen *et al.* 1994;Mould *et al.* 1998). Also, as the integrin profile of MM cells has not been examined, it is possible that there is aberrant expression of these integrins in MM (in both the murine model and humans), which may be important therapeutically (should the LID vector be proven to work by specific peptide targeting). This would be an important future study.

There is evidence that the α5β1 integrin is itself important in cancer and cancer metastasis. In colon cancer α5β1 expression is associated with highly invasive tumour cell lines but poorly invasive lines have reduced expression (Gong *et al.* 1997). In lymphoma, T cell leukaemia virus type I (HTLV1) infected T cells have increased α5β1, which is associated with increased adhesion of T cell leukaemia cells to the ECM and dendritic cells leading to lymphoma formation (Hasegawa *et al.* 1998). In mice, α5β1 is up-regulated in the development of spindle cell carcinoma in the late stages of mouse skin carcinogenesis (Gomez and Cano 1995). Finally, in metastatic deposition in the liver, α5β1 expression increases the attachment of tumour

cells to hepatocytes and inhibition of α5β1 also reduced colorectal metastasis to the liver(Kemperman *et al.* 1994;Stoeltzing *et al.* 2003).

Exposure of cells to DNA can produce toxicity. Interestingly, the MM cells appear to tolerate higher levels of DNA in transfection with the LID vector than non-malignant cells. For example, human foetal lung fibroblast (HFLI) cells suffer toxic effects at concentrations of DNA that MM cells tolerate well i.e. 1-2 μg/ml transfection medium. The greater tolerance of these cells to higher DNA levels is likely to be one reason why this system produces good transfection efficiency in MM cells. Using green fluorescent protein (GFP), the transfection efficiency was estimated as 15-20% using 2μg/ml DNA and 20-30% using 5μg/ml DNA. As the cell population increases *in vitro* (following transfection), the number of cells expressing GFP also increases (section 3.2.1.3). This may be due to sharing of GFP protein in the cytoplasm as the cell divides (GFP has a half-life of approximately 26 hours) or by the sharing of multiply transfected plasmids during cell division. In either situation, the implication is that a significant level of transfection has occurred and that for the purposes of these studies the transfection rate remains constant for the duration of the experiments. This was important for further experiments, where the level of plasmid transcription and protein expression could be assumed to be consistent and constant.

When higher concentrations of DNA (5μg/ml) were used to transfect the MM cells higher transfection rates (20-35%) were achieved at the cost of reduced total cell number, implying toxic effects. Therefore these higher doses were not used for general experiments. However, it is worth noting that despite this apparent toxicity following transfection, cell numbers still doubled at the same rate (36 hours) as cells transfected using lower DNA concentrations. The toxicity therefore seems to occur at the point of application of the transfection medium, but is not prolonged.

Using the retroviral method of transfection, stable transfections of Smad7 were achieved in all seven MM cell lines used. This allowed studies on the effects of Smad7 on collagen production. This method was used, instead of LID transient transfection, for experiments measuring hyp and in the animal model, as the LID vector only transfected approximately 20% of cells, which was not sufficient for studies of collagen production, as a change in collagen production of 20% was not enough to produce a significant change. This is not surprising as Smad7 is an

intracellular protein involved in specific signalling events; transfection will only have an effect on transfected cells, with no cell bystander effect envisaged.

The co-expression of GFP using the IRES vector insert gave a simple method to check that the cells were still expressing Smad7. The level of vector expression (as assessed by the intensity of GFP) was higher in the human cell lines than the murine cells, although all murine lines were successfully transfected, as assessed by GFP expression using con-focal microscopy. The level of Smad7 expression was enough to reduce Smad signalling but not enough to completely block it. This enabled assessment of reduced Smad signalling rather than complete inhibition and for the purposes of these experiments was probably more ideal since total blockade of Smad signalling may have resulted in other pathways becoming active. Hence these results are due to reduced Smad signalling rather than complete inhibition. The reduced expression in the murine cell lines compared with the human lines was not totally unexpected since the vector was derived from human immunodeficiency virus and designed principally for the transfection of human cell lines. Over a period of time and multiple passages the expression of GFP, and so also of Smad7, was observed to become less and so passage of these cells was limited.

Effects of Smad7 transfection on collagen production - three approaches were used to assess these effects at gene, protein and biological levels:

1) To assess the collagen gene response to manipulations of the TGFβ pathway, stimulation of collagen gene expression was examined by measuring the response of the α_1(I) pro-collagen gene promoter basally and following TGFβ stimulation. A construct, linking the promoter region to the luciferase gene, was transfected into MM cells, allowing rapid assessment of gene responses without having to quantify mRNA levels using Northern blotting. To perform these experiments only transient transfection of the MM cells was required as the assay was performed over 24 hours. This method gives rapid results and avoids the use of radio-labelled markers, necessary for mRNA detection in standard Northern blotting.

2) To assess the response at the protein level, hyp production was measured in MM cells grown *in vitro*. For these experiments cells were stably transfected with Smad7 or a control vector.

3) Finally, to assess the *in vivo* effects of Smad7-transfection, the growth of tumours derived from transfected cells was observed and compared with controls and the tumour collagen contents measured.

3.2.12.1 Procollagen gene promoter responses

As luciferase activity, generated by the gene promoter reporter construct, is only produced by the cells transfected with the construct, the transfection efficiency is unimportant, as long as there is enough to produce measurable levels of luciferase. It also enabled dual transfections to be carried out using Smad7 and the reporter constructs. The level of luciferase activity was high compared with other cell types being transfected with these reporter systems in our laboratory e.g. HFLI cells – data not shown. This may reflect higher transfection rates in these cells compared with other cell lines or that there is greater activity of the collagen gene promoter in MM cells.

Dual transfections of the reporter and Smad7 were used to assess the effect of Smad7 on collagen gene promoter activity. The reporter was first shown to be responsive to TGFβ_1 by measuring luciferase activity following exposure. As expected the activity increased following TGFβ_1, which was consistent with the base line studies of chapter 3.1 and confirmed that the reporter responded appropriately. To confirm the effects of Smad7 transfection on the collagen response in non-malignant cells, human foetal lung fibroblast (HFLI) cells were dual transfected with a pro-collagen reporter and the Smad7 vector. These cells produce large amounts of collagen in response to TGFβ (Coker *et al.* 1997) and this has been shown to occur via the Smad pathway (Roberts *et al.* 2001). As predicted, Smad7 over-expression inhibited the response to TGFβ_1 in these cells and the basal level of reporter activity was also significantly decreased (section 3.2.6). This confirmed that in a cell line known to signal through the Smad pathway in response to TGFβ, over-expression of Smad7 inhibited the collagen response as expected.

In MM cells however, the finding that transfecting cells with Smad7 increased the collagen gene response without inhibiting the response to TGFβ (section 3.2.5) was very surprising. It has previously been reported that the Smad pathway is the predominant pathway for TGFβ signalling and has been shown in other cell lines to

be necessary for the production of collagen (Inagaki *et al.* 2001;Poncelet and Schnaper 2001;Schnabl *et al.* 2001;Zhao *et al.* 2002a). Therefore Smad7 was predicted to inhibit activity of the reporter. Indeed, in other systems previously examined, Smad7 expression has been shown to inhibit collagen production. For example in adult primary cardiac fibroblasts over-expression of Smad7 suppressed the production of collagen I and III (Wang *et al.* 2002). In pulmonary fibrosis IL-7 inhibited fibroblast TGF-beta production and signalling by increasing Smad7 levels (Huang *et al.* 2002). In addition, in a bleomycin induced model of lung fibrosis, transfection of Smad7 into the airways inhibited fibrosis as assessed by collagen production (Nakao *et al.* 1999).

Unique Smad7 response in MM cells - In MM cells this paradoxical response to transfection with Smad7 has not been reported elsewhere or in any other cell line. This suggests a unique effect in these cells. This finding was consistent using murine (AC29 and AB22) and human (Ju77) MM cell lines (using a different human α2(I) procollagen gene promoter reporter construct in the human cells). The response was therefore not specific to either the MM cell line used, the species or to the specific procollagen I gene promoter reporter.

There are a number of possible explanations for this finding. The first is that the collagen response in MM cells involves pathways other than the Smad pathway. This has been demonstrated in other systems. For instance, in peritoneal mesothelial cells, inhibition of p38 kinase (MAPK signalling) resulted in collagen inhibition (assessed by Northern blot) with normal activation of Smad2 following TGFβ stimulation. Activation of p38 kinase after TGFβ occurred at 15 min in these experiments, as did Smad2 activation (Hung *et al.* 2003). Basal collagen production was not assessed and responses only at mRNA level were measured. The possibility of alternative signalling pathways being involved in the collagen response of MM cells to TGFβ stimulation are discussed and investigated in chapter 3.3.

Another explanation is that the response to Smad7 has changed in these cells, in that there may be an aberrant response to TGFβ. This may be due to changes in other steps in the TGFβ pathway (such as at the receptor or downstream of the Smad pathway) resulting in an altered response to Smad7. Alternatively, Smad7 may have other functions in these cells yet to be described, which rely on a direct effect of Smad7, possibly as a transcription factor. These points will be discussed later.

Despite results showing a large increase in basal activity following Smad7 transfection with further increases in response to TGFβ, the fold increase in activity above basal levels following TGFβ was reduced in Smad7 transfected cells compared with the controls. This would suggest some inhibition of the TGFβ response, despite the enhanced basal levels of activity in Smad7 transfected cells.

An interesting finding of note, not directly related to the specific effects of Smad7 transfection, is that reporter activity was seen to increase when dual control transfections are performed compared with transfection of the reporter alone. The reasons for this are unclear, especially considering that the amount of reporter cDNA used in the dual transfections was half of that used in the singly transfected reporter control. Whether it is due to increased transfection efficiency when two cDNAs are combined or an increased activity of the reporter is unclear, but interestingly the same result occurs in the hands of other users of the LID transfection system (personal communication from Dr Steven Hart). The mechanism of this effect has yet to be elucidated, but it appears to be a consistent finding in different cell lines transfected.

3.2.12.2 Collagen production

The second method of assessing the collagen response was to measure it at the protein level by assaying hyp production using HPLC. To assess the effect of Smad7 on TGFβ-induced collagen production it was necessary to transfect the MM cells by a retroviral system, as explained above. The stability and efficiency of expression was demonstrated by the co-expression of GFP, visualised using fluorescent light microscopy, as discussed above. There are non-specific effects of stable transfection and the importance of having a control stable over-expresser is demonstrated by the consistently reduced collagen production by control transfected cells compared with the non-transfected controls.

Collagen production was found to be increased in Smad7 expressing cells compared with both non-transfected and transfected controls (section 3.2.8). In the control transfected cells there was a reduction in collagen production compared with non-transfected controls due to a non-specific effect of stable transfection. The reason for this small reduction of collagen production in the stably transfected control cells is unclear. A speculative explanation may be that there is competition for substrates

between vector and normal gene responses in the formation of protein, the control vector resulting in the production of GFP. Since the Smad7 transfected cells are also producing GFP (due to the IRES component of the vector, which links the Smad7 cDNA with GFP cDNA) then the increased collagen production following Smad7 transfection has also overcome this non-specific inhibitory effect.

The increased collagen production in the Smad7 expressing cells appears to be an effect predominantly on basal levels rather than in response to TGFβ. As with the results obtained from the procollagen gene promoter reporter, if fold increases in collagen production above basal levels are calculated, then Smad7 transfection results in a reduced response to TGFβ. This is not because the cells have reached their maximum output of collagen synthesis, as the result in 3.1 shows that the collagen production can increase further with higher TGFβ stimulation. These findings are consistent for both murine (AB22) and human (Ju77) MM cell lines and are consistent when assessing both the gene response (luciferase reporter) and protein response (HPLC).

The results suggest that the basal regulation of collagen synthesis may be independent of TGFβ stimulated collagen production. The role of the Smad pathway is difficult to determine as reduced activity due to Smad7 transfection results in increased basal collagen production but may reduce the TGFβ response. This implies that alternative pathways to Smad regulate basal collagen production, but Smad is still involved in the TGFβ response. This does not explain why there is increased basal collagen production following Smad7 transfection. This could occur by Smad7 having a direct effect perhaps acting as a transcription factor, or by interacting with other pathways that are regulating basal collagen synthesis.

Smad7 transfection of MM cells unexpectedly increased their collagen production *in vitro*. To assess the effect of Smad7 over-expression *in vivo* a murine model of MM was used. The original hypothesis predicted that over-expressing Smad7 would inhibit tumour growth. This was expected not only because of its effect on inhibition of collagen production but also by blocking other tumour enhancing effects of TGFβ such as its pro-angiogenic and immune suppressing functions (described in section 1.6.9 – 1.6.11). However, after finding enhanced collagen production in MM-Smad7 cells *in vitro* the predicted outcome *in vivo* became less certain. If collagen production enhances tumour growth then Smad7 transfection

would now be predicted to result in larger tumours. This is exactly what was observed.

Results section 3.2.9 shows that tumours derived from MM-Smad7 cells grew larger than control cells and this was a consistent trend in the three different murine MM cell lines used. The effect of stable transfection with the control vector was to reduce tumour growth compared with the non-transfected controls. This was consistent with the collagen measurements made *in vitro* that showed increased collagen production by Smad7 transfected cells and reduced collagen production in the control transfected cells. The collagen content of the tumours was measured using HPLC and demonstrated that all three murine cell lines show a consistent trend toward Smad7-MM cell derived tumours having increased tumour collagen concentration. Therefore, the results are consistent both *in vitro* and *in vivo* and demonstrate that Smad7 transfection results in increased collagen production and increased tumour growth. These findings are consistent with the theory that increased collagen production results in increased tumour growth.

In chapter 3.1, TGFβ neutralising antibodies were demonstrated to result in smaller tumours with reduced collagen content – the opposite to the findings of Smad7 transfection. There may be differences in the concentration or bioavailability of TGFβ at the MM cell surface and it is unclear as to how much TGFβ synthesised by the MM cells acts as an autocrine factor and how much as a paracrine factor. Why neutralising TGFβ should have the opposite effect to over-expression of Smad7 is discussed further in chapter 4.

There is no direct correlation between tumour size and collagen content when all tumours are assessed together i.e. larger tumours in the non-Smad7 group have less collagen concentration than similar size tumours in the Smad7 group. The Smad7 tumours have a greater collagen concentration per se and therefore, tumours do not have less collagen simply because they are smaller. So although the mechanism by which the Smad7 induces increased collagen production is not known, the resultant increased tumour growth supports the theory of a link between collagen production and tumour growth.

3.3 TGFβ induced collagen production and MAPK signalling

TGFβ stimulates collagen production in MM cells and inhibition of TGFβ using TGFβ neutralising antibodies inhibits tumour growth. Over-expression of Smad7 however, the inhibitory component of the Smad pathway, enhances rather than inhibits collagen production basally. One possible explanation for this finding is that MM cells use different pathways to regulate basal and TGFβ-induced collagen production. The mitogen activated protein kinase (MAPK) pathways are the most likely candidates (for reasons explained in the discussion section 3.3.10). The role of MAPK in this system was therefore examined.

3.3.1 TGFβ stimulated ERK 1/2 activity in MM cells

To assess ERK1/2 activity following $TGF\beta_1$ stimulation in MM cells, the level of phosphorylated ERK1/2 (i.e. activated ERK) following $TGF\beta_1$ treatment was assessed by Western blot analysis, as described in section 2.6. Confluent MM cells were stimulated with 1ng/ml $TGF\beta_1$ in serum-free conditions and the level of phosphorylated ERK1/2 assessed at 1 - 90 minutes after treatment. Figure 3.3.1 shows the rapid activation of ERK1/2 (bands at 42 (ERK1) and 44 kDa (ERK2) on the Western blot) at 5 min after TGFβ exposure with activity trailing off rapidly. By 30 min the cell has returned to basal levels of activity. TGFβ-induced activation of ERK 1/2 occurring as rapidly as 5 minutes has not previously been reported. Further time-points did not show any delayed or second peak of activity.

3.3.2 Inhibition of ERK1/2 activation using UO126 in MM cells

Figure 3.3.2 shows the effects of using the MEK inhibitor UO126, a specific inhibitor of ERK activation that prevents the phosphorylation of ERK1/2 by inhibiting MEK1 (responsible for phosphorylation of ERK). UO126 (10 μM) applied to the cells 15 min before $TGF\beta_1$ exposure was shown to block activation of ERK in MM cells (as seen in other cell types) confirming that this compound is effective in MM cells.

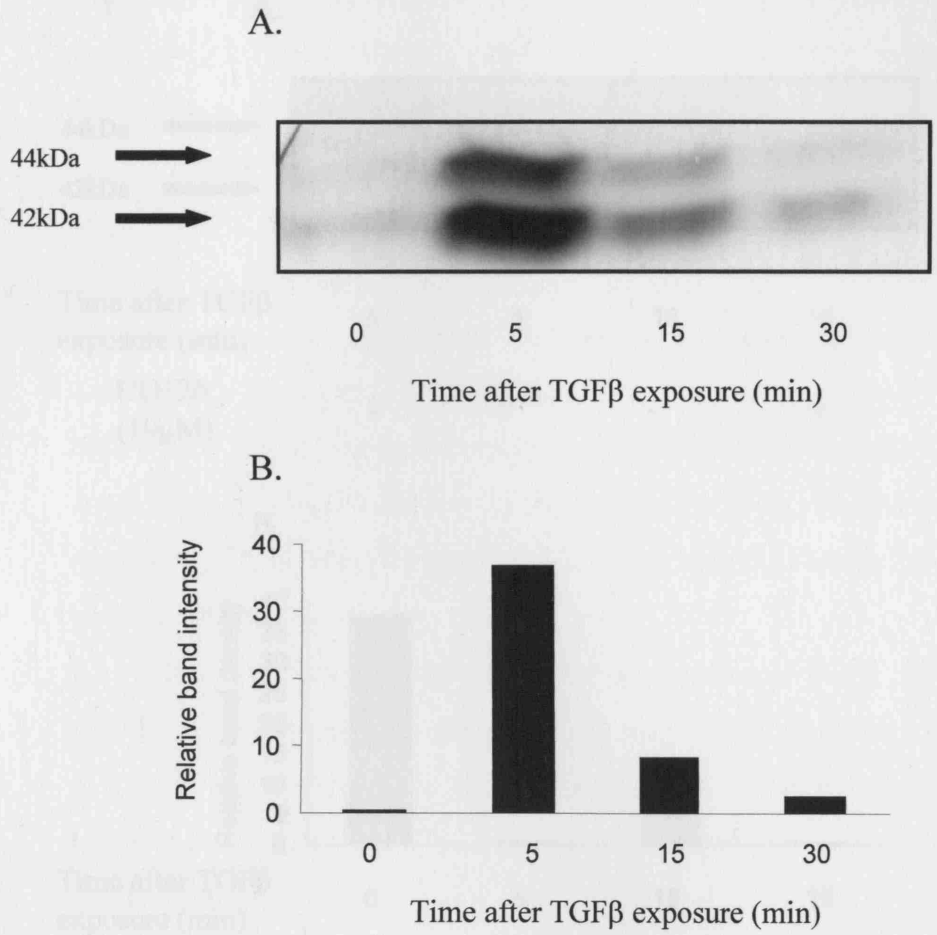

Figure 3.3.1. Phosphorylated ERK levels following $TGF\beta_1$ stimulation in AC29 cells. **A.** Western blot showing phosphorylated ERK 1/2 after stimulation of AC29 cells with $TGF\beta_1$ (1ng/ml). The activity was measured at the time points indicated following TGFβ exposure by using antibodies to phosphorylated ERK 1/2 (1:1000 dilution, Cell signalling Inc) and visualised by secondary HRP labelled staining. **B.** shows the relative band intensities of the Western blot demonstrating the rapid increase in activated ERK levels peaking 5 minutes after exposure to $TGF\beta_1$, returning to near basal levels by 30 minutes.

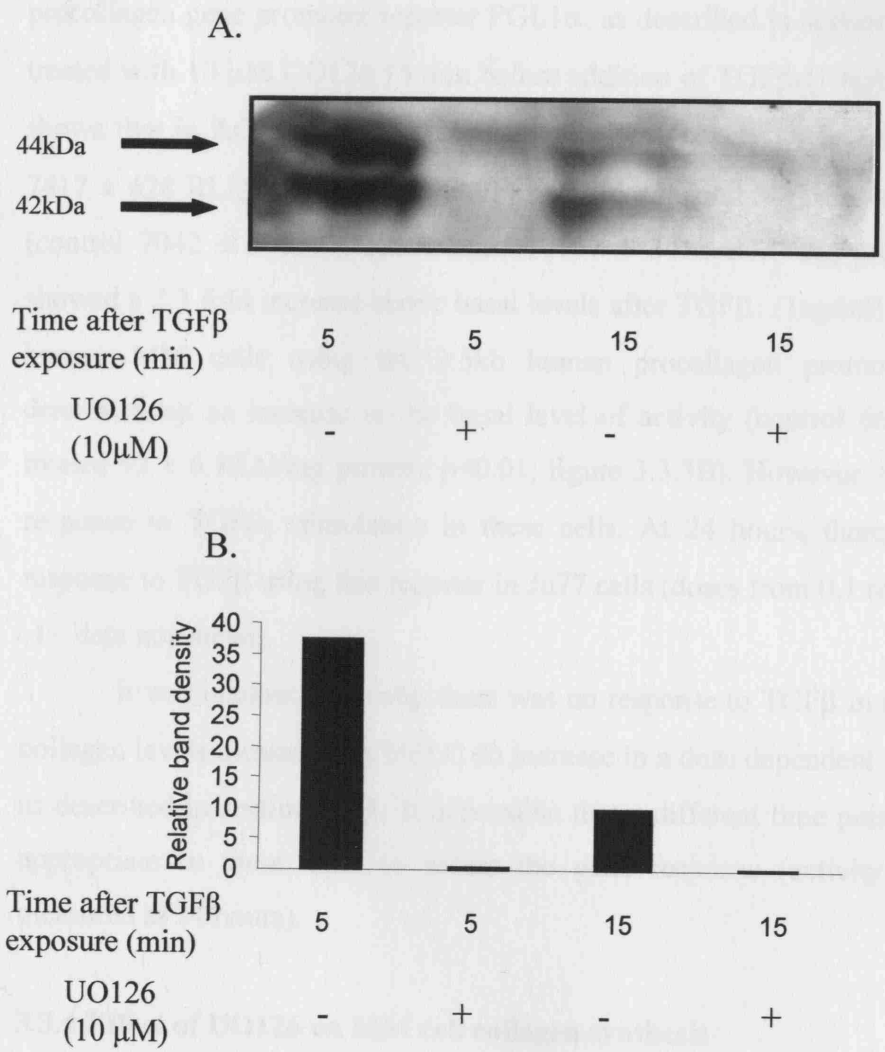

Figure 3.3.2 Blocking ERK activation in AC29 cells using the specific inhibitor UO126. **A.** Section from a Western blot showing phosphorylated ERK 1/2 after stimulation of AC29 cells with $TGF\beta_1$ (1ng/ml) with and without UO126. **B.** shows the relative density of the bands at the time points indicated. The inhibition of ERK activity using UO126 is clearly demonstrated and is consistent at both 5 and 15 minutes after TGFβ exposure.

3.3.3 Effect of blocking ERK on procollagen gene promoter reporter activity

Cells were grown to confluence in 24 well plates and transfected with the procollagen gene promoter reporter PGL1α, as described in section 2.5.1. Cells were treated with 10 μM UO126 15 min before addition of $TGF\beta_1$(1 ng/ml). Figure 3.3.3A shows that in AC29 cells, UO126 increased PGL1α activity basally (2957 ± 709 to 7417 ± 628 RLU/mg protein, $p<0.01$) and did not inhibit $TGF\beta_1$-stimulated activity (control 7042 ± 575, UO126 treated 17137 ± 3418 RLU/mg protein), which still showed a 2.3 fold increase above basal levels after $TGF\beta_1$ (1ng/ml). Analysis of Ju77 human MM cells using the 3.5kb human procollagen promoter reporter also demonstrated an increase in the basal level of activity (control 66 ± 5 and UO126 treated 92 ± 6 RLU/mg protein, $p<0.01$, figure 3.3.3B). However, there was no dose response to $TGF\beta_1$ stimulation in these cells. At 24 hours, there was no reporter response to TGFβ using this reporter in Ju77 cells (doses from 0.1 to 10 ng/ml $TGF\beta_1$) – data not shown.

It was unclear as to why there was no response to TGFβ in the JU77 cells, as collagen levels measured by HPLC do increase in a dose dependent manner to $TGF\beta_1$ as described in section 3.1.1. It is possible that a different time point would be more appropriate in these cells to assess the gene response (activity levels were all measured at 24 hours).

3.3.4 Effect of UO126 on MM cell collagen synthesis

Following the increased basal activity of the procollagen promoter gene seen in MM cells after treatment with UO126, HPLC assessment of hyp production was used to measure the effects of UO126 on collagen protein synthesis. AC29 cells were grown to confluence in 24 well plates and pre-incubated with UO126 (10μM) at least 15 min before treatment with $TGF\beta_1$ (1ng/ml). Collagen production was quantified after 24 hr incubation, as described in section 2.5.7. Figure 3.3.4 shows that the UO126 treated cells produced more collagen (nmol/10^6cells/24hr) than untreated controls both basally (control 0.26 ± 0.009, UO126 treated 0.49 ± 0.019, $p<0.01$) and after TGFβ stimulation (control 0.58 ± 0.003, UO126 treated 0.72 ± 0.020, $p<0.01$). The effect is predominantly seen as an increase in the basal production of collagen

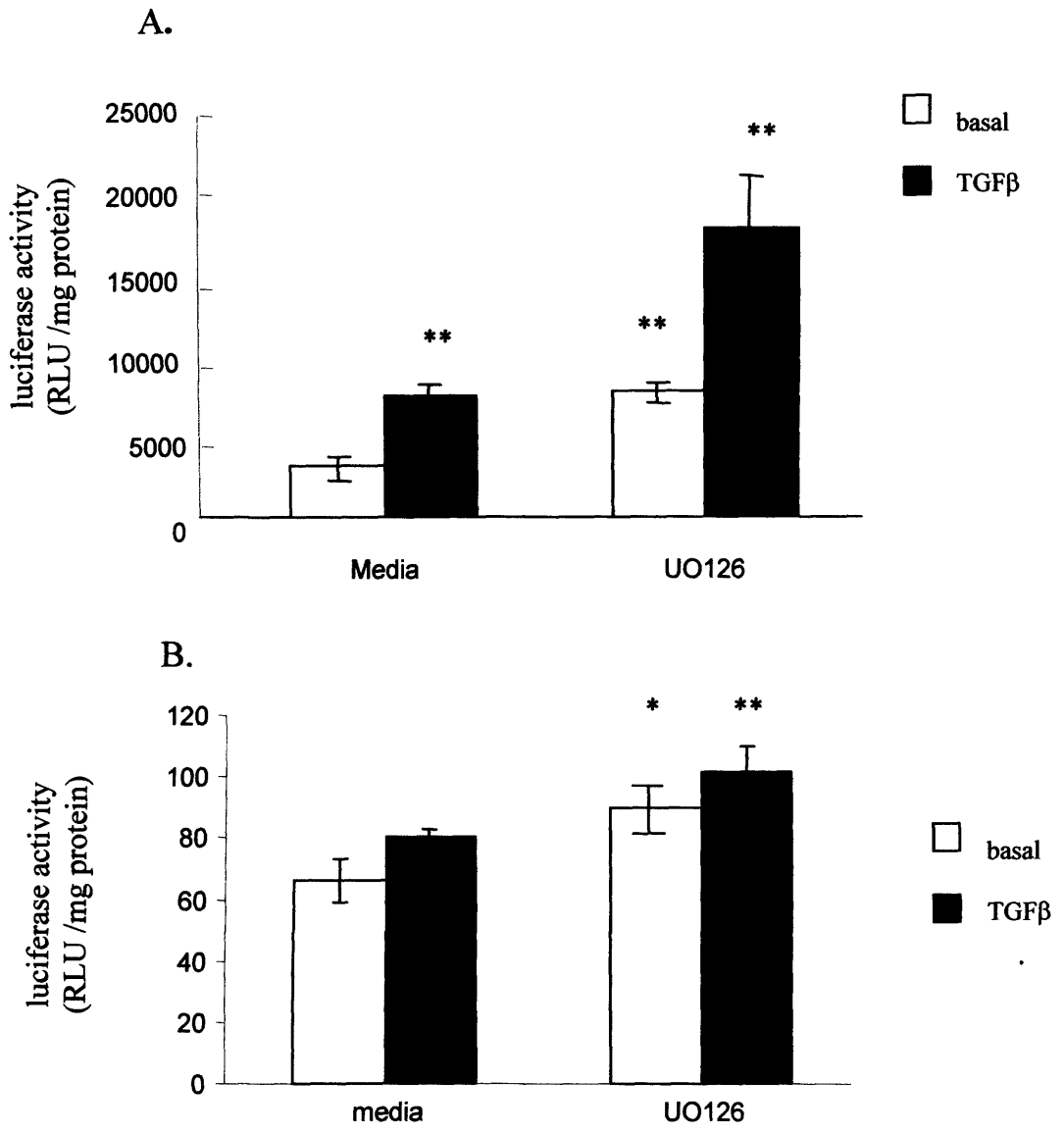

Figure 3.3.3 Increased activity of the transfected pro-collagen gene promoter luciferase reporter with UO126. **A.** Pro-collagen gene promoter reporter PGLIα(I) activity expressed as RLU/mg protein in AC29 cells 24 hours after $TGF\beta_1$ (1ng/ml) exposure in the presence of UO126 (10 μM) showing an increase in basal activity (empty bars) and a similar fold increase in $TGF\beta_1$ stimulated activity (black bars). **B.** activity of the 3.5kb human procollagen gene promoter reporter expressed as RLU/mg protein in Ju77 cells after $TGF\beta_1$ in the presence of UO126 also showing increased activity in these human MM cells. Bars represent the mean of four replicates per group ± SEM. * = $p < 0.05$, ** = $p < 0.01$ compared with basal control levels.

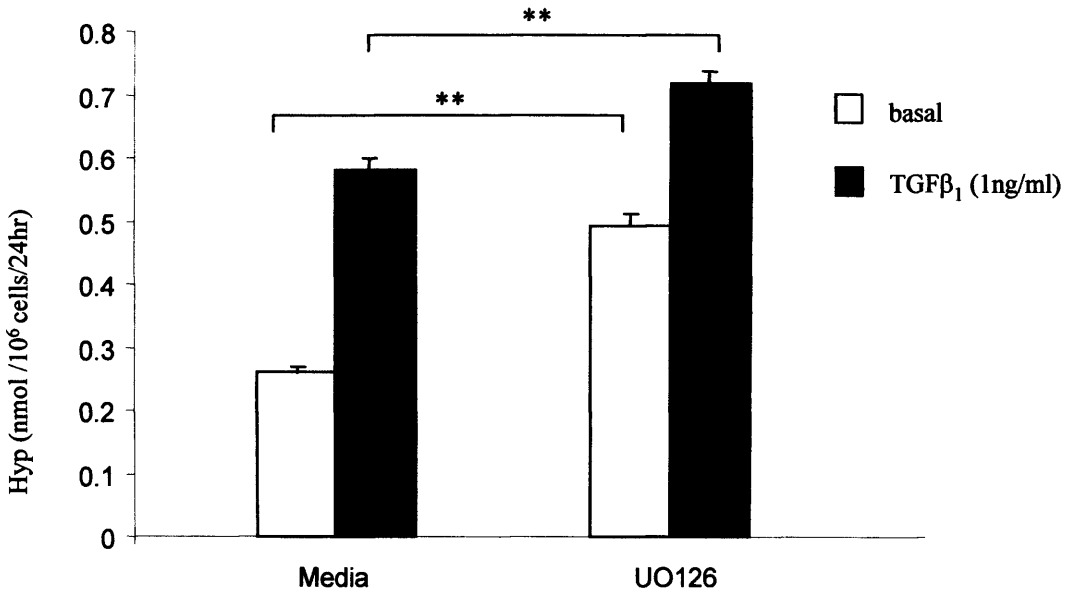

Figure 3.3.4 Hydroxyproline production by AC29 cells following UO126 (ERK inhibitor) exposure. Basal levels of hyp production (empty bars) significantly increase in the presence of UO126 (10μM) in AC29 cells with further increases in collagen synthesis in response to $TGF\beta_1$(filled bars). Each bar represents the mean of 6 replicates ± SEM (** = $p < 0.01$). This graph is representative for three repeat experiments.

with the fold increase following TGFβ$_1$ stimulation in the UO126 group (1.6 fold) slightly less than the non-UO126 treated group (2.2 fold). This result was confirmed in 2 repeat experiments represented in table 3.3.1.

	Collagen production (hyp production nmol / 10^6 cells / 24 hr)			
	Repeat experiment 1		**Repeat experiment 2**	
	Basal	**TGFβ treated**	**Basal**	**TGFβ treated**
Control cells	0.15 ± 0.003	0.386 ± 0.017	0.27 ± 0.010	0.62 ± 0.004
UO126 treated	0.31 ± 0.015	0.55 ± 0.020	0.52 ± 0.021	0.77 ± 0.022

Table 3.3.1 Results of repeat experiments assessing the effects of treatment with the ERK1/2 inhibitor UO126 (10μM) on the production of collagen by AC29 cells basally and in response to TGFβ$_1$ (1ng / ml). The increased production of collagen basally and in response to TGFβ is consistent with the result shown in figure 3.3.4.

3.3.5 TGFβ stimulated p38 kinase activity in MM cells

To assess p38 kinase activity following TGFβ stimulation in MM cells, the level of activated phosphorylated p38 kinase following TGFβ treatment was assessed by Western blot analysis, as described in section 2.6. Confluent MM cells in serum-free conditions were stimulated with 1ng/ml TGFβ$_1$ and the level of phosphorylated p38 kinase assessed at 1 – 60 minutes after treatment. As with ERK activity described in section 3.31, p38 kinase activation occurred rapidly following TGFβ$_1$, peaking by 5 minutes and returning to baseline by 60 minutes, as shown in figure 3.3.5.

3.3.6 Effects of inhibiting p38 kinase in murine MM cells on collagen production assessed using a pro-collagen gene promoter reporter assay

Murine AC29 cells were transfected with the murine procollagen gene promoter reporter, PGL1α, and human JU77 cells with the human 3.5kb procollagen promoter, and both treated with the specific p38 kinase inhibitor SB203580 (10μM), as described in section 2.5. In AC29 cells figure 3.3.6A shows a non-significant trend for an increase in basal and TGFβ$_1$-induced activity of the reporter in the presence of

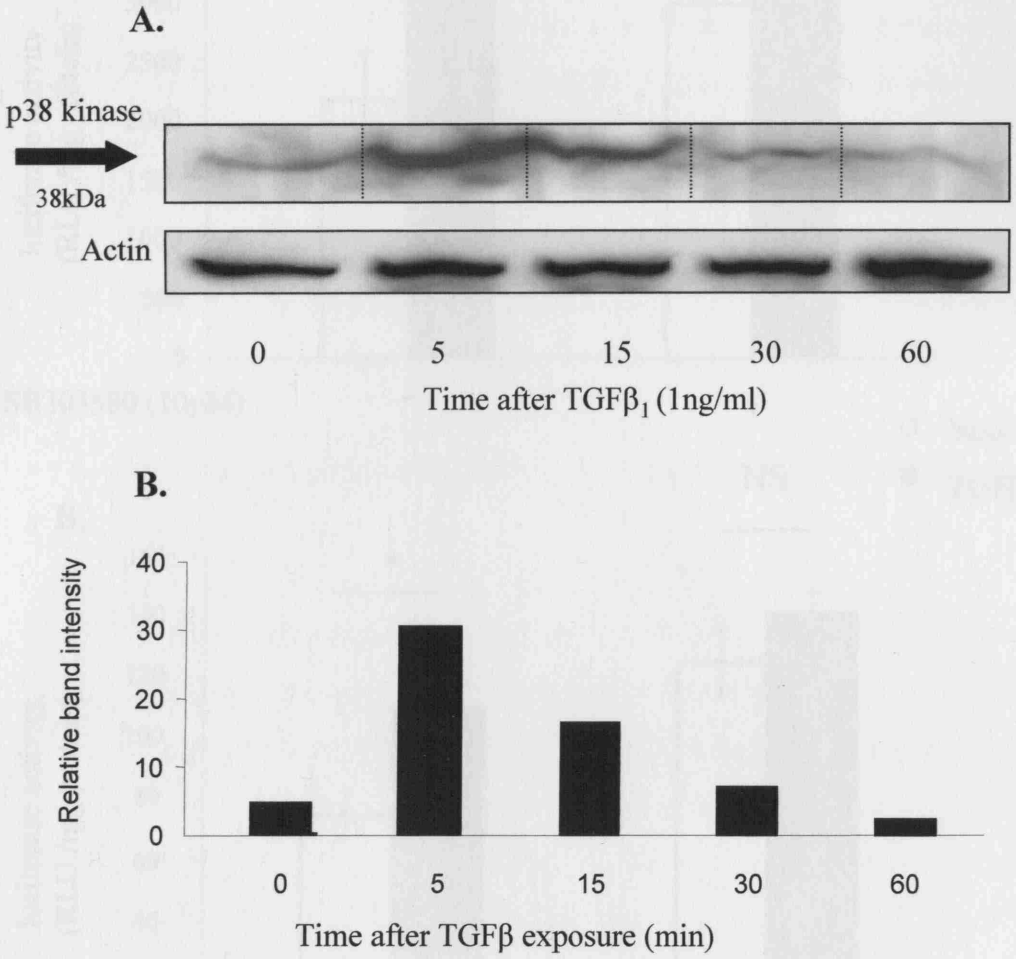

Figure 3.3.5 $TGF\beta_1$ induced p38 kinase activity in AC29 cells. **A** Western blot showing phosphorylated p38 kinase (i.e. activated p38 kinase) after stimulation of AC29 cells with $TGF\beta_1$ (1 ng/ml). The activity was measured at the time points indicated following TGFβ exposure, using antibodies to the phosphorylated p38 kinase (1:100 dilution) and visualised by secondary HRP labelled antibody staining (1:1000). The blot shows activation of p38 kinase 5 min after $TGF\beta_1$ stimulation with a return to basal levels of activity by 60 min. **B**. The band intensity of the Western blot above is shown.

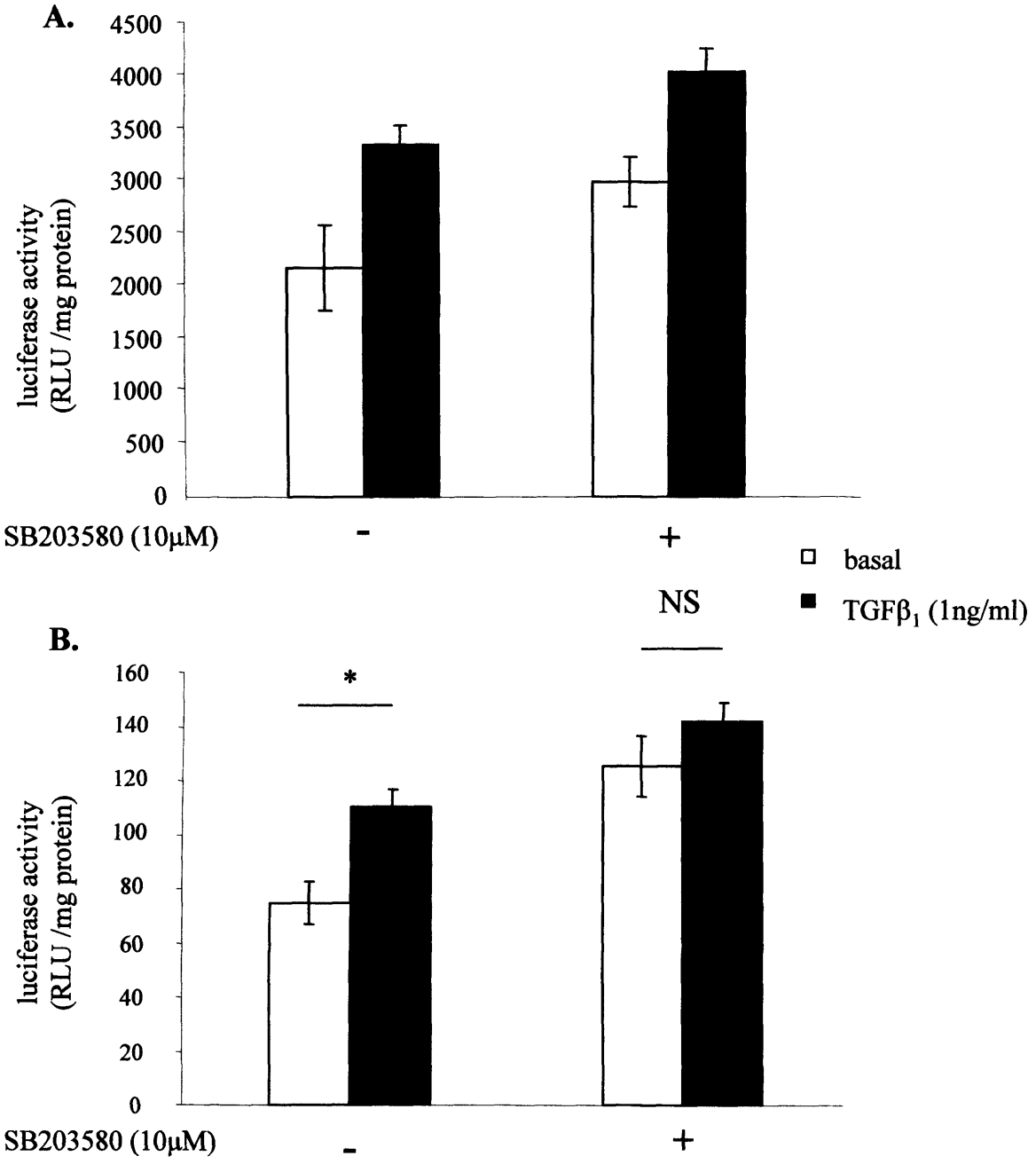

Figure 3.3.6 The effect of inhibiting p38 kinase (using SB203580) on pro-collagen gene promoter activity in AC29 cells. **A.** Activity of the PGL1α reporter at 24 hours (expressed as RLU/mg protein) in AC29 cells following $TGF\beta_1$ (1ng/ml) stimulation in the presence of SB203580 (10 μM), showing a trend for increased activity basally (empty bars) and a small reduction in the fold increase in activity following $TGF\beta_1$ stimulation. Bars are the mean of four replicates per group ± SEM. **B.** A repeat experiment showing a significant increase in activity following $TGF\beta_1$ stimulation in the non-SB203580 treated cells that is lost in the presence of SB203580. (* = $p < 0.01$, NS = non-significant)

SB203580. There was a small decrease in the $TGF\beta_1$-induced activity with fold increases above basal levels of 1.5 and 1.1 in the control and SB203580 treated groups respectively. In a repeat experiment (figure 3.3.6B) the same pattern is seen basally and in response to $TGF\beta_1$ in the presence of SB203580, with a similar reduction in the response to TGFβ.

In JU77 cells there appeared to be little effect on reporter activity at 24 hours either basally or in response to $TGF\beta_1$. Figure 3.3.7 shows two repeat experiments using JU77 cells in which SB203580 had no reproducible effects on luciferase activity. Other investigators in our laboratory have also reported inconsistencies using SB203580 and this reporter system, while investigating other cell lines. Due to the difficulties using this inhibitor with the gene reporter system further data was obtained by measuring hyp levels using HPLC to assess collagen production.

3.3.7 Hydroxyproline production by MM cells after SB203580 inhibition of p38 kinase

HPLC measurements of hyp levels were used to examine the effects of SB203580 on collagen synthesis in MM cells. AC29 cells were grown to confluence in 24 well plates and then treated with SB203580 (10μM) at least 15 min before $TGF\beta_1$ (1ng/ml) stimulation. Collagen production was quantified after 24 hr incubation, as described in section 2.5.6 Figure 3.3.8 shows that in contrast to the affect on the gene promoter activity (section 3.3.7) the SB203580 treated cells had small but significantly reduced hyp levels (nmol/10^6cells/24hr) compared with untreated controls both basally (control 0.48 ± 0.015, SB203580 treated 0.39 ± 0.024, $p<0.05$) and after TGFβ stimulation (control 0.59 ± 0.015, SB203580 treated 0.47 ± 0.037, $p<0.05$). The reduction was seen predominantly on the basal response as the fold increase following TGFβ treatment was the same for cells both exposed and not exposed to SB203580. This result was consistent in two repeat experiments (results shown in table 3.3.2). This result suggests that p38 kinase may have a role in the regulation of collagen production in MM cells but is unlikely to play a significant role in the TGFβ regulated collagen response.

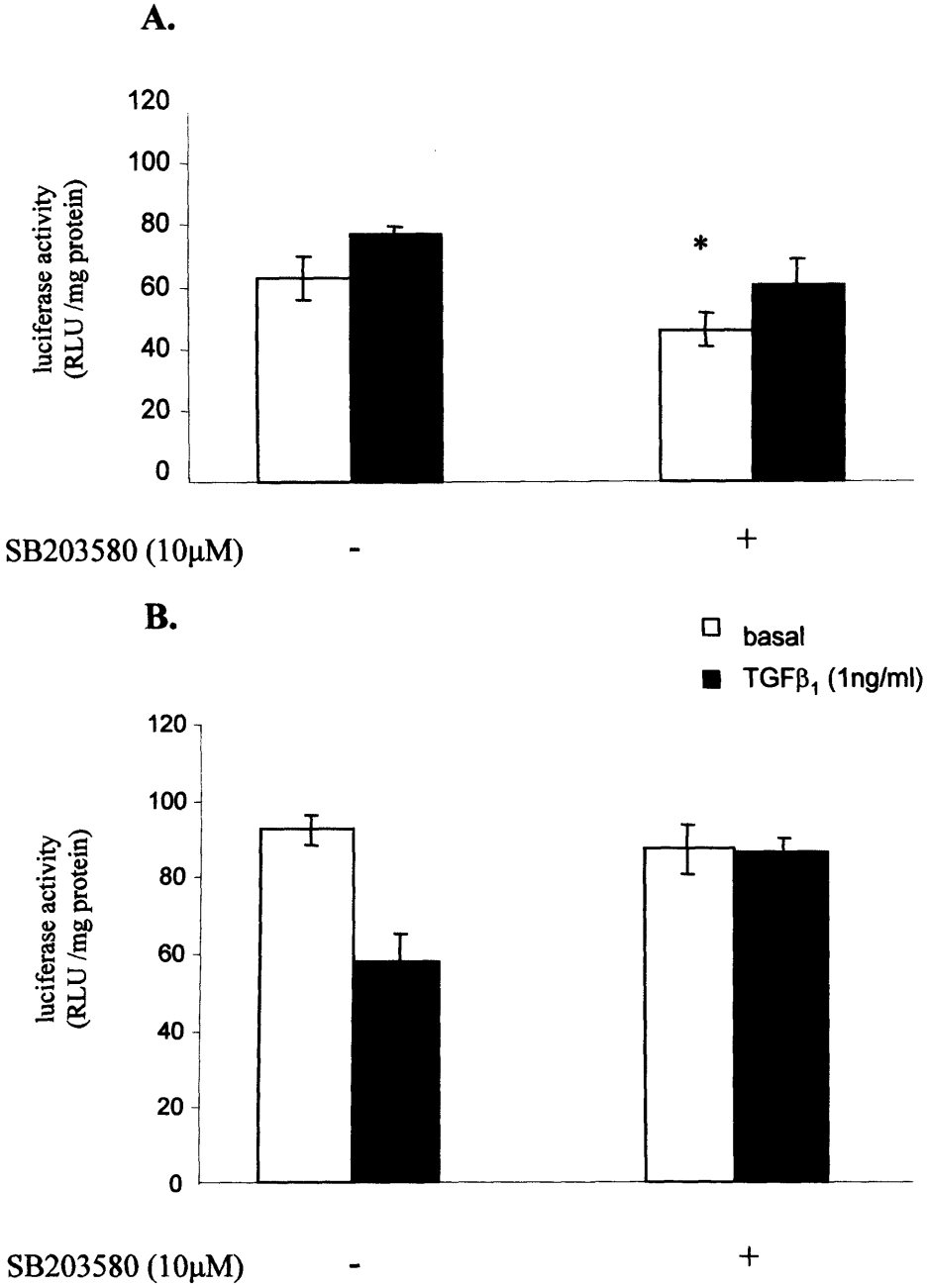

Figure 3.3.7 The effect of inhibiting p38 kinase (using SB203580) on procollagen gene promoter activity in JU77 cells. **A.** Activity of the 3.5kb 1α(I) procollagen gene promoter reporter, expressed as RLU/mg protein, in Ju77 cells was inhibited basally by a small but significant amount (empty bars) in the presence of SB203580. There was no significant change in activity 24 hour after $TGF\beta_1$ stimulation. **B.** In a repeat experiment there was no inhibition of basal activity. Bars represent the mean of four replicates per group ± SEM (* = $p < 0.05$).

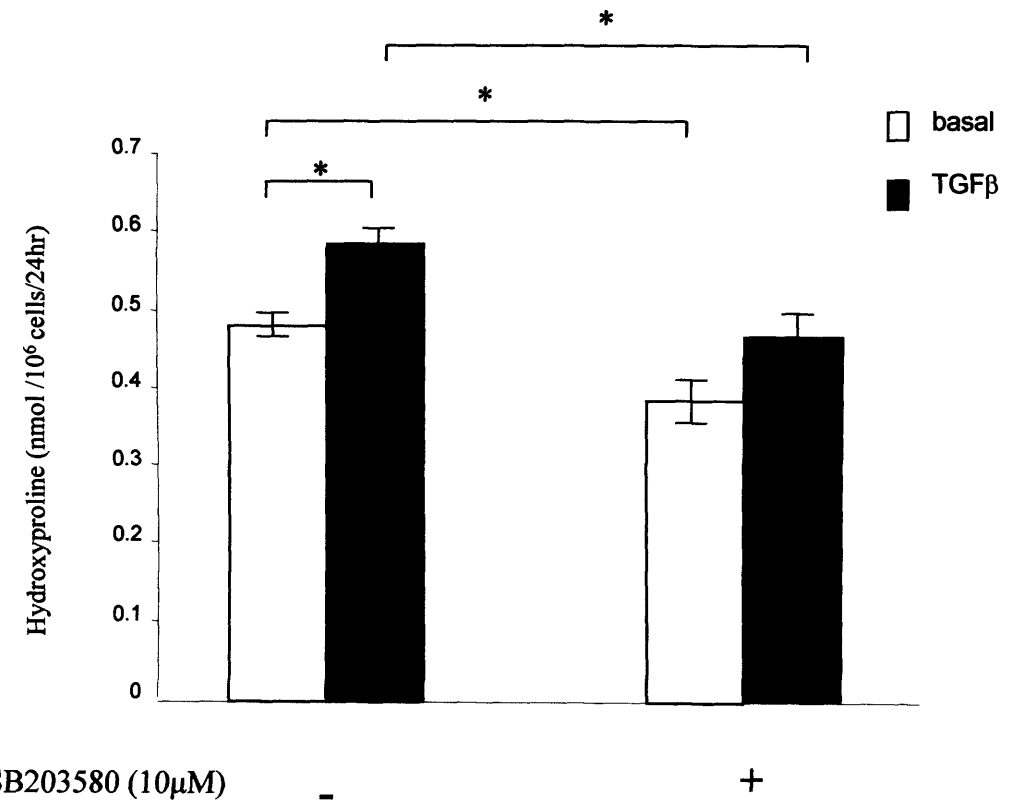

Figure 3.3.8 The effect of SB203580 on basal and TGFβ-induced collagen production in AC29 cells. Hydroxyproline production in AC29 cells 24 hours after $TGF\beta_1$ (1ng/ml) in the presence of the p38 kinase inhibitor SB203580 demonstrating a small but significant inhibition of basal collagen production (empty bars). Each bar represents the mean of 6 replicates ± SEM. * = $p < 0.05$

	Collagen production (hyp production nmol / 10^6 cells / 24 hr)			
	Repeat experiment 1		Repeat experiment 2	
	Basal	**TGFβ treated**	**Basal**	**TGFβ treated**
Control cells	0.76 ± 0.065	0.729 ± 0.049	0.483 ± 0.015	0.589 ± 0.014
SB203580 treated	0.674 ± 0.023	0.625 ± 0.027	0.388 ± 0.024	0.471 ± 0.037

Table 3.3.2 Results of repeat experiments assessing the effects of treatment with the p38 kinase inhibitor SB203580 (10μM) on the production of collagen by AC29 cells basally and in response to $TGF\beta_1$ (1ng / ml). The decreased production of collagen basally and in response to TGFβ is consistent with the result shown in figure 3.3.9.

3.3.8 Hydroxyproline production by MM cells after SB202190 inhibition of p38 kinase

Recent published data has shown that at 10μM the SB203580 compound also inhibits ALK5 – the TGFβ type I receptor (Inman *et al.* ;Laping *et al.* 2002). These studies examined the inhibitory effects of a number of "specific" inhibitor compounds, including another p38 kinase inhibitor, SB202190. They demonstrated that SB202190 and SB203580inhibit ALK5 at I_c50 values of 6 and 3 μM respectively and inhibit p38 kinase with I_c50 values of 1μM and 490 nM respectively. The effects of these compound on collagen production by MM cells was therefore repeated using SB202190 at 1.5μM and 15 μM, at which doses the compound should specifically inhibit p38 kinase and both p38 kinase and ALK5 respectively. The experiment was performed in two murine cell lines, AB22 and AC29.

Figure 3.3.9A shows that inhibition of p38 kinase in AC29 cells significantly inhibits basal collagen production. There was no apparent inhibition of TGFβ-induced collagen production. However, as there was no response to TGFβ in the AC29 cells in the untreated control cells, this TGFβ-induced response is difficult to interpret. The reason for this lack of TGFβ-induced response in the AC29 control cells is unclear.

However, it was a recurrent problem with the AC29 cell line during these later experiments and also a finding of a colleague in the laboratory using these cells. (Interestingly, the basal level of collagen production was increased, 1.5 nmol hyp/10^6 cells/24hr, compared with earlier experiments, 0.72 nmol hyp/10^6 cells/24hr -see section 3.3.1). Given the loss of the TGFβ response, the significance of the responses to TGFβ in combination with the inhibitor (SB202190) are not interpretable but are shown for completeness. What is demonstrated by these experiments is that the basal production of collagen is reduced significantly by inhibiting p38 kinase activity. The additional simultaneous inhibition of ALK5, by using the higher dose of the inhibitor, makes no significant difference to basal collagen production in AC29 cells. This would imply that the role of p38 kinase in basal collagen production is at least as significant, if not more significant, than that of ALK5. This theory could be tested by specifically inhibiting ALK5, but the agent recently developed to do this (Callahan *et al.* 2002) was not available.

In AB22 cells (figure 3.3.9B), there was a trend toward a reduction in basal collagen production, but in this cell line the TGFβ response was inhibited by SB202190. In this cell line the TGFβ response of the control cells had not been lost as it had with the AC29 cells and so some interpretation of the inhibitor's effect on the TGFβ response could be made. When ALK5 was also inhibited, using the higher concentration of SB202190, then the basal collagen production was significantly inhibited compared with control. The TGFβ response was also inhibited - but not as completely as when there was inhibition of p38 kinase alone.

These results are difficult to interpret as they show a different response between the two cell lines tested. However, the AC29 cell line was not responding as predicted in the control cells either and so over interpretation of these findings should therefore be avoided. The consistent finding from these experiments was that inhibition of p38 kinase appears to inhibit basal collagen production in two MM cells lines tested and inhibits the TGFβ response in one of those cell lines. P38 kinase does therefore appear to have a significant role in regulating collagen production.

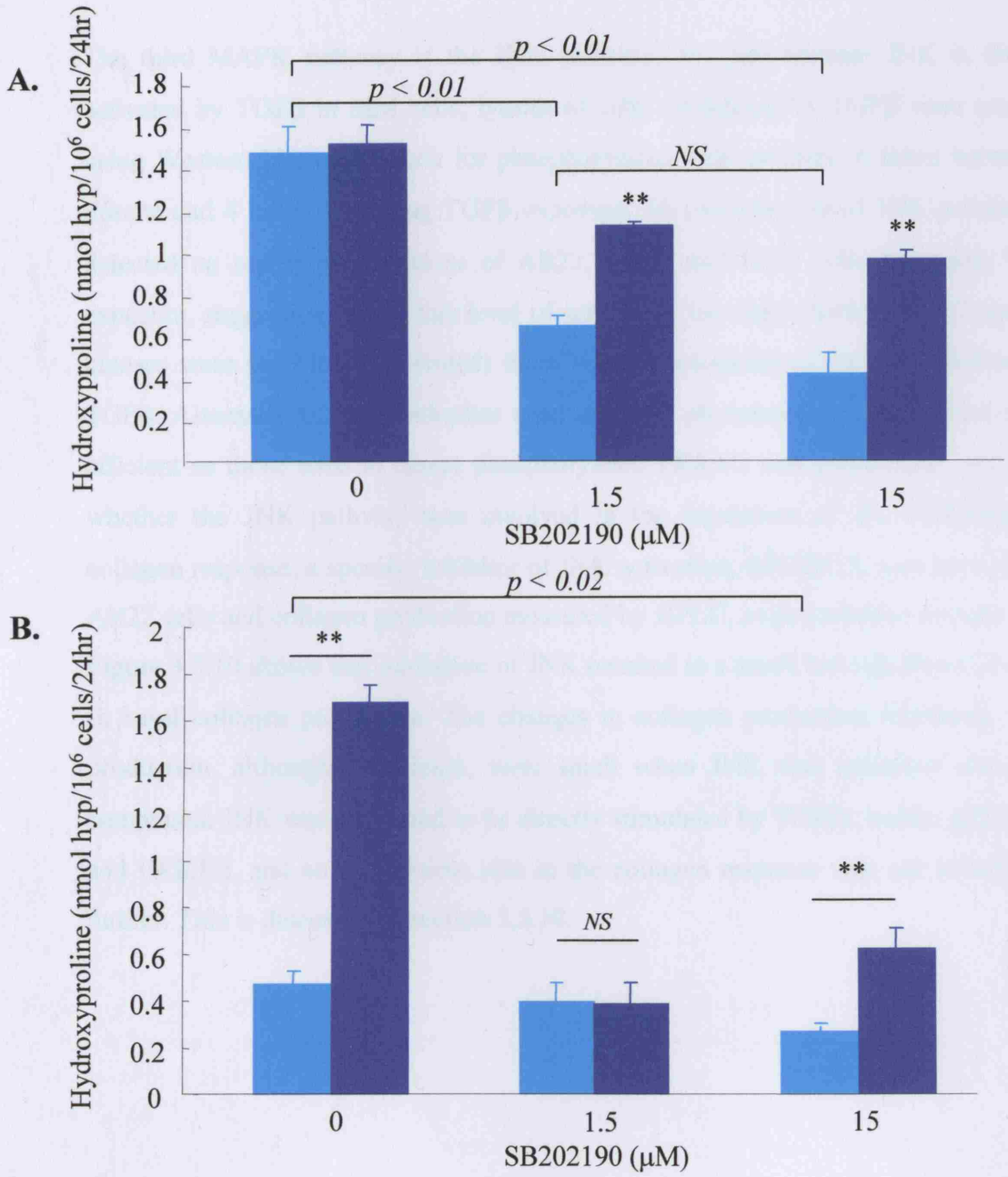

Figure 3.3.9. Hydroxyproline levels were measured in AC29 (**A**) and AB22 (**B**) MM cells in the presence of SB202190 at 1.5 μM (specific inhibition of p38 kinase) and 15μM (inhibition of p38 kinase and ALK5) 24 hours after stimulation with $TGF\beta_1$ (1ng/ml). In AB22 cells there is a reduction in basal collagen production and a marked decrease in the TGFβ1 induced collagen production when either p38 kinase is inhibited or when both p38 and ALK5 are inhibited. The AC29 cells have high basal levels of collagen production with no increased production in response to $TGF\beta_1$. ■ = Basal collagen in 0% FCS DMEM. ■ = TGFβ (1ng/ml). ** = $p < 0.01$ compared with basal level

3.3.9 Inhibition of Jun N-terminal kinase (JNK) activation

The third MAPK pathway is the JNK pathway. To find whether JNK is directly activated by TGFβ in MM cells, lysates of cells stimulated by TGFβ were assessed using Western blotting to look for phosphorylated JNK proteins at times between 1 minute and 4 hours following TGFβ exposure. No phosphorylated JNK protein was detected on repeat examinations of AB22, AC29 and JU77 cells following TGFβ exposure, suggesting that at this level of sensitivity (at which both ERK 1/2 and p38 kinases were seen to be activated) there was no activation of the JNK pathway by TGFβ. Alternatively, the antibodies used to detect phosphorylated JNK were not as efficient as those used to detect phosphorylated ERK1/2 and p38 kinase. To assess whether the JNK pathway was involved in the regulation of the TGFβ-induced collagen response, a specific inhibitor of JNK activation, SP600125, was used to treat AB22 cells and collagen production measured by HPLC, as described in section 2.5.6. Figure 3.3.10 shows that inhibition of JNK resulted in a small but significant increase in basal collagen production. The changes in collagen production following TGFβ production, although significant, were small when JNK was inhibited using this compound. JNK was not found to be directly stimulated by $TGF\beta_1$, unlike p38 kinase and ERK1/2, and so its possible role in the collagen response was not investigated further. This is discussed in section 3.5.10.

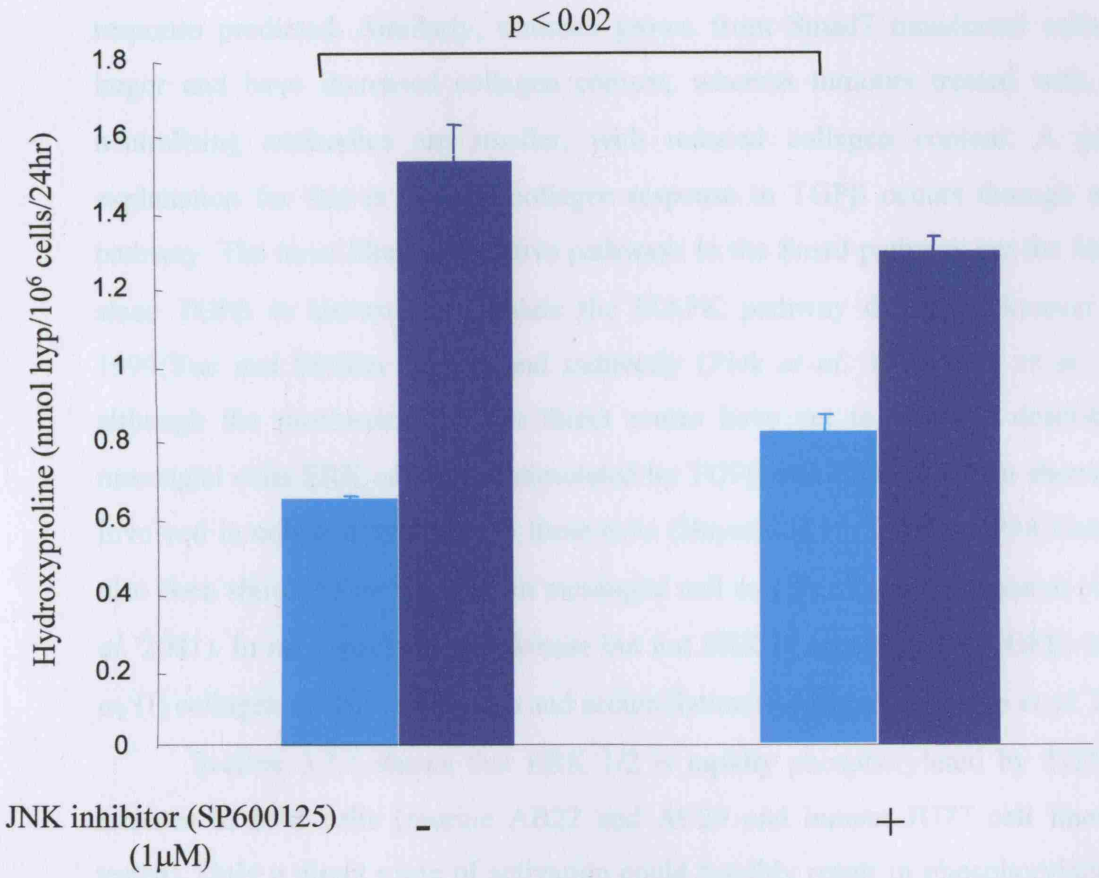

Figure 3.3.10. Collagen production in AB22 cells 24 hours after treatment with $TGF\beta_1$ (1ng/ml) in the presence of the specific JNK inhibitor SP600125 (1μM). The basal collagen production increased in the presence of SP600125 but the response to $TGF\beta_1$ was reduced. ■ = Basal collagen in 0% FCS DMEM. ■ = TGFβ (1ng/ml) stimulated. This experiment was repeated once with similar findings.

3.3.10 Discussion

In chapters 3.1 and 3.2 it was shown that blocking the Smad pathway in MM cells appears to increase rather than inhibit collagen production - the opposite to the response predicted. Similarly, tumours grown from Smad7 transfected cells grow larger and have increased collagen content, whereas tumours treated with TGFβ neutralising antibodies are smaller, with reduced collagen content. A possible explanation for this is that the collagen response to TGFβ occurs through another pathway. The most likely alternative pathways to the Smad pathway are the MAPKs, since TGFβ is known to stimulate the MAPK pathway directly (Hocevar *et al.* 1999;Yue and Mulder 2000a) and indirectly (Piek *et al.* 1999;Sano *et al.* 1999), although the mechanisms of the direct routes have yet to be fully described. In mesangial cells ERK activity is stimulated by TGFβ and ERK has been shown to be involved in collagen synthesis in these cells (Hayashida *et al.* 1999). P38 kinase has also been shown to be involved in mesangial cell α_1 (I) collagen production (Chin *et al.* 2001). In rat myoblasts, p38 kinase but not ERK is necessary for TGFβ_1-induced α_2 (I) collagen mRNA expression and accumulation (Rodriguez-Barbero *et al.* 2002).

Section 3.3.1 shows that ERK 1/2 is rapidly phosphorylated by TGFβ at 5 minutes in MM cells (murine AB22 and AC29 and human JU77 cell lines were tested). Only a direct route of activation could feasibly result in phosphorylation this fast, although the mechanism of this route is unknown. In other cells ERK activation has been shown to usually occur by 20 minutes following TGFβ (and p38 kinase in 30 minutes (Chin *et al.* 2001)). In these other cell lines, an intermediary such as TAK1 is thought to play a role. Rapid activation of ERK by other growth factor receptors has been demonstrated previously. For example, in COS-7 cells (a commonly used cell line derived from the kidney of an African green monkey) cross-talk between the insulin-like growth factor 1 (IGF-1) receptor and EGFR has been demonstrated in which transactivation of the EGF receptor mediates IGF-1-stimulated ERK1/2 activation(Roudabush *et al.* 2000). Stimulation of the epidermal growth factor receptor (EGFR) results in activation of the ERK pathway in exactly the same pattern as found in these MM cells following TGFβ i.e. rapid activation peaking by 5 minutes with return to baseline levels of activity by 30 minutes. The pattern of Smad activation following TGFβ is completely different, with a slower onset and peak

activity occurring at 1-2 hours (see section 3.2.4). The mechanism by which ERK (and p38 kinase) are activated by TGFβ is unknown, but TGFβ mediated transactivation of EGFR has been reported previously in glomerular mesangial cells(Uchiyama-Tanaka *et al.* 2002). In that study, transactivation of EGFR was mediated by an intermediate molecule, heparin binding EGF, which was processed and released via phosphotidylcholine-phospholipase C PKC. Subsequent activation of ERK and p38 kinase were involved in fibronectin expression via transcriptional regulation without requiring new protein expression.

As rapid activation of the ERK and p38 kinase pathways was found in the MM cells, these pathways appeared to be good candidates for a signalling pathway involved in TGFβ-induced collagen production. However, by using the ERK pathway inhibitor UO126, an inhibitor of MAPK kinase (MEK1), there was no inhibition in the basal collagen response when examined using a procollagen gene promoter assay or by measurement of hyp with HPLC (section 3.3.3 and 3.3.4). There was enhancement of the basal collagen production seen using both assay systems, in both murine (AC29) and human (Ju77) MM cell lines. As with the response to over-expression of Smad7, the major effect seemed to be on the basal collagen response with only a small decrease in the fold amplification of collagen production following TGFβ.

When p38 kinase, another member of the MAPK signalling family, was examined, there was again rapid activation (phosphorylation) of p38 protein 5 minutes after $TGF\beta_1$ stimulation (see section 3.3.5). Two specific inhibitors of p38 kinase, SB203580 and SB202190, were used to examine the collagen response. The procollagen gene promoter response was inconsistent between cell lines and between different procollagen reporter genes. Other workers in our laboratory have found similar inconsistencies when using these compounds with the collagen promoter reporter gene assay, which suggest another possible interaction between the compounds and the reporter construct. The results found when using these inhibitors in combination with the procollagen reporter were therefore difficult to interpret and the findings of experiments measuring the actual collagen production using HPLC were thought to more accurately reflect their effects.

Measurement of collagen using HPLC showed a significant decrease in collagen production when cells were treated with SB203580 or SB202190, and this

was true at both the higher and lower doses of SB202190, which had been found to be more specific to either p38 kinase inhibition (lower dose) or combined inhibition of p38 kinase and ALK5 (higher dose). This would imply that p38 kinase is involved in the collagen synthesis pathway, most likely at a regulatory level of basal production. Its role in the TGFβ-induced increased production is more difficult to determine. As already described, recent work has shown that the higher dose of the compound SB203580 (10μM) also results in inhibition of ALK5 i.e. inhibition of Smad3 phosphorylation following TGFβ stimulation (Laping *et al.* 2002). There have been a number of reports in the last 1-2 years suggesting that p38 kinase is an essential part of the TGFβ stimulated collagen response. For example TGFβ induces collagen synthesis in cultured myoblasts and this was reported to be via p38 kinase (Rodriguez-Barbero *et al.* 2002). However, to determine this result the workers used SB203580 at 10μM and so would have also been inhibiting Smad3 phosphorylation by ALK5. Similarly, in hepatic stellate lines p38 kinase was reported to regulate α1(I) procollagen mRNA levels by TNFα and TGFβ (Varela-Rey *et al.*). Again this work relied on the higher dose of SB203580. In fact most of the published data in this area has used inhibitors at these higher doses that were at the time unknown to inhibit Smad3 phosphorylation.

The p38 kinase pathway has been examined using methods that do not involve "specific" inhibitors. In murine mesangial cells, work using targeted disruption of the Mkk gene that encodes for MKK3 an upstream activator of p38 kinase, showed that p38 kinase was not activated by TGFβ when this gene was disrupted. Also the TGFβ-stimulated pro-α1(I) collagen expression was inhibited when the MKK3 was non-functional, but the TGFβ-induced fibronectin and PAI response were not affected (Wang *et al.*). These data do support the basic findings published using the inhibitors that propose a role for p38 kinase in the TGFβ collagen response.

P38 kinase does appear to be important in the collagen response but its degree of involvement remains poorly described because of the problems in using these "specific" inhibitors. At lower doses (2μM for SB203580 and 1.5μM for SB202190) these inhibitors have been shown to be specific for p38 kinase (Chen *et al.* 1999;Laping *et al.* 2002;Yamanaka *et al.* 2003). At these doses there is a marked decrease in basal collagen production by one murine MM cell line, AC29, with little effect upon the TGFβ stimulated response, whereas another murine cell line, AB22,

showed only a small reduction of basal collagen production but a marked reduction in the response to TGFβ. These data suggest that the p38 kinase pathway plays a significant role in the control of collagen production but do not elucidate the exact nature of the effect.

The third MAPK signalling pathway, JNK, does not appear to play a direct role in the TGFβ-induced collagen response of MM cells. JNK was not found to be activated by TGFβ. However, as with ERK signalling, it may have some role in regulating basal collagen production. The MAPK pathways do appear to be involved in collagen production in these cells but their exact roles remain elusive. The ERK pathway would appear to have a regulatory role in suppressing the basal collagen production by MM cells given that its inhibition with UO126 resulted in increased collagen production. The role of p38 kinase is more difficult to interpret from the experiments performed given the difficulties with the inhibitor described above. However, if blocking p38 kinase has these specific effects then one can deduce that it has a role in enhancing collagen production and may enhance the effects of TGFβ.

3.4 ALK1 and ALK5 TGFβ type I receptor expression on Mesothelioma cells and the effect of Smad7 expression

The Smad pathway appears to be activated normally in MM cells (see section 3.2.4) and over-expression of Smad7, via transfection, reduces activity of the pathway (section 3.2.8). TGFβ increases collagen production by MM cells and previous work has shown that the collagen stimulating effects of TGFβ occur through the Smad pathway(Roberts *et al.* 2001). Over-expression of Smad7 in MM cells however, results in enhanced collagen expression (section 3.2.9) and tumour growth (section 3.2.10). In contrast, TGFβ antibodies do reduce tumour collagen content and growth in this model, as shown in section 3.1.6 & 3.1.10. Examination of the MAPK pathways as an alternative signalling cascade for the collagen stimulating effects of TGFβ show that although these pathways may be involved in collagen regulation, and are indeed activated by TGFβ in these cells (ERK1/2, p38 kinase but not JNK), they do not appear to be responsible for the TGFβ stimulating effects on collagen production (see chapter 3.3). An alternative explanation for the apparently paradoxical effects of Smad7 transfection (compared with the effects of TGFβ antibodies) might be found at the level of the receptor since the antibodies are likely to function in the extracellular space and Smad7 has intracellular effects.

3.4.1 Type I TGFβ receptor expression on MM cells

To examine MM cell expression of the two isoforms of the TGFβ type I receptor that can respond to TGFβ, ALK1 and ALK5, tumour sections derived from the murine model were stained immunohistochemically for ALK1 and ALK5 using specific antibodies, as described in section 2.8.2.

Figure 3.4.1 shows that both ALK1 and ALK5 are present in MM cells and that the distribution and density of the two isoforms is similar. Distribution of both ALK1 and ALK5 is increased around the tumour borders with no differences in expression between the two isoforms. There was reduced expression of ALK1 and ALK5 in the central areas of the tumour as shown in figure 3.4.2. Previous histology, described in chapter 3.1 suggested that tumour activity was higher at the edges of the

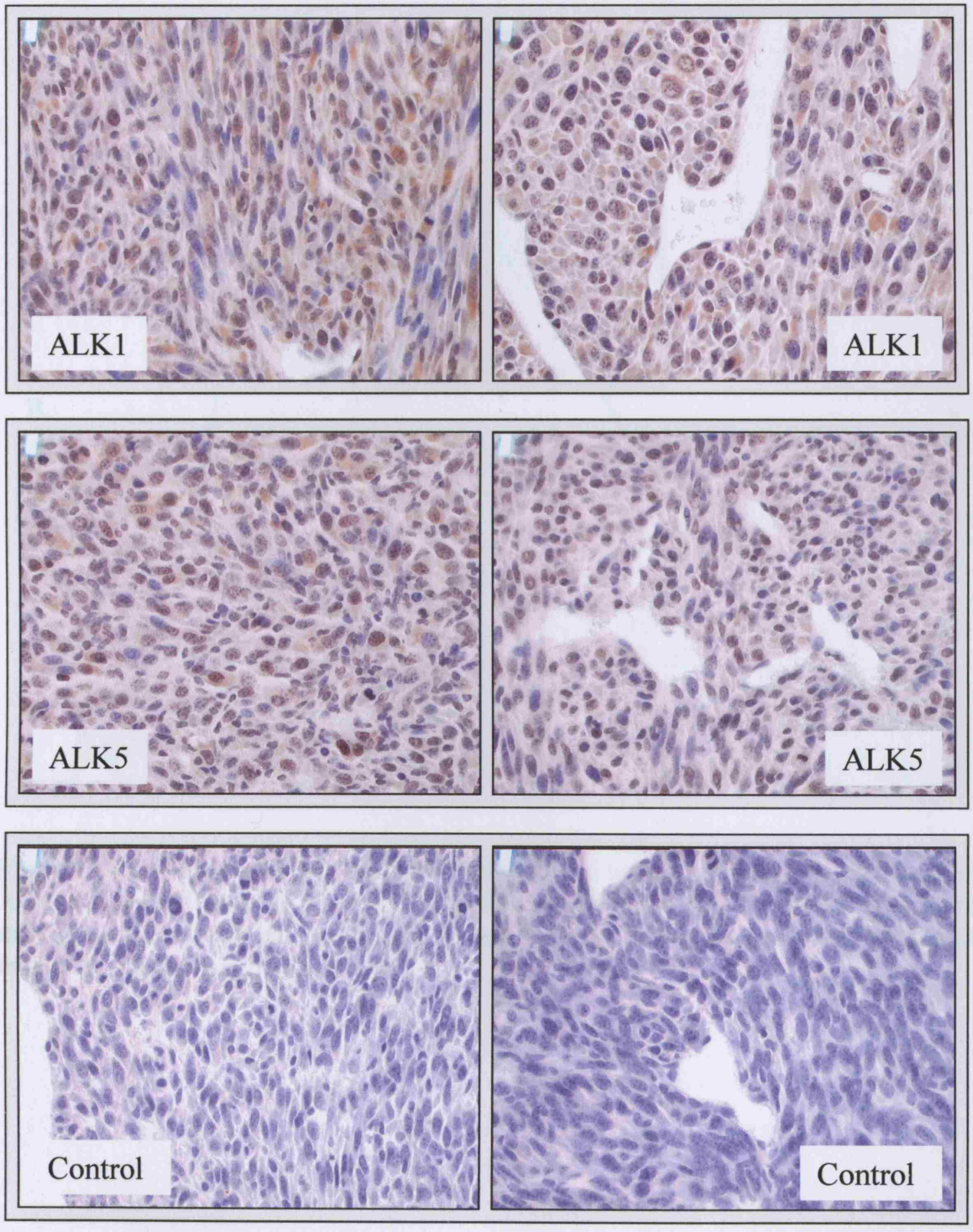

Figure 3.4.1 Immunohistochemical staining of TGFβ type I receptors ALK1 and ALK5 and a control matched antibody in sections from AB22 derived tumours (magnification x 40). The sections have been counter-stained with haematoxylin. Each section is taken from approximately the same area of tumour. The presence of both ALK1 and ALK5, predominantly in the cell cytoplasm is demonstrated by the brown stained areas.

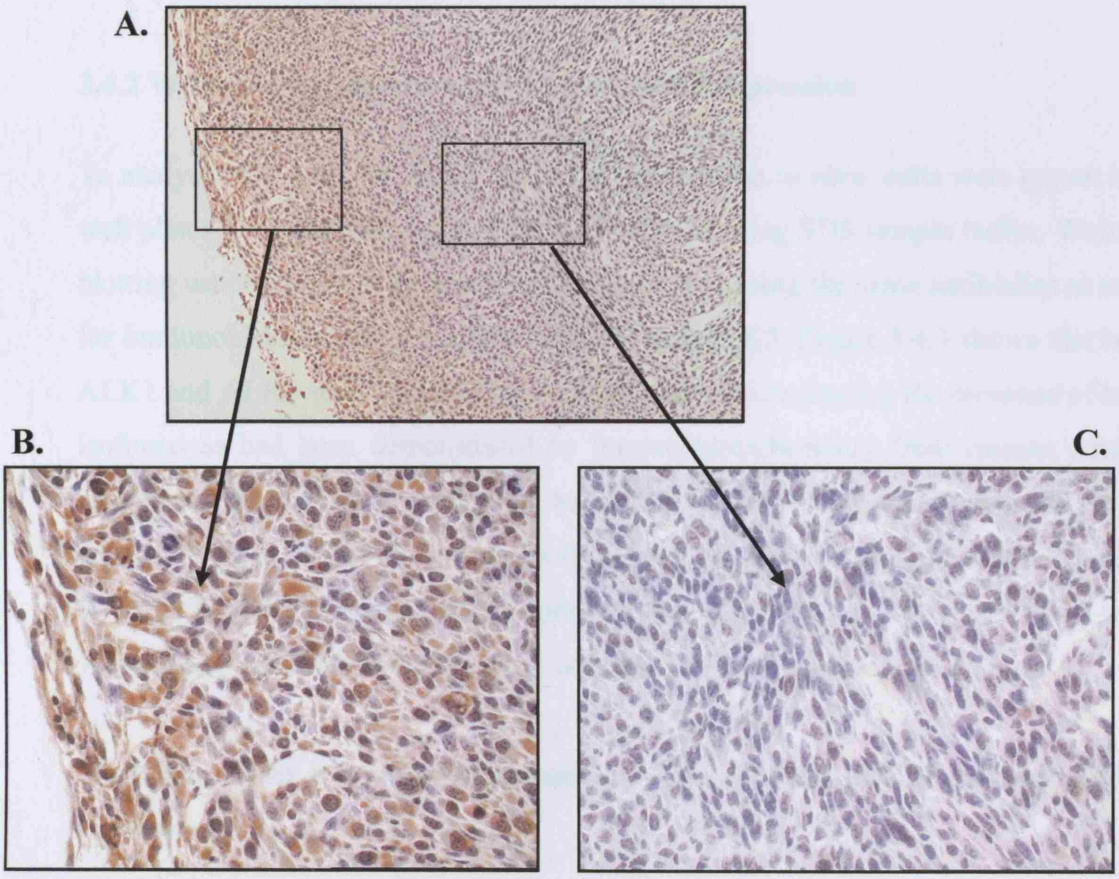

Figure 3.4.2 Section through AB1 MM cell derived tumour stained with antibody to ALK1 (**A**, magnification x 10) and counter-stained with haematoxylin. ALK1 is detected throughout the section but particularly toward the edge of the tumour, demonstrated in images **B** and **C** (magnification x 40).

tumour – this is where tumour growth, local invasion and the majority of angiogenesis is thought to occur and where the collagen-rich tumour capsule is found.

3.4.2 Western blot analysis of ALK1 and ALK5 expression

To analyse MM cells for ALK1 and ALK5 expression *in vitro,* cells were grown in 6 well plates to confluence and cell lysates extracted using SDS sample buffer. Western blotting was performed, as described in section 2.6, using the same antibodies as used for immunohistochemistry specific to ALK1 and ALK5. Figure 3.4.3 shows that both ALK1 and ALK5 were detected by Western blotting, confirming the presence of both isoforms as had been demonstrated by immunohistochemistry from murine tumour sections. This technique could not be used to quantify the expression of ALK1 compared with ALK5 as the antibodies used to identify the two isoforms have different binding affinities. Bands appeared at a molecular weight of 94kDa for both ALK1 and ALK5, which corresponds with the TGFβ type I receptor complex.

3.4.3 The effect of Smad7 expression on tumour MM cell ALK1 and ALK5 expression

After binding to the type I TGFβ receptor Smad7 initiates the down-regulation of the receptor by ubiquination. To examine whether Smad7 caused a down-regulation of either or both of the type I receptor isoforms, the expression of ALK1 and ALK5 were assessed on sections from tumours grown from Smad7-transfected MM cells and compared with those from control-transfected or non-transfected cells. Sections from AB22, AB1 and AC29 derived tumours were stained immunohistochemically for the expression of ALK1 and ALK5, as described in section 2.8.2. Sections from between 3 and 6 tumours from each cell type were examined for their ALK1 and ALK5 expression. There appeared to be a trend toward a reduction in tumour ALK expression in Smad7 transfected cell derived tumours with a more marked reduction in ALK5 than ALK1, an example is shown in figure 3.4.4. However, there were large variations within tumour groups with some showing no apparent differences between tumours derived from Smad7-transfected cells and those derived from control cells in terms of ALK expression. Also with individual tumours there were often wide variations in the expression of ALK receptors and this

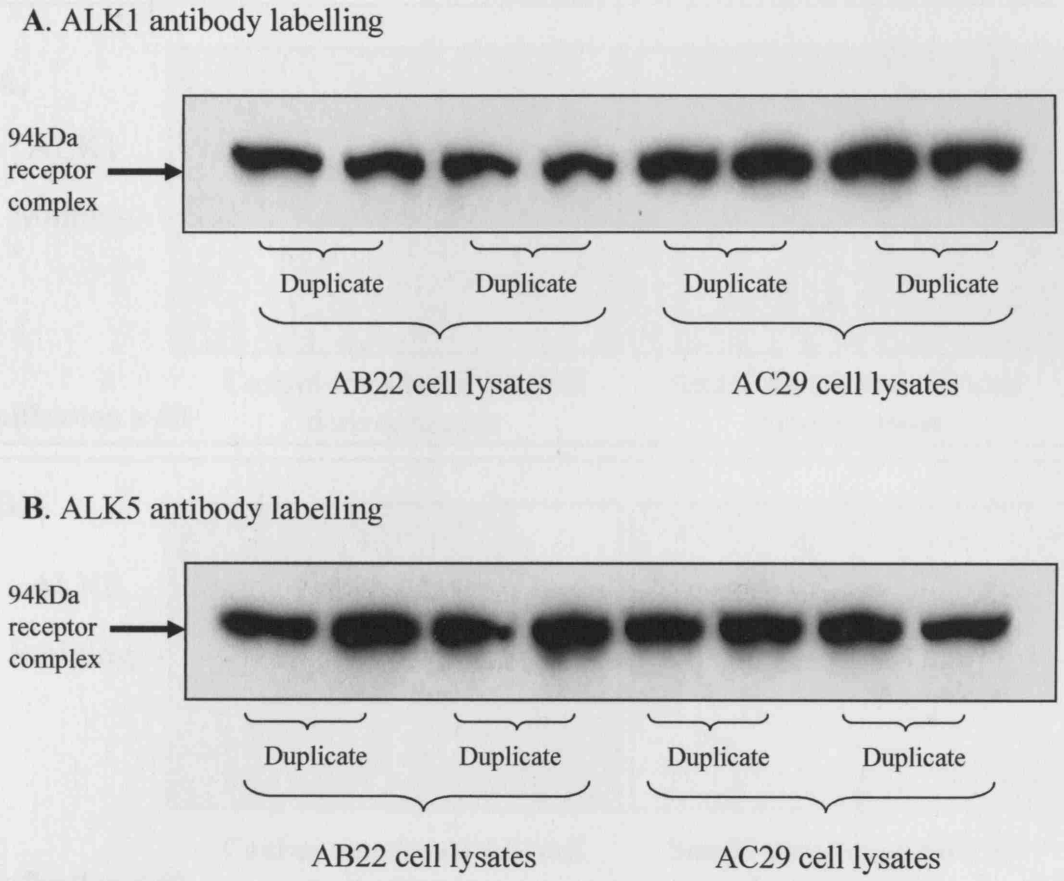

Figure 3.4.3 Western blot of AB22 and AC29 cell lysates using either ALK1 or ALK5 antibody labelling. In **A** separate duplicates, derived from different culture dish wells, of AB22 cells and AC29 cells are labelled for ALK1 expression, demonstrating the presence of ALK1. In **B** the same lysates are labelled with ALK5 specific antibodies, demonstrating the presence of ALK5.

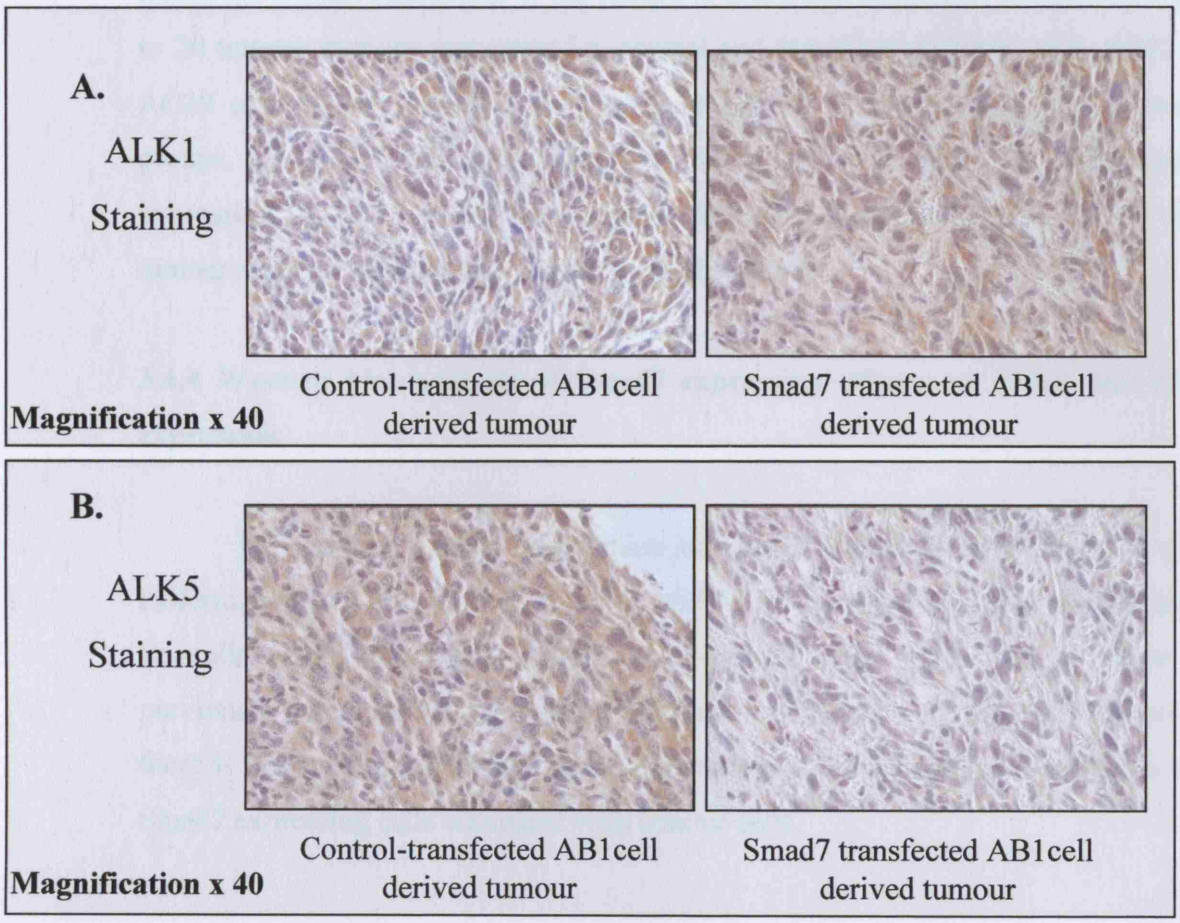

Figure 3.4.4. Sections from tumours derived from control transfected and Smad7 transfected AB1 cells stained immunohistochemically for ALK1 (panel A) and ALK5 (panel B). The sections from the control transfected tumours are taken from the same tumour. Similarly, the sections from the Smad7 transfected cell derived tumour are from the same tumour. There is an apparent down-regulation of ALK5 in the Smad7 transfected tumours. Sections are counter stained with haematoxylin.

heterogeneity of ALK1 and ALK5 expression between samples made it impossible to assess the overall expression of the receptors using this technique. After analysing up to 20 tumour sections per group i.e. control and Smad7 transfected AB1, AB22 and AC29 cell derived tumours, no consistent pattern of change was found between groups. Therefore, the overall analysis was that there were no differences in expression of ALK1 or ALK5 receptors following transfection with Smad7 when tumour sections were stained immunohistochemically.

3.4.4 Western blot analysis of Smad7 expression effects on ALK1 and ALK5 expression

To examine whether transfection of Smad7 altered the expression of either isoform, Western blot analysis of ALK1 and ALK5 protein expression was performed on cells stably expressing Smad7. JU77-Smad7 cells were used as these had previously demonstrated the highest expression of Smad7. Figure 3.4.5 shows that there is no apparent difference in the expression of either isoform detected in these Smad7 expressing cells compared with control cells.

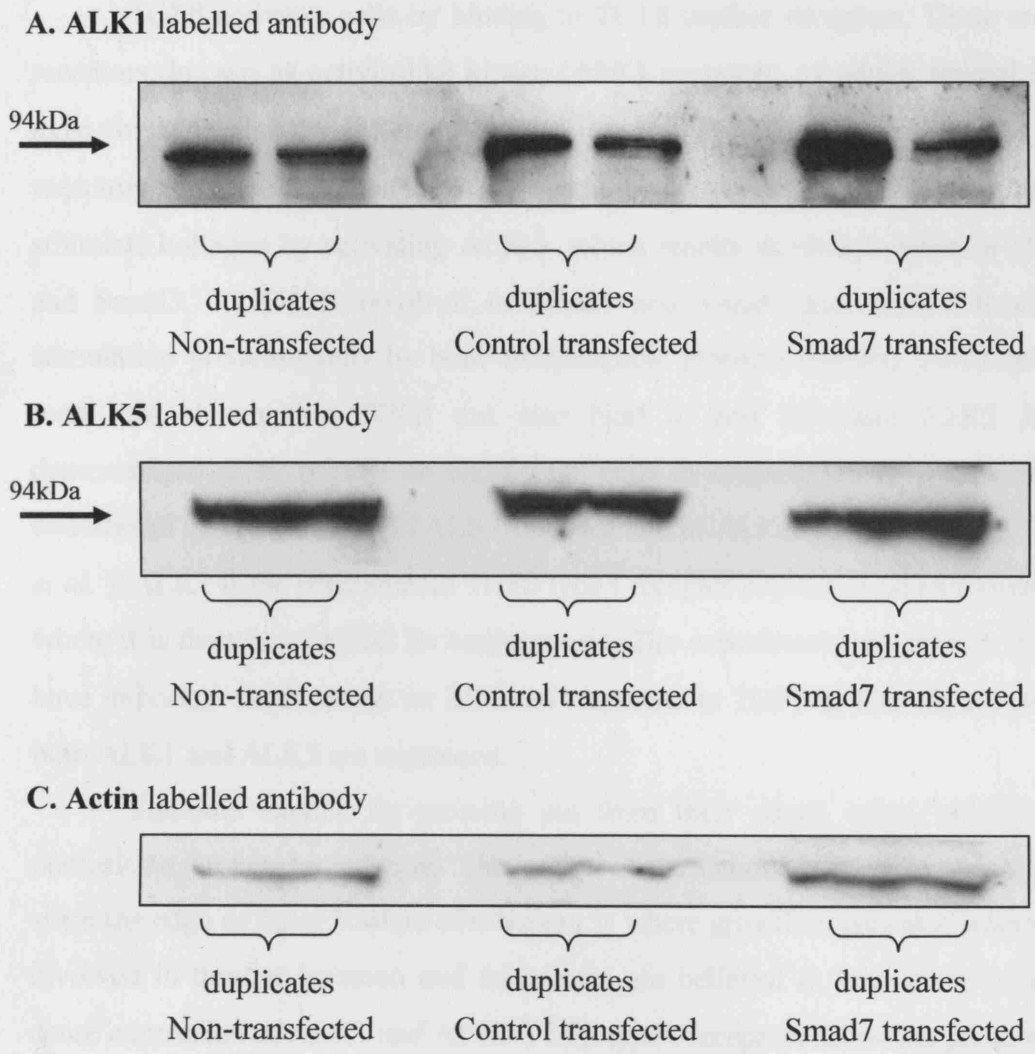

Figure 3.4.5 Western blot of cell lysates from non-transfected, control or Smad7 transfected JU77 cells . ALK1 **(A)** and ALK5 **(B)** antibody labelling was used to assess for changes in expression following Smad7 transfection. When corrected for protein loading by comparison with actin antibody labelled blots **(C)** there were no significant differences detected between groups.

3.4.5 Discussion

TGFβ activates cells by binding to TGFβ surface receptors. These are type I receptors, known as activin-like kinase (ALK) receptors, of which several isotopes exist for activation by different members of the TGFβ/activin family, and type II receptors that are ubiquitous for TGFβ signalling (see section 1.4). TGFβ is thought to stimulate collagen by activating ALK-5, which results in phosphorylation of Smad2 and Smad3. ALK-1 is involved in Smad1 and Smad5 activation following cell stimulation predominantly by bone morphogenic proteins (BMPs). However, recent work has shown that TGFβ can also bind to and stimulate ALK1 (recently demonstrated to be present on endothelial cells in conjunction with ALK5) and in endothelial cells the effects of ALK1 opposes that of ALK5 (Goumans *et al.* 2002;Oh *et al.*). ALK1 is the predominant TGFβ type I receptor expressed on endothelial cells, where it is thought essential for angiogenesis. The experiments reported in this thesis have important implications for MM cell responses to TGFβ as they demonstrate that both ALK1 and ALK5 are expressed.

Tumours expand by growing out from their edges, often leaving central necrosis as the tumour enlarges. This region of the tumour is therefore highly active, since the edge or outer borders of a tumour is where growth occurs and where factors involved in tumour invasion and metastases are believed to have their action. The dense expression of ALK1 and ALK5 TGFβ type I receptors occurring predominantly within this border region is consistent with these receptors being of importance to the regulation of tumour growth. The specific roles of the two isoforms are unknown in these cells and clearly need to be investigated further.

TGFβ is thought to signal predominantly through ALK5 in activating the Smad pathway. The high expression of ALK1 as well as ALK5, the receptor predicted to be expressed, was a surprising and novel finding. It is possible that the high expression of ALK1 explains the anomalous results obtained when the cells are transfected with Smad7 compared to treatment with TGFβ-neutralising antibodies. Smad7 only causes intracellular inhibition whereas the antibodies are thought to neutralise TGFβ before it binds to the cell receptor. Smad7 may be inhibiting the activation of only one of these two TGFβ type I receptors. This would be postulated to be ALK5 rather than ALK1, as ALK5 is the normal TGFβ signalling receptor. In BMP signalling, which occurs through ALK1, Smad6 is the inhibitory Smad protein.

ALK1 and ALK5 may have divergent or even opposing actions on MM cells, as they do in endothelial cells, in response to TGFβ. In endothelial cells, TGF-beta induces phosphorylation of Smad1/5 and Smad2 and these effects can be blocked by selective inhibition of ALK1 or ALK5 expression respectively. The TGF-beta/ALK5/Smad2/3 pathway **inhibited** endothelial cell migration and proliferation, whereas the TGF-beta/ALK1/Smad1/5 pathway **induced** migration and proliferation(Goumans *et al.* 2002;Oh *et al.*). These results suggest that there is a fine balance between ALK1 and ALK5 in regulating endothelial cell migration and proliferation.

Smad7 is thought to block ALK5 but may not block ALK1, which may still function in response to TGFβ and this may produce a pro-tumorigenic response. If ALK5 has an inhibitory role on ALK1 (as shown in endothelial cells, (Oh *et al.*)) or was independently anti-tumorigenic, then inhibition of ALK5 would enhance the effects of ALK1. Neutralising antibodies would result in reduced or no binding of TGFβ to the cells and so any different response of ALK1 and ALK5 would not be revealed.

There is a suggestion of enhanced down-regulation of ALK5 receptors by Smad7 expression in the immunohistochemically stained sections but this result is not convincing in these preliminary experiments. Down-regulation of the ALK5 receptor does not need to occur for inhibition of ALK5 activation following Smad7 expression, but if demonstrated would provide strong evidence to back this hypothesis. Further work in this area is clearly of great interest. An assessment of Smad7/ALK5 binding and Smad7/ALK1 binding in MM cells by immuno-precipitation would be an important experiment in future work. There are new small molecular weight inhibitors, not available at the time of these experiments, that specifically inhibit ALK1 or ALK5 and these would be extremely useful in further investigating these findings(DaCosta *et al.* 2004;Laping *et al.* 2002).

Chapter 4. Summary, Conclusions and Future Work

4.1 Summary of Findings

4.1.1. MM cells, TGFβ and collagen

1. MM cells synthesise significant quantities of collagen in response to TGFβ stimulation in a dose dependent manner.
2. MM cells produce TGFβ in significant quantities that can be measured exogenously.
3. Neutralising antibodies to TGFβ result in inhibition of exogenous TGFβ stimulating effects *in vitro*, but do not affect the basal level of collagen produced by MM cells *in vitro*.
4. Tumours grown *in vivo* using a murine model of MM contain abundant collagen.
5. Neutralising TGFβ antibody treatment of mice inhibits tumour growth *in vivo* and this effect is more marked when $TGF\beta_2$-specific neutralising antibodies are used.
6. Tumours that have been inhibited by TGFβ neutralising antibodies contain less collagen than control tumours.

4.1.2. Transient transfection of MM cells with LID and stable transfection with a lentiviral system; the effects of Smad7 transfection on collagen production

1. LID transfects MM cells and is a useful tool for transient transfection *in vitro* to assess collagen gene responses.
2. Lentiviral transfection of MM cells produces stable transfectants of Smad7 producing MM cells that are useful to examine the effects of Smad7 on collagen protein synthesis and tumour growth *in vivo*.
3. Normal Smad activation is found in human fetal lung fibroblasts (HFL1 cells) and transient transfection of Smad7 using LID results in inhibition of collagen gene responses.
4. Normal Smad activation occurs in MM cells but inhibition using transient Smad7 transfection results in a greater basal level of collagen gene activity and no inhibition of TGFβ responses.

5. Stable transfection of Smad7 using the lentiviral system in MM cells results in decreased Smad activation in response to TGFβ (but not total blockade of the Smad pathway).
6. Stable Smad7 transfection of MM cells results in increased collagen protein production *in vitro.*
7. *In vivo* stable Smad7 transfection results in increased tumour growth and greater collagen content of tumours.

4.1.3. TGFβ, the MAPK pathways and collagen production in MM cells

1. TGFβ stimulation leads to rapid activation of ERK1/2 and p38 kinase in these cells that has not been reported elsewhere, suggesting direct activation of these pathways by TGFβ.
2. Inhibition of ERK1/2 activation results in increased collagen gene activity and increased basal collagen protein production.
3. p38 kinase inhibition results in a small decrease in basal collagen production.
4. JNK is not directly stimulated by TGFβ, but inhibition results in a small increase in collagen production.

4.1.4. ALK1 and ALK5 TGFβ type I receptors and MM cells

1. ALK1 and ALK5 protein is expressed by MM cells *in vitro.*
2. Both ALK1 and ALK5 receptors are expressed on tumours grown in a murine model .
3. No consistent discernable effect of Smad7 expression is seen on ALK1 and ALK5 expression in MM cells.

4.2 Conclusions

There are a number of key conclusions to be drawn from this work and several as yet unanswered questions that could lead to important further work. The first conclusion is that TGFβ and collagen are confirmed as highly important factors in the growth of MM tumours. Also, that an autocrine growth loop in MM tumours is extremely likely to involve these two factors, since this work confirms that MM cells produce TGFβ and respond to TGFβ by synthesising large amounts of collagen. These tumours are found to contain high amounts of collagen as a key component of the ECM and previous work has shown that the ECM is critical in the mechanisms allowing local tumour invasion (Buchholz *et al.* 2003;Ioachim *et al.* 2002;Jaskiewicz *et al.* 1993;Marshall and Hart 1996;Wernert 1997), metastasis (De Wever and Mareel 2003;Engbring and Kleinman 2003;Stewart *et al.* 2004) and protection of tumours from chemotherapeutic agents (Sethi *et al.* 1999). Inhibition of TGFβ, using neutralising antibodies, in a murine model of MM demonstrated that tumour growth could be reduced and that the collagen content of the tumours was also reduced. The murine model proved to be a robust and consistent tool for evaluating tumour growth *in vivo*.

The results obtained using TGFβ neutralising antibodies suggest that these in themselves might offer a therapeutic option. The experiments were performed to test the theory that TGFβ has an important role in MM tumour growth rather than as potential therapeutic agents. So why haven't these antibodies been considered as potential therapy for TGFβ? The use of TGFβ neutralising antibodies as therapeutic agents in cancer has a number of difficulties; they are not tumour specific; they can lead to the production of antibodies by the body that renders them ineffective beyond short-term usage; and they are very expensive to produce. A transfection method of inhibiting TGFβ was used to test the hypothesis further by inhibiting TGFβ in another manner and as a way of identifying possible targets for novel treatment. The Smad pathway is thought to be specific to TGFβ signalling and Smad7 is the negative feedback loop of that pathway. To use Smad7 to inhibit the pathway seemed to be an ideal way of using transfection techniques to inhibit the effects of TGFβ (transfection has the potential to allow tumour targeting, although this work does not specifically examine that potential). By over-expressing Smad7 in MM cells, the Smad pathway

should be inhibited and hence TGFβ signalling blocked. What this work revealed however was totally unexpected. Smad7 over-expression resulted in an increased collagen production by MM cells, assessed at gene and protein levels and tumours grew larger *in vivo*. The technique used to over-express Smad7 resulted in reduced but not totally inhibited Smad signalling. In retrospect this was a useful, although unplanned, feature of the technique, as a total blockade of Smad signalling may have resulted in the activation of alternative pathways that would be difficult to identify within the scope of this work. A reduced signalling capacity should therefore reflect a genuine biological response and also shows that the level of activity is important i.e. activation of the Smad pathway is not an all or none response.

Throughout these experiments *in vitro*, both the murine and human cell lines behaved in a similar manner and therefore the murine cells were confirmed as a useful model for use *in vivo*.

The remainder of these investigations focussed on why this paradoxical response occurred i.e. why inhibition of TGFβ using neutralising antibodies within the extracellular space had opposing effects to inhibition of the intracellular signalling. TGFβ had already been shown to increase collagen synthesis by MM cells and therefore pathways other than Smad were investigated as possible routes by which TGFβ may be signalling in these cells to increase collagen production.

The MAPK pathways were examined as the most likely alternative route for signalling since previous work had shown that these pathways can be involved in collagen synthesis (see chapter 3.3 discussion). The results demonstrated that TGFβ does directly stimulate ERK1/2 and p38 kinase, possibly by a novel mechanism, since activation occurred at 5 minutes after TGFβ stimulation. Smad activation occurred normally in these cells at 20 minutes and so could not be an up-stream event to explain MAPK activation. Previous work has demonstrated TGFβ activating these pathways indirectly after 15-20 minutes (see discussion chapter 3.3). This novel finding was important, as it suggested a possible role for these pathways in the collagen response of MM cells to TGFβ. However, ERK1/2 inhibition resulted in increased MM cell collagen production, suggesting that ERK1/2 has an inhibitory role in MM collagen synthesis. Inhibition of p38 kinase did result in decreased collagen production, but this was mainly of basal collagen levels and although statistically significant was only a small reduction. There were no consistent effects on the TGFβ

stimulated collagen response. It is possible that these pathways have other roles in tumorigenesis linked to TGFβ in these tumours to explain their rapid activation but this is likely to be a separate mechanism to that involving collagen.

The contrast between the results of extracellular inhibition of TGFβ compared with the intracellular signalling inhibition lead to the further hypothesis that something unusual was occurring at the cell surface i.e. at the interface between TGFβ and intracellular signalling and how Smad7 was interacting at this point. Therefore the TGFβ receptor was examined. The TGFβ family of proteins signal by binding to the ubiquitous TGFβ type II receptor, which then combines with the type I receptor activating an intracellular phosphorylation site. There are a number of isotypes of the type I receptor and TGFβ activates ALK5 in most normal cells. In endothelial cells it also activates ALK1, which appears to have opposing effects to ALK5 activation in these cells. The current investigations found that MM cells also express both ALK1 and ALK5, another novel finding that might be important in explaining why Smad7 transfection had such unexpected results. The preliminary results of this work were unable to show a difference between expression of ALK1 and ALK5 but it may be the Smad7 interaction with these receptors that is causing the increased collagen production and increased tumour growth. Smad7 is known to bind to the type I receptor in order to inhibit its phosphorylation site and block signalling. Binding of Smad7 also results in the down-regulation of the receptor by stimulating ubiquination. TGFβ normally signals through the ALK5 receptor and Smad7 is known to bind to this. Smad6, the inhibitory Smad for BMP signalling, is known to bind to ALK1 to inhibit its action. What is unclear is the nature, if any, of the interaction between Smad7 and ALK1. This and the interaction between Smad7 and ALK5 receptors in MM cells could be a focus for further work. Specific blocking of ALK1 or ALK5 using recently developed inhibitors may reveal a difference in their actions that may be key to MM cell growth.

In conclusion, this work confirms the hypothesis that TGFβ and collagen are important for MM tumour growth and that TGFβ inhibition reduces tumour growth. Transfection of Smad7 is not a candidate to use as a therapy in itself but its use has revealed novel findings in MM that warrant further investigation.

There are two directions in which this work could be continued. The first is the further exploration of these findings in an attempt to elucidate mechanisms that may identify specific therapeutic targets. The second is to use these results to devise approaches that might be of therapeutic use. I chose to pursue the mechanism of Smad7's paradoxical effect rather than using that result as a way of indicating a specific therapeutic direction – for instance inhibiting Smad7. By taking this approach, there have probably been more questions than answers produced. However, the presence of both ALK1 and ALK5 TGFβ receptors was an unexpected and novel finding, which opens potentially exciting avenues for further investigation. To examine this further the interaction of Smad7 with these two receptors could be assessed histochemically by using labelled Smad7 and labelled ALK1 or ALK5. Or from the experiments already performed, Western analysis using antibodies to ALK1 or ALK5 in conjunction with Flag antibodies (the peptide label attached to the transfected Smad7), could be used to establish if Smad7 interacts with one, both or neither of the two ALK receptors. Similarly the interaction of TGFβ with the ALK receptors could be assessed in the same manner.

As an alternative approach, there are now specific inhibitors of ALK1 and ALK5 (not available during the period that this work was performed) that would demonstrate potential differences in their roles. If these demonstrated that of one these two isoforms was more important as a tumour promoter then clearly this could be examined as a therapeutic target in MM. Such experiments may also show a divergent action between the two different receptor isoforms that might also be utilised. For instance, if one were pro-tumorigenic and the other anti-tumorigenic then some way of forcing cell expression of one rather than the other might inhibit tumour growth. The examination of normal mesothelial cells for expression of ALK1 and ALK5 would be an important further experiment to assess whether this phenomenon was part of the malignant transformation.

Smad7 is the inhibitory Smad for TGFβ signalling, but there is another inhibitory Smad – Smad6, which is the inhibitory Smad for BMP signalling. Smad6 is targeted to ALK1 in that pathway and so its effects in these ALK1 expressing MM cells could be very interesting, especially if there are divergent roles for ALK1 and

ALK5. Similarly a combination of Smad6 and Smad7 transfection may also produce interesting results – perhaps a greater inhibition of TGFβ that might produce similar effects to those of the neutralising antibodies.

The alternative line of investigation to expand this work would be to examine what happens if Smad7 became the target, since Smad7 has been shown to enhance tumour growth. Smad7 could be blocked using techniques such as antisense or preferably by the more recent and exciting method of RNA interference (RNAi)(Milhavet *et al.* 2003) that is superseding antisense techniques. The consequences of blocking Smad7 would be very interesting, although further work would be required to establish mechanisms.

There are a number of experiments that could be done to refine the work presented here further. These could include an assessment of the other TGFβ pro-tumorigenic effects i.e. angiogenesis and immunosuppression. These could be examined in a number of ways including micro-blood vessel counts and infiltration of tumours by T-cells. These effects of TGFβ may be in part due to its effects on non-malignant cells surrounding the tumour stroma. Antibodies to TGFβ may inhibit these effects, whereas Smad7 transfection of MM cells may not. This is important as a further possible explanation as to why there are opposing effects between extracellular and intracellular inhibition of TGFβ.

This work opens a number of possible avenues for further investigation that I believe might lead to the identification of a novel target in MM, which currently remains very insensitive to therapy. The peak of the MM epidemic is yet to occur in developed countries that have banned the use of asbestos. In developing countries, which are expanding their use of asbestos, the problem is going to increase for many years.

References

Abdel-Wahab, N., Wicks, S. J., Mason, R. M. and Chantry, A. Decorin suppresses transforming growth factor-beta-induced expression of plasminogen activator inhibitor-1 in human mesangial cells through a mechanism that involves Ca2+-dependent phosphorylation of Smad2 at serine-240. *Biochem. J.*, 2002, 362: 643-649.

Abdollah, S., Macias-Silva, M., Tsukazaki, T., Hayashi, H., Attisano, L. and Wrana, J. L. TbetaRI phosphorylation of Smad2 on Ser465 and Ser467 is required for Smad2-Smad4 complex formation and signaling. *J. Biol. Chem.*, 1997, 272: 27678-27685.

Abe, M., Harpel, J. G., Metz, C. N., Nunes, I., Loskutoff, D. J. and Rifkin, D. B. An assay for transforming growth factor-beta using cells transfected with a plasminogen activator inhibitor-1 promoter-luciferase construct. *Anal. Biochem.*, 1994, 216: 276-284.

Adams, V. I., Unni, K. K., Muhm, J. R., Jett, J. R., Ilstrup, D. M. and Bernatz, P. E. Diffuse malignant mesothelioma of pleura. Diagnosis and survival in 92 cases. *Cancer*, 1986, 58: 1540-1551.

Adjei, A. A. Pemetrexed (Alimta): a novel multitargeted antifolate agent. *Expert. Rev. Anticancer Ther.*, 2003, 3: 145-156.

Afrakhte, M., Moren, A., Jossan, S., Itoh, S., Sampath, K., Westermark, B., Heldin, C. H., Heldin, N. E. and ten Dijke, P. Induction of inhibitory Smad6 and Smad7 mRNA by TGF-beta family members. *Biochem. Biophys. Res. Commun.*, 1998, 249: 505-511.

Akhurst, R. J. and Derynck, R. TGF-beta signaling in cancer--a double-edged sword. *Trends Cell Biol.*, 2001, 11: S44-S51.

Akiyoshi, S., Inoue, H., Hanai, J., Kusanagi, K., Nemoto, N., Miyazono, K. and Kawabata, M. c-Ski acts as a transcriptional co-repressor in transforming growth factor-beta signaling through interaction with smads. *J. Biol. Chem.*, 1999, 274: 35269-35277.

Albo, D., Berger, D. H. and Tuszynski, G. P. The effect of thrombospondin-1 and TGF-beta 1 on pancreatic cancer cell invasion. *J. Surg. Res.*, 1998, 76: 86-90.

Andreasen, P. A., Kjoller, L., Christensen, L. and Duffy, M. J. The urokinase-type plasminogen activator system in cancer metastasis: a review. *Int. J. Cancer*, 1997, 72: 1-22.

Annes, J. P., Munger, J. S. and Rifkin, D. B. Making sense of latent TGFbeta activation. *J. Cell Sci.*, 2003, 116: 217-224.

Antony, V. B. Immunological mechanisms in pleural disease. *Eur. Respir. J.*, 2003, 21: 539-544.

Asplund, T., Versnel, M. A., Laurent, T. C. and Heldin, P. Human mesothelioma cells produce factors that stimulate the production of hyaluronan by mesothelial cells and fibroblasts. *Cancer Res.*, 1993, 53: 388-392.

Atkinson, J. J. and Senior, R. M. Matrix metalloproteinase-9 in lung remodeling. *Am. J. Respir. Cell Mol. Biol.*, 2003, 28: 12-24.

Baas, P. Predictive and prognostic factors in malignant pleural mesothelioma. *Curr. Opin. Oncol.*, 2003, 15: 127-130.

Barbanti-Brodano, G., Sabbioni, S., Martini, F., Negrini, M., Corallini, A. and Tognon, M. Simian virus 40 infection in humans and association with human diseases: results and hypotheses. *Virology*, 2004, 318: 1-9.

Baris, B., Demir, A. U., Shehu, V., Karakoca, Y., Kisacik, G. and Baris, Y. I. Environmental fibrous zeolite (erionite) exposure and malignant tumors other than mesothelioma. *J. Environ. Pathol. Toxicol. Oncol.*, 1996, 15: 183-189.

Barrett, J. C. Cellular and molecular mechanisms of asbestos carcinogenicity: implications for biopersistence. *Environ. Health Perspect.*, 1994, 102 Suppl 5: 19-23.

Barrett, J. C., Lamb, P. W. and Wiseman, R. W. Multiple mechanisms for the carcinogenic effects of asbestos and other mineral fibers. *Environ. Health Perspect.*, 1989, 81: 81-89.

Basso, D., Mazza, S., Greco, E., Belluco, C., Roveroni, G., Navaglia, F., Nitti, D., Lise, M. and Plebani, M. Metastatic colorectal cancer stimulates collagen synthesis by fibroblasts. *Anticancer Res.*, 2001, 21: 2665-2670.

Beeh, K. M., Beier, J., Kornmann, O. and Buhl, R. Sputum matrix metalloproteinase-9, tissue inhibitor of metalloprotinease-1, and their molar ratio in patients with chronic obstructive pulmonary disease, idiopathic pulmonary fibrosis and healthy subjects. *Respir. Med.*, 2003, 97: 634-639.

Bellone, G., Carbone, A., Tibaudi, D., Mauri, F., Ferrero, I., Smirne, C., Suman, F., Rivetti, C., Migliaretti, G., Camandona, M., Palestro, G., Emanuelli, G. and Rodeck, U. Differential expression of transforming growth factors-beta1, -beta2 and -beta3 in human colon carcinoma. *Eur. J. Cancer*, 2001, 37: 224-233.

Benigni, A., Zoja, C., Corna, D., Zatelli, C., Conti, S., Campana, M., Gagliardini, E., Rottoli, D., Zanchi, C., Abbate, M., Ledbetter, S. and Remuzzi, G. Add-on anti-TGF-beta antibody to ACE inhibitor arrests progressive diabetic nephropathy in the rat. *J. Am. Soc. Nephrol.*, 2003, 14: 1816-1824.

Benjamin, L. E., Golijanin, D., Itin, A., Pode, D. and Keshet, E. Selective ablation of immature blood vessels in established human tumors follows vascular endothelial growth factor withdrawal. *J. Clin. Invest*, 1999, 103: 159-165.

Berking, C., Takemoto, R., Schaider, H., Showe, L., Satyamoorthy, K., Robbins, P. and Herlyn, M. Transforming growth factor-beta1 increases survival of human melanoma through stroma remodeling. *Cancer Res.*, 2001, 61: 8306-8316.

Bignon, J., Monchaux, G., Sebastien, P., Hirsch, A. and Lafuma, J. Human and experimental data on translocation of asbestos fibers through the respiratory system. *Ann. N. Y. Acad. Sci.*, 1979, 330: 745-750.

Bitzer, M., von Gersdorff, G., Liang, D., Dominguez-Rosales, A., Beg, A. A., Rojkind, M. and Bottinger, E. P. A mechanism of suppression of TGF-beta/SMAD signaling by NF-kappa B/RelA. *Genes Dev.*, 2000, 14: 187-197.

Boast, S., Su, M. W., Ramirez, F., Sanchez, M. and Avvedimento, E. V. Functional analysis of cis-acting DNA sequences controlling transcription of the human type I collagen genes. *J. Biol. Chem.*, 1990, 265: 13351-13356.

Bocchetta, M., Di, R., I, Powers, A., Fresco, R., Tosolini, A., Testa, J. R., Pass, H. I., Rizzo, P. and Carbone, M. Human mesothelial cells are unusually susceptible to simian virus 40-mediated transformation and asbestos cocarcinogenicity. *Proc. Natl. Acad. Sci. U. S. A*, 2000, 97: 10214-10219.

Bosman, F. T., de Bruine, A., Flohil, C., van der, W. A., ten Kate, J. and Dinjens, W. W. Epithelial-stromal interactions in colon cancer. *Int. J. Dev. Biol.*, 1993, 37: 203-211.

Boumediene, K., Takigawa, M. and Pujol, J. P. Cell density-dependent proliferative effects of transforming growth factor (TGF)-beta 1, beta 2, and beta 3 in human chondrosarcoma cells HCS-2/8 are associated with changes in the expression of TGF-beta receptor type I. *Cancer Invest*, 2001, 19: 475-486.

Boutin, C., Dumortier, P., Rey, F., Viallat, J. R. and De Vuyst, P. Black spots concentrate oncogenic asbestos fibers in the parietal pleura. Thoracoscopic and mineralogic study. *Am. J. Respir. Crit Care Med.*, 1996, 153: 444-449.

Brandt, S., Kopp, A., Grage, B. and Knabbe, C. Effects of tamoxifen on transcriptional level of transforming growth factor beta (TGF-beta) isoforms 1 and 2 in tumor tissue during primary treatment of patients with breast cancer. *Anticancer Res.*, 2003, 23: 223-229.

Breier, G., Blum, S., Peli, J., Groot, M., Wild, C., Risau, W. and Reichmann, E. Transforming growth factor-beta and Ras regulate the VEGF/VEGF-receptor system during tumor angiogenesis. *Int. J. Cancer*, 2002, 97: 142-148.

Brown, J. D., DiChiara, M. R., Anderson, K. R., Gimbrone, M. A., Jr. and Topper, J. N. MEKK-1, a component of the stress (stress-activated protein kinase/c- Jun N-terminal kinase) pathway, can selectively activate Smad2-mediated transcriptional activation in endothelial cells. *J. Biol. Chem.*, 1999, 274: 8797-8805.

Buchholz, M., Biebl, A., Neebetae, A., Wagner, M., Iwamura, T., Leder, G., Adler, G. and Gress, T. M. SERPINE2 (protease nexin I) promotes extracellular matrix production and local invasion of pancreatic tumors in vivo. *Cancer Res.*, 2003, 63: 4945-4951.

Burdorf, A., Dahhan, M. and Swuste, P. Occupational characteristics of cases with asbestos-related diseases in The Netherlands. *Ann. Occup. Hyg.*, 2003, 47: 485-492.

Butel, J. S., Jafar, S., Wong, C., Arrington, A. S., Opekun, A. R., Finegold, M. J. and Adam, E. Evidence of SV40 infections in hospitalized children. *Hum. Pathol.*, 1999, 30: 1496-1502.

Bydder, S., Phillips, M., Joseph, D. J., Cameron, F., Spry, N. A., DeMelker, Y. and Musk, A. W. A randomised trial of single-dose radiotherapy to prevent procedure tract metastasis by malignant mesothelioma. *Br. J. Cancer*, 2004, 91: 9-10.

Callahan, J. F., Burgess, J. L., Fornwald, J. A., Gaster, L. M., Harling, J. D., Harrington, F. P., Heer, J., Kwon, C., Lehr, R., Mathur, A., Olson, B. A., Weinstock, J. and Laping, N. J. Identification of novel inhibitors of the transforming growth factor beta1 (TGF-beta1) type 1 receptor (ALK5). *J. Med. Chem.*, 2002, 45: 999-1001.

Caminschi, I., Venetsanakos, E., Leong, C. C., Garlepp, M. J., Robinson, B. W. and Scott, B. Cytokine gene therapy of mesothelioma. Immune and antitumor effects of transfected interleukin-12. *Am. J. Respir. Cell Mol. Biol.*, 1999, 21: 347-356.

Campa, J. S., McAnulty, R. J. and Laurent, G. J. Application of high-pressure liquid chromatography to studies of collagen production by isolated cells in culture. *Anal. Biochem.*, 1990, 186: 257-263.

Carbone, M., Kratzke, R. A. and Testa, J. R. The pathogenesis of mesothelioma. *Semin. Oncol.*, 2002, 29: 2-17.

Carbone, M., Pass, H. I., Miele, L. and Bocchetta, M. New developments about the association of SV40 with human mesothelioma. *Oncogene*, 2003, 22: 5173-5180.

Carter, J. J., Madeleine, M. M., Wipf, G. C., Garcea, R. L., Pipkin, P. A., Minor, P. D. and Galloway, D. A. Lack of serologic evidence for prevalent simian virus 40 infection in humans. *J. Natl. Cancer Inst.*, 2003, 95: 1522-1530.

Cataldo, D., Munaut, C., Noel, A., Frankenne, F., Bartsch, P., Foidart, J. M. and Louis, R. Matrix metalloproteinases and TIMP-1 production by peripheral blood granulocytes from COPD patients and asthmatics. *Allergy*, 2001, 56: 145-151.

Ceresoli, G. L., Locati, L. D., Ferreri, A. J., Cozzarini, C., Passoni, P., Melloni, G., Zannini, P., Bolognesi, A. and Villa, E. Therapeutic outcome according to histologic subtype in 121 patients with malignant pleural mesothelioma. *Lung Cancer*, 2001, 34: 279-287.

Cerrano, P. G., Jasani, B., Filiberti, R., Neri, M., Merlo, F., De Flora, S., Mutti, L. and Puntoni, R. Simian virus 40 and malignant mesothelioma (Review). *Int. J. Oncol.*, 2003, 22: 187-194.

Chalfie, M., Tu, Y., Euskirchen, G., Ward, W. W. and Prasher, D. C. Green fluorescent protein as a marker for gene expression. *Science*, 1994, 263: 802-805.

Chen, S. J., Yuan, W., Mori, Y., Levenson, A., Trojanowska, M. and Varga, J. Stimulation of type I collagen transcription in human skin fibroblasts by TGF-beta: involvement of Smad 3. *J. Invest Dermatol.*, 1999, 112: 49-57.

Chen, Y. G., Hata, A., Lo, R. S., Wotton, D., Shi, Y., Pavletich, N. and Massague, J. Determinants of specificity in TGF-beta signal transduction. *Genes Dev.*, 1998, 12: 2144-2152.

Chen, Y. G. and Massague, J. Smad1 recognition and activation by the ALK1 group of transforming growth factor-beta family receptors. *J. Biol. Chem.*, 1999, 274: 3672-3677.

Cheng, D., Lee, Y. C., Rogers, J. T., Perkett, E. A., Moyers, J. P., Rodriguez, R. M. and Light, R. W. Vascular endothelial growth factor level correlates with transforming growth factor-beta isoform levels in pleural effusions. *Chest*, 2000, 118: 1747-1753.

Cheng, J. Q., Jhanwar, S. C., Klein, W. M., Bell, D. W., Lee, W. C., Altomare, D. A., Nobori, T., Olopade, O. I., Buckler, A. J. and Testa, J. R. p16 alterations and deletion mapping of 9p21-p22 in malignant mesothelioma. *Cancer Res.*, 1994, 54: 5547-5551.

Chin, B. Y., Mohsenin, A., Li, S. X., Choi, A. M. and Choi, M. E. Stimulation of pro-alpha(1)(I) collagen by TGF-beta(1) in mesangial cells: role of the p38 MAPK pathway. *Am. J. Physiol Renal Physiol*, 2001, 280: F495-F504.

Chin, L., Pomerantz, J. and DePinho, R. A. The INK4a/ARF tumor suppressor: one gene--two products--two pathways. *Trends Biochem. Sci.*, 1998, 23: 291-296.

Churg, A. and DePaoli, L. Clearance of chrysotile asbestos from human lung. *Exp. Lung Res.*, 1988, 14: 567-574.

Cicala, C., Pompetti, F. and Carbone, M. SV40 induces mesotheliomas in hamsters. *Am. J. Pathol.*, 1993, 142: 1524-1533.

Clark, D. A. and Coker, R. Transforming growth factor-beta (TGF-beta). *Int. J. Biochem. Cell Biol.*, 1998, 30: 293-298.

Coker, R. K., Laurent, G. J., Shahzeidi, S., Lympany, P. A., du Bois, R. M., Jeffery, P. K. and McAnulty, R. J. Transforming growth factors-beta 1, -beta 2, and -beta 3 stimulate fibroblast procollagen production in vitro but are differentially expressed during bleomycin-induced lung fibrosis. *Am. J. Pathol.*, 1997, 150: 981-991.

Cook, J. W., Sterman, D. H., Singhal, S., Smythe, W. R. and Kaiser, L. R. Suramin inhibits the growth of malignant mesothelioma in vitro, and in vivo, in murine flank and intraperitoneal models. *Lung Cancer*, 2003, 42: 263-274.

Craighead, J. E. and Mossman, B. T. The pathogenesis of asbestos-associated diseases. *N. Engl. J. Med.*, 1982, 306: 1446-1455.

Cramers, P., Ruevekamp, M., Oppelaar, H., Dalesio, O., Baas, P. and Stewart, F. A. Foscan uptake and tissue distribution in relation to photodynamic efficacy. *Br. J. Cancer*, 2003, 88: 283-290.

Crowe, D. L. and Shuler, C. F. Regulation of tumor cell invasion by extracellular matrix. *Histol. Histopathol.*, 1999, 14: 665-671.

DaCosta, B. S., Major, C., Laping, N. J. and Roberts, A. B. SB-505124 is a selective inhibitor of transforming growth factor-beta type I receptors ALK4, ALK5, and ALK7. *Mol. Pharmacol.*, 2004, 65: 744-752.

Dahlman, T., Lammerts, E., Wik, M., Bergstrom, D., Grimelius, L., Westermark, K., Rubin, K. and Heldin, N. E. Fibrosis in undifferentiated (anaplastic) thyroid carcinomas: evidence for a dual action of tumour cells in collagen type I synthesis. *J. Pathol.*, 2000, 191: 376-386.

Dang, D., Yang, Y., Li, X., Atakilit, A., Regezi, J., Eisele, D., Ellis, D. and Ramos, D. M. Matrix metalloproteinases and TGFbeta1 modulate oral tumor cell matrix. *Biochem. Biophys. Res. Commun.*, 2004, 316: 937-942.

Dang-Tan, T., Mahmud, S. M., Puntoni, R. and Franco, E. L. Polio vaccines, Simian Virus 40, and human cancer: the epidemiologic evidence for a causal association. *Oncogene*, 2004, 23: 6535-6540.

Darland, D. C. and D'Amore, P. A. TGF beta is required for the formation of capillary-like structures in three-dimensional cocultures of 10T1/2 and endothelial cells. *Angiogenesis.*, 2001, 4: 11-20.

Datto, M. B., Hu, P. P., Kowalik, T. F., Yingling, J. and Wang, X. F. The viral oncoprotein E1A blocks transforming growth factor beta- mediated induction of p21/WAF1/Cip1 and p15/INK4B. *Mol. Cell Biol.*, 1997, 17: 2030-2037.

Davidson, B., Givant-Horwitz, V., Lazarovici, P., Risberg, B., Nesland, J. M., Trope, C. G., Schaefer, E. and Reich, R. Matrix metalloproteinases (MMP), EMMPRIN (extracellular matrix metalloproteinase inducer) and mitogen-activated protein kinases (MAPK): co-expression in metastatic serous ovarian carcinoma. *Clin. Exp. Metastasis*, 2003, 20: 621-631.

Davis, J. M., Beckett, S. T., Bolton, R. E., Collings, P. and Middleton, A. P. Mass and number of fibres in the pathogenesis of asbestos-related lung disease in rats. *Br. J. Cancer*, 1978, 37: 673-688.

Davis, M. R., Manning, L. S., Whitaker, D., Garlepp, M. J. and Robinson, B. W. Establishment of a murine model of malignant mesothelioma. *Int. J. Cancer*, 1992, 52: 881-886.

de Caestecker, M. P., Piek, E. and Roberts, A. B. Role of transforming growth factor-beta signaling in cancer. *J. Natl. Cancer Inst.*, 2000, 92: 1388-1402.

de Jong, J. S., van Diest, P. J., van, d., V and Baak, J. P. Expression of growth factors, growth-inhibiting factors, and their receptors in invasive breast cancer. II: Correlations with proliferation and angiogenesis. *J. Pathol.*, 1998, 184: 53-57.

De Rienzo, A., Tor, M., Sterman, D. H., Aksoy, F., Albelda, S. M. and Testa, J. R. Detection of SV40 DNA sequences in malignant mesothelioma specimens from the United States, but not from Turkey. *J. Cell Biochem.*, 2002, 84: 455-459.

de Vries, W. J. and Long, M. A. Treatment of mesothelioma in Bloemfontein, South Africa. *Eur. J. Cardiothorac. Surg.*, 2003, 24: 434-440.

De Wever, O. and Mareel, M. Role of tissue stroma in cancer cell invasion. *J. Pathol.*, 2003, 200: 429-447.

Delporte, C., Redman, R. S. and Baum, B. J. Relationship between the cellular distribution of the alpha(v)beta3/5 integrins and adenoviral infection in salivary glands. *Lab Invest*, 1997, 77: 167-173.

Denhardt, D. T. Oncogene-initiated aberrant signaling engenders the metastatic phenotype: synergistic transcription factor interactions are targets for cancer therapy. *Crit Rev. Oncog.*, 1996, 7: 261-291.

Deraco, M., Casali, P., Inglese, M. G., Baratti, D., Pennacchioli, E., Bertulli, R. and Kusamura, S. Peritoneal mesothelioma treated by induction chemotherapy, cytoreductive surgery, and intraperitoneal hyperthermic perfusion. *J. Surg. Oncol.*, 2003, 83: 147-153.

Derynck, R., Akhurst, R. J. and Balmain, A. TGF-beta signaling in tumor suppression and cancer progression. *Nat. Genet.*, 2001, 29: 117-129.

Derynck, R., Zhang, Y. and Feng, X. H. Smads: transcriptional activators of TGF-beta responses. *Cell*, 1998, 95: 737-740.

Doll, R. Mortality from lung cancer in asbestos workers. *Br. J. Ind. Med.*, 1955, 12: 81-86.

Ebisawa, T., Fukuchi, M., Murakami, G., Chiba, T., Tanaka, K., Imamura, T. and Miyazono, K. Smurf1 interacts with transforming growth factor-beta type I receptor through Smad7 and induces receptor degradation. *J. Biol. Chem.*, 2001, 276: 12477-12480.

Edwards, J. G., Abrams, K. R., Leverment, J. N., Spyt, T. J., Waller, D. A. and O'Byrne, K. J. Prognostic factors for malignant mesothelioma in 142 patients: validation of CALGB and EORTC prognostic scoring systems. *Thorax*, 2000, 55: 731-735.

Edwards, J. G., McLaren, J., Jones, J. L., Waller, D. A. and O'Byrne, K. J. Matrix metalloproteinases 2 and 9 (gelatinases A and B) expression in malignant mesothelioma and benign pleura. *Br. J. Cancer*, 2003, 88: 1553-1559.

Ehlers, E. M., Bakhshandeh, A., Wiedemann, G. and Kuhnel, W. Invasiveness of human pleural mesothelioma cells is influenced in vitro by the three-dimensional structure of the ECM and its composition. *Ann. Anat.*, 2002, 184: 417-424.

Emri, S., Demir, A., Dogan, M., Akay, H., Bozkurt, B., Carbone, M. and Baris, I. Lung diseases due to environmental exposures to erionite and asbestos in Turkey. *Toxicol. Lett.*, 2002, 127: 251-257.

Engbring, J. A. and Kleinman, H. K. The basement membrane matrix in malignancy. *J. Pathol.*, 2003, 200: 465-470.

Faouzi, S., Le Bail, B., Neaud, V., Boussarie, L., Saric, J., Bioulac-Sage, P., Balabaud, C. and Rosenbaum, J. Myofibroblasts are responsible for collagen synthesis in the stroma of human hepatocellular carcinoma: an in vivo and in vitro study. *J. Hepatol.*, 1999, 30: 275-284.

Feldman, A. L., Libutti, S. K., Pingpank, J. F., Bartlett, D. L., Beresnev, T. H., Mavroukakis, S. M., Steinberg, S. M., Liewehr, D. J., Kleiner, D. E. and Alexander, H. R. Analysis of factors associated with outcome in patients with malignant peritoneal mesothelioma undergoing surgical debulking and intraperitoneal chemotherapy. *J. Clin. Oncol.*, 2003, 21: 4560-4567.

Fitzpatrick, D. R., Bielefeldt-Ohmann, H., Himbeck, R. P., Jarnicki, A. G., Marzo, A. L. and Robinson, B. W. Transforming growth factor-beta: antisense RNA-mediated inhibition affects anchorage-independent growth, tumorigenicity and tumor-infiltrating T-cells in malignant mesothelioma. *Growth Factors*, 1994, 11: 29-44.

Franchi, A., Benvenuti, S., Masi, L., Malentacchi, C., Arganini, L., Brandi, M. L. and Santucci, M. TGF-beta isoform and receptor expression in giant cell tumor and giant cell lesions of bone. *Appl. Immunohistochem. Mol. Morphol.*, 2001, 9: 170-175.

Frederick, J. P., Liberati, N. T., Waddell, D. S., Shi, Y. and Wang, X. F. Transforming growth factor beta-mediated transcriptional repression of c-myc is dependent on direct

binding of Smad3 to a novel repressive Smad binding element. *Mol. Cell Biol.*, 2004, 24: 2546-2559.

Friedberg, J. S., Mick, R., Stevenson, J., Metz, J., Zhu, T., Buyske, J., Sterman, D. H., Pass, H. I., Glatstein, E. and Hahn, S. M. A phase I study of Foscan-mediated photodynamic therapy and surgery in patients with mesothelioma. *Ann. Thorac. Surg.*, 2003, 75: 952-959.

Frizelle, S. P., Rubins, J. B., Zhou, J. X., Curiel, D. T. and Kratzke, R. A. Gene therapy of established mesothelioma xenografts with recombinant p16INK4a adenovirus. *Cancer Gene Ther.*, 2000, 7: 1421-1425.

Fukasawa, H., Yamamoto, T., Suzuki, H., Togawa, A., Ohashi, N., Fujigaki, Y., Uchida, C., Aoki, M., Hosono, M., Kitagawa, M. and Hishida, A. Treatment with anti-TGF-beta antibody ameliorates chronic progressive nephritis by inhibiting Smad/TGF-beta signaling. *Kidney Int.*, 2004, 65: 63-74.

Garlepp, M. J. and Leong, C. C. Biological and immunological aspects of malignant mesothelioma. *Eur. Respir. J.*, 1995, 8: 643-650.

Gerwin, B. I., Lechner, J. F., Reddel, R. R., Roberts, A. B., Robbins, K. C., Gabrielson, E. W. and Harris, C. C. Comparison of production of transforming growth factor-beta and platelet-derived growth factor by normal human mesothelial cells and mesothelioma cell lines. *Cancer Res.*, 1987, 47: 6180-6184.

Giancotti, F. G. and Ruoslahti, E. Integrin signaling. *Science*, 1999, 285: 1028-1032.

Gibbs, A. R., Stephens, M., Griffiths, D. M., Blight, B. J. and Pooley, F. D. Fibre distribution in the lungs and pleura of subjects with asbestos related diffuse pleural fibrosis. *Br. J. Ind. Med.*, 1991, 48: 762-770.

Gold, L. I., Jussila, T., Fusenig, N. E. and Stenback, F. TGF-beta isoforms are differentially expressed in increasing malignant grades of HaCaT keratinocytes, suggesting separate roles in skin carcinogenesis. *J. Pathol.*, 2000, 190: 579-588.

Gomez, M. and Cano, A. Expression of beta 1 integrin receptors in transformed mouse epidermal keratinocytes: upregulation of alpha 5 beta 1 in spindle carcinoma cells. *Mol. Carcinog.*, 1995, 12: 153-165.

Gong, J., Wang, D., Sun, L., Zborowska, E., Willson, J. K. and Brattain, M. G. Role of alpha 5 beta 1 integrin in determining malignant properties of colon carcinoma cells. *Cell Growth Differ.*, 1997, 8: 83-90.

Goodman, M., Teta, M. J., Hessel, P. A., Garabrant, D. H., Craven, V. A., Scrafford, C. G. and Kelsh, M. A. Mesothelioma and Lung Cancer Among Motor Vehicle Mechanics: a Meta-analysis. *Ann. Occup. Hyg.*, 2004, 48: 309-326.

Gorelik, L. and Flavell, R. A. Transforming growth factor-beta in T-cell biology. *Nat. Rev. Immunol.*, 2002, 2: 46-53.

Goumans, M. J., Valdimarsdottir, G., Itoh, S., Rosendahl, A., Sideras, P. and ten Dijke, P. Balancing the activation state of the endothelium via two distinct TGF- beta type I receptors. *EMBO J.*, 2002, 21: 1743-1753.

Graff, J. M., Bansal, A. and Melton, D. A. Xenopus Mad proteins transduce distinct subsets of signals for the TGF beta superfamily. *Cell*, 1996, 85: 479-487.

Greenberg, M. Knowledge of the health hazard of asbestos prior to the Merewether and Price report of 1930. *Soc. Hist Med.*, 1994, 7: 493-516.

Greenberg, M. Biological effects of asbestos: New York Academy of Sciences 1964. *Am. J. Ind. Med.*, 2003, 43: 543-552.

Grotendorst, G. R., Rahmanie, H. and Duncan, M. R. Combinatorial signaling pathways determine fibroblast proliferation and myofibroblast differentiation. *FASEB J.*, 2004, 18: 469-479.

Grove, C. S. and Lee, Y. C. Vascular endothelial growth factor: the key mediator in pleural effusion formation. *Curr. Opin. Pulm. Med.*, 2002, 8: 294-301.

Gulumian, M. The role of oxidative stress in diseases caused by mineral dusts and fibres: current status and future of prophylaxis and treatment. *Mol. Cell Biochem.*, 1999, 196: 69-77.

Hagedorn, H. G., Bachmeier, B. E. and Nerlich, A. G. Synthesis and degradation of basement membranes and extracellular matrix and their regulation by TGF-beta in invasive carcinomas (Review). *Int. J. Oncol.*, 2001, 18: 669-681.

Hahn, S. A., Schutte, M., Hoque, A. T., Moskaluk, C. A., da Costa, L. T., Rozenblum, E., Weinstein, C. L., Fischer, A., Yeo, C. J., Hruban, R. H. and Kern, S. E. DPC4, a candidate tumor suppressor gene at human chromosome 18q21.1. *Science*, 1996, 271: 350-353.

Hanafusa, H., Ninomiya-Tsuji, J., Masuyama, N., Nishita, M., Fujisawa, J., Shibuya, H., Matsumoto, K. and Nishida, E. Involvement of the p38 mitogen-activated protein kinase pathway in transforming growth factor-beta-induced gene expression. *J. Biol. Chem.*, 1999, 274: 27161-27167.

Harris, L. V. and Kahwa, I. A. Asbestos: old foe in 21st century developing countries. *Sci. Total Environ.*, 2003, 307: 1-9.

Hart, P. J., Deep, S., Taylor, A. B., Shu, Z., Hinck, C. S. and Hinck, A. P. Crystal structure of the human TbetaR2 ectodomain--TGF-beta3 complex. *Nat. Struct. Biol.*, 2002, 9: 203-208.

Hart, S. L., Arancibia-Carcamo, C. V., Wolfert, M. A., Mailhos, C., O'Reilly, N. J., Ali, R. R., Coutelle, C., George, A. J., Harbottle, R. P., Knight, A. M., Larkin, D. F., Levinsky, R. J., Seymour, L. W., Thrasher, A. J. and Kinnon, C. Lipid-mediated enhancement of transfection by a nonviral integrin- targeting vector. *Hum. Gene Ther.*, 1998, 9: 575-585.

Hasegawa, H., Nomura, T., Kishimoto, K., Yanagisawa, K. and Fujita, S. SFA-1/PETA-3 (CD151), a member of the transmembrane 4 superfamily, associates preferentially with alpha 5 beta 1 integrin and regulates adhesion of human T cell

leukemia virus type 1-infected T cells to fibronectin. *J. Immunol.*, 1998, 161: 3087-3095.

Hashimoto, Y., Kohri, K., Akita, H., Mitani, K., Ikeda, K. and Nakanishi, M. Efficient transfer of genes into senescent cells by adenovirus vectors via highly expressed alpha v beta 5 integrin. *Biochem. Biophys. Res. Commun.*, 1997, 240: 88-92.

Hayashida, T., Poncelet, A. C., Hubchak, S. C. and Schnaper, H. W. TGF-beta1 activates MAP kinase in human mesangial cells: a possible role in collagen expression. *Kidney Int.*, 1999, 56: 1710-1720.

Heldin, C. H., Miyazono, K. and ten Dijke, P. TGF-beta signalling from cell membrane to nucleus through SMAD proteins. *Nature*, 1997, 390: 465-471.

Hessel, P. A., Teta, M. J., Goodman, M. and Lau, E. Mesothelioma among brake mechanics: an expanded analysis of a case-control study. *Risk Anal.*, 2004, 24: 547-552.

Hill, C., Flyvbjerg, A., Rasch, R., Bak, M. and Logan, A. Transforming growth factor-beta2 antibody attenuates fibrosis in the experimental diabetic rat kidney. *J. Endocrinol.*, 2001, 170: 647-651.

Hirao, T., Bueno, R., Chen, C. J., Gordon, G. J., Heilig, E. and Kelsey, K. T. Alterations of the p16(INK4) locus in human malignant mesothelial tumors. *Carcinogenesis*, 2002, 23: 1127-1130.

Hjelmeland, M. D., Hjelmeland, A. B., Sathornsumetee, S., Reese, E. D., Herbstreith, M. H., Laping, N. J., Friedman, H. S., Bigner, D. D., Wang, X. F. and Rich, J. N. SB-431542, a small molecule transforming growth factor-beta-receptor antagonist, inhibits human glioma cell line proliferation and motility. *Mol. Cancer Ther.*, 2004, 3: 737-745.

Hocevar, B. A., Brown, T. L. and Howe, P. H. TGF-beta induces fibronectin synthesis through a c-Jun N-terminal kinase-dependent, Smad4-independent pathway. *EMBO J.*, 1999, 18: 1345-1356.

Huang, M., Sharma, S., Zhu, L. X., Keane, M. P., Luo, J., Zhang, L., Burdick, M. D., Lin, Y. Q., Dohadwala, M., Gardner, B., Batra, R. K., Strieter, R. M. and Dubinett, S. M. IL-7 inhibits fibroblast TGF-beta production and signaling in pulmonary fibrosis. *J. Clin. Invest*, 2002, 109: 931-937.

Huang, S. and Chakrabarty, S. Regulation of fibronectin and laminin receptor expression, fibronectin and laminin secretion in human colon cancer cells by transforming growth factor-beta 1. *Int. J. Cancer*, 1994, 57: 742-746.

Hung, K. Y., Huang, J. W., Chen, C. T., Lee, P. H. and Tsai, T. J. Pentoxifylline modulates intracellular signalling of TGF-beta in cultured human peritoneal mesothelial cells: implications for prevention of encapsulating peritoneal sclerosis. *Nephrol. Dial. Transplant.*, 2003, 18: 670-676.

Huse, M., Muir, T. W., Xu, L., Chen, Y. G., Kuriyan, J. and Massague, J. The TGF beta receptor activation process: an inhibitor- to substrate-binding switch. *Mol. Cell*, 2001, 8: 671-682.

Inagaki, Y., Mamura, M., Kanamaru, Y., Greenwel, P., Nemoto, T., Takehara, K., ten Dijke, P. and Nakao, A. Constitutive phosphorylation and nuclear localization of Smad3 are correlated with increased collagen gene transcription in activated hepatic stellate cells. *J. Cell Physiol*, 2001, 187: 117-123.

Inman, G. J., Nicolas, F. J., Callahan, J. F., Harling, J. D., Gaster, L. M., Reith, A. D., Laping, N. J. and Hill, C. S. SB-431542 is a potent and specific inhibitor of transforming growth factor-beta superfamily type I activin receptor-like kinase (ALK) receptors ALK4, ALK5, and ALK7.

Ioachim, E., Charchanti, A., Briasoulis, E., Karavasilis, V., Tsanou, H., Arvanitis, D. L., Agnantis, N. J. and Pavlidis, N. Immunohistochemical expression of extracellular matrix components tenascin, fibronectin, collagen type IV and laminin in breast cancer: their prognostic value and role in tumour invasion and progression. *Eur. J. Cancer*, 2002, 38: 2362-2370.

Itoh, Y. and Nagase, H. Matrix metalloproteinases in cancer. *Essays Biochem.*, 2002, 38: 21-36.

Iwatsubo, Y., Pairon, J. C., Boutin, C., Menard, O., Massin, N., Caillaud, D., Orlowski, E., Galateau-Salle, F., Bignon, J. and Brochard, P. Pleural mesothelioma: dose-response relation at low levels of asbestos exposure in a French population-based case-control study. *Am. J. Epidemiol.*, 1998, 148: 133-142.

Jagirdar, J., Lee, T. C., Reibman, J., Gold, L. I., Aston, C., Begin, R. and Rom, W. N. Immunohistochemical localization of transforming growth factor beta isoforms in asbestos-related diseases. *Environ. Health Perspect.*, 1997, 105 Suppl 5: 1197-1203.

Janne, P. A., Taffaro, M. L., Salgia, R. and Johnson, B. E. Inhibition of epidermal growth factor receptor signaling in malignant pleural mesothelioma. *Cancer Res.*, 2002, 62: 5242-5247.

Jaskiewicz, K., Chasen, M. R. and Robson, S. C. Differential expression of extracellular matrix proteins and integrins in hepatocellular carcinoma and chronic liver disease. *Anticancer Res.*, 1993, 13: 2229-2237.

Jenkins, R. G., Herrick, S. E., Meng, Q. H., Kinnon, C., Laurent, G. J., McAnulty, R. J. and Hart, S. L. An integrin-targeted non-viral vector for pulmonary gene therapy. *Gene Ther.*, 2000, 7: 393-400.

Jenkins, R. G., Meng, Q. H., Hodges, R. J., Lee, L. K., Bottoms, S. E., Laurent, G. J., Willis, D., Ayazi, S. P., McAnulty, R. J. and Hart, S. L. Formation of LID vector complexes in water alters physicochemical properties and enhances pulmonary gene expression in vivo. *Gene Ther.*, 2003, 10: 1026-1034.

Jester, J. V., Barry-Lane, P. A., Petroll, W. M., Olsen, D. R. and Cavanagh, H. D. Inhibition of corneal fibrosis by topical application of blocking antibodies to TGF beta in the rabbit. *Cornea*, 1997, 16: 177-187.

Jin, H. and Varner, J. Integrins: roles in cancer development and as treatment targets. *Br. J. Cancer*, 2004, 90: 561-565.

Joshi, T. K. and Gupta, R. K. Asbestos in developing countries: magnitude of risk and its practical implications. *Int. J. Occup. Med. Environ. Health*, 2004, 17: 179-185.

Kaarteenaho-Wiik, R., Soini, Y., Pollanen, R., Paakko, P. and Kinnula, V. L. Over-expression of tenascin-C in malignant pleural mesothelioma. *Histopathology*, 2003, 42: 280-291.

Kallianpur, A. R., Carstens, P. H., Liotta, L. A., Frey, K. P. and Siegal, G. P. Immunoreactivity in malignant mesotheliomas with antibodies to basement membrane components and their receptors. *Mod. Pathol.*, 1990, 3: 11-18.

Kanzaki, T., Olofsson, A., Moren, A., Wernstedt, C., Hellman, U., Miyazono, K., Claesson-Welsh, L. and Heldin, C. H. TGF-beta 1 binding protein: a component of the large latent complex of TGF-beta 1 with multiple repeat sequences. *Cell*, 1990, 61: 1051-1061.

Kasuga, I., Ishizuka, S., Minemura, K., Utsumi, K., Serizawa, H. and Ohyashiki, K. Malignant pleural mesothelioma produces functional granulocyte-colony stimulating factor. *Chest*, 2001, 119: 981-983.

Kauppila, S., Stenback, F., Risteli, J., Jukkola, A. and Risteli, L. Aberrant type I and type III collagen gene expression in human breast cancer in vivo. *J. Pathol.*, 1998, 186: 262-268.

Keerthisingam, C. B., Jenkins, R. G., Harrison, N. K., Hernandez-Rodriguez, N. A., Booth, H., Laurent, G. J., Hart, S. L., Foster, M. L. and McAnulty, R. J. Cyclooxygenase-2 deficiency results in a loss of the anti-proliferative response to transforming growth factor-beta in human fibrotic lung fibroblasts and promotes bleomycin-induced pulmonary fibrosis in mice. *Am. J. Pathol.*, 2001, 158: 1411-1422.

Kemperman, H., Wijnands, Y., Meijne, A. M. and Roos, E. TA3/St, but not TA3/Ha, mammary carcinoma cell adhesion to hepatocytes is mediated by alpha 5 beta 1 interacting with surface-associated fibronectin. *Cell Adhes. Commun.*, 1994, 2: 45-58.

Khasigov, P. Z., Podobed, O. V., Gracheva, T. S., Salbiev, K. D., Grachev, S. V. and Berezov, T. T. Role of matrix metalloproteinases and their inhibitors in tumor invasion and metastasis. *Biochemistry (Mosc.)*, 2003, 68: 711-717.

Kim, S. J., Angel, P., Lafyatis, R., Hattori, K., Kim, K. Y., Sporn, M. B., Karin, M. and Roberts, A. B. Autoinduction of transforming growth factor beta 1 is mediated by the AP-1 complex. *Mol. Cell Biol.*, 1990, 10: 1492-1497.

Kinnula, V. L. Oxidant and antioxidant mechanisms of lung disease caused by asbestos fibres. *Eur. Respir. J.*, 1999, 14: 706-716.

Klominek, J., Baskin, B. and Hauzenberger, D. Platelet-derived growth factor (PDGF) BB acts as a chemoattractant for human malignant mesothelioma cells via PDGF receptor beta-integrin alpha3beta1 interaction. *Clin. Exp. Metastasis*, 1998, 16: 529-539.

Kobie, J. J., Wu, R. S., Kurt, R. A., Lou, S., Adelman, M. K., Whitesell, L. J., Ramanathapuram, L. V., Arteaga, C. L. and Akporiaye, E. T. Transforming growth factor beta inhibits the antigen-presenting functions and antitumor activity of dendritic cell vaccines. *Cancer Res.*, 2003, 63: 1860-1864.

Koivunen, E., Wang, B. and Ruoslahti, E. Isolation of a highly specific ligand for the alpha 5 beta 1 integrin from a phage display library. *J. Cell Biol.*, 1994, 124: 373-380.

Kolb, M., Margetts, P. J., Galt, T., Sime, P. J., Xing, Z., Schmidt, M. and Gauldie, J. Transient transgene expression of decorin in the lung reduces the fibrotic response to bleomycin. *Am. J. Respir. Crit Care Med.*, 2001, 163: 770-777.

Konig, J. E., Tolnay, E., Wiethege, T. and Muller, K. M. Expression of vascular endothelial growth factor in diffuse malignant pleural mesothelioma. *Virchows Arch.*, 1999, 435: 8-12.

Koskinen, K., Pukkala, E., Martikainen, R., Reijula, K. and Karjalainen, A. Different measures of asbestos exposure in estimating risk of lung cancer and mesothelioma among construction workers. *J. Occup. Environ. Med.*, 2002, 44: 1190-1196.

Kratzke, R. A., Otterson, G. A., Lincoln, C. E., Ewing, S., Oie, H., Geradts, J. and Kaye, F. J. Immunohistochemical analysis of the p16INK4 cyclin-dependent kinase inhibitor in malignant mesothelioma. *J. Natl. Cancer Inst.*, 1995, 87: 1870-1875.

Krecicki, T., Zalesska-Krecicka, M., Jelen, M., Szkudlarek, T. and Horobiowska, M. Expression of type IV collagen and matrix metalloproteinase-2 (type IV collagenase) in relation to nodal status in laryngeal cancer. *Clin. Otolaryngol.*, 2001, 26: 469-472.

Kretzschmar, M., Doody, J., Timokhina, I. and Massague, J. A mechanism of repression of TGFbeta/ Smad signaling by oncogenic Ras. *Genes Dev.*, 1999, 13: 804-816.

Krueger, T., Altermatt, H. J., Mettler, D., Scholl, B., Magnusson, L. and Ris, H. B. Experimental photodynamic therapy for malignant pleural mesothelioma with pegylated mTHPC. *Lasers Surg. Med.*, 2003, 32: 61-68.

Kruklitis, R. J., Singhal, S., Delong, P., Kapoor, V., Sterman, D. H., Kaiser, L. R. and Albelda, S. M. Immuno-gene therapy with interferon-beta before surgical debulking delays recurrence and improves survival in a murine model of malignant mesothelioma. *J. Thorac. Cardiovasc. Surg.*, 2004, 127: 123-130.

Kuwahara, M., Takeda, M., Takeuchi, Y., Kuwahara, M., Harada, T. and Maita, K. Transforming growth factor beta production by spontaneous malignant mesothelioma cell lines derived from Fisher 344 rats. *Virchows Arch.*, 2001, 438: 492-497.

Laden, F., Stampfer, M. J. and Walker, A. M. Lung cancer and mesothelioma among male automobile mechanics: a review. *Rev. Environ. Health*, 2004, 19: 39-61.

Lagord, C., Berry, M. and Logan, A. Expression of TGFbeta2 but not TGFbeta1 correlates with the deposition of scar tissue in the lesioned spinal cord. *Mol. Cell Neurosci.*, 2002, 20: 69-92.

Landrigan, P. J., Nicholson, W. J., Suzuki, Y. and Ladou, J. The hazards of chrysotile asbestos: a critical review. *Ind. Health*, 1999, 37: 271-280.

Laping, N. J., Grygielko, E., Mathur, A., Butter, S., Bomberger, J., Tweed, C., Martin, W., Fornwald, J., Lehr, R., Harling, J., Gaster, L., Callahan, J. F. and Olson, B. A. Inhibition of transforming growth factor (TGF)-beta1-induced extracellular matrix with a novel inhibitor of the TGF-beta type I receptor kinase activity: SB-431542. *Mol. Pharmacol.*, 2002, 62: 58-64.

Larsson, J., Goumans, M. J., Sjostrand, L. J., van Rooijen, M. A., Ward, D., Leveen, P., Xu, X., ten Dijke, P., Mummery, C. L. and Karlsson, S. Abnormal angiogenesis but intact hematopoietic potential in TGF-beta type I receptor-deficient mice. *EMBO J.*, 2001, 20: 1663-1673.

Law, M. R., Gregor, A., Hodson, M. E., Bloom, H. J. and Turner-Warwick, M. Malignant mesothelioma of the pleura: a study of 52 treated and 64 untreated patients. *Thorax*, 1984, 39: 255-259.

Lechner, J. F., Tesfaigzi, J. and Gerwin, B. I. Oncogenes and tumor-suppressor genes in mesothelioma--a synopsis. *Environ. Health Perspect.*, 1997, 105 Suppl 5: 1061-1067.

Lee, T. C., Zhang, Y., Aston, C., Hintz, R., Jagirdar, J., Perle, M. A., Burt, M. and Rom, W. N. Normal human mesothelial cells and mesothelioma cell lines express insulin-like growth factor I and associated molecules. *Cancer Res.*, 1993, 53: 2858-2864.

Lee, Y. C. and Lane, K. B. The many faces of transforming growth factor-beta in pleural diseases. *Curr. Opin. Pulm. Med.*, 2001, 7: 173-179.

Leigh, J. and Driscoll, T. Malignant mesothelioma in Australia, 1945-2002. *Int. J. Occup. Environ. Health*, 2003, 9: 206-217.

Letterio, J. J. and Roberts, A. B. Regulation of immune responses by TGF-beta. *Annu. Rev. Immunol.*, 1998, 16: 137-161.

Li, J. H., Zhu, H. J., Huang, X. R., Lai, K. N., Johnson, R. J. and Lan, H. Y. Smad7 inhibits fibrotic effect of tgf-Beta on renal tubular epithelial cells by blocking smad2 activation. *J. Am. Soc. Nephrol.*, 2002, 13: 1464-1472.

Ling, H., Li, X., Jha, S., Wang, W., Karetskaya, L., Pratt, B. and Ledbetter, S. Therapeutic Role of TGF-beta-Neutralizing Antibody in Mouse Cyclosporin A Nephropathy: Morphologic Improvement Associated with Functional Preservation. *J. Am. Soc. Nephrol.*, 2003, 14: 377-388.

Lippmann, M. Asbestos exposure indices. *Environ. Res.*, 1988, 46: 86-106.

Liu, F., Hata, A., Baker, J. C., Doody, J., Carcamo, J., Harland, R. M. and Massague, J. A human Mad protein acting as a BMP-regulated transcriptional activator. *Nature*, 1996, 381: 620-623.

Liu, Z., Dobra, K., Hauzenberger, D. and Klominek, J. Expression of hyaluronan synthases and hyaluronan in malignant mesothelioma cells. *Anticancer Res.*, 2004, 24: 599-603.

Liu, Z., Ivanoff, A. and Klominek, J. Expression and activity of matrix metalloproteases in human malignant mesothelioma cell lines. *Int. J. Cancer*, 2001, 91: 638-643.

Lux, A., Attisano, L. and Marchuk, D. A. Assignment of transforming growth factor beta1 and beta3 and a third new ligand to the type I receptor ALK-1. *J. Biol. Chem.*, 1999, 274: 9984-9992.

Ma, L. J., Jha, S., Ling, H., Pozzi, A., Ledbetter, S. and Fogo, A. B. Divergent effects of low versus high dose anti-TGF-beta antibody in puromycin aminonucleoside nephropathy in rats. *Kidney Int.*, 2004, 65: 106-115.

Madri, J. A., Pratt, B. M. and Tucker, A. M. Phenotypic modulation of endothelial cells by transforming growth factor-beta depends upon the composition and organization of the extracellular matrix. *J. Cell Biol.*, 1988, 106: 1375-1384.

Maeda, H. and Shiraishi, A. TGF-beta contributes to the shift toward Th2-type responses through direct and IL-10-mediated pathways in tumor-bearing mice. *J. Immunol.*, 1996, 156: 73-78.

Maeda, J., Ueki, N., Ohkawa, T., Iwahashi, N., Nakano, T., Hada, T. and Higashino, K. Transforming growth factor-beta 1 (TGF-beta 1)- and beta 2-like activities in malignant pleural effusions caused by malignant mesothelioma or primary lung cancer. *Clin. Exp. Immunol.*, 1994, 98: 319-322.

Manning, C. B., Vallyathan, V. and Mossman, B. T. Diseases caused by asbestos: mechanisms of injury and disease development. *Int. Immunopharmacol.*, 2002a, 2: 191-200.

Manning, G., Whyte, D. B., Martinez, R., Hunter, T. and Sudarsanam, S. The protein kinase complement of the human genome. *Science*, 2002b, 298: 1912-1934.

Manning, L. S., Whitaker, D., Murch, A. R., Garlepp, M. J., Davis, M. R., Musk, A. W. and Robinson, B. W. Establishment and characterization of five human malignant mesothelioma cell lines derived from pleural effusions. *Int. J. Cancer*, 1991, 47: 285-290.

Marshall, J. F. and Hart, I. R. The role of alpha v-integrins in tumour progression and metastasis. *Semin. Cancer Biol.*, 1996, 7: 129-138.

Marzo, A. L., Fitzpatrick, D. R., Robinson, B. W. and Scott, B. Antisense oligonucleotides specific for transforming growth factor beta2 inhibit the growth of malignant mesothelioma both in vitro and in vivo. *Cancer Res.*, 1997, 57: 3200-3207.

Maschler, S., Grunert, S., Danielopol, A., Beug, H. and Wirl, G. Enhanced tenascin-C expression and matrix deposition during Ras/TGF-beta-induced progression of mammary tumor cells. *Oncogene*, 2004, 23: 3622-3633.

Masood, R., Kundra, A., Zhu, S., Xia, G., Scalia, P., Smith, D. L. and Gill, P. S. Malignant mesothelioma growth inhibition by agents that target the VEGF and VEGF-C autocrine loops. *Int. J. Cancer*, 2003, 104: 603-610.

Massague, J. TGF-beta signal transduction. *Annu. Rev. Biochem.*, 1998, 67: 753-791.

Masuda, Y., Kizaki, M., Ueno, H., Mori, S., Takayama, N., Muto, A., Matsushita, H., Ikeda, E., Kawai, Y. and Ikeda, Y. Chronic myelogenous leukemia (CML) associated with granulocyte colony- stimulating factor (G-CSF)-producing mesothelioma. *Leukemia*, 1995, 9: 1591-1594.

Matejuk, A., Dwyer, J., Hopke, C., Vandenbark, A. A. and Offner, H. Opposing roles for TGF-beta1 and TGF-beta3 isoforms in experimental autoimmune encephalomyelitis. *Cytokine*, 2004, 25: 45-51.

McAllister, K. A., Grogg, K. M., Johnson, D. W., Gallione, C. J., Baldwin, M. A., Jackson, C. E., Helmbold, E. A., Markel, D. S., McKinnon, W. C., Murrell, J. and . Endoglin, a TGF-beta binding protein of endothelial cells, is the gene for hereditary haemorrhagic telangiectasia type 1. *Nat. Genet.*, 1994, 8: 345-351.

McCaughey, W. T., Colby, T. V., Battifora, H., Churg, A., Corson, J. M., Greenberg, S. D., Grimes, M. M., Hammar, S., Roggli, V. L. and Unni, K. K. Diagnosis of diffuse malignant mesothelioma: experience of a US/Canadian Mesothelioma Panel. *Mod. Pathol.*, 1991, 4: 342-353.

McCulloch, J. Asbestos mining in Southern Africa, 1893-2002. *Int. J. Occup. Environ. Health*, 2003, 9: 230-235.

Meredith, J. E., Jr., Fazeli, B. and Schwartz, M. A. The extracellular matrix as a cell survival factor. *Mol. Biol. Cell*, 1993, 4: 953-961.

Middleton, G. W., Smith, I. E., O'Brien, M. E., Norton, A., Hickish, T., Priest, K., Spencer, L. and Ashley, S. Good symptom relief with palliative MVP (mitomycin-C, vinblastine and cisplatin) chemotherapy in malignant mesothelioma. *Ann. Oncol.*, 1998, 9: 269-273.

Milhavet, O., Gary, D. S. and Mattson, M. P. RNA interference in biology and medicine. *Pharmacol. Rev.*, 2003, 55: 629-648.

Mimuro, J., Sawdey, M., Hattori, M. and Luskutoff, D. J. cDNA for bovine type 1 plasminogen activator inhibitor (PAI-1). *Nucleic Acids Res.*, 1989, 17: 8872.

Minamoto, T., Ooi, A., Okada, Y., Mai, M., Nagai, Y. and Nakanishi, I. Desmoplastic reaction of gastric carcinoma: a light- and electron- microscopic immunohistochemical analysis using collagen type-specific antibodies. *Hum. Pathol.*, 1988, 19: 815-821.

Mitchev, K., Dumortier, P. and De Vuyst, P. 'Black Spots' and hyaline pleural plaques on the parietal pleura of 150 urban necropsy cases. *Am. J. Surg. Pathol.*, 2002, 26: 1198-1206.

Mo, J., Fang, S. J., Chen, W. and Blobe, G. C. Regulation of ALK-1 signaling by the nuclear receptor LXRbeta. *J. Biol. Chem.*, 2002, 277: 50788-50794.

Monnet, I., Breau, J. L., Moro, D., Lena, H., Eymard, J. C., Menard, O., Vuillez, J. P., Chokri, M., Romet-Lemonne, J. L. and Lopez, M. Intrapleural infusion of activated macrophages and gamma-interferon in malignant pleural mesothelioma: a phase II study. *Chest*, 2002, 121: 1921-1927.

Monneuse, O., Beaujard, A. C., Guibert, B., Gilly, F. N., Mulsant, P., Carry, P. Y., Benoit, M. and Glehen, O. Long-term results of intrathoracic chemohyperthermia (ITCH) for the treatment of pleural malignancies. *Br. J. Cancer*, 2003, 88: 1839-1843.

Moses, H. L., Yang, E. Y. and Pietenpol, J. A. TGF-beta stimulation and inhibition of cell proliferation: new mechanistic insights. *Cell*, 1990, 63: 245-247.

Mould, A. P., Burrows, L. and Humphries, M. J. Identification of amino acid residues that form part of the ligand- binding pocket of integrin alpha5 beta1. *J. Biol. Chem.*, 1998, 273: 25664-25672.

Moustakas, A., Pardali, K., Gaal, A. and Heldin, C. H. Mechanisms of TGF-beta signaling in regulation of cell growth and differentiation. *Immunol. Lett.*, 2002, 82: 85-91.

Muers, M. F., Rudd, R. M., O'Brien, M. E., Qian, W., Hodson, A., Parmar, M. K. and Girling, D. J. BTS randomised feasibility study of active symptom control with or without chemotherapy in malignant pleural mesothelioma: ISRCTN 54469112. *Thorax*, 2004, 59: 144-148.

Mulatero, C., Surentheran, T., Breuer, J. and Rudd, R. M. Simian virus 40 and human pleural mesothelioma. *Thorax*, 1999, 54: 60-61.

Muller, K. M., Schmitz, I. and Konstantinidis, K. Black spots of the parietal pleura: morphology and formal pathogenesis. *Respiration*, 2002, 69: 261-267.

Muraoka, R. S., Dumont, N., Ritter, C. A., Dugger, T. C., Brantley, D. M., Chen, J., Easterly, E., Roebuck, L. R., Ryan, S., Gotwals, P. J., Koteliansky, V. and Arteaga, C. L. Blockade of TGF-beta inhibits mammary tumor cell viability, migration, and metastases. *J. Clin. Invest*, 2002, 109: 1551-1559.

Murphy-Ullrich, J. E. and Poczatek, M. Activation of latent TGF-beta by thrombospondin-1: mechanisms and physiology. *Cytokine Growth Factor Rev.*, 2000, 11: 59-69.

Mutsaers, S. E. Mesothelial cells: their structure, function and role in serosal repair. *Respirology.*, 2002, 7: 171-191.

Nabeshima, K., Inoue, T., Shimao, Y. and Sameshima, T. Matrix metalloproteinases in tumor invasion: role for cell migration. *Pathol. Int.*, 2002, 52: 255-264.

Nakao, A., Afrakhte, M., Moren, A., Nakayama, T., Christian, J. L., Heuchel, R., Itoh, S., Kawabata, M., Heldin, N. E., Heldin, C. H. and ten Dijke, P. Identification of Smad7, a TGFbeta-inducible antagonist of TGF-beta signalling. *Nature*, 1997, 389: 631-635.

Nakao, A., Fujii, M., Matsumura, R., Kumano, K., Saito, Y., Miyazono, K. and Iwamoto, I. Transient gene transfer and expression of Smad7 prevents bleomycin-induced lung fibrosis in mice. *J. Clin. Invest*, 1999, 104: 5-11.

Naldini, L., Blomer, U., Gallay, P., Ory, D., Mulligan, R., Gage, F. H., Verma, I. M. and Trono, D. In vivo gene delivery and stable transduction of nondividing cells by a lentiviral vector. *Science*, 1996, 272: 263-267.

Nasreen, N., Mohammed, K. A., Hardwick, J., Van Horn, R. D., Sanders, K., Kathuria, H., Loghmani, F. and Antony, V. B. Low molecular weight hyaluronan induces malignant mesothelioma cell (MMC) proliferation and haptotaxis: role of CD44 receptor in MMC proliferation and haptotaxis. *Oncol. Res.*, 2002, 13: 71-78.

Nath, R. K., Kwon, B., Mackinnon, S. E., Jensen, J. N., Reznik, S. and Boutros, S. Antibody to transforming growth factor beta reduces collagen production in injured peripheral nerve. *Plast. Reconstr. Surg.*, 1998, 102: 1100-1106.

Neuzil, J., Swettenham, E. and Gellert, N. Sensitization of mesothelioma to TRAIL apoptosis by inhibition of histone deacetylase: role of Bcl-xL down-regulation. *Biochem. Biophys. Res. Commun.*, 2004, 314: 186-191.

Newham, P. and Humphries, M. J. Integrin adhesion receptors: structure, function and implications for biomedicine. *Mol. Med. Today*, 1996, 2: 304-313.

Nilsson, E. E. and Skinner, M. K. Role of transforming growth factor beta in ovarian surface epithelium biology and ovarian cancer. *Reprod. Biomed. Online.*, 2002, 5: 254-258.

Nishimura, S. L. and Broaddus, V. C. Asbestos-induced pleural disease. *Clin. Chest Med.*, 1998, 19: 311-329.

Norman, J. T., Lindahl, G. E., Shakib, K., En-Nia, A., Yilmaz, E. and Mertens, P. R. The Y-box binding protein YB-1 suppresses collagen alpha 1(I) gene transcription via an evolutionarily conserved regulatory element in the proximal promoter. *J. Biol. Chem.*, 2001, 276: 29880-29890.

Oh, S. P., Seki, T., Goss, K. A., Imamura, T., Yi, Y., Donahoe, P. K., Li, L., Miyazono, K., ten Dijke, P., Kim, S. and Li, E. Activin receptor-like kinase 1

modulates transforming growth factor- beta 1 signaling in the regulation of angiogenesis.

Ohbayashi, H. Matrix metalloproteinases in lung diseases. *Curr. Protein Pept. Sci.*, 2002, 3: 409-421.

Ohmori, T., Yang, J. L., Price, J. O. and Arteaga, C. L. Blockade of tumor cell transforming growth factor-betas enhances cell cycle progression and sensitizes human breast carcinoma cells to cytotoxic chemotherapy. *Exp. Cell Res.*, 1998, 245: 350-359.

Ohno, S., Tachibana, M., Fujii, T., Ueda, S., Kubota, H. and Nagasue, N. Role of stromal collagen in immunomodulation and prognosis of advanced gastric carcinoma. *Int. J. Cancer*, 2002, 97: 770-774.

Ordonez, N. G. Value of E-cadherin and N-cadherin immunostaining in the diagnosis of mesothelioma. *Hum. Pathol.*, 2003, 34: 749-755.

Oshima, M., Oshima, H. and Taketo, M. M. TGF-beta receptor type II deficiency results in defects of yolk sac hematopoiesis and vasculogenesis. *Dev. Biol.*, 1996, 179: 297-302.

Ozvaran, M. K., Cao, X. X., Miller, S. D., Monia, B. A., Hong, W. K. and Smythe, W. R. Antisense oligonucleotides directed at the bcl-xl gene product augment chemotherapy response in mesothelioma. *Mol. Cancer Ther.*, 2004, 3: 545-550.

Pache, J. C., Janssen, Y. M., Walsh, E. S., Quinlan, T. R., Zanella, C. L., Low, R. B., Taatjes, D. J. and Mossman, B. T. Increased epidermal growth factor-receptor protein in a human mesothelial cell line in response to long asbestos fibers. *Am. J. Pathol.*, 1998, 152: 333-340.

Paek, D. Asbestos problems yet to explode in Korea. *Int. J. Occup. Environ. Health*, 2003, 9: 266-271.

Papp, T., Schipper, H., Pemsel, H., Bastrop, R., Muller, K. M., Wiethege, T., Weiss, D. G., Dopp, E., Schiffmann, D. and Rahman, Q. Mutational analysis of N-ras, p53, p16INK4a, p14ARF and CDK4 genes in primary human malignant mesotheliomas. *Int. J. Oncol.*, 2001, 18: 425-433.

Pasche, B. Role of transforming growth factor beta in cancer. *J. Cell Physiol*, 2001, 186: 153-168.

Pass, H. I., Mew, D. J., Carbone, M., Donington, J. S., Baserga, R. and Steinberg, S. M. The effect of an antisense expression plasmid to the IGF-1 receptor on hamster mesothelioma proliferation. *Dev. Biol. Stand.*, 1998, 94: 321-328.

Pass, H. I., Temeck, B. K., Kranda, K., Thomas, G., Russo, A., Smith, P., Friauf, W. and Steinberg, S. M. Phase III randomized trial of surgery with or without intraoperative photodynamic therapy and postoperative immunochemotherapy for malignant pleural mesothelioma. *Ann. Surg. Oncol.*, 1997, 4: 628-633.

Paulus, W., Baur, I., Huettner, C., Schmausser, B., Roggendorf, W., Schlingensiepen, K. H. and Brysch, W. Effects of transforming growth factor-beta 1 on collagen synthesis, integrin expression, adhesion and invasion of glioma cells. *J. Neuropathol. Exp. Neurol.*, 1995, 54: 236-244.

Pelucchi, C., Malvezzi, M., La Vecchia, C., Levi, F., Decarli, A. and Negri, E. The Mesothelioma epidemic in Western Europe: an update. *Br. J. Cancer*, 2004, 90: 1022-1024.

Perlman, R., Schiemann, W. P., Brooks, M. W., Lodish, H. F. and Weinberg, R. A. TGF-beta-induced apoptosis is mediated by the adapter protein Daxx that facilitates JNK activation. *Nat. Cell Biol.*, 2001, 3: 708-714.

Peto, J., Decarli, A., La Vecchia, C., Levi, F. and Negri, E. The European mesothelioma epidemic. *Br. J. Cancer*, 1999, 79: 666-672.

Piek, E., Heldin, C. H. and ten Dijke, P. Specificity, diversity, and regulation in TGF-beta superfamily signaling. *FASEB J.*, 1999, 13: 2105-2124.

Poncelet, A. C. and Schnaper, H. W. Sp1 and Smad proteins cooperate to mediate transforming growth factor- beta 1-induced alpha 2(I) collagen expression in human glomerular mesangial cells. *J. Biol. Chem.*, 2001, 276: 6983-6992.

Prehn, R. T. Relationship of tumor immunogenicity to concentration of the oncogen. *J. Natl. Cancer Inst.*, 1975, 55: 189-190.

Ramirez, F. and Pereira, L. The fibrillins. *Int. J. Biochem. Cell Biol.*, 1999, 31: 255-259.

Randall, R. A., Howell, M., Page, C. S., Daly, A., Bates, P. A. and Hill, C. S. Recognition of phosphorylated-Smad2-containing complexes by a novel Smad interaction motif. *Mol. Cell Biol.*, 2004, 24: 1106-1121.

Reed, C. C., Gauldie, J. and Iozzo, R. V. Suppression of tumorigenicity by adenovirus-mediated gene transfer of decorin. *Oncogene*, 2002, 21: 3688-3695.

Roberts, A. B., Piek, E., Bottinger, E. P., Ashcroft, G., Mitchell, J. B. and Flanders, K. C. Is Smad3 a major player in signal transduction pathways leading to fibrogenesis? *Chest*, 2001, 120: 43S-47S.

Roberts, A. B. and Sporn, M. B. Physiological actions and clinical applications of transforming growth factor-beta (TGF-beta). *Growth Factors*, 1993, 8: 1-9.

Robinson, B. W., Creaney, J., Lake, R., Nowak, A., Musk, A. W., de Klerk, N., Winzell, P., Hellstrom, K. E. and Hellstrom, I. Mesothelin-family proteins and diagnosis of mesothelioma. *Lancet*, 2003, 362: 1612-1616.

Robinson, C. F., Petersen, M. and Palu, S. Mortality patterns among electrical workers employed in the U.S. construction industry, 1982-1987. *Am. J. Ind. Med.*, 1999, 36: 630-637.

Rodriguez-Barbero, A., Obreo, J., Yuste, L., Montero, J. C., Rodriguez-Pena, A., Pandiella, A., Bernabeu, C. and Lopez-Novoa, J. M. Transforming growth factor-beta1 induces collagen synthesis and accumulation via p38 mitogen-activated protein

kinase (MAPK) pathway in cultured L(6)E(9) myoblasts. *FEBS Lett.*, 2002, 513: 282-288.

Roudabush, F. L., Pierce, K. L., Maudsley, S., Khan, K. D. and Luttrell, L. M. Transactivation of the EGF receptor mediates IGF-1-stimulated shc phosphorylation and ERK1/2 activation in COS-7 cells. *J. Biol. Chem.*, 2000, 275: 22583-22589.

Roushdy-Hammady, I., Siegel, J., Emri, S., Testa, J. R. and Carbone, M. Genetic-susceptibility factor and malignant mesothelioma in the Cappadocian region of Turkey. *Lancet*, 2001, 357: 444-445.

Rowland-Goldsmith, M. A., Maruyama, H., Matsuda, K., Idezawa, T., Ralli, M., Ralli, S. and Korc, M. Soluble type II transforming growth factor-beta receptor attenuates expression of metastasis-associated genes and suppresses pancreatic cancer cell metastasis. *Mol. Cancer Ther.*, 2002, 1: 161-167.

Ruffie, P., Feld, R., Minkin, S., Cormier, Y., Boutan-Laroze, A., Ginsberg, R., Ayoub, J., Shepherd, F. A., Evans, W. K., Figueredo, A. and . Diffuse malignant mesothelioma of the pleura in Ontario and Quebec: a retrospective study of 332 patients. *J. Clin. Oncol.*, 1989, 7: 1157-1168.

Ruzek, M. C., Hawes, M., Pratt, B., McPherson, J., Ledbetter, S., Richards, S. M. and Garman, R. D. Minimal effects on immune parameters following chronic anti-TGF-beta monoclonal antibody administration to normal mice. *Immunopharmacol. Immunotoxicol.*, 2003, 25: 235-257.

Salzman, S. A., Mazza, J. J. and Burmester, J. K. Regulation of colony-stimulating factor-induced human myelopoiesis by transforming growth factor-beta isoforms. *Cytokines Cell Mol. Ther.*, 2002, 7: 31-36.

Sano, Y., Harada, J., Tashiro, S., Gotoh-Mandeville, R., Maekawa, T. and Ishii, S. ATF-2 is a common nuclear target of Smad and TAK1 pathways in transforming growth factor-beta signaling. *J. Biol. Chem.*, 1999, 274: 8949-8957.

Sasaki, A., Naganuma, H., Satoh, E., Kawataki, T., Amagasaki, K. and Nukui, H. Participation of thrombospondin-1 in the activation of latent transforming growth factor-beta in malignant glioma cells. *Neurol. Med. Chir (Tokyo)*, 2001, 41: 253-258.

Savage, C., Das, P., Finelli, A. L., Townsend, S. R., Sun, C. Y., Baird, S. E. and Padgett, R. W. Caenorhabditis elegans genes sma-2, sma-3, and sma-4 define a conserved family of transforming growth factor beta pathway components. *Proc. Natl. Acad. Sci. U. S. A*, 1996, 93: 790-794.

Scarpa, S., Giuffrida, A., Fazi, M., Coletti, A., Palumbo, C., Pass, H. I., Procopio, A. and Modesti, A. Migration of mesothelioma cells correlates with histotype-specific synthesis of extracellular matrix. *Int. J. Mol. Med.*, 1999, 4: 67-71.

Schnabl, B., Kweon, Y. O., Frederick, J. P., Wang, X. F., Rippe, R. A. and Brenner, D. A. The role of Smad3 in mediating mouse hepatic stellate cell activation. *Hepatology*, 2001, 34: 89-100.

Sebastien, P., Janson, X., Gaudichet, A., Hirsch, A. and Bignon, J. Asbestos retention in human respiratory tissues: comparative measurements in lung parenchyma and in parietal pleura. *IARC Sci. Publ.*, 1980, 237-246.

Sekelsky, J. J., Newfeld, S. J., Raftery, L. A., Chartoff, E. H. and Gelbart, W. M. Genetic characterization and cloning of mothers against dpp, a gene required for decapentaplegic function in Drosophila melanogaster. *Genetics*, 1995, 139: 1347-1358.

Senan, S. Indications and limitations of radiotherapy in malignant pleural mesothelioma. *Curr. Opin. Oncol.*, 2003, 15: 144-147.

Sethi, T., Rintoul, R. C., Moore, S. M., MacKinnon, A. C., Salter, D., Choo, C., Chilvers, E. R., Dransfield, I., Donnelly, S. C., Strieter, R. and Haslett, C. Extracellular matrix proteins protect small cell lung cancer cells against apoptosis: a mechanism for small cell lung cancer growth and drug resistance in vivo. *Nat. Med.*, 1999, 5: 662-668.

Shapiro, G. I., Edwards, C. D. and Rollins, B. J. The physiology of p16(INK4A)-mediated G1 proliferative arrest. *Cell Biochem. Biophys.*, 2000, 33: 189-197.

She, Y., Lee, F., Chen, J., Haimovitz-Friedman, A., Miller, V. A., Rusch, V. R., Kris, M. G. and Sirotnak, F. M. The epidermal growth factor receptor tyrosine kinase inhibitor ZD1839 selectively potentiates radiation response of human tumors in nude mice, with a marked improvement in therapeutic index. *Clin. Cancer Res.*, 2003, 9: 3773-3778.

Sheers, G. and Coles, R. M. Mesothelioma risks in a naval dockyard. *Arch. Environ. Health*, 1980, 35: 276-282.

Shi, Y. and Massague, J. Mechanisms of TGF-beta signaling from cell membrane to the nucleus. *Cell*, 2003, 113: 685-700.

Siriwardena, D., Khaw, P. T., King, A. J., Donaldson, M. L., Overton, B. M., Migdal, C. and Cordeiro, M. F. Human antitransforming growth factor beta(2) monoclonal antibody--a new modulator of wound healing in trabeculectomy: a randomized placebo controlled clinical study. *Ophthalmology*, 2002, 109: 427-431.

Stander, M., Naumann, U., Dumitrescu, L., Heneka, M., Loschmann, P., Gulbins, E., Dichgans, J. and Weller, M. Decorin gene transfer-mediated suppression of TGF-beta synthesis abrogates experimental malignant glioma growth in vivo. *Gene Ther.*, 1998, 5: 1187-1194.

Stanton, M. F., Layard, M., Tegeris, A., Miller, E., May, M., Morgan, E. and Smith, A. Relation of particle dimension to carcinogenicity in amphibole asbestoses and other fibrous minerals. *J. Natl. Cancer Inst.*, 1981, 67: 965-975.

Stanton, M. F., Laynard, M., Tegeris, A., Miller, E., May, M. and Kent, E. Carcinogenicity of fibrous glass: pleural response in the rat in relation to fiber dimension. *J. Natl. Cancer Inst.*, 1977, 58: 587-603.

Steele, J. P., Shamash, J., Evans, M. T., Gower, N. H., Tischkowitz, M. D. and Rudd, R. M. Phase II study of vinorelbine in patients with malignant pleural mesothelioma. *J. Clin. Oncol.*, 2000, 18: 3912-3917.

Sterman, D. H., Treat, J., Litzky, L. A., Amin, K. M., Coonrod, L., Molnar-Kimber, K., Recio, A., Knox, L., Wilson, J. M., Albelda, S. M. and Kaiser, L. R. Adenovirus-mediated herpes simplex virus thymidine kinase/ganciclovir gene therapy in patients with localized malignancy: results of a phase I clinical trial in malignant mesothelioma. *Hum. Gene Ther.*, 1998, 9: 1083-1092.

Stetler-Stevenson, W. G., Aznavoorian, S. and Liotta, L. A. Tumor cell interactions with the extracellular matrix during invasion and metastasis. *Annu. Rev. Cell Biol.*, 1993, 9: 541-573.

Stewart, D. A., Cooper, C. R. and Sikes, R. A. Changes in extracellular matrix (ECM) and ECM-associated proteins in the metastatic progression of prostate cancer. *Reprod. Biol. Endocrinol.*, 2004, 2: 2.

Stoeltzing, O., Liu, W., Reinmuth, N., Fan, F., Parry, G. C., Parikh, A. A., McCarty, M. F., Bucana, C. D., Mazar, A. P. and Ellis, L. M. Inhibition of integrin alpha5beta1 function with a small peptide (ATN-161) plus continuous 5-FU infusion reduces colorectal liver metastases and improves survival in mice. *Int. J. Cancer*, 2003, 104: 496-503.

Strizzi, L., Catalano, A., Vianale, G., Orecchia, S., Casalini, A., Tassi, G., Puntoni, R., Mutti, L. and Procopio, A. Vascular endothelial growth factor is an autocrine growth factor in human malignant mesothelioma. *J. Pathol.*, 2001a, 193: 468-475.

Strizzi, L., Vianale, G., Catalano, A., Muraro, R., Mutti, L. and Procopio, A. Basic fibroblast growth factor in mesothelioma pleural effusions: correlation with patient survival and angiogenesis. *Int. J. Oncol.*, 2001b, 18: 1093-1098.

Sugarbaker, D. J., Jaklitsch, M. T., Bueno, R., Richards, W., Lukanich, J., Mentzer, S. J., Colson, Y., Linden, P., Chang, M., Capalbo, L., Oldread, E., Neragi-Miandoab, S.,

Swanson, S. J. and Zellos, L. S. Prevention, early detection, and management of complications after 328 consecutive extrapleural pneumonectomies. *J. Thorac. Cardiovasc. Surg.*, 2004, 128: 138-146.

Summerford, C., Bartlett, J. S. and Samulski, R. J. AlphaVbeta5 integrin: a co-receptor for adeno-associated virus type 2 infection. *Nat. Med.*, 1999, 5: 78-82.

Sun, Y., Liu, X., Ng-Eaton, E., Lodish, H. F. and Weinberg, R. A. SnoN and Ski protooncoproteins are rapidly degraded in response to transforming growth factor beta signaling. *Proc. Natl. Acad. Sci. U. S. A*, 1999, 96: 12442-12447.

Suzuki, C., Murakami, G., Fukuchi, M., Shimanuki, T., Shikauchi, Y., Imamura, T. and Miyazono, K. Smurf1 regulates the inhibitory activity of Smad7 by targeting Smad7 to the plasma membrane. *J. Biol. Chem.*, 2002.

Suzuki, Y. Pathology of human malignant mesothelioma--preliminary analysis of 1,517 mesothelioma cases. *Ind. Health*, 2001, 39: 183-185.

Suzuki, Y. and Kohyama, N. Malignant mesothelioma induced by asbestos and zeolite in the mouse peritoneal cavity. *Environ. Res.*, 1984, 35: 277-292.

Takayama, K., Ueno, H., Pei, X. H., Nakanishi, Y., Yatsunami, J. and Hara, N. The levels of integrin alpha v beta 5 may predict the susceptibility to adenovirus-mediated gene transfer in human lung cancer cells. *Gene Ther.*, 1998, 5: 361-368.

Tanimura, S., Asato, K., Fujishiro, S. H. and Kohno, M. Specific blockade of the ERK pathway inhibits the invasiveness of tumor cells: down-regulation of matrix metalloproteinase-3/-9/-14 and CD44. *Biochem. Biophys. Res. Commun.*, 2003, 304: 801-806.

Tannock, I. F., Lee, C. M., Tunggal, J. K., Cowan, D. S. and Egorin, M. J. Limited penetration of anticancer drugs through tumor tissue: a potential cause of resistance of solid tumors to chemotherapy. *Clin. Cancer Res.*, 2002, 8: 878-884.

Tatebe, S., Matsuura, T., Endo, K., Doi, R., Goto, A., Sato, K. and Ito, H. Adenoviral transduction efficiency partly correlates with expression levels of integrin alphavbeta5, but not alphavbeta3 in human gastric carcinoma cells. *Int. J. Mol. Med.*, 1998, 2: 61-64.

Terranova, V. P., Liotta, L. A., Russo, R. G. and Martin, G. R. Role of laminin in the attachment and metastasis of murine tumor cells. *Cancer Res.*, 1982, 42: 2265-2269.

Terranova, V. P., Williams, J. E., Liotta, L. A. and Martin, G. R. Modulation of the metastatic activity of melanoma cells by laminin and fibronectin. *Science*, 1984, 226: 982-985.

Testa, J. R. and Giordano, A. SV40 and cell cycle perturbations in malignant mesothelioma. *Semin. Cancer Biol.*, 2001, 11: 31-38.

Togo, G., Toda, N., Kanai, F., Kato, N., Shiratori, Y., Kishi, K., Imazeki, F., Makuuchi, M. and Omata, M. A transforming growth factor beta type II receptor gene mutation common in sporadic cecum cancer with microsatellite instability. *Cancer Res.*, 1996, 56: 5620-5623.

Treasure, T., Waller, D., Swift, S. and Peto, J. Radical surgery for mesothelioma. *BMJ*, 2004, 328: 237-238.

Tsukazaki, T., Chiang, T. A., Davison, A. F., Attisano, L. and Wrana, J. L. SARA, a FYVE domain protein that recruits Smad2 to the TGFbeta receptor. *Cell*, 1998, 95: 779-791.

Tuxhorn, J. A., McAlhany, S. J., Yang, F., Dang, T. D. and Rowley, D. R. Inhibition of transforming growth factor-beta activity decreases angiogenesis in a human prostate cancer-reactive stroma xenograft model. *Cancer Res.*, 2002, 62: 6021-6025.

Uchida, K., Suzuki, H., Ohashi, T., Nitta, K., Yumura, W. and Nihei, H. Involvement of MAP kinase cascades in Smad7 transcriptional regulation. *Biochem. Biophys. Res. Commun.*, 2001, 289: 376-381.

Uchiyama-Tanaka, Y., Matsubara, H., Mori, Y., Kosaki, A., Kishimoto, N., Amano, K., Higashiyama, S. and Iwasaka, T. Involvement of HB-EGF and EGF receptor transactivation in TGF-beta- mediated fibronectin expression in mesangial cells. *Kidney Int.*, 2002, 62: 799-808.

Ueki, N., Nakazato, M., Ohkawa, T., Ikeda, T., Amuro, Y., Hada, T. and Higashino, K. Excessive production of transforming growth-factor beta 1 can play an important role in the development of tumorigenesis by its action for angiogenesis: validity of neutralizing antibodies to block tumor growth. *Biochim. Biophys. Acta*, 1992, 1137: 189-196.

Ueno, T., Hashimoto, O., Kimura, R., Torimura, T., Kawaguchi, T., Nakamura, T., Sakata, R., Koga, H. and Sata, M. Relation of type II transforming growth factor-beta receptor to hepatic fibrosis and hepatocellular carcinoma. *Int. J. Oncol.*, 2001, 18: 49-55.

Ulloa, L., Doody, J. and Massague, J. Inhibition of transforming growth factor-beta/SMAD signalling by the interferon-gamma/STAT pathway. *Nature*, 1999, 397: 710-713.

Valle, M. T., Porta, C., Megiovanni, A. M., Libener, R., Mele, L., Gaudino, G., Strizzi, L., Guida, R., Toma, S. and Mutti, L. Transforming growth factor-beta released by PPD-presenting malignant mesothelioma cells inhibits interferon-gamma synthesis by an anti-PPD CD4+ T-cell clone. *Int. J. Mol. Med.*, 2003, 11: 161-167.

van Ruth, S., Baas, P., Haas, R. L., Rutgers, E. J., Verwaal, V. J. and Zoetmulder, F. A. Cytoreductive surgery combined with intraoperative hyperthermic intrathoracic chemotherapy for stage I malignant pleural mesothelioma. *Ann. Surg. Oncol.*, 2003, 10: 176-182.

Varani, J. Interaction of tumor cells with the extracellular matrix. *Revis. Biol. Celular.*, 1987, 12: 1-113.

Varela-Rey, M., Montiel-Duarte, C., Oses-Prieto, J. A., Lopez-Zabalza, M. J., Jaffrezou, J. P., Rojkind, M. and Iraburu, M. J. p38 MAPK mediates the regulation of alpha1(I) procollagen mRNA levels by TNF-alpha and TGF-beta in a cell line of rat hepatic stellate cells(1).

Versnel, M. A., Claesson-Welsh, L., Hammacher, A., Bouts, M. J., van der Kwast, T. H., Eriksson, A., Willemsen, R., Weima, S. M., Hoogsteden, H. C., Hagemeijer, A. and . Human malignant mesothelioma cell lines express PDGF beta-receptors whereas cultured normal mesothelial cells express predominantly PDGF alpha-receptors. *Oncogene*, 1991, 6: 2005-2011.

Vogelzang, N. J., Rusthoven, J. J., Symanowski, J., Denham, C., Kaukel, E., Ruffie, P., Gatzemeier, U., Boyer, M., Emri, S., Manegold, C., Niyikiza, C. and Paoletti, P. Phase III study of pemetrexed in combination with cisplatin versus cisplatin alone in patients with malignant pleural mesothelioma. *J. Clin. Oncol.*, 2003, 21: 2636-2644.

von Gersdorff, G., Susztak, K., Rezvani, F., Bitzer, M., Liang, D. and Bottinger, E. P. Smad3 and Smad4 mediate transcriptional activation of the human Smad7 promoter by transforming growth factor beta. *J. Biol. Chem.*, 2000, 275: 11320-11326.

Wagner, J. C., SLEGGS, C. A. and MARCHAND, P. Diffuse pleural mesothelioma and asbestos exposure in the North Western Cape Province. *Br. J. Ind. Med.*, 1960, 17: 260-271.

Wang, B., Hao, J., Jones, S. C., Yee, M. S., Roth, J. C. and Dixon, I. M. Decreased Smad 7 expression contributes to cardiac fibrosis in the infarcted rat heart. *Am. J. Physiol Heart Circ. Physiol*, 2002, 282: H1685-H1696.

Wang, E., Dement, J. M. and Lipscomb, H. Mortality among North Carolina construction workers, 1988-1994. *Appl. Occup. Environ. Hyg.*, 1999, 14: 45-58.

Wang, L., Ma, R., Flavell, R. A. and Choi, M. E. Requirement of mitogen-activated protein kinase kinase 3 (MKK3) for activation of p38alpha and p38delta MAPK isoforms by TGF-beta 1 in muri.

Wernert, N. The multiple roles of tumour stroma. *Virchows Arch.*, 1997, 430: 433-443.

Whitaker, D., Papadimitriou, J. M. and Walters, M. N. The mesothelium and its reactions: a review. *Crit Rev. Toxicol.*, 1982, 10: 81-144.

White, C. Annual deaths from mesothelioma in Britain to reach 2000 by 2010. *BMJ*, 2003, 326: 1417.

Xavier, S., Piek, E., Fujii, M., Javelaud, D., Mauviel, A., Flanders, K. C., Samuni, A. M., Felici, A., Reiss, M., Yarkoni, S., Sowers, A., Mitchell, J. B., Roberts, A. B. and Russo, A. Amelioration of radiation-induced fibrosis: inhibition of transforming growth factor-beta signaling by halofuginone. *J. Biol. Chem.*, 2004, 279: 15167-15176.

Xu, Z., Armstrong, B. K., Blundson, B. J., Rogers, J. M., Musk, A. W. and Shilkin, K. B. Trends in mortality from malignant mesothelioma of the pleura, and production and use of asbestos in Australia. *Med. J. Aust.*, 1985, 143: 185-187.

Yamanaka, O., Saika, S., Okada, Y., Ooshima, A. and Ohnishi, Y. Effects of interferon-gamma on human subconjunctival fibroblasts in the presence of TGFbeta1: reversal of TGFbeta-stimulated collagen production. *Graefes Arch. Clin. Exp. Ophthalmol.*, 2003, 241: 116-124.

Yanagisawa, M., Nakashima, K., Takeda, K., Ochiai, W., Takizawa, T., Ueno, M., Takizawa, M., Shibuya, H. and Taga, T. Inhibition of BMP2-induced, TAK1 kinase-mediated neurite outgrowth by Smad6 and Smad7. *Genes Cells*, 2001, 6: 1091-1099.

Yang, E. Y. and Moses, H. L. Transforming growth factor beta 1-induced changes in cell migration, proliferation, and angiogenesis in the chicken chorioallantoic membrane. *J. Cell Biol.*, 1990, 111: 731-741.

Yeung, P. and Rogers, A. An occupation-industry matrix analysis of mesothelioma cases in Australia 1980-1985. *Appl. Occup. Environ. Hyg.*, 2001, 16: 40-44.

Yeung, P., Rogers, A. and Johnson, A. Distribution of mesothelioma cases in different occupational groups and industries in Australia, 1979-1995. *Appl. Occup. Environ. Hyg.*, 1999, 14: 759-767.

Yonekura, A., Osaki, M., Hirota, Y., Tsukazaki, T., Miyazaki, Y., Matsumoto, T., Ohtsuru, A., Namba, H., Shindo, H. and Yamashita, S. Transforming growth factor-beta stimulates articular chondrocyte cell growth through p44/42 MAP kinase (ERK) activation. *Endocr. J.*, 1999, 46: 545-553.

Yu, Q. and Stamenkovic, I. Cell surface-localized matrix metalloproteinase-9 proteolytically activates TGF-beta and promotes tumor invasion and angiogenesis. *Genes Dev.*, 2000, 14: 163-176.

Yue, J. and Mulder, K. M. Requirement of Ras/MAPK pathway activation by transforming growth factor beta for transforming growth factor beta 1 production in a Smad- dependent pathway. *J. Biol. Chem.*, 2000a, 275: 30765-30773.

Yue, J. and Mulder, K. M. Requirement of Ras/MAPK pathway activation by transforming growth factor beta for transforming growth factor beta 1 production in a smad- dependent pathway. *J. Biol. Chem.*, 2000b, 275: 35656.

Zanella, C. L., Timblin, C. R., Cummins, A., Jung, M., Goldberg, J., Raabe, R., Tritton, T. R. and Mossman, B. T. Asbestos-induced phosphorylation of epidermal growth factor receptor is linked to c-fos and apoptosis. *Am. J. Physiol*, 1999, 277: L684-L693.

Zellos, L. S. and Sugarbaker, D. J. Diffuse malignant mesothelioma of the pleural space and its management. *Oncology (Huntingt)*, 2002, 16: 907-913.

Zhao, J., Lee, M., Smith, S. and Warburton, D. Abrogation of Smad3 and Smad2 or of Smad4 gene expression positively regulates murine embryonic lung branching morphogenesis in culture. *Dev. Biol.*, 1998, 194: 182-195.

Zhao, J., Shi, W., Wang, Y. L., Chen, H., Bringas, P., Jr., Datto, M. B., Frederick, J. P., Wang, X. F. and Warburton, D. Smad3 deficiency attenuates bleomycin-induced

pulmonary fibrosis in mice. *Am. J. Physiol Lung Cell Mol. Physiol*, 2002a, 282: L585-L593.

Zhao, J., Sime, P. J., Bringas, P., Jr., Gauldie, J. and Warburton, D. Adenovirus-mediated decorin gene transfer prevents TGF-beta-induced inhibition of lung morphogenesis. *Am. J. Physiol*, 1999, 277: L412-L422.

Zhao, W., Kobayashi, M., Ding, W., Yuan, L., Seth, P., Cornain, S., Wang, J., Okada, F. and Hosokawa, M. Suppression of in vivo tumorigenicity of rat hepatoma cell line KDH-8 cells by soluble TGF-beta receptor type II. *Cancer Immunol. Immunother.*, 2002b, 51: 381-388.

Zocchi, L. Physiology and pathophysiology of pleural fluid turnover. *Eur. Respir. J.*, 2002, 20: 1545-1558.